2015

Rheological performance evaluation of asphalt modified with bio-based polymers

Conglin Chen
Iowa State University

Rheological performance evaluation of asphalt modified with bio-based polymers

by

Conglin Chen

A thesis submitted to the graduate faculty

in partial fulfillment of the requirements for the degree of

MASTER OF SCIENCE

Major: Civil Engineering (Civil Engineering Materials)

Program of Study Committee:
R. Christopher Williams, Major Professor
Vernon R. Schaefer
W. Robert Stephenson

Iowa State University

Ames, Iowa

2015

TABLE OF CONTENTS

ACKNOWLEDGEMENTS

First, I would like to give my special gratitude to my major professor, Dr. R. Chris Williams, for his guidance, encouragement, and patience. His financial support helped me concentrate on this research and my study. I also want to thank Dr. Stephenson for the guidance in the statistical study. Additionally, I would like to thank Dr. Schaefer and Dr. Stephen for being my committee members and I'm so grateful that I used to be one of the students in their courses in which I learnt a lot.

I also want to thank my laboratory graduate colleagues for the help they provided to me during my Master's study. I would like to thank Dr. Joseph Podolsky and Austin Hohmann for the help, guidance, and advice on this research.

Last but not least, I would like to express my deep gratitude and love to my parents, Dongfeng Chen and Yan Zhao, and my fiancé Yang Zhang, who always cheered me up and cared about everything in my life.

LIST OF TABLES

LIST OF FIGURES

ABSTRACT

Fuel-based polymers, used as modifiers and additives in asphalt cement binders, improve the rheological performance of the base asphalt binders, therefore increase the resistance to pavement distresses. However, demand for polymers that are biodegradable, environmentally friendly, and cost effective is increasing. Soybean oil used as an alternative in place of soft and rubbery elastomers polybutadiene derived from crude oil was synthesized to bio-based polymers via chemical synthesis methods Reversible Addition-Fragmentation chain Transfer (RAFT) and Atom Transfer Radical Polymerization (ATRP).

In this study, bio-based polymers (PS-PAESO and PS-PAESO-Cl) with different styrene parameters were blended at a dosage of 3% by weight to a base asphalt binder by the solvent blending approach and three different shear blending methods. The objective of this study was to characterize the rheological properties of bio-based polymer modified asphalt blends by conducting dynamic shear rheometer (DSR), rolling thin film oven (RTFO), pressurized aging vessel (PAV), and bending beam rheometer (BBR) based on the Superpave performance graded asphalt binder specifications. The complex modulus (G*), phase angle (δ), mass losses, and creep stiffness were determined to evaluate the rheological properties of the modified blends. Statistical analysis was conducted to evaluate the related factors that may influence the test results and to develop statistical modeling for predicting the bio-based polymers with appropriate styrene parameters that would optimize the rheological performance of the modified blends.

Results from high temperature performance tests show that the addition of bio-based polymer (PS-PAESO and PS-PAESO-PS) used in this study increase the critical high temperature of the base binder that indicate an improvement on the resistance of rutting at high temperature. The similar results are observed from the master curves and the black diagrams which both exhibit stiffer behavior of the base asphalt at higher temperatures after modification, which indicates a rubber-elastic network establishment within the blends. Whereas, these bio-based polymers do not substantially improve the resistance to low temperature thermal cracking based on the critical low temperature results. Another finding is the use of bio-based polymers generally widened the continuous performance grade range of the base asphalt binder, which indicates that the bio-based polymers reduce the

temperature susceptibility of the base asphalt binder. Furthermore, the statistical analysis on laboratory test results show no statistically significant difference between the three shear blending methods used in this study and no statistically significant difference between the polymer synthesis reaction durations. However, further statistical analysis by using block design on the shear blending methods and the polymer reaction durations shows there is statistically significant difference between the short and long reaction durations but no statistically significant difference between the shear blending methods. The finalized prediction models based on the response surface modeling present the same predicated styrene parameters in polymer to the test result analysis, which indicates that bio-based polymer with styrene parameters as lower molecular weight and lower styrene content are recommended for achieving higher critical high temperatures.

CHAPTER 1. INTRODUCTION

The rheological properties have significant impact on asphalt pavement performance. Primary pavement distresses such as rutting at high temperature, thermal cracking at low temperature, and fatigue cracking due to repeated traffic loading are related to the rheological properties of the asphalt materials in pavement construction. In order to improve the performance of asphalt binders, modifiers or additives such as SBS, SBR, and EVA have been used to modify asphalt. However, because of the high costs and the demand for non-fossil fuel-based polymers, bio-based polymers have been invented to simulate the chemical properties of fuel-based polymers.

The study discussed in this thesis is to evaluate the rheological properties of modified asphalt binders by using the bio-based polymers (PS-PAESO, PS-PAESO-Cl) produced at Iowa State University. This chapter describes the industry and technical problems with respect to the goals, objectives, and methodology used in this study. The final section of this chapter presents the organization of this thesis.

INDUSTRY AND TECHNICAL PROBLEMS

As the increasing price and the globally limited resources of crude oil, the cost of fuel-based polymers keeps increasing. For the purpose of finding an alternative product instead of fuel-based polymers, researchers have been focusing on using agricultural resources such as linseed, rapeseed, and soybean oil to synthesize bio-based polymers via chemical reactions. These types of bio-based polymers are biodegradable, environmentally friendly, and cost competitive. More importantly, the triglycerides in these agricultural plant seeds can be synthesized into the soft and rubbery elastomers which can be an alternatives to polybutadiene in fuel-based polymers such as styrene-butadiene-styrene (SBS) and styrene-butadiene (SB), so the bio-based polymers are expected to improve the rheological properties of asphalt binder like the fuel-base polymers.

However, there is limited research focusing on bio-based polymer modification in asphalt binder. The technical problems are associated with the compatibility between the base asphalt and the bio-based polymer, the bio-based polymer modification ability in asphalt binder at both high and low temperatures, and the application of the bio-based polymer modified asphalt in hot mix asphalt.

GOALS AND OBJECTIVES OF THE RESEARCH

The first goal of this research was to determine and evaluate the rheological properties and the performance grade of modified asphalt binders by using different styrene parameters (i.e. styrene molecular weight and styrene content) of bio-based polymers (PS-PAESO, PS-PAESO-Cl). The second goal was to further associate laboratory results with the statistical modeling to create the prediction models for the recommended bio-based polymer styrene parameters (i.e. styrene molecular weight and styrene content) for further studies.

The specific objectives of this research are to:

- conduct laboratory rheological tests to evaluate the modification effects of these bio-based polymers according to asphalt blends rheological performance;
- perform statistical analysis based on the laboratory test results to determine if different shear blending methods and different polymer chemical synthesis reaction durations would differ the rheological properties of bio-based modified blends; and
- perform statistical response surface modeling via the step-down regression process based on the laboratory test results to create prediction models for the recommended bio-based polymer styrene parameters (i.e. styrene molecular weight and styrene content) that can provide sufficient improvement on elasticity of the base asphalt binders at high temperature.

METHODOLOGY

The bio-based polymers (PS-PAESO and PS-PAESO-Cl) were laboratory-produced polymers from department of Chemical & Biological Engineering at Iowa State University. The modified asphalt blends by using bio-based polymers were tested following the Superior Performing Asphalt Pavements (Superpave) performance graded asphalt binder specifications. The primary tests performed on modified asphalt blends were the dynamic shear rheometer (DSR) high temperature performance grades tests on unaged and the rolling thin-film oven (RTFO) short-term aged modified asphalt blends, the RTFO short-term aging process on unaged modified asphalt blends, the Pressure aging vessel (PAV) long-term aging for the RTFO short-term aged residuals, and the bending beam rheometer (BBR) low temperature performance tests on the PAV long-term aging residuals. The mass losses of modified asphalt blends after the

RTFO short-term aging were calculated. The master curves and the black diagrams were developed for both unaged and the RTFO short-term aged modified blends.

A single-factor analysis of variance (ANOVA) model was performed to assess the factors that could affect the rheological performance of the bio-based polymer modified blends. A least square means comparisons were performed using Tukey's honestly significant differences (HSD) test with α=0.05. Response surface modeling was developed with the major factors and their interactions effects to optimize the key influencing parameters for creating the prediction models. The JMP (version: Pro 12) statistical software was the computer program used for performing the analysis of variance and response surfacing modeling.

ORGANIZATION OF THE DOCUMENT

Following this introductory chapter, this thesis is organized into four additional chapters. Chapter 2 provides background information and reviews previous literature related to this study. Chapter 3 describes the experimental materials and the overall testing plans and methods used in this study. Chapter 4 discusses the laboratory results and statistical analysis results for characterizing the rheological properties of the modified asphalt blends. Chapter 5 summarizes the conclusions and key findings derived from the results and reports some suggestions for future research. Supporting materials are included as appendices that follow the list of works cited.

KEY TERMS

Rheological property, performance grade, bio-based polymer, asphalt modification, response surface model.

CHAPTER 2. BACKGROUND/LITERATURE REVEIW

BACKGROUND OF ASPHALT

Asphalt is a dark brown to black cementitious material which is widely used in the world. Due to properties of waterproofing and adhesiveness (McIntosh 2008), in the ancient Middle East, asphalt was used for mortar between bricks and stones, to cement artworks etc. (Abraham 1938). In 1830, asphalt became generally used for pavements, flat roofs, and the lining of cisterns in France and England (Lewis 2006). For modern usage, approximately 85% asphalt is consumed for making asphalt concrete for road surface in United States (NAPA 2011).

Commercially used asphalt are natural asphalts and petroleum asphalts. According to Bunger et al. (1979), the remains of ancients, microscopic algae and other once living things were deposited in the place where organisms lived such as mud on the bottom of the ocean or lakes. As a result, natural asphalt will be formed by these remains under the heat (above 50°C) and pressure in the earth. However, the majority of asphalt used today is obtained from carefully refined residue of the distillation process of selected crude petroleum (Wikipedia 2015).

The Components of Asphalt

Based on the study of Corbett (1969), the selective adsorption-desorption method (Figure 1) was conducted to separate and quantify the components of asphalt. According to Corbett's results, asphalt consists of four major compounds which are asphaltenes, polar aromatics, naphthene aromatics, and saturates. These four compounds directly relate to the performance and properties of asphalt (Corbett 1969).

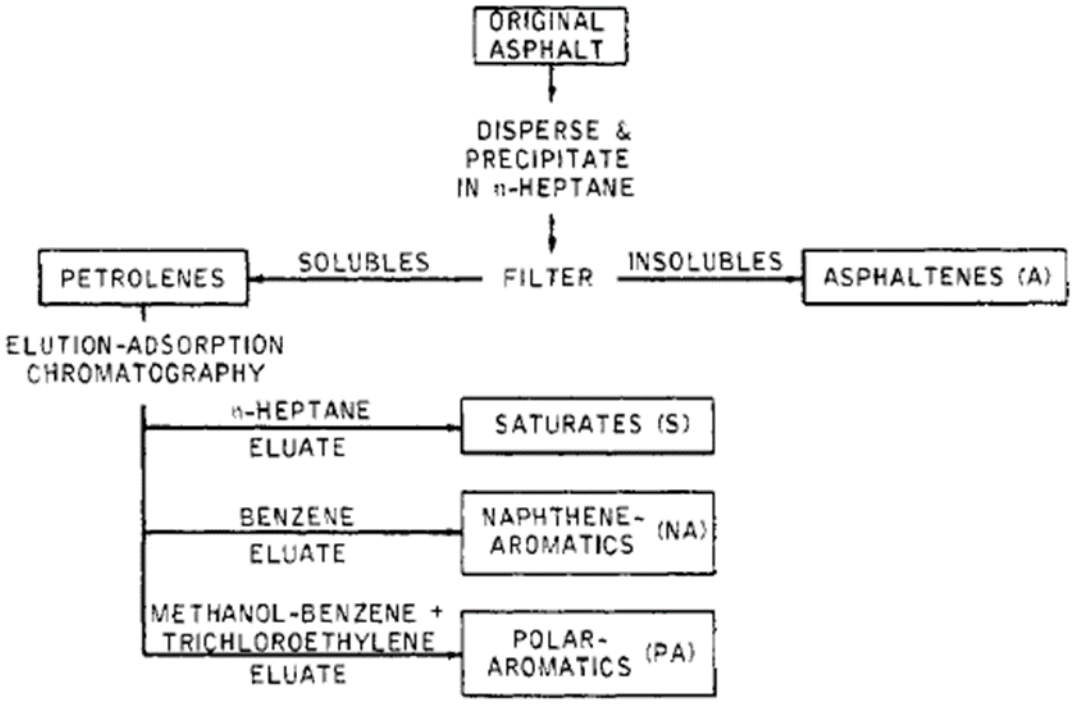

Figure 1. Selective adsorption-desorption method (Corbett 1969)

Asphaltenes

Asphaltenes are dark brown, friable solid or semi-solid at ambient temperature, which precipitated by n-pentane when there are higher amounts. Because asphaltenes are highest polarity component, they have very high tendency to interact and associate with aggregate. As studies showed (Roberts et al. 1996; Yang et al. 2007), asphalt varies from one to another as the amounts and characteristics of asphaltenes are different. Moreover, asphaltenes are one of important roles in asphalt components which are the viscosity-building ("bodying") also relate mostly to the property of temperature susceptibility of asphalt cement and owe the highest molecular weight. Therefore, according to researchers, if low content of asphaltenes (less than around 10 percent) or weakly associating asphaltenes is utilized, the association between aggregate and asphalt in hot-mix asphalt (HMA) would be tender (Roberts et al. 1996). Asphaltenes usually possess 5-20% of asphalt (Yang et al. 2007).

Saturates

According to Roberts et al. (1996), "Saturates are the first fraction to emerge from the column when eluted (desorbed) with n-heptane." Furthermore, "Saturates are liquid at ambient temperatures and hardly change with time" (Roberts et al. 1996). Saturates are a-lack-polar

chemical functional groups, which is susceptible to temperature and the percentage saturates correlates with softening point of asphalt (Roberts et al. 1996) Saturates are lubricator and softener of asphalt whose have low average molecular weight. Saturates possess 5-20% of asphalt (Yang et al. 2007).

Naphthene Aromatics (NA)

"Naphthene aromatics emerge as the second fraction when eluted with a more polar aromatic solvent such as benzene or toluene" (Roberts et al. 1996). Naphthene aromatics are normally dark brown gluey liquid at ambient temperatures. They are considered to be the softening component and the aging friction in asphalt (Roberts et al. 1996), who owe low average molecular weight in asphalt. Naphthene aromatics generally possess 40-60% of asphalt (Yang et al. 2007).

Polar Aromatics (PA)

"They are the final fraction to emerge from the column when eluted with a highly polar mixture of alcohol and benzene (or toluene)" (Roberts et al. 1996). Polar aromatics are yellow to brown solid or semi-solid at ambient temperatures with the most polar property. They have intermediate average molecular weight and relate to ductility and aging fractions of asphalt (Roberts et al. 1996). Polar aromatics possess 15-30% of asphalt (Yang et al. 2007).

Superpave Performance Graded Asphalt Binder Specification

The Superpave system developed by the Strategic Highway Research Program (SHRP) and the specification is evaluated based on American Association of State Highway and Transportation Officials (AASHTO) and American Society for Testing and Materials (ASTM). The Superpave asphalt binder specification is proposed for evaluating modified and unmodified asphalt rheological properties by conducting required sets of testing which are RTFO, PAV, DSR, RV, BBR, and DTT. Three critical stages of binder testing are required to perform and simulate serving conditions during binder's life. Performing testing on original binder is the first stage of transportation, storage, and handling. The second stage is by performing the RTFO (making binder film exposes to heat and air that represents the process of asphalt during hot mixing, hauling, and laydown conditions) to simulate the process of binder's mixing production and construction. The third stage is by conducting the PAV to make binder expose to heat and pressure to simulate years of in-serve aging in a pavement (SMD 1996). The Superpave binder test equipment and purposes are shown in Table 1.

Table 1. Superpave binder test equipment (SMD 1996)

Equipment	Purpose
Rolling thin-film oven (RTFO) Pressure aging vessel (PAV)	Simulate binder aging (hardening) characteristics
Dynamic shear rheometer (DSR)	Measure binder properties at high and intermediate temperatures
Rotational viscometer (RV)	Measure binder properties at high temperatures
Bending beam Rheometer (BBR) Direct tension tester (DTT)	Measure binder properties at low temperatures

Performance graded (PG) (SMD 1996)

Performance graded (PG) binders are defined by PG XX-XX with the testing modulus from BBR (low temperature) and DSR (high temperature) as shown in Figure 2. For example, PG 64-22, which means the high temperature grade is 64°C and the low temperature grade is -22°C. Because the grading system is based on climate, this graded binder should be expected to serve in an environment in which an average seven-day maximum pavement temperature of 64°C and a minimum pavement design temperature of -22°C with adequate physical properties.

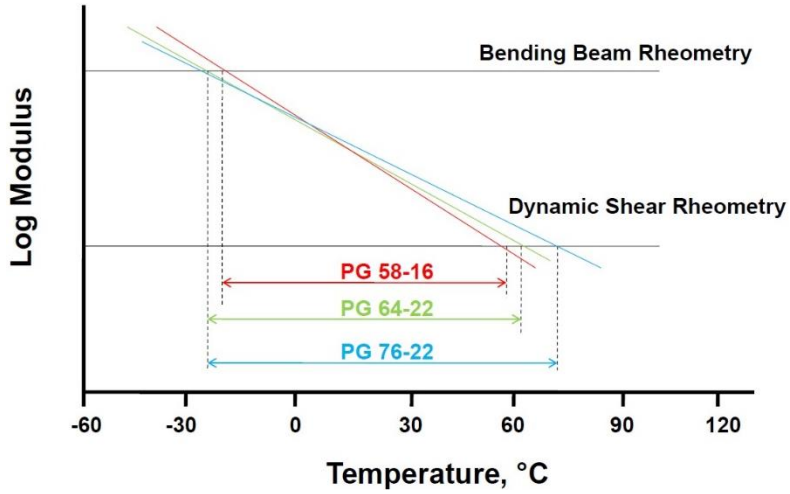

Figure 2. Performance graded asphalt (Kluttz 2012)

Useful temperature interval (UTI) (Kluttz 2012)

Useful temperature interval is the minimum to maximum temperature range getting from the high temperature binder testing DSR and low temperature binder testing BBR where the binder

is expected to perform properly. This interval often refers to as the "True Grade" or "Continuous Grade" of the binder.

HMA Pavement Distresses Related to Asphalt Cement Rheological Properties

The rheological properties of asphalt cement binder such as ductility, viscosity, temperature susceptibility, etc., which has an important effect on pavement performance. Some specific types of pavement distresses are related to the rheological properties of asphalt cement (Roberts et al. 1996). Primarily, these pavement distresses in asphalt pavement are high temperature permanent deformation, low temperature thermal cracking and load-associated fatigue cracking.

High temperature permanent deformation

Rutting, shoving and distortion are typical permanent deformation. Wheel path rutting is the most common form of rutting, which could be visually appeared with depressions forming in the wheel tracks parallel to the traffic line direction (Figure 3). This permanent rutting is caused by the consolidation of one or more layers as a result of repetitive shear stresses. Also, because of the accumulation of plastic deformation in the asphalt pavement with repeated applied loads at upper service temperatures. There are a lot of causes of rutting, such as aggregate shape and property problem, asphalt content issue and designed highway structure problem (Rowlett 1990). However, two indicators of potential rutting could be binders with high temperature susceptibility and binders that do not harden upon oxidation. As for these two binder properties issues, polymer modification could be used in the binder to generally stiffen it and reduce the temperature susceptibility to provide a more elastic and as well as less viscous material (Lewandowski 1994; Kluttz 2012).

Figure 3. High temperature pavement deformation (rutting) (BMT 2013)

Load-associated fatigue cracking

Fatigue cracking occurs in asphalt pavements when there is continuous application of loads over a long period of time. Fatigue cracking is also called alligator cracking, the cracks are shown in Figure 4. The major reason for fatigue cracking is related to the repeated traffic loads and volumes that exceed the pavement design criteria. Additionally, other reasons such as the low binder content for pavement construction, the high stiffness of asphalt binder due to aging, poor bearing capacity of supporting layers, etc. (Lewandowski 1994). To be concluded, load-associated fatigue cracking is influenced by the pavement structure, the asphalt binder properties, and the mixture properties (Kluttz 2012).

Figure 4. Load-associated fatigue cracking (Road Science 2015)

Low-temperature thermal cracking

Thermal shrinkage cracking occurs under the condition of thermal cycle where the temperature reaches a critical low temperature. When the tensile stress exceeds the tensile strength of the asphalt pavement, cracking will appear. This low temperature cracking usually causes cracks transverse to the pavement direction as shown in Figure 5. The causes for this cracking are because of stiff binders, low binder content and high dust to asphalt ratio. However, low temperature thermal cracking is also mainly influenced by the asphalt binder properties. Therefore, the use of modifiers can improve the low temperature flexibility and strength of the asphalt mixture (Kluttz 2012).

Figure 5. Low-temperature thermal cracking (Road Science 2015)

Stripping and aging

Stripping is caused by the greater affinity of aggregate's surface for water than asphalt. Then the loss bond between aggregates and asphalt binder will appear which typically starts at the HMA bottom layer and progresses upward. Modifiers and additives can be used to change the surface of aggregates from hydrophilic (water-loving) to hydrophobic (water-hating) to reduce the moisture susceptibility and improve adhesion of the binder to aggregates (Lewandowski 1994; Kluttz 2012).

Aging or embrittlement of asphalt binder occurs during the mixing and laydown process and the service life of the asphalt pavement. Oxidation and loss of light causes the stiffness and reduction of flexibility of asphalt binder. Polymers have been found to be helpful lower the apparent age hardening (Lewandowski 1994; Kluttz 2012).

BACKGROUND OF POLYMER IN ASPHALT

As discussed above, most of the pavement distresses occur related to the properties of asphalt binder. Terrell and Epps (1988) give a more in-depth list of reasons for using modified binders and mixtures:

- Obtain softer asphalt binder at low service temperatures and reduce cracking;
- Obtain stiffer asphalt binder at high temperature and reduce rutting;
- Reduce viscosity at construction temperature;
- Increase strength and stability of asphalt mixtures;
- Improve abrasion resistance of asphalt mixtures;
- Reduce raveling of asphalt mixtures;
- Reduce low temperature cracking of asphalt pavements;
- Improve workability and compaction of asphalt mixtures;
- Accelerate early stiffening of tender asphalt mixtures;
- Improve fatigue resistance of asphalt mixtures;
- Upgrade marginal asphalt binders;
- Rejuvenate aged asphalt binders;
- Reinforce asphalt binders as an extender;
- Permit thicker asphalt films on aggregates;
- Improve bonding and reduce stripping between asphalt binders and aggregates;
- Reduce flushing or bleeding of asphalt mixtures;
- Improve resistance to aging or oxidation of asphalt binders and asphalt mixtures;
- Reduce structural thickness of asphalt pavement layers;
- Reduce life cycle costs of asphalt pavements; and
- Improve overall performance of asphalt pavements.

Since the Arab oil embargo of the 1970's, the crude sources of asphalt cement have changed which made the asphalt cement not as sticky as it used to be. Moreover, the refinery processes have changed for producing more gasoline and less asphalt cement from crude oil (Corun 2015). In order to improve resistance of pavement distresses, mend total lifecycle cost of the asphalt pavement, make asphalt binder sustainable and enhance the safety of pavements, researchers are focusing on using polymer modification in asphalt to improve its physical properties for longevity serving.

In 1873, Samuel Whiting was granted a patent for using 1% by weight quantity of latex from the balata plant in asphalt paving mixture. In 1902, A French rubberized asphalt paving company laid rubberized asphalt road (Thompson and Hoiberg 1979). In the 1930's, British and French constructed numerous test roads (Shuler and Epps 1982). Utah Department of Transportation (UDOT) has been using polymers since the late 1960's. UDOT examined 33 field projects by using polymers (Lewandowski 2004).

> "The AC-20R polymerized asphalt concrete pavement sections constructed in 1989 were performing with virtually no thermal cracking, which justified the use of polymerized asphalt for mitigating thermal cracking" (Peterson and Anderson 1998).

Kentucky Department of Transportation started a study to estimate if unmodified performance graded binders manufactured with different modifiers (SBR, chemically modified, and straight run) performances the same as modifiers (SBS). Results showed no substantial rutting appeared on pavements and all pavements except SBR showed thermal cracking. Alabama Department of Transportation (ADOT) has been using SBR in overlays since 1983 and Taxes Department of Transportation (TxDOT) also constructed field testing modified pavement with SBR to compare with unmodified asphalt pavements. All data from ADOT and TxDOT showed the same results that SBR modified asphalt pavement could significantly increase the pavement life as shown in Figure 6 (Lewandowski 2004). Polymer modified HMA shows a substantially lower rut depth and less possibility of fatigue cracking as shown in Figure 7 (Harold 2004).

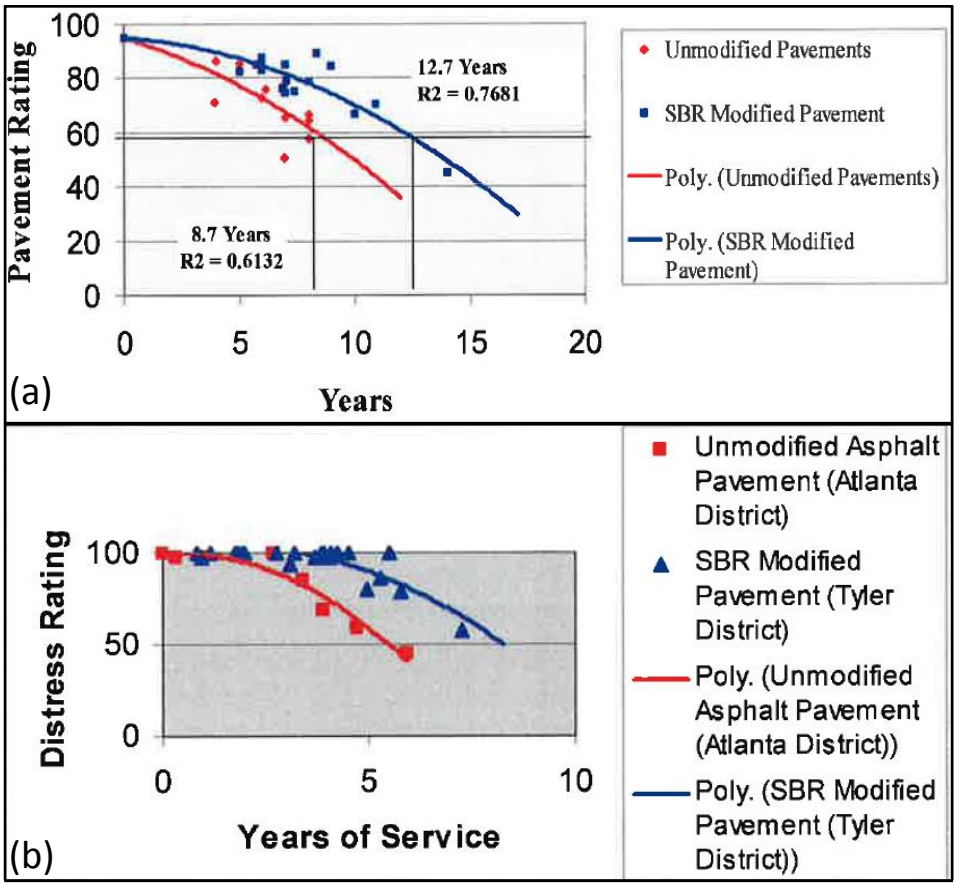

Figure 6. Distress rating versus years of service of SBR modified and unmodified asphalt pavement from (a) ADOT and (b) TxDOT (Lewandowski 2004)

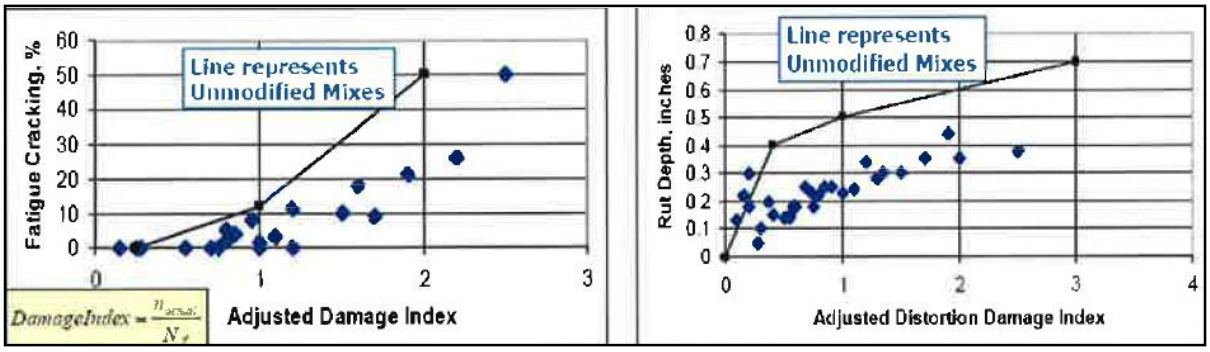

Figure 7. Modified versus unmodified performance of fatigue cracking and rut depth (Harold 2004)

Colorado Department of Transportation (CDOT) initiated a study in 1991 by using different categories of polymer which defined in the AASHTO Task Force 31. Five separate locations were selected in Colorado for evaluation both the sections with polymer modified and without

polymer modified (Harmelink 1997). Locations, asphalt binder types and modifiers applied are shown in Table 2.

Table 2. Location, asphalt binder and modifier (Harmelink 1997)

Location	Asphalt Binder Used	Corresponding SHRP Grading	Task Force 31 Type and Grade	Modifier
I-70 near Flager	AC20 Conoco Denver	PG 64-22	–	–
	AC20 P ELF Pueblo	PG 70-28	Type I-D	SB
I-25 near Pueblo	AC20 Diamond Shamrock	PG 58-16	–	–
	AC20R ELF Pueblo	PG 64-28	Type II-B	SB Tri-Block
	AC20P ELF Pueblo	PG 70-28	Type I-D	SB
I-25 in Denver	AC20 Conoco	PG 64-22	–	–
	AC20P ELF Pueblo	PG 70-28	Type I-D	SB
Santa Fe Drive in Littleton	AC20 Conoco Denver	PG 64-22	–	–
	AC20P ELF Pueblo	PG 70-28	Type I-D	SB
Brighton Boulevard in Denver	AC10 Conoco Denver	PG 58-22	–	–
	AC20P ELF Pueblo	PG 70-28	Type I-D	SB
	AC20P ELF Pueblo	PG 70-28	Type III-D	EVA

Each site selected had significant traffic loadings to determine the effectiveness of the polymer modified asphalt with respecting to rutting from 1991 to 1996 after construction. Evaluations were performed each spring and fall of each year including deflection measurements, cracking measurements, rutting measurements, visual observation and cores testing for in-place voids determination (Harmelink 1997).

As the conclusion of the study, it was determined that rutting was not a significant distress found in any of the projects and no reduction of in-place voids was recorded. In general, cracking was found to be less in the polymer modified sections as compared to the control sections. In most of the cases both longitudinal and transverse cracking were at least 50% less in the polymer modified sections as compared to the control sections. According to the accumulated cracking results gained from these observation years (Harmelink 1997):

- I-70 near Flagler (SB): minor reduction in cracking in polymerized section to control section;

- I-25 near Pueblo (SB Tri-Block): about 2/3 less transverse cracking in polymerized section as compared to rubber test section and about ¾ less than control section; about 1/3 less longitudinal cracking in polymerized section to control section;
- I-25 in Denver (SB): about 1/3 less general cracking in polymerized section than control section;
- Santa Fe Drive in Littleton (SB): the addition of the polymerized section was inconclusive because the premature pavement failure; and
- Brighton Boulevard in Denver (SB, EVA): less cracking in SB polymerized section than both EVA and control section.

Generally, cracking data indicated that the polymers such as SBS and SB enhanced the overall performance of the pavement (Harmelink 1997).

Polymers for Asphalt Modification

The word of "Polymer" is from the Greek. "Poly" means many and "Mer" means units. A polymer is a large molecule which is consisted of many (poly) smaller molecular units called "monomers" by chemical reaction (Kluttz 2012). There are a large variety of categories of modifiers used for asphalt modification: The purpose of which modifier should be applied is dependent on the pavement distresses encounter and the type of asphalt will be modified. Most of the polymer-modifier manufacturers suggest to improve asphalt properties such as its resistance to high temperature permanent deformation especially rutting, low temperature flexibility, fatigue resistance, tensile strength, to reduce temperature susceptibility etc. (Lewandowski 1994). Figure 8 shows the ideal modified asphalt binder compared to a conventional asphalt binder based on the evaluation of stiffness in different in-service temperatures. In low service temperature, modifiers significantly lower the creep stiffness of asphalt binders than conventional asphalt binders, therefore, the resistance to thermal cracking has been improved (Isacsson and Lu 1999). In high service temperature, modifiers increase the stiffness and elasticity and reduce the phrase angle of asphalt binder for rutting distresses (Bahia and Anderson 1995). Three groups of polymer-modifiers used in asphalt paving industry can be roughly categorized as block copolymers and other thermoplastics, synthetic and natural rubbers, and others (Lewandowski 1994).

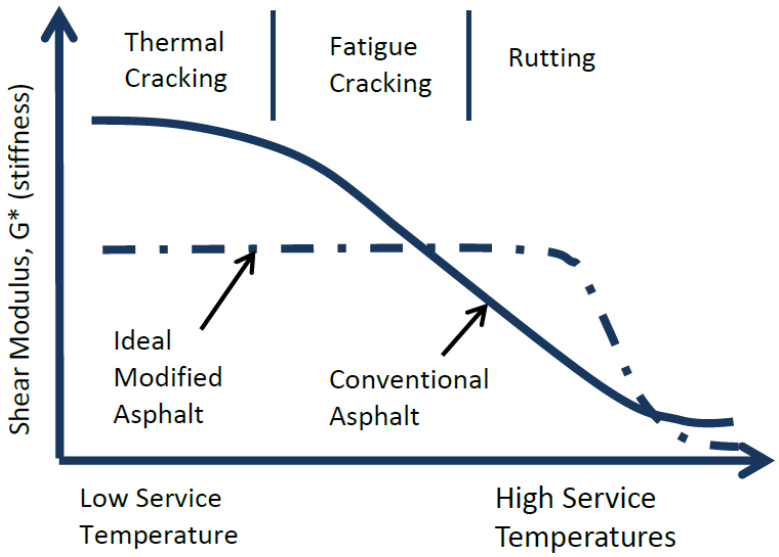

Figure 8. Effects of polymer modification in asphalt binder (Shuler and Epps 1982)

Block copolymers and other thermoplastics (Hines 1993)

This group of modifiers is mainly made up of block copolymers which means if two different monomers are randomly mixed and reacted together, a new polymer with very different physical properties is created. This group can also be divided into two general categories: elastomers (rubber) and plastomers (plastic).

Elastomers resist deformation when there is stress applied and will recover shape quickly as soon as the stress is removed. Asphalt with elastomers modified could add very little strength to asphalt but make it more flexible and behave like an elastomer. Elastomers or rubbers used as asphalt modifiers are including natural rubber (NR), styrene-butadiene rubber (SBR) latexes or SBR, styrene-butadiene-styrene (SBS) block copolymers, styrene-isoprene-styrene (SIS) block copolymers etc.

Plastomers have a tough, rigid, three dimensional network which could resist deformation. Using plastomers as modifier in asphalt could generally increase the stiffness moduli of HMA pavements and can be helpful exhibit quick early strength when loading applied. Plastomers or plastics as asphalt modifiers are including polyethylene, polypropylene, ethyl vinyl acetate (EVA), polyvinyl chloride (PVC), ethylene propylene (EPDM) etc.

Synthetic and natural rubbers (Lewandowski 1994)

This group of modifiers consists of synthetic and natural rubbers, in order not to flow at high temperature, a crosslinking agent is always required to form a continuous network. Homopolymers such as natural rubber (NR), polybutadiene (PBD), polyisoprene (PI) and poly

(2-chloro-1, 3-butadiene) are made up this group. Random copolymers like styrene butadiene rubber (SBR) are also included.

Others (ground tire, fibers, etc.) (Lewandowski 1994)

The remaining types of modifiers are loosely grouped to "others" category, which includes ground tire, fibers and antistripping agents.

BIO-BASED POLYMERS

In order to improve rutting resistance, thermal cracking, fatigue damage, stripping, temperature susceptibility, and meet the specification of pavement in-service performance, using polymer as small amount of asphalt substitute is necessary for improving the rheological properties of original asphalt binder (Lewandowski 1994). As known in asphalt modification industry, SB and SBS are the most commonly used modifiers. However, because of the shortage of styrene-butadiene polymers for the asphalt industry (Romagosa 2008), the desire for renewable natural resources, the increasing price of petroleum derivatives, and the demands for environmentally friendly material are rising (Podolsky et al. 2015). More importantly, bio-based polymers offer significant contributions by reducing the dependence on fossil fuels and making positive environmental impacts like reduced carbon dioxide emissions. As reported, the worldwide interest in bio-based polymers has accumulated in recent years due to the desire and demand for finding non-fossil fuel-based polymers. As indicated by ISI Web of Sciences and Thomas Innovations, there is an incredible increase in the number of publication citations on bio-based polymers and applications in recent years, as shown in Figure 9 (Chen and Patel 2012; Babu et al. 2013). In 2004, there was only around 500 times publications citations while after seven years (2011) the citation increased 8 times. The same increasing trend was found in patents application as well. Approximately 3 times increasing in bio-based polymer patents application from 2005 to 2012. As a result, there is a worldwide demand for replacing petroleum-derived raw materials with renewable resource-based raw materials for the production of polymers.

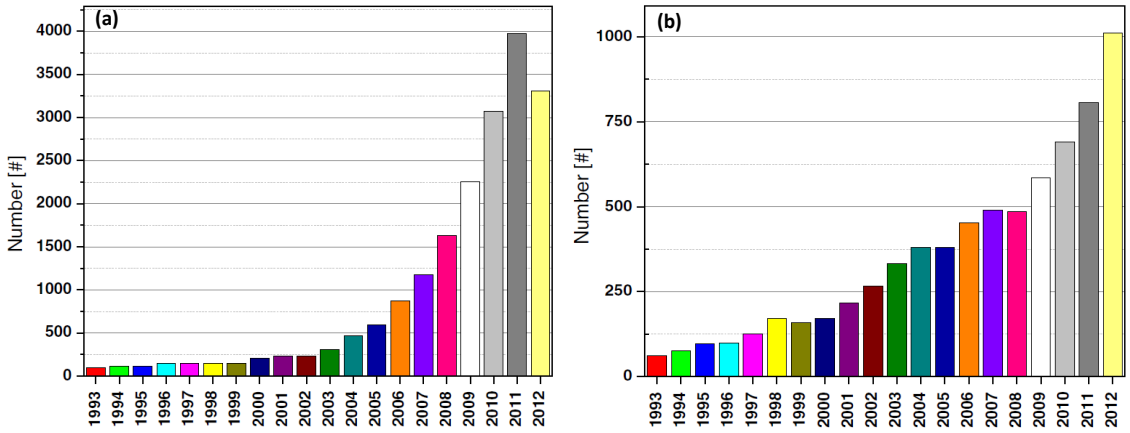

Figure 9. Citation trends of (a) publications and (b) patents on bio-based polymers in recent years (Babu et al. 2013)

Recently, based on researchers' study, they found out the bio-oils can be generated from biomass materials like microalgae (Chailleux et al. 2012), animal waste (Fini 2011; Mills-beale 2012), corn stover (Rsouf 2010), urban yard waste (Hill and Jennings 2011), tea and coffee residue (Chaiya 2011; Uzun 2010), rapeseed and soybean (Onay and Koçkar 2006; Şensöz and Kaynar 2006), etc. Vegetable oils are one of the cheapest and most abundant, annually renewable natural resources available in large quantities from various oil (Andjelkovic et al. 2005). Whereas soybean oil is the most abundant vegetable oil which possesses around 30% of the world's vegetable oil supply. Moreover, soybean oil owes multiple carbon double bonds which are especially suitable for polymerization (Williams et al. 2014). Not only regarding as a food resources, since soybean oil is readily available for large scale production, it also has wide industrial applications. More than 600 million pounds of soybean oil production annually in the United State are used for nonedible applications, the production of industry materials are included as well (Rus 2010). Thus, lots of researchers have been focused on the direct synthesis of copolymers of oils with synthetic polymers (Cakmakli et al. 2004) such as copolymerization of oils with styrene (Gultekin et al. 2000), divinylbenzene-styrene, and the cationic polymerization of epoxidized drying oils (Cakmakli et al. 2004).

Thermoplastic Elastomers (TPEs)

Thermoplastic elastomer (TPEs) are a group of polymers exhibit elastic properties that also have the ability to be processed and recycled as thermoplastics. Typically, properties of elastomer are high strain, weak intermolecular forces, reversible, and immediate responses

(Shanks and Kong 2012). They are composed of an amorphous domains which are commonly known as the "soft" phase and enclosed by crystalline domains which are referred as the "hard" phase (Figure 10) (Hernández et al. 2015). The soft phase can be polybutadiene, poly (ethylene-co-alkene), polyisobutylene, poly (oxyethylene), poly (ester), polysiloxane or any of the typical rubbery elastomers while the hard phase are polystyrene, poly (methylmethacrylate), urethane, ionomer – poly (ethylene-co-acrylic acid) (sodium, Mg, Zn salt), ethylene propylene diene monomer, and fluropolymers. In asphalt modification industry, the most commonly used elastomeric polymers are styrenic block copolymers (SBCs). There are two types of SBCs widely used, which are styrene-butadiene (SB) AB diblock polymers and styrene-butadiene-styrene (SBS) ABA triblock polymers. The structure of styrenic TPEs is shown in Figure 11.

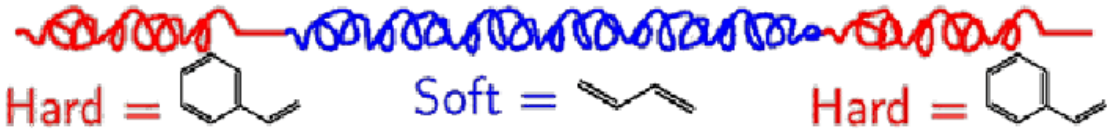

Figure 10. Representation of a typical styrenic block copolymer thermoplastic elastomer. The crystalline domains are colored in red while the amorphous domain is colored in blue (Hernández et al. 2015)

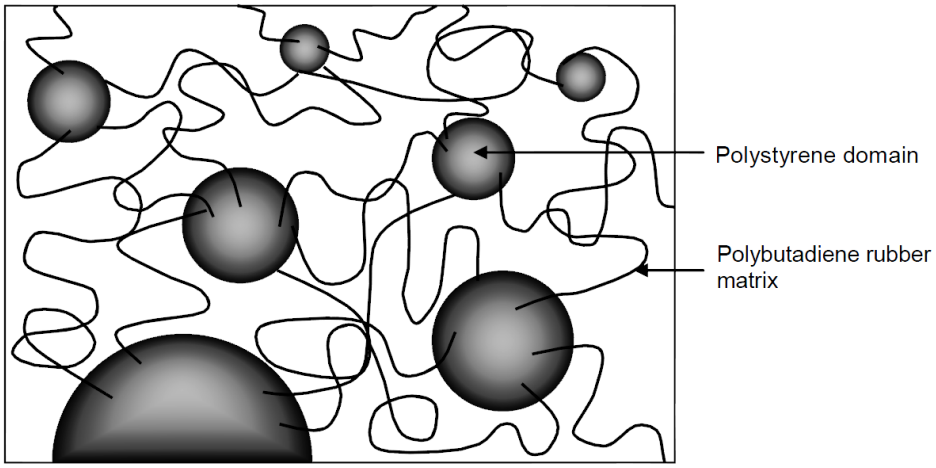

Figure 11. Schematic of a styrene-butadiene-styrene block copolymer (Shanks and Kong 2012)

As for SBS, in order to uniformly disperse the polymer, between 2 and 5 % by total weight of the binder will be added in to asphalt binder through mixing and shear blending at high

temperature. A continuous three-dimensional network will form thoroughly when blending SBS with asphalt since the elastomeric phase of SBS copolymer absorbs the maltenes fraction from asphalt and swells up to nine times its initial volume, which will significantly modify asphalt properties (Yildirim 2007; Brûlé et al. 1988; Airey 2003).

According to Airey (2004), DSR tests were performed on original asphalt binder (Bitumen A and Bitumen B) and SBS polymerized original asphalt binder with various dosages (A3 and B3 (3%), A5 and B5 (5%), and A7 and B7 (7%)). The principle viscoelastic parameters obtained from DSR (the complex modulus (G*) and phase angle (δ)) were interpreted by producing rheological master curves at a reference temperature of 25°C using the time-temperature superposition principle (TTSP) and shift factors determined for the G* master curves as shown in Figure 12 and Figure 13. As results, master curves in Figure 12 of bitumen A Polymers Modified Bitumen (PMBs) both show a significant increase in G* with increasing polymer content at low frequencies high temperatures comparing to original asphalt binder "Bitumen A". The phase angle master curves for the SBS PMBs (Figure 13) show a reduction in phase angle with modification, which indicates the presence of polymer elastic networks or entanglements in modified binders. In conclusion of Airey (2004), at high temperatures, the polymer could be helpful provide stiffness while its network turns to flow by increasing complex modulus of binder mixture. At low temperatures, the polymer network is formed by the physical cross-linking of polystyrene while the polybutadiene elastic property provides the resistance of low temperature cracking (Airey 2004).

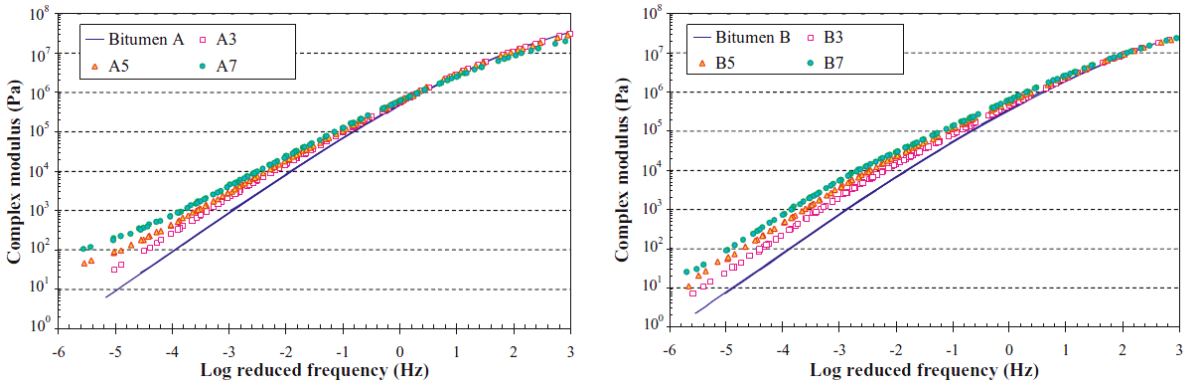

Figure 12. Master curves of complex modulus at 25°C for SBS PMBs (Airey 2004)

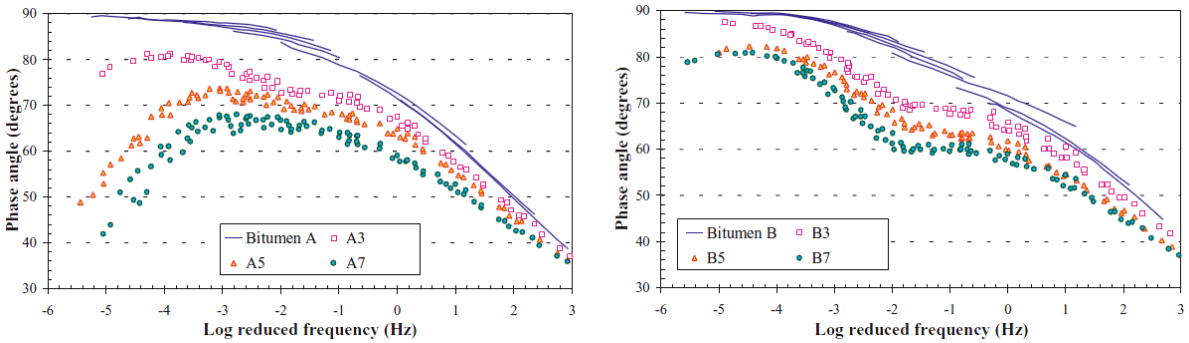

Figure 13. Master curves of phase angle at 25°C for SBS PMBs (Airey 2004)

The same effects of SBS modified asphalt binder's properties were obtained from Chen et al. (2002). Asphalt Binder AC-30 was mixed with five dosages of SBS (3, 5, 6, 7, and 9%). DSR was used to measure the complex shear moduli of these blends. The complex modulus for SBS-modified asphalt at different dosages is illustrated in Figure 14. As the results shown in Figure 14, the complex modulus increases as a function of the amount of SBS copolymer when the SBS copolymer modified asphalt binder. At 3% SBS, the local SBS networks begin to form which can enforce the asphalt binder. At 5% SBS, the local networks begin to interact forming a critical network that leads to a sharp increase in the complex modulus. Based on these studies above, with the little dosage of SBS polymer's incorporation, both the performance and temperature range will improve.

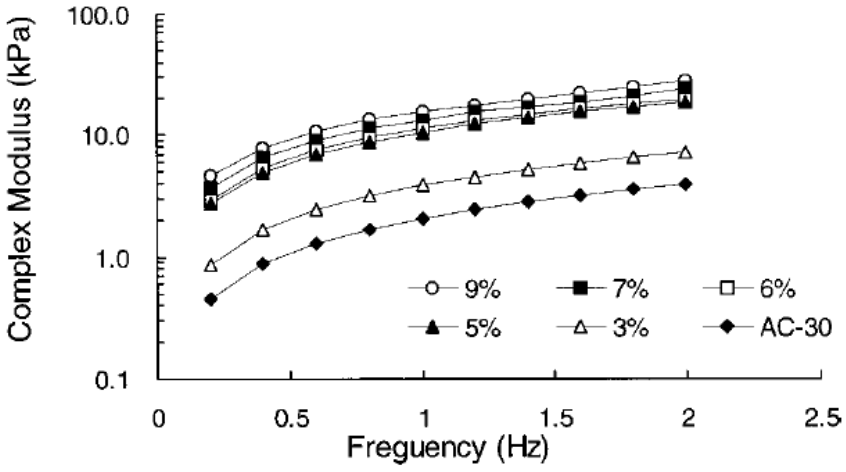

Figure 14. Complex modulus of styrene-butadiene-styrene-modified asphalt at 60°C (Chen et al. 2002)

The compatibility and storage stability of styrene-butadiene-styrene copolymer modified asphalt

As mentioned in previous section "The components of Asphalt", asphalt is a heterogeneous material which consists of immiscible of asphaltenes and maltenes. Asphaltenes are polyatomic hydrocarbons of relatively high molecular weight; maltenes are a mixture of saturates, aromatics, and resins (Browarzik et al. 1999; Murgich et al. 1996). The asphaltenes and maltenes are different in both amount and composition. The maltenes are the lightest components which contain the low molecular weight components, whereas the asphaltenes are the heaviest components of asphalt binder matrix which are the dispersed phase with solid particles of high molecular weight (Alonso et al. 2010). Because the molecular weights of the polymeric chains are higher than or similar to those of the asphaltenes. If there is an imbalance between the components, a phase separation may happen when the polymer chains compete for the solvency of the maltenes fraction. A phase separation means incompatibility between the asphalt and polymer (Fernandes et al. 2008).

Compatibility can be defined as the state of dispersion between two dissimilar components. Good PMBs compatibility can be achieved by carefully selection of its two components. Low compatibility may result in poor storage stability, which in turn leads to separation of polymeric and bituminous phases and inconsistent binder quality (Lu and Isacsson 1997). In most cases, compatibility is influenced concurrently by various factors such as bitumen composition, polymer chain architecture, the molecular weight distribution, polymer content and also mixing process (Lu and Isacsson 1997; Lu and Isacsson 2000).

Lu and Isacsson (1997) found out, at a given polymer content, better compatibility and higher storage stability can be obtained when the modified binders produced from bitumen with higher content of aromatics. Moreover, the storage stability of modified binders decreased with increasing SBS content. Furthermore, in the investigation, they compared the degree of dispersion between branched SBS polymer and linear SBS polymer. Because the degree of SBS dispersion in asphalt binders would influence storage stability and the rheological properties of modified asphalt binders. As results, Linear SBS displayed a finer dispersion in modified asphalt binder and a lower phase separation was observed during hot storage compared to branched SBS polymer (Lu and Isacsson 1997). According to Masson et al. (2003), lower stability of branched polymeric structure SBS in asphalt binders was not because of its chain structure but its high molecular weight. Since liner SBS polymers owes molecular weights between 1300,000 to

170,000 daltons and branched SBS polymers have molecular weights between 210,000 to 350,000 daltons (Williams et al. 2014).

High demand for butadiene market (Romagosa 2008)

Since 2008, there is a shortage of styrene-butadiene polymers for asphalt industry. The shortage includes linear SBS polymers, radial SBS polymers, and diblock SB etc. The reason why there is a shortage of SBS polymer is because of the shortage of butadiene. Butadiene is not produced on purpose, it is a by-product of the production of ethylene. Styrene and butadiene are two basic monomers for SBS polymer which are both obtained as by-product from ethylene production. Ethylene is made through a steam cracking process which is one of the many resulting products. The ethylene production process is shown in Figure 15. The raw materials for these crackers can either feed gas like ethane, butane and propane or can feed liquid petroleum product such as gas, oil or naphtha. As shown in Figure 15, butadiene and other chemicals beneath it are produced only as a by-product of cracking liquid feeds. Economically, ethane as gas feed raw material is less costly than liquid feeds. In May 2008, the cost to produce a pound of ethylene using ethane feed was $0.20 cheaper compared to naphtha feed per pound. As a result, cracker operators are running more gas feed and producing less butadiene. Butadiene production in 2008 is projected to be approximately 70-75% of 2007 production. Basic on the fact of above, the Association of Modified Asphalt Producers (AMAP) suggested (Romagosa 2008) “prudent planners should be working on the basis that availability of SBS polymers will remain tight for the immediate future.”

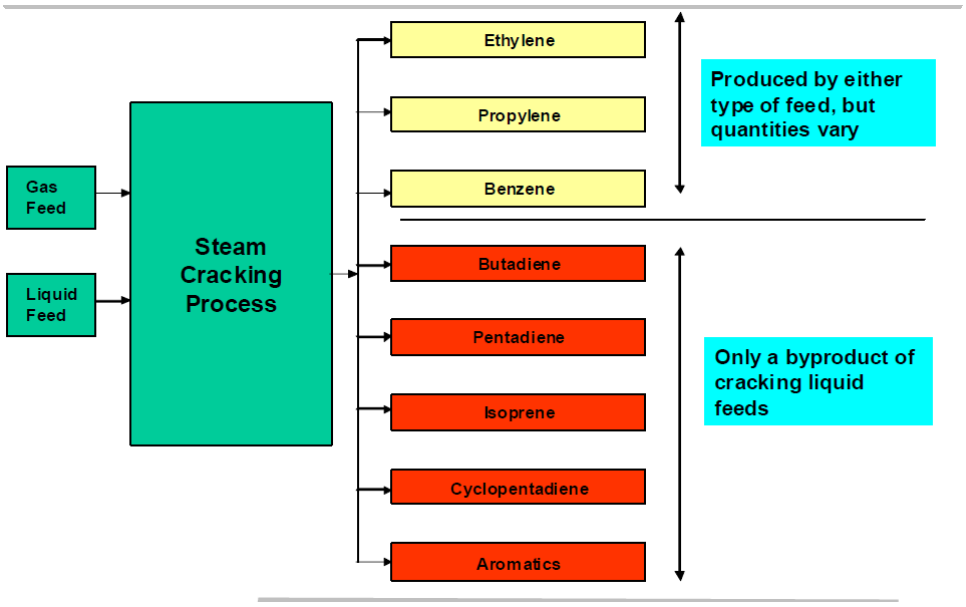

Figure 15. Ethylene production process (Romagosa 2008)

As the structure of SBS copolymer shown in Figure 11, the styrene composition is about 10-30 wt% of the spherical styrene domains compared to the matrix of butadiene domains. The glass transition temperature of polystyrene is at around 100°C (Tg =100°C). The polybutadiene (Tg< -90°C) matrix will be liquid when temperature is below the glass transition temperature (Tg =100°C) of polystyrene. However, the glassy state polystyrene will serve as physical crosslinks that bounds the liquid polybutadiene in middle. Because the glass transition temperature of polybutadiene is pretty low at around -90°C, when the temperature is above the glass transition temperature of polystyrene, the entire SBS or SB elastomer will melt or in the rubbery state, where they are soft, flexible, pliable and easy to process (Williams et al. 2014). Polybutadiene has a Tg of -90°C while as reported cross-linked poly (soybean oil) has Tg value of -56°C (Yang et al. 2010). Therefore, based on styrenic block copolymers, the poly (soybean oil) could be an ideal candidate to serve as the liquid component in thermoplastic elastomers (Williams et al. 2014).

Polymers Synthesized from Vegetable Oils

Definition

Biopolymers are made from natural renewable resources which are completely biodegradable, and nontoxic as alternatives to petroleum-based polymers (Lukkassen and Meidell 2011).

Vegetable oils are renewable sources. For industrial purpose, they primarily originate from five basic crops: soybean, oil palm, rapeseed, sunflower, and coconut (Cuperus and Derksen 1996). The world supply of vegetable oils mainly from ten major countries: USA, Brazil, China, India, Canada, Europe, Africa, Australia, New Zealand, and Japan (Baumann et al. 1988). The makeup of vegetable oils is usually triglycerides from three fatty acids (FAs) that are connected with a glycerol as shown in Figure 16 (La Scala and Wool 2005).

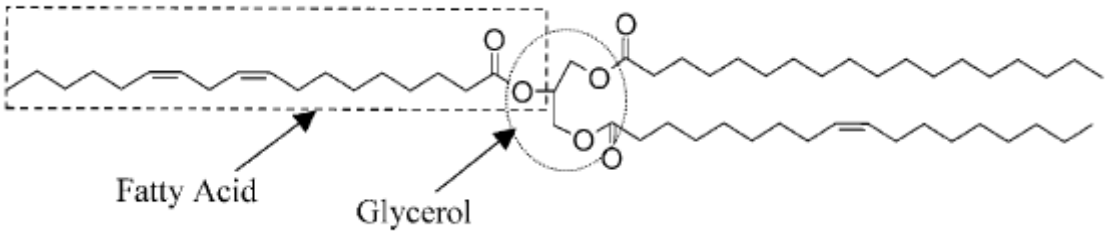

Figure 16. The molecular structure of a typical triglyceride molecule. Three fatty acids are connected to a glycerol center (Scala and Wool 2005)

Researchers are very interested in the new crops that contain a higher percentage of desirable fatty acid (FA) or a lower percentage of undesirable fatty acids (FA), and those owe a unique fatty acid (FA) (Cuperus and Derksen 1996). A list of common FA is shown in Table 3.

Table 3. Common fatty acids found in common vegetable oils (Hernández et al. 2015)

Fatty Acid	Formula	Structure	Occurrence
Oleic	$C_{18}H_{34}O_2$	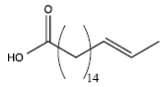	olive oil, pecan oil, canola oil, peanut oil, macadamia nut oil, sesame oil
Linoleic	$C_{18}H_{32}O_2$	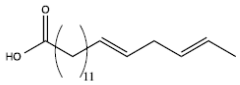	safflower oil, sunflower oil, soybean oil, cottonseed oil
α-Linolenic	$C_{18}H_{30}O_2$	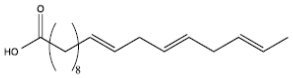	linseed oil and in lower levels in many other seed oils
α-Eleostearic	$C_{18}H_{34}O_3$	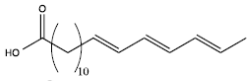	tung oil, bitter gourd seed oil
Ricinoleic	$C_{18}H_{34}O_3$	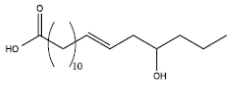	castor oil
Stearic	$C_{18}H_{36}O_2$	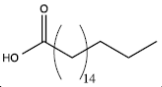	plant fats

Functionalization of the fatty acyl chain in FAs via epoxidation can be used to produce components of bioadvantaged polymers such as epoxy resins, polyurethanes or polyesters (Rus

2010). The molecular structure of FAs in vegetable oils provides quite a number of reactive sites for functionalization which including the double bond, the allylic carbons, the ester group, and the carbon alpha to the ester group, as shown in Figure 17(Bunker and Wool 2002).

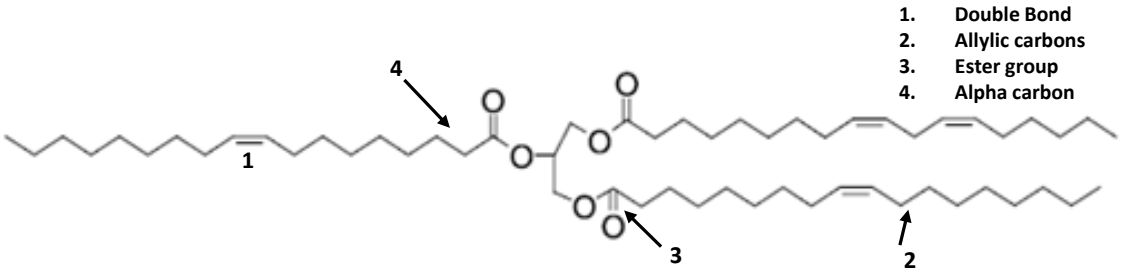

Figure 17. Diagram of a triglyceride molecule with different functionalities (Bunker and Wool 2002)

Vegetable oils as renewable raw materials are excellent for polymerizing to thermosetting polymers. Because the presence of multiple C=C bonds makes these natural resources become useful polymeric materials and have opportunities for monomer modification and polymerization. In other words, the C=C double bonds in triglycerides makes it possible to attach some functional groups via chemical modification and pathways to functionalize triglycerides and FA (Galià et al. 2010). For converting to industrial useful plastics, there are three methods: FA C=C bond functionalization, subsequent copolymerization, and direct copolymerization of the FA C=C bonds with a variety of alkene comonomers (Andjelkovic et al. 2005).

However, not all vegetable oils are suitable for use in polymerization. For those unmodified vegetable oils that contain mostly isolated C=C double bonds possess low reactivities which make them unsuitable for polymerization, such as soybean oil, peanut oil, sunflower oil, and canola oil. Whereas, thermal or cationic polymerization can be used on vegetable oils with higher reactivities which contain naturally occurring conjugated C=C double bonds like tung oil or bitter gourd seed oil (Li and Larock 2003; Galià et al. 2010). Thus, besides directing polymerization of C=C double bonds, considerable efforts have been devoted to modify C=C double bonds into more reactive functional groups that could be helpful and efficient to further the polymerization of triglycerides (Galià et al. 2010).

In 1960s, Nevin (1966) firstly invented the acrylation of vegetable oils, which made the oils very susceptible to chain growth polymerization (Nevin 1966). In the early 1990s, Crivello and Narayan (1992) utilized the photoinitiators like triarylsulfonium salt that made monomers mainly

soybean oils (SBO) rapidly and efficiently photopolymerized cationically. The main polymerization they conducted was the cationic photopolymerization of epoxidized oils, which gave the results of good adhesion and mechanical properties with vegetable oils contained both unsaturated oils and naturally epoxidized oils that can be polymerized directly (Crivello and Narayan 1992).

Since 1997, Wool et al. (2000) has been working on synthesis and application of liquid resins derived mainly from plant triglycerides as raw material to get high modulus thermosetting polymers which were suitable for using alone or as matrix polymer in fiber reinforced composites. The synthesis was using soybean-triglycerides with suitable comonomers and reactants that functionalized and render the plant triglyceride polymerized. The free radical initiated addition, condensation or ring opening polymerization were the major polymerization reactions involved. The functionalization of triglycerides was used in conjunction with reactive diluents, accelerators, viscosity modifiers, cross-linking, toughening, and coupling agents. The liquid resins were mixed with initiators, catalyst, the reinforcing fibers, and chain extended or cross-linked to give the final cured composite (Wool et al. 2000).

In 1998, Petrovic et al. (2000) successfully converted the C=C double bonds of soybean oil into polyols by epoxidizing the C=C bonds of the triglyceride oil, followed by oxirane ring-opening of the epoxidized oil (Guo et al. 2002; Guo et al. 2000). In order to follow the demands for pressure sensitive adhesive (PSA), Bunker et al. (2003) was using miniemulsion polymerization to synthesize these adhesive by renewable resource (eg. plant oils) as monomers. Their resulting polymer has shown physical properties comparable to petroleum based polymers. Moreover, the polymers derived from a renewable resource display typical PSA properties (Bunker et al. 2003).

Andjelkovic et al. (2006) utilized the cationic copolymerization of different soybean oils (SBO) and alkenes in the presence of a modified boron trifluoride diethyl etherate (BEF) as initiator to get a series of new polymeric materials ranging from elastomers to tough and rigid plastics. They found out soybean oil polymers possess a good combination of thermal and mechanical properties such as excellent damping and shape memory properties (Andjelkovic et al. 2006).

Bonnaillie and Wool (2007) implemented a pressurized carbon dioxide foaming process produced polymeric forms from acrylated epoxidized soybean oil (AESO). The AESO was cured

with a free-radical initiator. Cobalt naphtenate was used as an accelerator to promote quick foam cure at low temperature (40-50°C) (Bonnaillie and Wool 2007). Lately, bio-based polyols from epoxidized soybean oil (ESO) and castor oil fatty acid were developed by Zhang et al. (2013) using solvent-free/catalyst-free method which is a 100% bio-based content environmentally friendly method. (Zhang et al. 2013).

As illustrated previous synthetic methods above, there are numbers of examples of vegetable oils modification combined with thermal, cationic or free radical polymerization methods that have yielded thermoset plastics. However, triglyceride of vegetable oil cannot be used on its own without further modification. The FA must be suitably functionalized to add polymerisable functionalities which will be helpful in curing process. The purpose of these modification is to reach a higher level of molecular weight and cross-link density, and to incorporate chemical functionalities that impact stiffness in a polymer network as well, which also can become more comparable to other conventional liquid molding resin already available in market (Adekunle 2014).

Chemical functionalities of soybean oil (SBO)

Wool et al. (2000) have reported that there are various synthetic methods by which an epoxidized vegetable oil triglyceride can be suitable functionalized (Wool et al. 2000). The modifications were done with various reagents, as example of a vegetable crop that contains a long-chain FA, which makes the material more flexible, is epoxidized soybean oil (ESO) (Rus 2010). Soybean oil (SBO) is one of many readily available renewable resources. Currently, most soybean oil (SBO) is used for food applications. Refined soybean oil (SBO) is consisted of 99% triglycerides. These triglycerides are composed of eight different FA ranging in length from 14 to 22 carbons long (Lu et al. 2005), as shown in Figure 18(a). The average molecular weight of a triglyceride is approximately 871g/mol with an average functionality of 4.6 C=C double bonds per triglyceride (Pryde 1979). ESO is manufactured by epoxidation of C=C double bonds of soybean oil triglyceride with hydrogen peroxide, either in acetic or formic acid [Figure 18 (b)], and it is available industrially in large quantities at reasonable cost (Park et al. 2004). To introduce the acrylate functional group, the ESO is reacted with ethylenically substituted carboxylic acids, such as acrylic acid to form AESO [Figure 18 (c)] (Lu et al. 2005). Synthesis of acrylated epoxidized soybean oil (AESO) is shown in Figure 18. The resulting monomer is then copolymerized with styrene to form rigid polymers via controlled radical polymerization

techniques, such as atom transfer radical polymerization (ATRP) and reversible addition-fragmentation chain-transfer polymerization (RAFT).

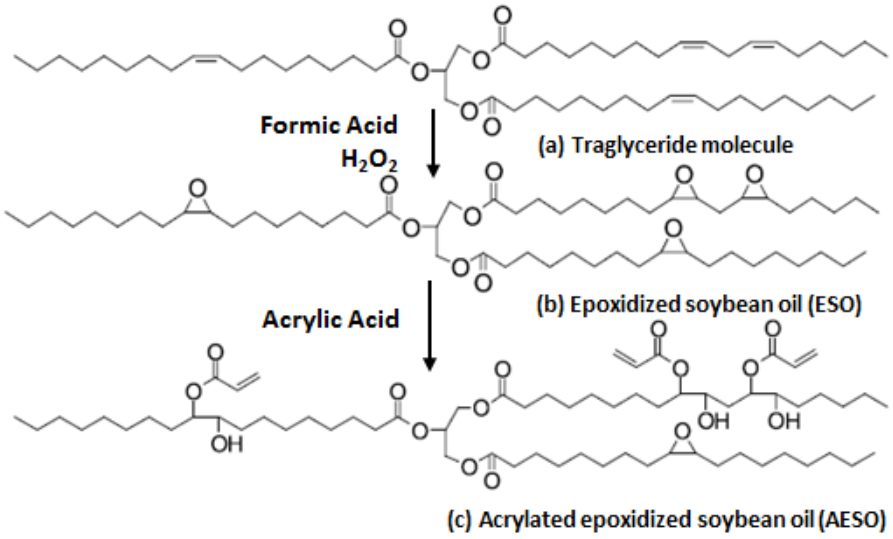

Figure 18. Synthesis of acrylated epoxidized soybean oil (AESO) from soybean oil (Lu et al. 2005)

Atom transfer radical polymerization (ATRP) (Matyjaszewski et al. 1997)

ATRP is one of the controlled (living) radical polymerizations via which could synthesize well-defined polymers with properties of low polydistersities and complex architectures. ATRP needs to have monomer, initiator, catalyst, counter catalyst, and ligand. An important participate in this polymerization is a copper(I) complex, CuX/2L (X=Cl or Br, and L=2,2'-bipyridine [bipy] or a 4,4'-disubstituted-2, 2'-bipyridine). The polymerization step contains CuX/2L is responsible for the controlled behavior of the polymerizations since CuX/2L activates reversibly the dormant polymer chain via a halogen atom transfer reaction. The mechanism of ATRP is shown in Figure 19.

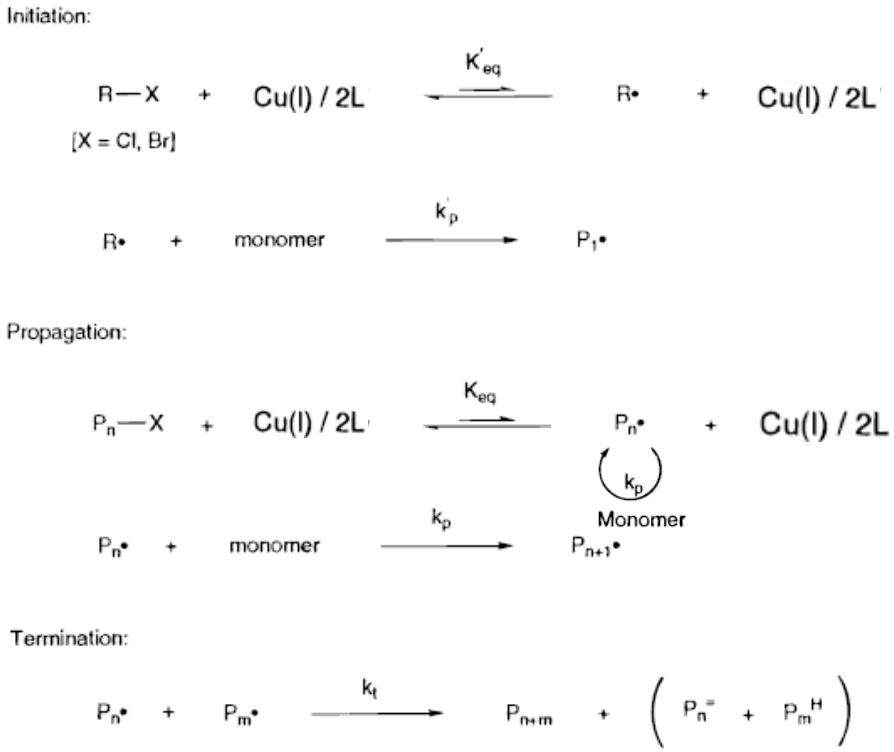

Figure 19. Mechanism of ATRP (Matyjaszewski et al. 1997)

Reversible addition-fragmentation chain transfer (RAFT)

RAFT was developed in Australia by G. Moad, E. Rizzardo and S.H. Tang from the Commonwealth Scientific and Industrial Research Organization and they first introduced the technique in 1998 (Moad et al. 2005, Hernández et al. 2015). The RAFT process can synthesis numbers of well-defined architectural polymers such as homo-, gradient, diblock, triblock, star polymers and more complex architectures like microgels and polymer brushes etc. (Moad et al. 2005, Hernández et al. 2015).

There are three major steps in the mechanism of RAFT which are initiation, propagation, and termination. The mechanism and sequences of RAFT polymerization is shown in Figure 20. The RAFT polymerization reaction starts with initiation. In the stage of initiation, it needs to add an agent who has the ability of decomposing to form free radical fragments from the initiator. After these free radical fragments attacks a monomer, the initiation will be accomplished by producing a propagating radical ($P^{\cdot}_n$). The additional monomers are added in initiation stage for producing a growing polymer chain. In the propagation step, the propagating radical ($P^{\cdot}_n$) adds to a chain transfer agent (CTA) like a thiocarbonylthio compound (RSC(Z)=S, 1) followed by fragmentation of the intermediate radical (2) forming a dormant polymer chain with a

thiocarbonylthio ending ($P_nS(Z)C=S$, 3) and a new radical ($R^{\cdot}$). This new radical ($R^{\cdot}$) will react with monomer forms a new propagating radical ($P^{\cdot}_m$). In the chain of propagation step, ($P^{\cdot}_n$) and ($P^{\cdot}_m$) reach equilibrium and the dormant polymer chain (3) offers an equal probability to all polymer chains to grow at the same rate and allows polymers to be synthesized with narrow polydispersity. The termination step is when the polymerization is completed or stopped, most chain retain the thiocarbonylthio end group and can isolated as stable materials (Moad et al. 2006; Williams et al. 2014, Hernández et al. 2015).

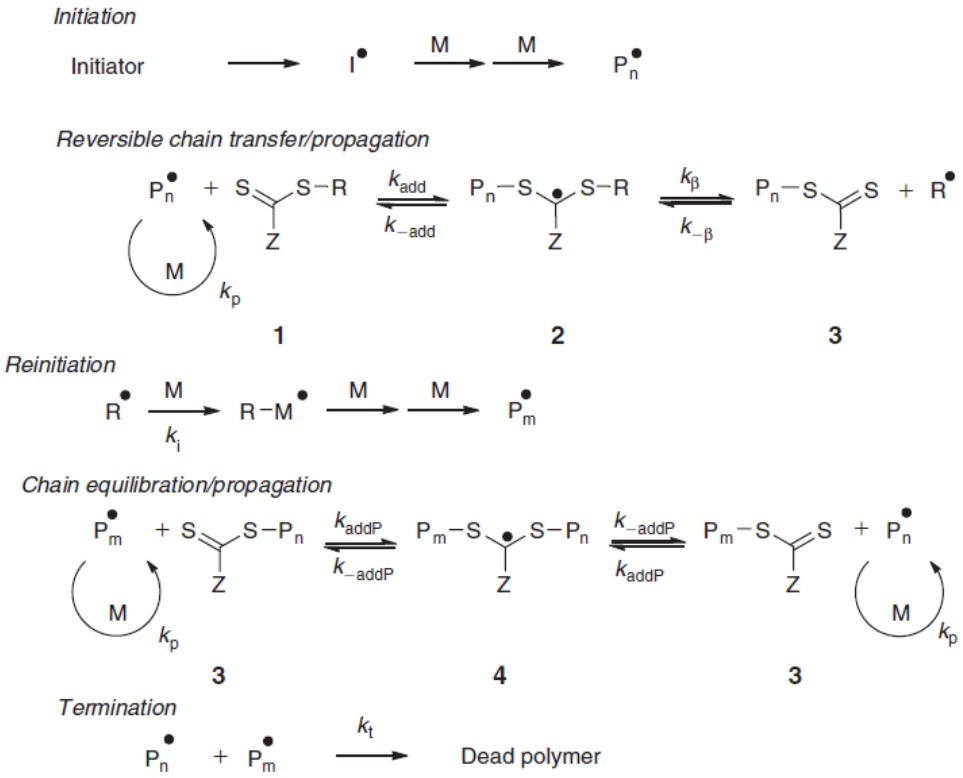

Figure 20. Mechanism of RAFT polymerization (Moad et al. 2006)

In order to form a thermoplastic block copolymer, such as triblock copolymers polystyrene-b-polyAESO-b-polystyrene (PS-PAESO-PS), a radically polymerizable triglyceride monomer (AESO) was polymerized with polystyrene via RAFT polymerization by using a free radical initiator and CTA (Williams et al. 2014). Hernández et al. (2015) reported, "The use of AESO (with different degrees of acrylation) instead of petroleum-based chemical butadiene as a renewable substitute of the "soft" phase in the production of tunable branched styrenic based TPEs via RAFT".

In order to evaluate the effective of bio-based polymer (PS-PAESO and PS-PAESO-PS) modification, asphalt modification tests were performed by the Civil Engineering Department at Iowa State University, research group led by Dr. Chris Williams. As results of Dr. Williams and coworkers, rheology test results showed the bio-based polymer (PS-PAESO and PS-PAESO-PS) has the ability to widen the grade range of asphalt and reduced its temperature susceptibility. Furthermore, they can also enhance the performance properties of asphalt binder especially for the improvement of rutting resistance for high temperature. Therefore, the biopolymers were effective in improving the high temperature performance, however, not as effective in retaining the low stiffness modulus of the base asphalt (Williams et al. 2014).

CHAPTER 3. EXPERIMENTAL PLAN AND TESTING METHODS

The experimental program of this study was designed to evaluate the rheological properties of base asphalt binder after blending with bio-based polymers (PS-PAESO and PS-PAESO-Cl) with a certain percentage (3%) of total weight. Furthermore, high temperature performance grade and low temperature performance grade were identified for each type of bio-based polymer modified asphalt blend. The methods used in this study were selected to demonstrate the following objectives:

- by conducting different laboratory blending methods at different temperatures to evaluate the high and low temperature performance of bio-based polymer asphalt blends;
- by conducting different laboratory blending methods at different temperatures to evaluate the effects of various bio-based polymers on asphalt blend rheological properties; and
- to compare the high temperature and low temperature performance of each bio-based polymer modified asphalt blend and the base asphalt binder.

To address the objectives of this study, primary laboratory tests for asphalt binder were conducted by performing dynamic shear rheometer (DSR), rolling thin-film oven test (RTFO), pressurized aging vessel (PAV), and bending beam rheometer (BBR). In this chapter, the experimental materials used, the experimental plans designed, and the specific laboratory test procedures will be illustrated as follows.

EXPERIMENTAL MATERIALS

In this study, the primary materials used were the base asphalt binder and bio-based polymers (PS-PAESO and PS-PAESO-Cl).

Asphalt binder

The asphalt binder used as the base asphalt in the experiment was a soft asphalt cement graded as PG XX-34 from Flint Hills Resources Pine Bend Refinery in Rosemount, MN (Figure 21).

Figure 21. Flint Hill XX-34 Asphalt Cement

AESO

AESO was purchased from Sigma-Aldrich Company and used as received (Figure 22).

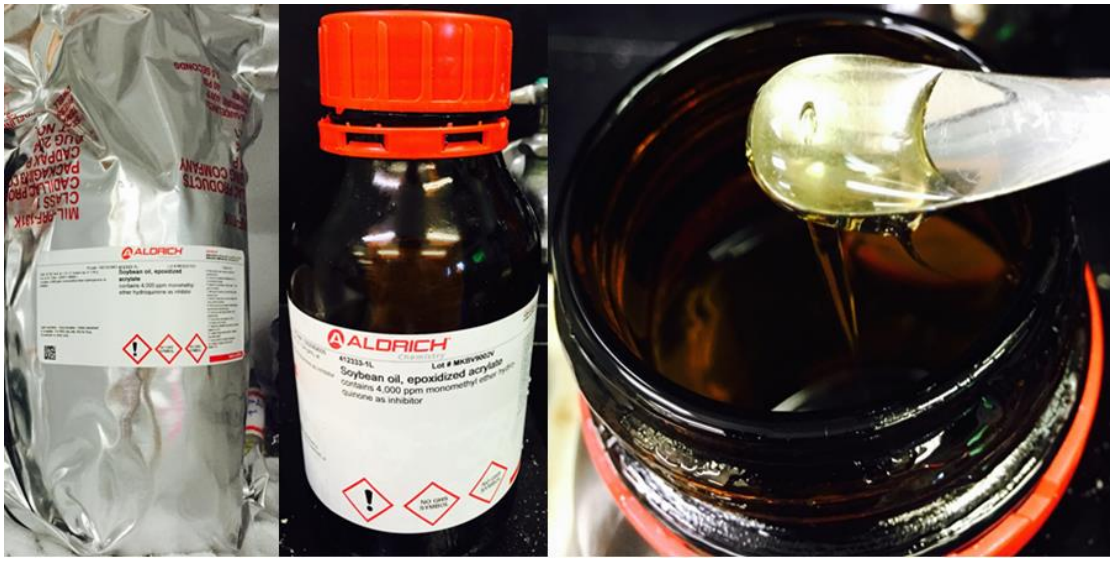

Figure 22. Sigma-Aldrich acrylated epoxidized soybean oil

Styrene

Styrene was purchased from Fisher Scientific and purified over basic aluminum cans (for pulling out inhibitors in styrene) followed by three freeze-pump-thaw cycles (Figure 23).

Figure 23. Purified styrene

Azobisisobutyronitrile (AIBN)

AIBN was crystalline and needle-like solids (Figure 24). In this study it was used as initiator in each polymerized reaction.

Figure 24. Azobisisobutyronitrile (AIBN)

Methylhydroquinone (MHQ)

MHQ was purchased from Sigma-Aldrich Company and used as received (Figure 25). It was used as inhibitor in each polymerized reaction in this study. Inhibitor in the polymer reaction was used as a stabilizer to prevent premature degradation.

Figure 25. Methylhydroquinone (MHQ)

Bio-based polymers synthesis

Synthesis of Styrene via Reversible Addition-Fragmentation Chain Transfer Polymerization (RAFT)

Monomer (styrene), initiator (AIBN), chain transfer agent (CTA) (EOBT or PPBD), and sufficient solvent were mixed in a 100mL round-bottomed flask (RBF) with different mass value ratio of initiator to CTA to monomer. The reaction flask was purged with argon for approximately 30 minutes to remove oxygen in RBF during the process before increasing reaction temperature. The reaction was run at 100°C. The reaction duration depended on the molecular weight needed. Final product of PS with EOBT as CTA is shown in Figure 26.

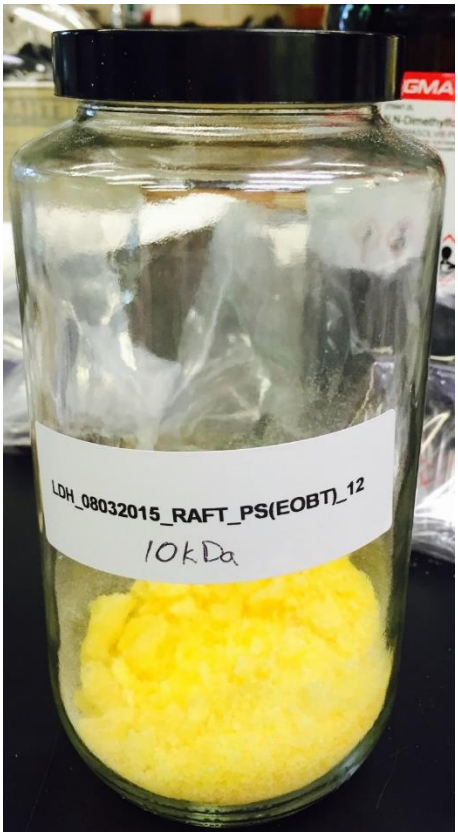

Figure 26. PS with EOBT as CTA

Synthesis of Poly (Acrylated Epoxidized Soybean Oil) (PAESO) via RAFT

Monomer (AESO), initiator (AIBN), chain transfer agent (CTA) (EOBT and PPBD), and sufficient solvent were mixed in a 100mL round-bottomed flask (RBF) with different mass value ratio of initiator to CTA to monomer. The reaction flask was purged with argon for approximately 30 to 60 minutes to remove oxygen in RBF during the process before increasing reaction temperature. The reaction was run at 70°C. The reaction duration depended on the molecular weight needed.

Synthesis of Poly (Styrene-B-AESO) via RAFT

AESO monomer was dissolved in solvent (Toluene, Dioxane, Tetrahydrofuran [THF], or Methyltetrahydrofuran [MeTHF]) in RBF. Polystyrene (PS) was added to RBF, and then dissolved initiator (AIBN) was added to RBF. Stir blending the mixture in water bath until PS dissolved [Figure 27 (a)]. The reaction flask was purged with argon for approximately 20 minutes to remove oxygen in RBF during the process before increasing reaction temperature [Figure 27 (b)]. The reaction was run at around 75°C for five to six hours. The product was cooled down to room temperature and coagulated in excess methanol or water. The product was

stirred in mixed solution of methanol and ethanol to remove unreacted AESO monomer. Then the product was dissolved in dioxane, and the inhibitor (MHQ) was added by one or two percent of total weight into the dissolved solution. The final product was vacuum dried, or air dried, or schlenk line dried for 24 hours at room temperature. The PS-PAESO diblock polymer before and after drying is shown in Figure 28. Final well-ground product of PS-PAESO with EOBT and PPBD as CTA is shown in Figure 29.

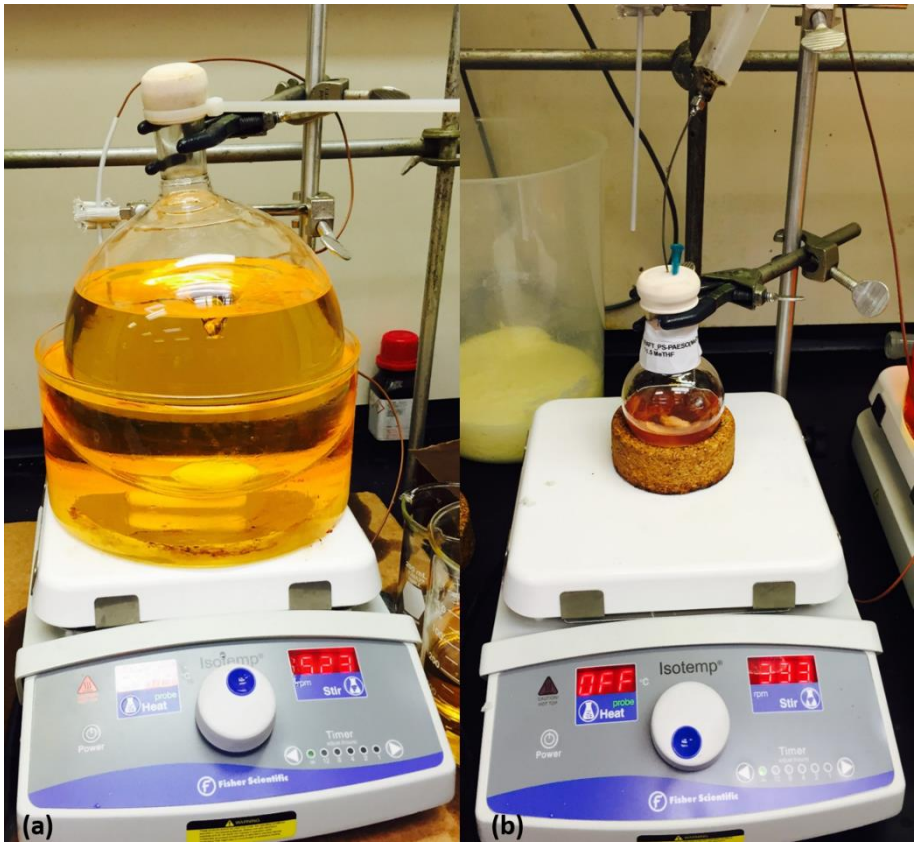

Figure 27. (a) Stirred blending and (b) purging under argon

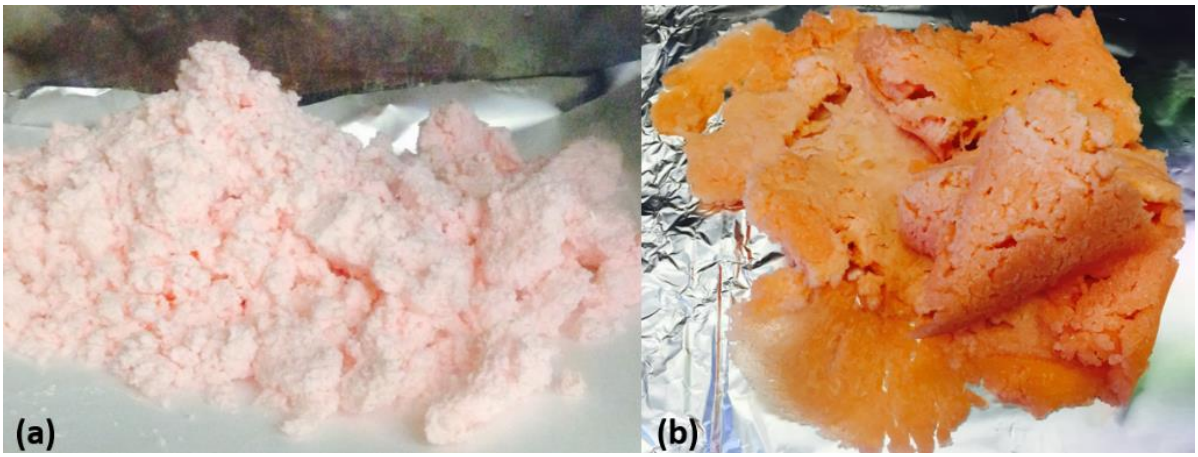

Figure 28. PS-PAESO diblock polymer (a) before drying and (b) after drying

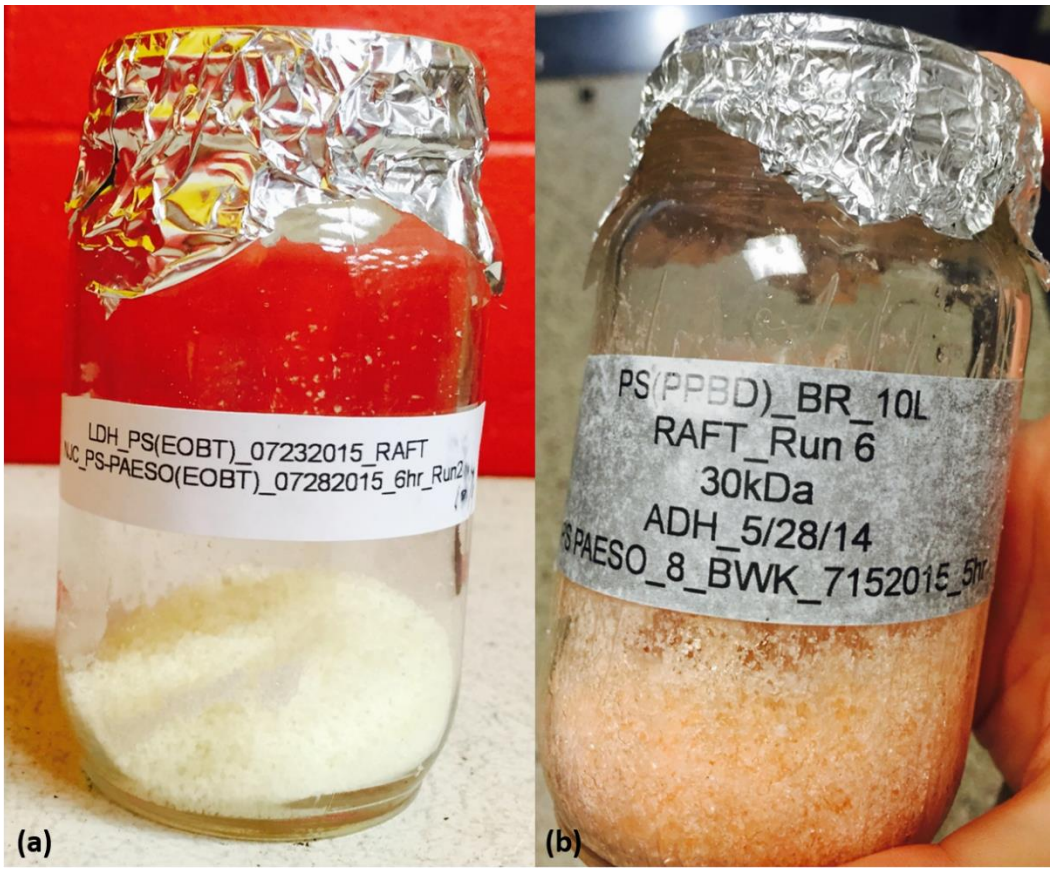

Figure 29. PS-PAESO with CTA of (a) EOBT and (b) PPBD

Synthesis of Poly (Styrene-B-AESO-B-Chloride) via ATRP

The poly (styrene-b-AESO) diblock was used as monomer, and the monomer was reacted with initiator [benzyl chloride (BCl)], catalyst [cooper(I) chloride(Cu_ICl)], counter catalyst [cooper(II) chloride ($Cu_{II}Cl$)], and ligand [*N*,*N*,*N*′,*N*′,*N*′′-pentamethyldiethylenetriamine (PMDTA)]. Final well-ground product of PS-PAESO-Cl is shown in Figure 30.

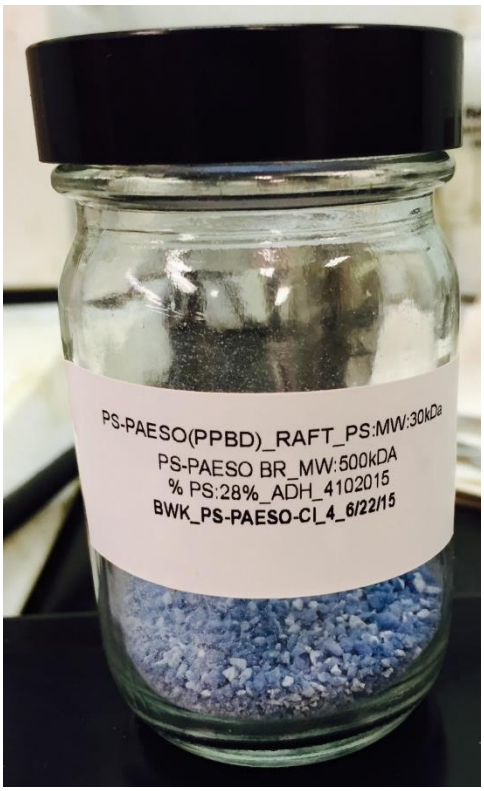

Figure 30. Well-ground PS-PAESO-Cl

EXPERIMENTAL PLAN AND TESTING METHODS

The bio-based polymers (PS-PAESO and PS-PAESO-Cl) used in this study were made with different target styrene molecular weights and styrene contents of PS-PAESO and PS- PAESO-Cl with various polymer reaction durations. The bio-based polymer making plans with corresponding asphalt blend codes were tabulated and summarized in Table 4 and Table 5.

Table 4. The bio-based polymer making plan with corresponding asphalt blend codes for Solvent Blending

Solvent Blending				
Styrene Content,%	**Styrene Molecular Weight, kDa**			**Reaction duration, hr**
	15	30	45	8
20	Blend A	Blend F	Blend K	
25	Blend B	Blend G	Blend L	
30	Blend C	Blend H	Blend M	
35	Blend D	Blend I	Blend N	
40	Blend E	Blend J	Blend O	

Table 5. The bio-based polymer making plan with corresponding asphalt blend codes for Shear Blending

Shear Blending				
Styrene Content,%	**Styrene Molecular Weight, kDa**			**Reaction Length, hr**
	10	20	30	
30	–	–	Blend 21	4
30			Blend 14	5
30			Blend 4	6
20	Blend 13		–	8
25	Blend 25,Blend 27	Blend 26	Blend1,Blend2,Blend3, Blend 11, Blend 12, Blend 8	
30	Blend 18,Blend 23, Blend 24	–	Blend 9,Blend 15	
35	Blend 28		–	
40	–		Blend 6,Blend 10	
30			Blend 17	9
30			Blend 19	10
30			Blend 16	11
30			Blend 20	12

Note: Blend 1, blend 2, and blend 3 were used shear blending method A (shear blended at 180°C for 3hr); blend 8, blend 6, and blend 10 were used shear blending method C (shear blended at 120°C for 30min and increased temperature to 195°C for another 90min); the rest of blends were used shear blending method B (shear blended at 190°C for 3hr).

Rheology is the primary factor that can be helpful to predict the future performance of modified asphalt binder using in pavements. Therefore, the experimental plans were designed to determine the rheological properties of asphalt blends with different bio-based polymers by different blending methods. Thirty different bio-based polymers were blended with base asphalt, 15 out of the 30 were shear blended and the other 15 were solvent blended both with a dosage of 3% of total weight (asphalt binder weight + polymer weight). Table 6 shows the corresponding

testing codes and each bio-based polymer name. Furthermore, the polymer basic properties such as molecular weight, polydispersity, polystyrene content etc. were concerned as well, which can be the major factors influence the modified properties of the base modified asphalt binder. The specific experimental plan of both modified asphalt binder and bio-based polymers and the test methods are shown in Figure 31 and discussed in detail hereafter.

Table 6. Experimental blends' codes with corresponding bio-based polymer names

Blending Method	Blend Code	Bio-based Polymer Name
Solvent blending	A	PS_MW:15kDa_Content:20%
	B	PS_MW:15kDa_Content:25%
	C	PS_MW:15kDa_Content:30%
	D	PS_MW:15kDa_Content:35%
	E	PS_MW:15kDa_Content:40%
	F	PS_MW:30kDa_Content:20%
	G	PS_MW:30kDa_Content:25%
	H	PS_MW:30kDa_Content:30%
	I	PS_MW:30kDa_Content:35%
	J	PS_MW:30kDa_Content:40%
	K	PS_MW:45kDa_Content:20%
	L	PS_MW:45kDa_Content:25%
	M	PS_MW:45kDa_Content:30%
	N	PS_MW:45kDa_Content:35%
	O	PS_MW:45kDa_Content:40%
Control Group (no blending)	0	Base asphalt binder PG XX-34
Shear Blending at 180°C for 3hr	1	PS_MW:30kDa_Content:25% PS-PAESO-Cl (crashed in methanol, coagulated with H2O) w/o MHQ_8hr
	2	PS_MW:30kDa_Content:25% PS-PAESO-Cl (crashed with H2O) w/o MHQ_8hr
	3	PS(PPBD)_MW:30kDa_Content:25% PS-PAESO-Cl w/o MHQ_8hr
Shear Blending at 120°C (30min) and 195°C (90min)	5	Reserved
	6	PS_MW:30kDa_Content40% PS-PAESO_MHQ:1%_8hr
	8	PS_MW:30kDa_Content:28% PS-PAESO-Cl_ w/o MHQ_8hr
	10	PS_MW:30kDa_Content:40% PS-PAESO_MHQ:1%_8hr
Shear Blending at 190°C for 3hr	4	PS_MW:30kDa_Content:30% PS-PAESO_MHQ:2%_6hr
	7	Base asphalt processed in shear mill w/o polymer

Blending Method	Blend Code	Bio-based Polymer Name
	9	PS(PPBD)_MW:30kDa_Content:30% PS-PAESO_MHQ:2%_8hr
	10	PS_MW:30kDa_Content:40% PS-PAESO_MHQ:1%_8hr
	11	PS_MW:30kDa_Contents:25% PS-PAESO_MHQ:2%_8hr
	12	PS_MW:30kDa_Content:25% PS-PAESO-Cl_MHQ:2%_8hr
	13	PS(EOBT)_MW:10kDa_Content:20% PS-PAESO(EOBT)_MHQ:2%_8hr
	14	PS(PPBD)_MW:30kDa_Content:30% PS-PAESO_MHQ2%_5hr
	15	PS(EOBT)_ MW:30kDa_Content:30% PS-PAESO_MHQ:1.2%_8hr
	16	PS(PPBD)_ MW:30kDa_Content:30% PS-PAESO_MHQ:2%_11hr
	17	PS(PPBD)_MW:30kDa_Content:30% PS-PAESO_MHQ:2%_9hr
	18	PS(EOBT)_MW:10kDa_Content:30% PS-PAESO_MHQ:2%_8hr
	19	PS(PPBD)_MW:30kDa_Content:30% PS-PAESO_MHQ:2%_10hr
	20	PS_MW:30kDa_Content:30% PS-PAESO_MHQ:2%_12hr
	21	PS(EOBT)_MW:30kDa_Content:30% PS-PAESO_MHQ:2%_4hr
	22	Reserved
	23	PS(EOBT)_MW:10kDa_Content:30% PS-PAESO_MHQ:2%_8hr
	24	PS(EOBT)_MW:10kDa_Content:30% PS-PAESO_MHQ:2%_8hr
	25	PS(EOBT)_MW:10kDa_Content:25% PS-PAESO_MHQ:2%_8hr
	26	PS(EOBT)_MW:20kDa_Content:25% PS-PAESO_MHQ:2%_8hr
	27	PS(EOBT)_MW:10kDa_Content:25% PS-PAESO_MHQ:2%_8hr
	28	PS(EOBT)_MW:10kDa_Content:35% PS-PAESO_MHQ:2%_8hr

Note: PS indicates poly styrene; PAESO indicated poly acrylated epoxidized soybean oil; PPBD and EOBT are two different CTA; MW indicates molecular weight; Content indicates the percentage of PS in total polymer; MHQ is the inhibitor used in polymer reactions.

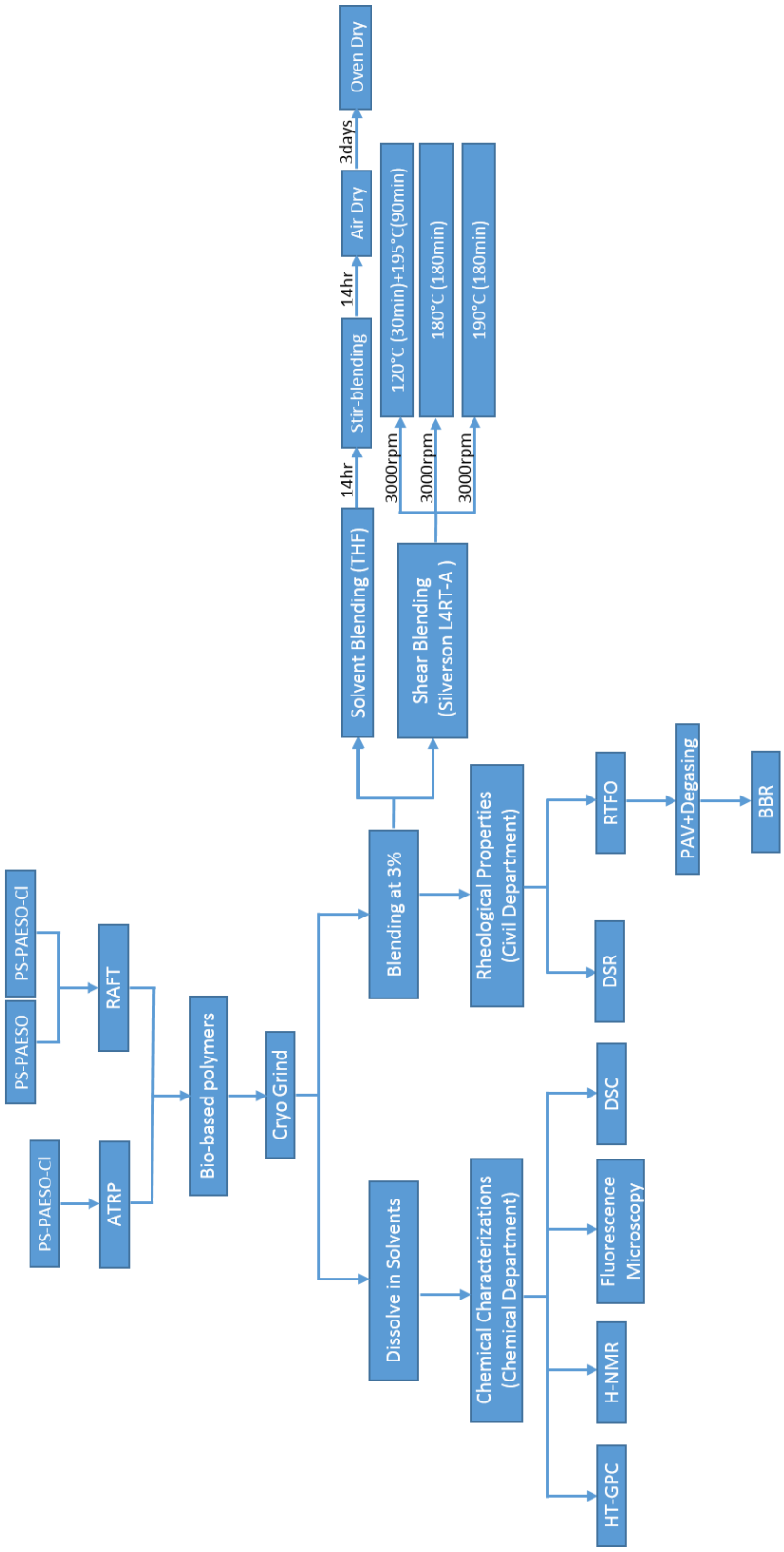

Figure 31. Experimental plan and testing methods

Bio-based polymer testing plan

The production and testing for the characteristics of bio-based polymers were conducted by researchers in the department of Chemical & Biological Engineering at Iowa State University. The tests performed and purposes are discussed as follows:

High temperature gel permeation chromatography (HT-GPC)

HT-GPC is a very commonly-used and important device in polymer industry. The advantage of HT-GPC is that it is a major way to measure not only molecular weight but the molecular weight distribution. The broadness of the distribution is related to the basic properties of polymer such as strength, toughness, brittleness, melt viscosity, chemical resistance and solubility. As a result, the HT-GPC provides key information to predict the processability and material properties of a polymer (Agilent Technologies 2015). The HT-GPC used in this study is shown in Figure 32.

Figure 32. High temperature gel permeation chromatography (HT-GPC)

Hydrogen nuclear magnetic resonance (H-NMR)

H-NMR is the most powerful and useful tool available for the structure determination of molecule. H-NMR was used to study the percentage of polystyrene on the diblock and triblock. From the results spectrum graph, each integral rise can be assigned to a particular number of hydrogens in molecule. These picks are helpful to confirm the amount of styrene has been reacted (Wade 2003, Softic et al. 2014).

Fluorescence microscopy

Compared to conventional microscope, a fluorescence microscope uses a much higher intensity light to illuminate the sample. This light excites fluorescence species in the sample, which emits lower energy light of a longer wavelength. The most significant feature of a florescent microscope is that the fluorescing areas can be observed in the microscope and shine out against a dark background with high contrast, in other words, it produces magnified images of the sample (Tripathy 2004). In this study, the fluorescence microscopy (Leica DFC7000 T) was used to determine the dispersion of polymer added within asphalt blends and the compatibility between polymer and asphalt binder after blending. The fluorescence microscopy (Leica DFC7000 T) and microscopy slides of samples are shown in Figure 33.

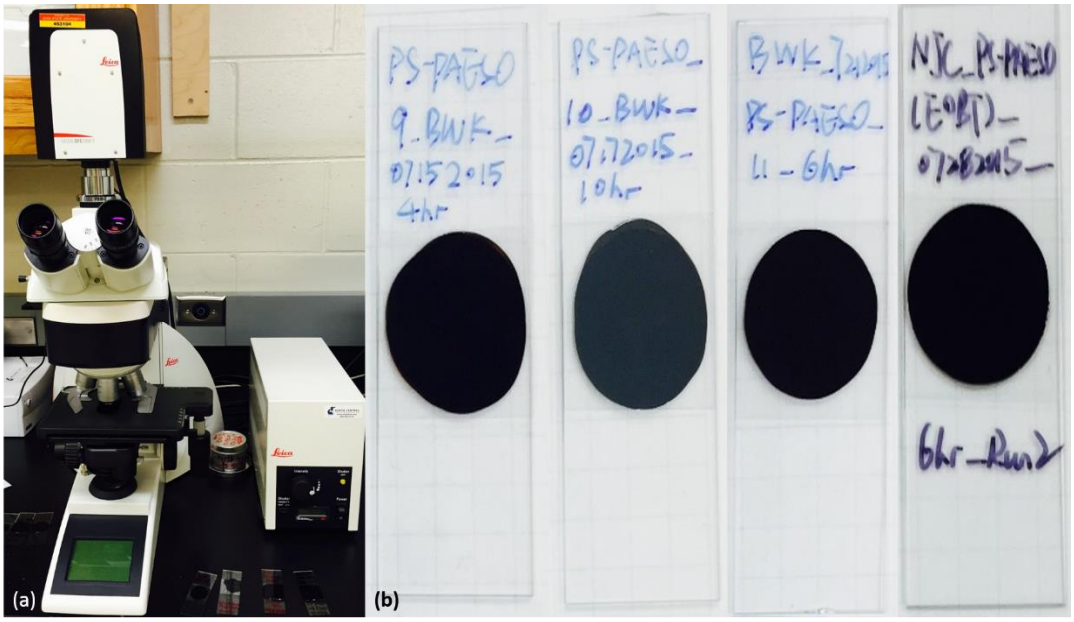

Figure 33. (a) Fluorescence microscopy (Leica DFC7000 T) and (b) microscopy slides of samples

Differential scanning calorimetry (DSC)

DSC is for determining thermal characteristics of polymers. Thermal characteristics such as melting point, melting range, heat capacity, crystallization, glass transition temperatures, thermal stability and decomposition temperatures can all be tested by DSC. In this study, DSC was mainly used to determine a first-order transition (melting) temperature and a second-order endothermic transition (glass transition) temperature. DSC used in this study was a reaction calorimetry (Mettler Toledo – RC1e), which is shown in Figure 34.

Figure 34. Reaction calorimetry (Mettler Toledo – RC1e)

Blending approaches designing plan

The approaches of blending polymers with the base asphalt binder has significant effects on the compatibility of asphalt blends. Moreover, the blending temperature, rotation rate, and duration have effects on the chain branching, crosslinking degree and architecture of the polymer in asphalt, which results in different rheology properties of asphalt blends. In order to investigate the most desirable blending design for improving rheology properties of asphalt blends, variety of different blending designs have been conducted including a low temperature solvent blending approach and other three high temperature shear blending approach.

During the processes of these blending approaches, there was a crucial step for polymers to achieve better blending compatibility, which was represented as cryo grinding. Cryo grinding was a procedure to make polymer to be small particles and to be easier for blending with the base

asphalt binder. Once the PS-PAESO polymer was dry enough and ready for blending, it was a big chunk of polymer (Figure 35), which was difficult and inconvenient to thoroughly blend with the base asphalt binder.

Figure 35. Well-dried PS-PAESO polymer

Cryo grinding of polymer processed with consistent argon supply, which was for avoiding water and oxygen in the air to reach polymers [Figure 36 (a)]. Furthermore, liquid nitrogen [Figure 36 (b)] was used on polymer to freeze it and make it brittle and fragile for easily grinding [Figure 36 (c)]. Figure 37 shows the polymer conditions before and after grinding.

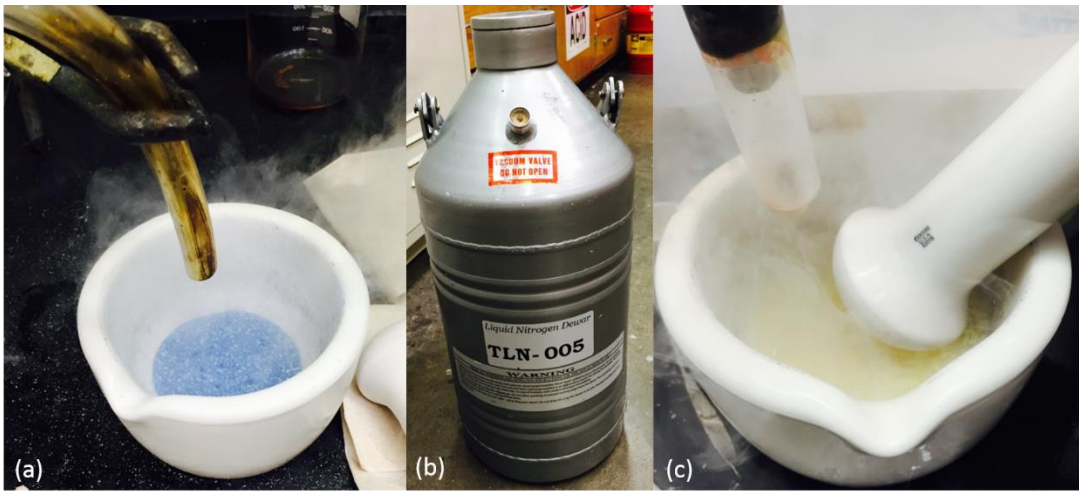

Figure 36. Cryo grinding of polymer with (a) consistent argon, (b) liquid nitrogen, and (c) grinding process

Figure 37. PS-PAESO polymer (a) before and (b) after grinding

The entire blending procedurals are discussed as follows:

Solvent blending (low temperature blending)

The purpose of solvent blending was to blend polymer into asphalt binder without using temperatures higher than 110°C. There were three major steps in solvent blending which were stir-blending, air dry, and oven dry.

Stir-blending was blending using a stir with certain blending rotation rate. The appearance of a vertex is helpful to mix the blends to be homogenous. The practical procedures in this study are described as follows:

- Identified the base asphalt binder weight and heated it up to thorough flow condition and poured a certain amount of it into a beaker;
- Identified the amount of polymer that needs to be added to base asphalt binder and calculated the polymer weight needed for modification which was always as 3% of the total blends weight in this study;
- Solvent [Tetrahydrofuran (THF)] was then added to the base asphalt binder as the weight ratio of 1.0:1.0 and poured the solvent to the same beaker;
- Got polymers cryo ground (with constant argon and liquid nitrogen when grounding) and dropped the polymer into the asphalt-solvent mixture, and then put the beaker on a stir plate and put a stir bar in the mixture for blending;
- A piece of tin foil sheet was placed on the top of beaker to cover samples and ensure solvent cannot evaporate during stir-blending; and
- A vertex presented when stir-blending at the rate of around 1500rpm and stir-blend should keep going for approximate 14 hours.

Air drying aims at using air blows off enough THF so that the blends samples cannot splash while in the oven dry step. The practical procedures in this study are described as follows:

- After stir-blending for around 14 hours, the well-blended mixtures (asphalt/solvent/polymer) was poured into an aluminum foil tray; and
- Put the tray on the experimental hood with the compressed air that can blow over the mixture for drying for approximate 14 hours.

Oven drying is to remove all of the THF from the sample at the temperature below 110°C. The practical procedures in this study are described as follows:

- Preheated the oven to 110°C; and
- Placed the tray into the oven when reheated to proper temperature and oven dry it for 3 days.

Shear blending (high temperature blending)

Mechanical mixers are often used to mix dry powder materials or combined easily-mixed solutions or to solve a solid material in a solution. The device is designed to have a constant motor rotation rate. The required time of mixing depends on the type of materials and the operator's option as along as a homogenized mixture is obtained (Hasan et al. 2012).

High shear mixers are of the most applicable mixers which are used in mixing asphalt and polymers. The high shear mixers used in this study for asphalt-polymer shear-blending were a Silverson L4RT-A shear mixer [Figure 38 (a)] and a Silverson L5M-A shear mixer [Figure 38 (b)]. The shear heads used for both shear mixers were the square-hole high shear screen as shown in Figure 39. This kind of shear heads provides exceptionally high shear rates, which is ideal for the rapid size reduction of soluble and insoluble granular solids and also suitable for the preparation of emulsions and fine colloidal suspensions. Shear blending helps to make the asphalt-polymer mixtures more homogeneous.

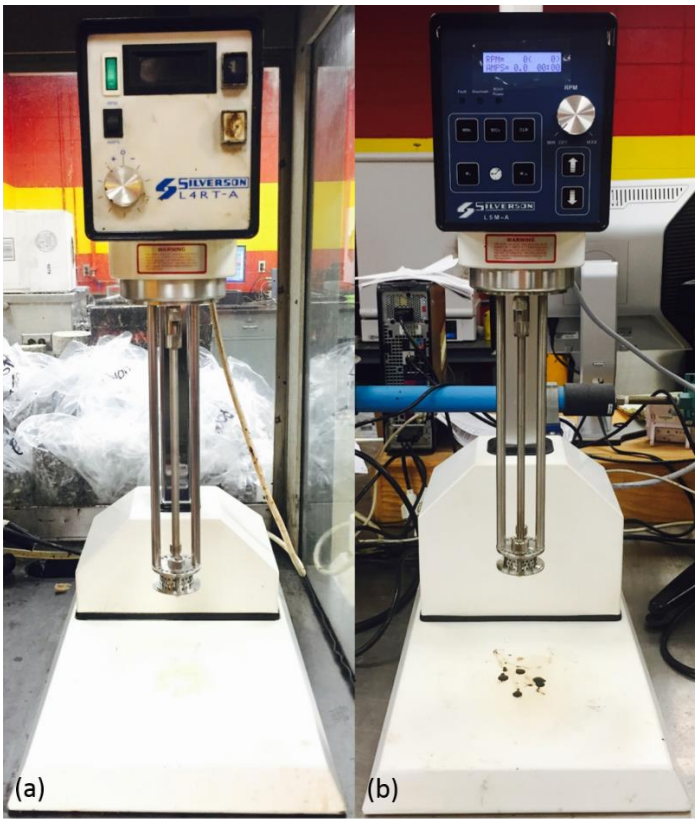

Figure 38. Silverson shear mixer (a) L4RT-A and (b) L5M-A

Figure 39. Shear head – square hole high shear screen

For shear blending, there were three blending methods used: shear blending at 180°C for 180 minutes (3 hours) (method A), shear blending at 190°C for 180 minutes (3 hours) (method B), and shear blending at 120°C for 30 minutes and 195°C for another 90minutes (method C). The practical procedures in this study are described as follows:

Shear blending at 180°C for 180 minutes (3 hours):

- Identified the weight of base asphalt binder in a quarter can and heated it up to 180°C;
- Identified the polymer would be used later and got it cryo ground (with constant argon and be crushed with liquid nitrogen);
- Calculated the polymer dosage which was the 3% of total weight; and
- Weighed out the well-ground polymer and added it by teaspoon within approximate 20 minutes when asphalt binder reached 180°C, and started shearing the mix at the rotation speed of 3000rpm for 180 minutes (3 hours).

Shear blending at 190°C for 180 minutes (3 hours):

- Identified the weight of base asphalt binder in a quarter can and heated it up to 190°C;
- Identified the polymer would be used later and got it cryo ground (with constant argon and be crushed with liquid nitrogen)
- Calculated the polymer dosage which was the 3% of total weight; and
- Weighed out the well-ground polymer and added it by teaspoon within approximate 20 minutes when asphalt binder reached 190°C, and started shearing the mix at the rotation speed of 3000rpm for 180 minutes (3 hours) (Figure 40).

Shear blending at 120°C for 30 minutes and 195°C for another 90minutes:

- Identified the weight of base asphalt binder in a quarter can and heated it up to 120°C;

- Got the identified polymer cryo ground and calculated the polymer dosage which was the 3% of total weight;
- Weighed out the cryo ground polymer (with constant argon and be crushed with liquid nitrogen) and added it by teaspoon over 10 minutes when asphalt binder reached 120°C, and started shearing the mix at the rotation speed of 3000rpm for 30 minutes;
- Increased the temperature to 195°C while kept the shear mill continuously running; and
- Maintained blending with the shear mill at 3000rpm for another 90minutes at 195°C.

Figure 40. Shear blending at 3000rpm, 190°C

Rheological testing plan: Superpave specifications and procedures

The objective of rheological testing plan in this study was to determine and evaluate the rheological properties of the unaged, the RTFO short-term aged, and long term aged bio-based polymer blended with the base asphalt binder (PG XX-34) based on Superpave specifications. To address the objectives of the testing section, the listed test specifications below have been followed to evaluate the performance grading of modified asphalt blends:

- ASTM D7175-08: Standard Test Method for Determining the Rheological Properties of Asphalt Binder Using a Dynamic Shear Rheometer;
- ASTM D2872-12: Standard Test Method for Effect of Heat and Air on a Moving Film of Asphalt (Rolling Thin-Film Oven Test);
- ASTM D6521-13: Standard Practice for Accelerated Aging of Asphalt Binder Using a Pressurized Aging Vessel (PAV);
- ASTM D6648-08: Standard Test Method for Determining the Flexural Creep Stiffness of Asphalt Binder Using the Bending Beam Rheometer (BBR); and
- ASTM D6373-15: Standard Specification for Performance Graded Asphalt Binder.

Dynamic shear rheometer (DSR)

The DSR is widely used as dynamic rheometer or oscillatory shear rheometer in the plastic industry. The DSR tests aim at characterizing the viscous and elastic behavior of asphalt binder at high and intermediate temperatures to predict rutting resistance and high temperature susceptibility. The DSR measures the complex modulus G* (G star) and phase angle δ (delta) of asphalt binder which are both significantly influenced by temperature and frequency of loading. The G* is the measurement of the total resistance of asphalt binder to deformation when exposed to repeatedly sheared. The δ represents the relative amounts of recoverable and non-recoverable deformation of the viscoelastic asphalt binder. The DSR tests performed at the speed of oscillation at 10 radians per second which is equal to approximate 1.59 Hz (cycles per second). Both strain and stress were measured during each oscillation cycle. A disk-shaped asphalt sample with a diameter equals the oscillating plate of the DSR is required for testing. There are two different types of diameter plate 25mm and 8mm with respect to the same size of the silicon molds. According to ASTM-D7175 (2008), 25mm parallel plates are used to test unaged and the RTFO short-term aged asphalt binders for predicting the resistance of rutting and 8mm parallel plates are used to test the PAV long-term aged asphalt binder for evaluating the susceptibility of

fatigue cracking. In this study, only 25mm diameter plates, 25mm diameter head, and 25mm diameter silicon molds (Figure 41) were used to test the critical high temperature of bio-based polymer modified asphalt binders (unaged) due to a lack of the PAV long-term aged materials for 8mm parallel plate. The DSR used and the tested sample made in this study is shown in Figure 42.

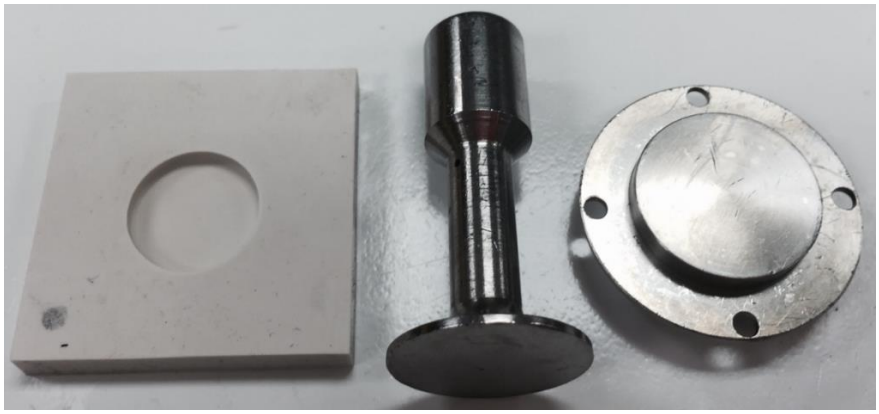

Figure 41. DSR 25mm diameter silicon mold, head, and plate

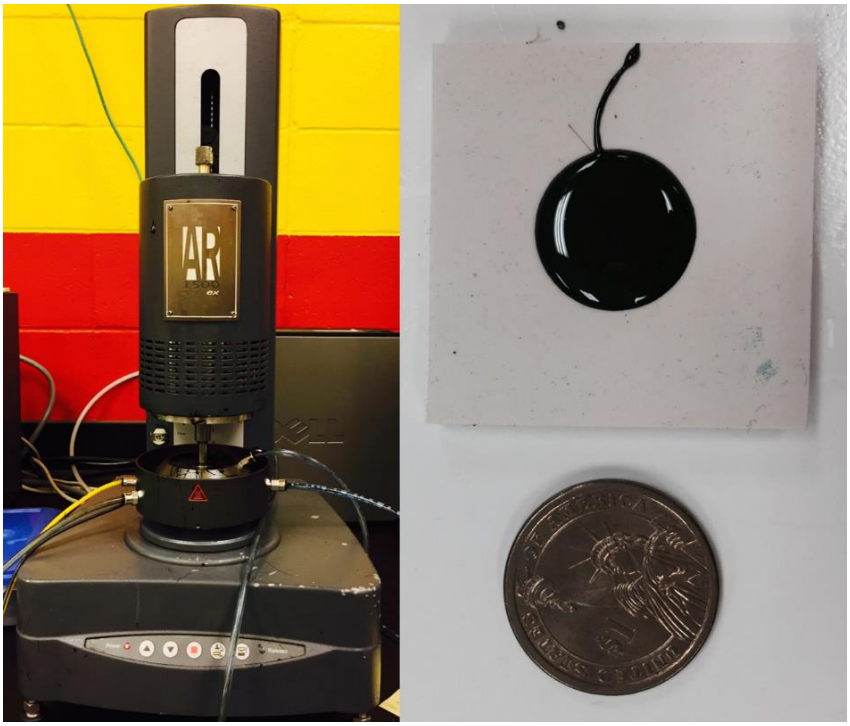

Figure 42. Dynamic Shear Rheometer (DSR) and the testing sample

The tests were conducted according to ASTM-D7175 (2008) and summarized as follows:

- Turned on the DSR device and preheated water bath to desired testing temperature (for this study, the original testing temperature for bio-based polymer modified asphalt binder was 52°C and lasted until the sample failed);
- The DSR samples were made in 25mm silicon molds directly after finishing shear blending bio-based polymer to the original asphalt binder and the sample sited in the mold for more than two hours before being subjected to loading into DSR;
- After loading the sample to the plates of the DSR, the plate was lowered down automatically;
- Then trimmed out extra materials after squashing, the testing started;
- The water bath was surrounded the sample and maintained testing temperature; and
- A computer controlled the DSR test parameters and recorded test results.

Rolling thin-film oven (RTFO)

The RTFO tests were conducted to simulate the asphalt binder aging during the manufacture and construction of HMA pavements according to ASTM-D2872 (2012). There are two main purposes for performing this test. One is to provide an aged binder for further testing and second is to determine the mass of volatiles lost during the testing process of exposing to heat and air flow rolling. The mass loss was calculated by Equation 1.

$$\text{Mass loss} = \frac{\text{Aged mass} - \text{Original mass}}{\text{Original mass}} \times 100 \quad (1)$$

The primary purpose for this study was the first one, to simulate asphalt binder aging and oxidation, however, several modified blends were also selected to evaluate the mass of volatiles. The RTFO device, glass container, 35.0±0.5g sample in glass container, and the glass container with sample after running the test were shown in Figure 43 and Figure 44 respectively. The tests were performed on original binder and asphalt binder blended with various types of bio-based polymers.

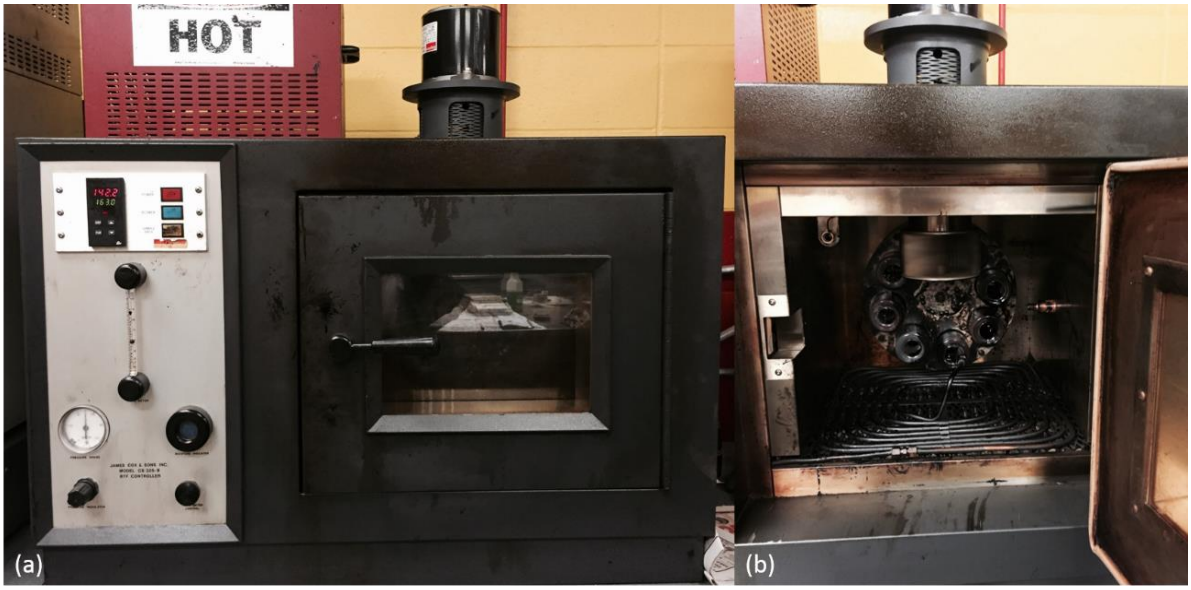

Figure 43. RTFO device (a) outside and (b) inside carriage

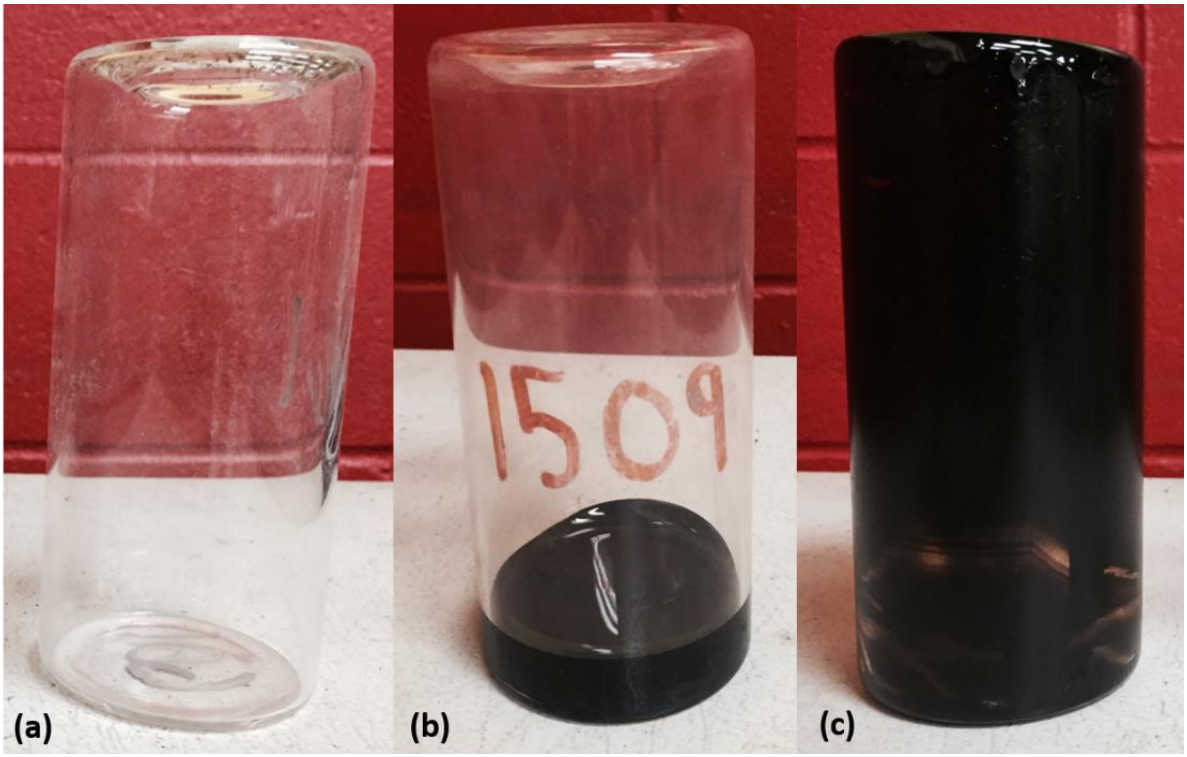

Figure 44. RTFO glass container (a) empty glass container, (b) glass container with 35±0.5g sample, and (c) glass container after running test

The testing procedures can be summarized as follows:

- The RTOF oven should be preheated to required aging temperature 163±0.5°C while heating up the asphalt binder in oven to thoroughly flowable condition but not to excess 150°C;
- The weight of each glass container was obtained and recorded;
- When asphalt binder was ready, poured 35±0.5g of the sample into a glass container and recorded the weight of binder, then turned the container to horizontal position;
- Put all the glass sample containers in the cooling rack to cool down to room temperature in 60-180 minutes;
- 8 glass containers with samples should be tested at each set, and in this study 4 of 8 glass containers were poured with the well-blended modified asphalt blends with same bio-based polymer;
- Loaded the glass containers to the carriage one by one, then closed the door of the RTFO device and started rotating the carriage at the rate of 15±0.2 r/min with the maintaining test temperature 163±0.5°C and the air flow rate of 4000±200mL/min. for 85minutes;
- After finishing the RTFO aging process, the weights of the RTFO residues with the glass containers were recorded;
- Then the residue was scraped out from the glass containers and kept the same modified asphalt blends residue in one aluminum container for further rheological property testing; and
- The mass loss of the asphalt blend was calculated.

Pressure aging vessel (PAV)

The PAV tests were conducted to simulate the effects of long term in-service aging of asphalt binder via exposing asphalt binder to high temperature (90°C, 100°C, or 110°C) and pressure (2.1 ±0.1MPa) for 20 hours. Based on the investigation of Bahia and Anderson (1995), the PAV could simulate the field aging of HMA pavement in-service occurs during 5 to 10 years. Because the PAV is for long-term aging, which means the tests should use the residue of short-term aging that has gone through the simulation of mixing and construction. Therefore, the sample should be tested through the RTFO process firstly, then the PAV process. The PAV device with sample rack and sample pans are shown in Figure 45.

Figure 45. PAV (a) PAV device, (b) sample rack, and (c) PAV pan with 50±0.5g sample

Testing procedures were followed ASTM-D6521 (2013) and summarized as below:

- Preheated the PAV oven until 100°C and heated up the RTFO residues to fluid;
- Poured each PAV pan at the mass of 50±0.5g (for this study, a bio-based polymer modified asphalt binder sample was poured on two pans each time and the PAV tests were conducted with 8 pans which were 4 different bio-based polymer modified asphalt binders one time);
- When the PAV oven hit 100°C, placed the filled pans to the sample rack;
- Put the sample rack with pans into the vessel and closed the lid immediately to avoid excessive heat loss;
- Turned on the gas supply and the device started aging until the pressure reached 2.1 ±0.1MPa;
- The temperature and air pressure maintained inside the pressure vessel for 20h±10min;
- After 20 hours, the pressure would be fully released gradually in eight to ten minutes;
- The sample rack needed to be removed from the PAV vessel and sample pans were taken out from the rack;
- After scraped each modified PAV residues to aluminum cans, degassing was required to perform;
- Degassing oven needed to be preheated at least one hour before the PAV was done;
- The residue cans were placed in the degassing oven (Figure 46) at 170°C for 30 minutes at a pressure of 15kPa absolute for removing foams in binders; and

- After degassing process, the PAV residues were ready for further testing.

Figure 46. (a) Degassing oven and (b) inside chamber

Bending beam rheometer (BBR)

The BBR was used to determine the low temperature susceptibility, thermal cracking potential, and the low temperature performance grade of asphalt binder. The BBR is designed to measure the amounts that a binder deflects or creeps under a constant loading at a constant low temperature which is related to the lowest service temperature of pavement. The low temperature was maintained by a mixing liquid bath that was a mixture of 1:1:1 ratio of ethylene glycol, methanol, and water. The test was performed by using the residues that had been aged in both RTFO and PAV. Thus, the test measured the condition of asphalt binder both had been exposed to hot mixing manufacture and the long-term in-service aging. The BBR device, the inside liquid bath, and the testing samples are shown in Figure 47. There were two main parameter results could be recorded which were creep stiffness and m-value. Creep stiffness is a measurement of how the tested asphalt binder resists the constant loading, and m-value is a measurement of the rate at which the creep stiffness changes with the loading time that is the slope of the log creep stiffness versus log time curve at any testing time. According to the Superpave binder specification requirement, the creep stiffness should be less than or equal to 300MPa and m-value should be greater than or equal to 0.300 when measured at a loading time of 60 seconds.

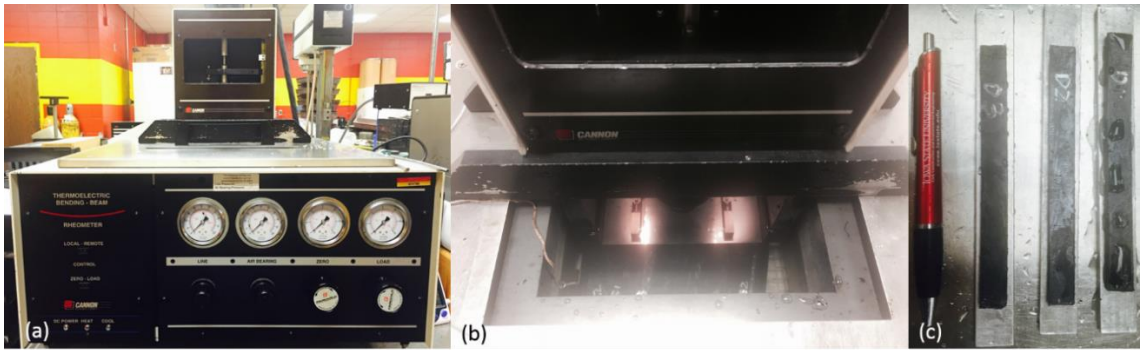

Figure 47. BBR (a) BBR device outside, (b) inside liquid bath, and (c) testing samples

Testing procedures were followed ASTM-D6648 (2008) and summarized as below:

- Six rectangular aluminum molds for one type of bio-based polymer modified asphalt binder PAV residue were prepared for making BBR testing samples;
- When the bio-based polymer modified asphalt binder PAV residue was heated to fluid, the asphalt binder was poured to the six molds;
- After a cooling period of approximate 45 to 60 minutes, excess asphalt binder was trimmed from the upper surface by using a hot spatula;
- Demolding was performed after the well-trimmed the molds with samples placed in iced water bath for 5 to 10 minutes;
- After demolding, the beams were conditioned in the BBR test bath for 60 minutes after the BBR device passed the calibration and the bath temperature was down to desired temperatures (for this study, the BBR testing low temperatures were -18°C and -24°C);
- Six beams for each modified asphalt binder were separated into two groups for the two testing temperatures -18C° and -24°C;
- After 60 minutes conditioning, the beams were tested and placed on the loading frame individually and subjected to a loading for 240 seconds; and
- The testing results of creep stiffness and m-value for each beam were recorded and shown in the program.

Developing master curve

In order to develop master curves for complex shear modulus (G*) of asphalt binder modified by bio-based polymers, in total of 28 bio-based polymer modified asphalt blends were prepared and tested in the DSR. Both unaged asphalt blends and the RTFO short-term aged

asphalt blends were tested by the DSR to obtain the principal viscoelastic parameters: the complex shear modulus (G*) and phase angle (δ).

All DSR tested samples in this study for developing master curve were performed under strain-control loading conditions under frequency sweeps between 0.1Hz to 100.0Hz (0.1, 0.1259, 0.1585, 0.1995, 0.2512, 0.3162, 0.3981, 0.5012, 0.631, 0.7943, 1,1.259, 1.585, 1.995, 2.512, 3.162, 3.981, 5.012, 6.31, 7.943, and 10Hz) at temperature between 20 and 58°C (20, 30, 46, and 58°C). All preformed DSR tests for developing master curves were undertaken with 25mm diameter and 1mm gap geometry.

The master curves for all tested bio-based polymer modified asphalt binders and the base asphalt binder were developed by using an empirical time-temperature superposition principle equation, which is also a numerical and non-functional form shift approach, named as Williams-Landel-Ferry Equation (WLF) equation. The objective of developing master curves was by using shift factors to appropriately shift the complex shear modulus (G*) at each frequency to overlap a smooth curve for comparing the rheological properties of each asphalt blends. Furthermore, the purpose of using WLF equation was to evaluate the accuracy that the manually shifted factors are comparing to the equation obtained shifting factors. The shifting factors were obtained by using WLF equation as shown in Equation 2,

$$\log a_T = \frac{(-C_1)\times(T-T_r)}{C_2+(T-T_r)} \quad (2)$$

where a_T is the shift factor, C_1 and C_2 are constants based on material properties, T is the measurement temperature (in K), and T_r is the reference temperature (in K) for this study T_r used 20°C.

The shifted frequencies were calculated by using the manually shifted factors at each testing temperature multiply the real testing frequencies. The master curves were plotted with the complex modulus (G*) as the Y-axis and the shifted frequencies as the X-axis. The X-axis also represented the temperature as low frequency representing for high temperature and vice versa. The Microsoft Excel Spreadsheet Solver function was used for the best fit of each set of data. This tool is able to adjust the empirical constants C_1 and C_2 to a proper value for minimizing the difference sum of value between the manually shifted factors and equation obtained shifting factors.

Developing black diagram

Since complex modulus (G*) cannot be the only parameter deciding the rheological properties of asphalt binder, the phase angle (δ) should also be taken into account to evaluate the rheological behavior of modified asphalt binder. Therefore, black diagrams were also developed by using phase angle (δ) as X-axial and complex modulus (G*) as Y-axial with the same data obtained from the DSR for master curves.

Statistical analysis

Response surface model is a combination of mathematical and statistical techniques used to identify factors that produce the best response and satisfy operating or process specifications with fewer experiments. It can also be used to identify optimum conditions that improve product quality by modeling the relationship between the independent variables which is always unknown (Chen et al. 2012, Cutright and Meza 2007). Therefore, the most crucial step for the response surface modeling is to find a suitable approximation for the true functional relationship between the response and the independent variables (Cutright and Meza 2007).

With the rheological performance of bio-based polymer modified blends at high and low temperatures as responses, respectively, the effects of independent factors (i.e. testing temperature, styrene molecular weight, and styrene content) were selected to develop the initial response surface modeling to find the true functional relationship through the step-down regression process based on the laboratory results obtained in the study. The statistical analysis was conducted by using statistical analysis computer software JMP (version: Pro 12) to evaluate the statistical difference between each of the factor that might have effects on the test results at a confidence level of 95%.

Response surface modeling and statistical transformation

The response surface modeling used in this study for the response has three independent variables, i.e. testing temperature, styrene molecular weight, and styrene content were selected. This modeling allows the formulation of a second-order polynomial model to describe the process, which includes three first-order model linear effects, three cross product factors, and three second-order quadratic items as presented in Equation 3,

$$y = \beta_0 + \beta_1 x_1 + \beta_2 x_2 + \beta_3 x_3 + \beta_{12} x_1 x_2 + \beta_{13} x_1 x_3 + \beta_{23} x_2 x_3 + \beta_{11} x_1^2 + \beta_{22} x_2^2 + \beta_{33} x_3^2 + \varepsilon \quad (3)$$

where y is the response as the testing results which relates to x_1,x_2, and x_3, three major factors styrene molecular weight (kDa), styrene content (%), and testing temperature (°C) respectively, β_0 is the intercept, $\beta_1 \ldots \beta_{33}$ are the coefficients, and ε is the random error component. The fit quality of the polynomial model was expressed by coefficient of determination R^2.

For each response, G*/sin (δ) for high temperature of unaged and the RTFO short-term aged modified asphalt binder, the m-value and the stiffness for low temperature of the PAV long-term aged modified asphalt binder, the data under unmodified state and two transformed state (logarithm base 10 and root square) was used to determine the most reliable model for predicting the appropriate styrene parameters (styrene molecular weight and styrene content) in polymer that provides improvement on elasticity of the modified blends at high temperature. The statistical step-down regression process was used in each response surface modeling to eliminate the variable that had the highest p-value until the final model determined by the variables that were all statistically significant difference in terms of the p-value was less than 0.05. The final prediction models of unmodified state, logarithm base 10 transformed state, and root square transformed state were compared by checking if the residuals followed a normal distribution and met the equal standard deviation conditions for determining the best model to use as statistical prediction model.

CHAPTER 4. RESULTS AND DISCUSSION

This chapter includes the rheological performance test results of the bio-based polymer modified asphalt blends. The test data obtained and analysis performed are listed and summarized based on the results according to the Superpave standard specifications. All tests were conducted according to the test methods and experimental plans illustrated in Chapter 3. This chapter was subdivided into five sections which can be summarized as follows. First, the high temperature performance grade test results for all unaged and the RTFO short-term aged bio-based polymer modified asphalt blends and unaged and the RTFO short-term aged base asphalt binder were discussed. The RTFO mass losses were calculated and listed according to Chapter 3. Second, the low temperature performance grade test results for the PAV long-term aged bio-based polymer modified asphalt blends were discussed, and the continuous performance grade ranges based on results of high and low temperature testing were tabulated. Third, the master curves were developed according to the William, Landel and Ferry (WLF) equation. Forth, the black diagrams of both unaged and the RTFO short-term aged bio-modified asphalt binders were developed for better evaluation of the rheological performance based on the changes in complex modulus (G*) and phase angle (δ). Fifth, the statistical analysis and statistical prediction modeling were performed on the laboratory test results.

HIGH TEMPERATURE PERFORMANCE GRADE

In this study, the high temperature continuous grades (critical high temperatures) were obtained by using the DSR on both unaged and the RTFO short-term aged asphalt materials (modified and unmodified) according to ASTM D7175 (2008). Furthermore, the high temperature performance grades of both unaged and the RTFO short-term aged asphalt materials (modified and unmodified) were determined according to ASTM D6373 (2015). Based on the Superpave standard specifications, the high temperature performance grades were determined on both unaged and the RTFO short-term aged DSR test results. However, the lower values of critical temperature were considered as the high temperature performance grade. According to the Superpave standard specifications, the continuous grades for unaged asphalt binder is based on the value of $|G^*|/\sin(\delta)$, which should be equal to 1.00kPa, whereas for the RTFO short-term aged asphalt binder the $|G^*|/\sin(\delta)$ should be equal to 2.20kPa, and these two values can be referred to the minimum requirements in the specification.

Unaged asphalt blends

For this section of tests, all samples were tested in the DSR by following the procedures illustrated in Chapter 3. Because the base asphalt binder used for this study was from Flint Hills, a PG XX-34 asphalt cement, all bio-based polymer modifications aimed at improving the high temperature performance grades of asphalt binders. Therefore, both the base asphalt binder and bio-based polymer modified asphalt binders were tested and compared consequently. The initial testing temperature started at 46°C, and the following test proceeded in 6°C increments until the critical high temperature was achieved (see Table 32 to Table 36 in Appendix A). The results of continuous grading on all tested modified and unmodified asphalt binder were obtained and are tabulated in Table 7.

Table 7. High temperature continuous grading for unaged unmodified and modified asphalt binders

Blending Method	Blend Code	Continuous Grades, °C
Solvent blending	A	56.4
	B	59.4
	C	60.5
	D	58.2
	E	63.0
	F	70.5
	G	76.2
	H	74.1
	I	72.4
	J	73.2
	K	59.7
	L	66.7
	M	62.5
	N	64.5
	O	60.6

Table7. continued

Blending Method	Blend Code	Continuous Grades, °C
Control Group (no blending)	0	53.4
Shear blending at 180°C for 3hr	1	54.8
	2	58.1
	3	56.0
Shear blending at 120°C for 30min and 195°C for 90min (total 120min)	5	Reserved
	6	56.1
	8	56.3
	10	55.8
Shear blending at 190°C for 3hr	4	55.0
	7	55.8
	9	56.4
	11	56.7
	12	56.3
	13	60.7
	14	53.1
	15	56.8
	16	57.8
	17	57.7
	18	60.0
	19	57.3
	20	56.9
	21	56.5
	22	Reserved
	23	56.8
	24	56.5
	25	53.7
	26	56.5
	27	57.5
	28	56.9

Note: The blending codes refer to Chapter 3.

Based on the results, the following conclusions can be made. By using the DSR to test the high continuous grades, the unaged base asphalt binder had a critical high temperature at 53.4°C. In comparison with the bio-based polymer blends, all modified results showed increases in the critical high temperature by using both solvent and shear blending approaches. Second, it was observed that solvent blending gained relative higher continuous grades than the other results from the three shear blending methods. Third, in the solvent blending results (Figure 48), the asphalt binder modified with 30kDa styrene molecular weight PS-PAESO polymer presented the average highest continuous grades as compared to the PS-PAESO with the 15kDa and 45kDa molecular weight of styrene. According to the Superpave standard specifications, the high temperature performance grade should be determined by both unaged and the RTFO short-term aged asphalt binders. Therefore, the RTFO short-term aged asphalt binders need to be tested to obtain $|G^*|/\sin(\delta)$ values for reliable performance grading.

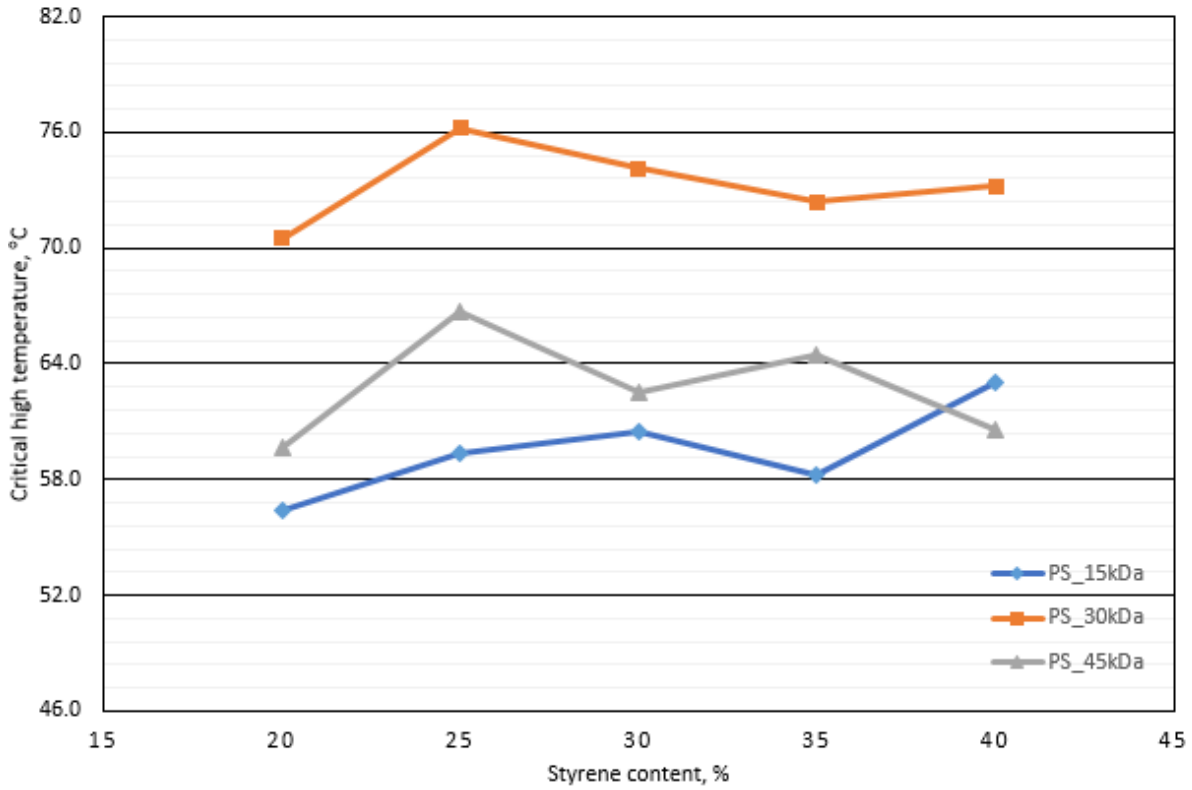

Figure 48. Solvent blending continuous grades results comparison

RTFO short-term aged asphalt blends

All tested modified and unmodified asphalt binders were respectively short-term aged in an RTFO oven at 163°C for 85minutes. According to Superpave standard specifications and ASTM

D2872 (2012), it is required that the mass loss of asphalt binder after the RTFO short-term aging process should be less than one percent. The results of mass loss for part of the modified asphalt binders were calculated based on the Equation (1) (see Chapter 3) and tabulated in Table 8. The test results for calculating mass loss are listed in Table 37 in Appendix A. Based on the mass loss results obtained, the selected bio-based polymer modified asphalt binders for confirming the mass loss were all less than one percent. Somehow, the mass loss results varied in accordance with the different molecular weights and the percentage contents of styrene without apparent order. However, all results calculated met the specified mass loss criteria for asphalt binder grading. Under this condition, it can be assumed that the bio-based polymers applied in general are not considered as volatile materials when blended with asphalt binders.

Table 8. Mass loss results for RTFO short-term aged modified asphalt binders

Blend Code	RTFO Mass Loss, %
3	0.36
12	0.50
13	0.43
18	0.35
23	0.78
24	0.71
25	0.71
26	0.93
27	0.92
28	0.50

Note: The blending codes refer to Chapter 3.

After modified and unmodified asphalt binders were short-term aged in an RTFO oven, high temperature performance grading were performed by using the DSR followed the same procedures as unaged asphalt blends. The initial testing temperature started at 46°C, and the following test proceeded in 6°C increments until the critical high temperature was achieved (see Table 38 to Table 42 in Appendix A). The asphalt materials will become stiffer due to the oxidation and high temperature during the RTFO aging process. The $|G^*|/\sin(\delta)$ criteria for

continuous grading of the RTFO short-term aged asphalt materials would be 2.20kPa due to the stiffening of the short-term aging binders. The DSR results of high temperature continuous grades for the RTFO short-term aged modified and unmodified asphalt binders were summarized in Table 9.

Table 9. High temperature continuous grading for the RTFO short-term aged unmodified and modified asphalt binders

Blending Method	Blend Code	Continuous Grades, °C
Control Group	0	53.7
Shear blending at 120°C for 30min and 195°C for 90min (total 120min)	6	57.5
	8	54.5
	10	66.8
Shear blending at 190°C for 3hr	4	55.0
	7	55.5
	9	55.5
	11	54.6
	12	55.7
	13	60.4
	14	55.9
	15	54.8
	16	55.6
	17	55.2
	18	62.0
	19	55.3
	20	55.2
	21	56.0
	22	Reserved
	23	55.2
	24	55.5
	25	56.3
	26	56.9
	27	59.1
	28	58.2

Note: The blending codes refer to Chapter 3.

In order to provide better understanding of the continuous grades for bio-based polymer modified asphalt blends and the base asphalt binder, the comparison of continuous grades results between unaged and the RTFO short-term aged modified and unmodified asphalt blends are listed in Table 10.

Table 10. Compared results of high temperature continuous grades

Blending Method	Blend Code	Continuous Grades, °C	
		Unaged	RTFO aged
Base asphalt binder	0	53.4	53.7
Base asphalt binder shear blended at 190°C, 3hr	7	55.8	55.5
Shear blending at 120°C for 30min and 195°C for 90min (total 120min)	6	56.1	57.5
	8	56.3	54.5
	10	55.8	66.8
Shear blending at 190°C for 3hr	4	55.0	55.0
	9	56.4	55.5
	11	56.7	54.6
	12	56.3	55.7
	13	60.7	60.4
	14	53.1	55.9
	15	56.8	54.8
	16	57.8	55.6
	17	57.7	55.2
	18	60.0	62.0
	19	57.3	55.3
	20	56.9	55.2
	21	56.5	56.0
	22	Reserved	Reserved
	23	56.8	55.2
	24	56.5	55.5
	25	53.7	56.3
	26	56.5	56.9
	27	57.5	59.1
	28	56.9	58.2

Note: The blending codes refer to Chapter 3.

Compared to unaged asphalt binders continuous grades, eight out of the 22 bio-based polymer blends increased the critical high temperature 1 to 2°C or even higher after the RTFO aging such as blends 6, 10, 14, 18, 25, 26, 27, and 28, whereas the rest of blends decreased 1 to 2°C after the RTFO aging process. However, it is difficult to explain why certain bio-based polymer blends increased the critical high temperature while others decreased the critical high temperature after short-term aging. Further investigation needs to be done towards this topic. Figure 49 shows the critical high temperature values of modified blends. Bio-based polymer modified asphalt blends presented a trend of increasing the high temperature continuous grades as compared to the base asphalt binder.

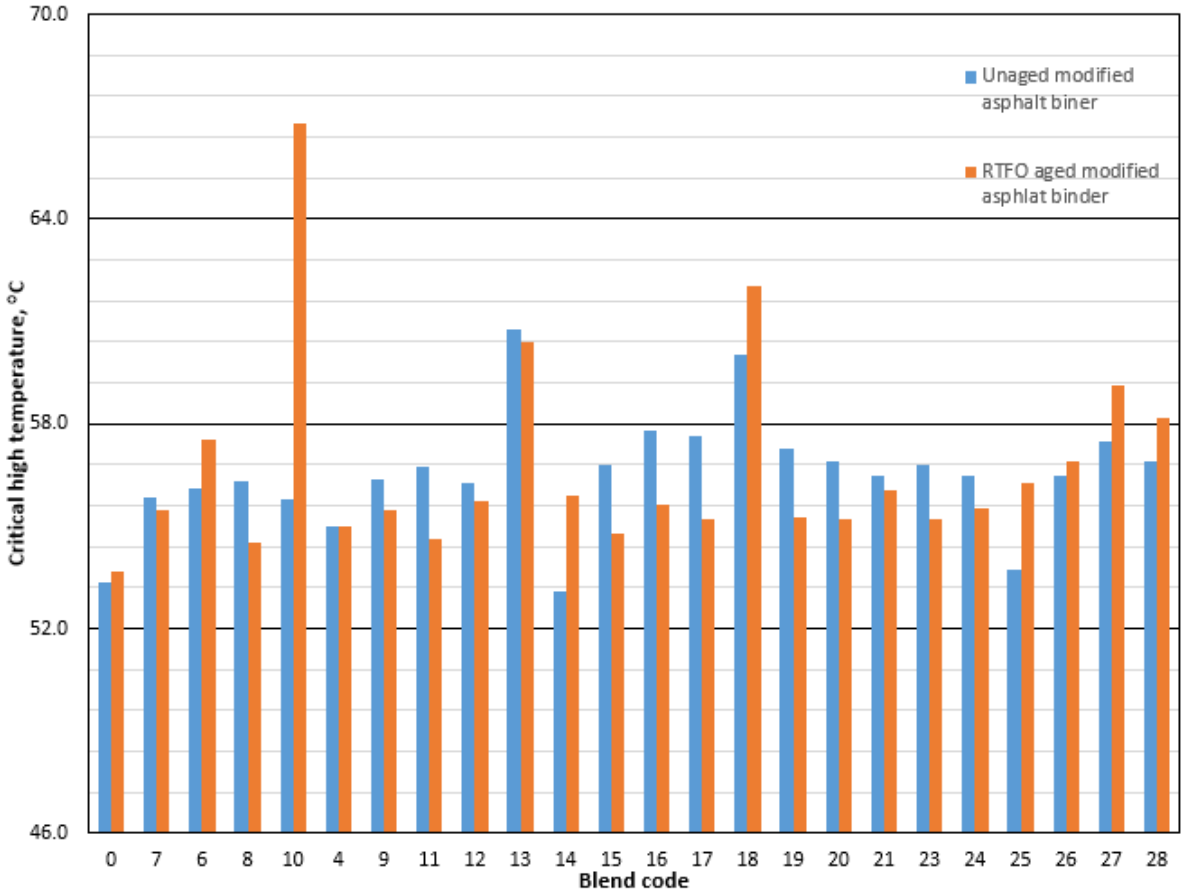

Figure 49. High temperature continuous grades of unaged and the RTFO short-term aged modified asphalt binder and the base asphalt binder

LOW TEMPERATURE PERFORMANCE GRADE

The low critical temperature continuous grades for all PAV long-term aged bio-based polymer modified asphalt blends were determined by using a BBR (see Chapter 3 for detailed test procedures). According to ASTM D6648 (2008), the criteria for the critical low temperature of are based on two parameters: the stiffness and the m-value at a loading time of 60 seconds in a BBR. A value is determined as critical low temperature when either the stiffness is greater than 300MPa or the m-value is less than 0.300. The low performance grading of the based binder used in this study was graded as -34. The low temperature continuous grades results (see Table 43 in Appendix A) obtained from the BBR testing are summarized in Table 11.

Asphalt binders which are polymer modified often improve one side of the performance grade which indicates either high temperature or low temperature benefit. Figure 50 shows the low temperature continuous grades of bio-based polymer modified blends. It was observed that 12 out of the 18 bio-based polymer modified asphalt blends presented temperature continuous grades with 1 or 2°C lower than the base asphalt critical low temperature. Therefore, these modified asphalt binder grades were not affected and still considered as - 34°C performance grade. However, the other six modified blends presented the polymers had negative effects on the critical low temperature as they increased the low temperature grade from -34°C to -28°C, such as blends 13, 18, 21, 23, 26, and 27. To summarize, the bio-based polymers used in this study had no effect on improving the low temperature performance grades. In other words, these polymers did not substantially improve the resistance to thermal cracking. However, according to the continuous performance grade ranges in Table 12 and Figure 51, 11 out of the 18 bio-based polymer blends were higher than the base asphalt binder's range. Thus, these bio-based polymers reduced the temperature susceptibility of the base asphalt binder.

Table 11. BBR results for low temperature continuous grades of the PAV long-term aged bio-polymers modified asphalt binders

Blend code	Continuous grade, °C
16	-35.5
20	-34.6
21	-32.8
17	-34.3
9	-34.6
15	-34.7
19	-37.0
11	-37.2
14	-35.5
13	-32.6
18	-31.5
12	-41.2
23	-33.5
24	-34.1
25	-35.4
26	-33.3
27	-33.5
28	-34.4

Note: The blending codes refer to Chapter 3.

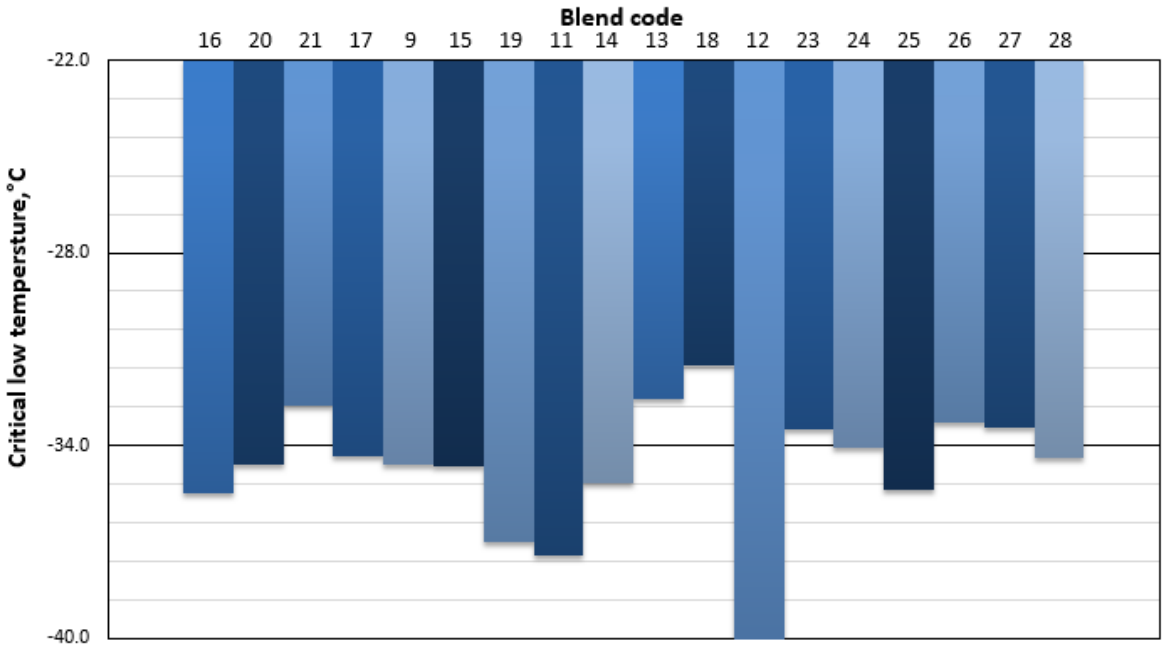

Figure 50. BBR results for low temperature continuous grades for the PAV long-term aged modified asphalt binders

Table 12. Continuous performance grade ranges of modified asphalt binders and the base asphalt binder

Blend Code	Continuous Grade Range, °C
0	89.7
13	93.0
25	89.1
27	91.0
18	91.5
23	88.7
24	89.6
28	91.3
26	89.8
21	88.8
14	88.2
11	92.0
12	96.9
9	90.1
15	89.4

Blend Code	Continuous Grade Range, °C
17	89.5
19	92.3
16	91.1
20	89.8

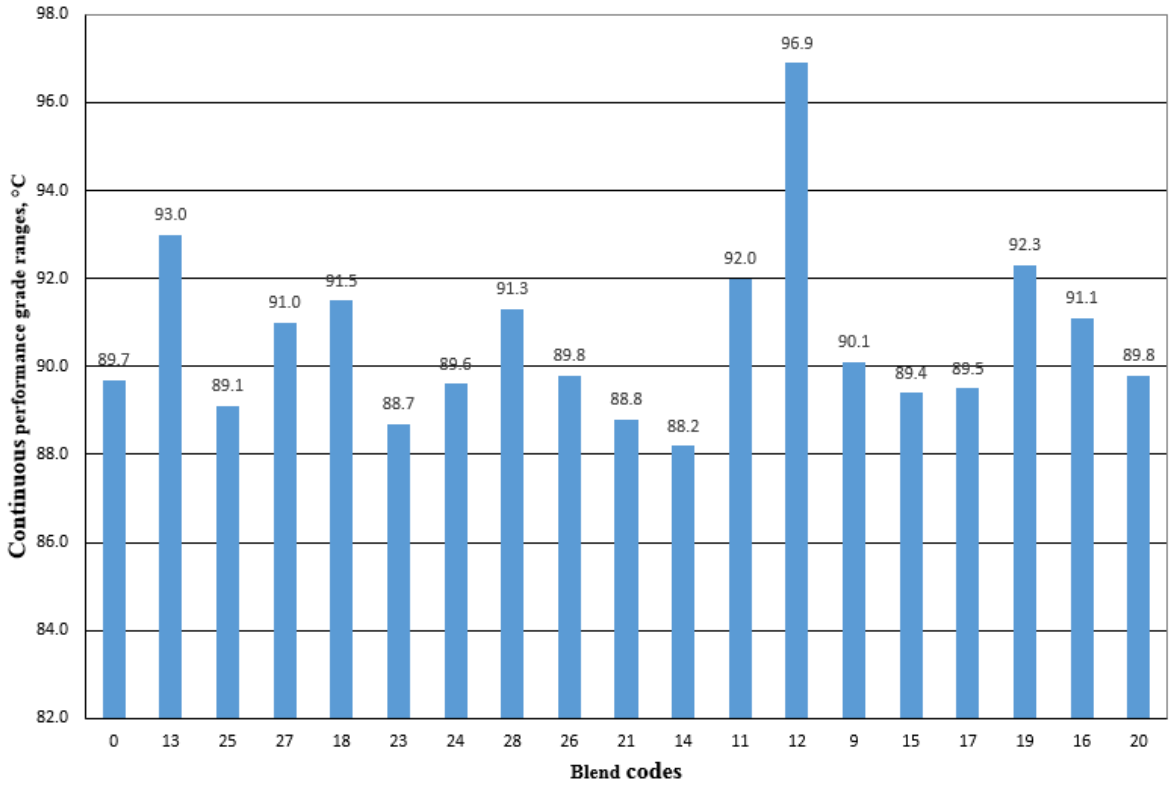

Figure 51. Continuous performance grade ranges of modified asphalt blends and the base asphalt binder

MASTER CURVES FOR BIO-BASED POLYMER MODIFIED ASPHALT BINDER

The master curves were developed by using William, Landel and Ferry (WLF) equation to calculate the most appropriate shift factors to shift the experimental complex modulus at each testing frequency. By comparing the overlapped best fit curves, the rheological properties of each modified asphalt blends can be observed at high, intermediate, and low temperatures.

The data were obtained from the DSR by testing unaged modified and the RTFO short-term aged modified asphalt blends. The complex modulus (G*) before and after RTFO short-term aging process at each testing temperature are shown in Figure 61 to Figure 103 in Appendix A. All developed master curves were using the manual frequency sweeps shifting factors which were perfectly matched with the WLF equation-calculated shift factors with adjusted coefficients (C_1 and C_2) in the formula at the reference temperature of 20°C. The master curves of the unaged bio-based polymer modified asphalt binders and the RTFO aged bio-based polymer modified asphalt binders are shown in Figure 52 and Figure 53, respectively.

For all unaged bio-based polymer modified asphalt binders, the results showed similar trend in the master curves. Comparing the unaged base asphalt binder master curve, the unaged modified asphalt binders were all stiffer at higher temperatures (lower frequency), intermediate temperatures (intermediate frequency), and lower temperature (higher frequency), which were resulted by the bio-based polymer modifications. Furthermore, it was observed that, unaged blends 13 and 18 were stiffer than any other modified asphalt binders, especially at higher temperatures (lower frequency). Unaged blend 13 had the highest complex modulus (G*) at higher temperatures, which could because the PS-PAESO polymer added to the base asphalt binder had the lowest molecular weight (10kDa) with the lowest styrene content (20%) among all the polymers.

For the RTFO short-term aged modified asphalt binders, all curves showed stiffer trend as expected, especially at higher temperatures (lower frequency). According to the master curves, all curves were observed with increasing complex modulus (G*) because of the aging process comparing to the unaged curves. This trend indicated improved resistance to rutting deformation. Moreover, the relative stiffer blends after the RTFO short-term aging were the modified asphalt blends with the lower styrene molecular weight. The same trend in both unaged and the RTFO short-term aged modified asphalt binder can be observed in Figure 54, which only has blend 13 against the base asphalt binder for display purposes. In summary, it can be proposed that the

styrene molecular weight and styrene content of the polymer have effects on the complex modulus (G*) of the modified asphalt blends, and also the lower molecular weight of styrene might have positive effects on the asphalt binder performance of rutting resistance at high temperature.

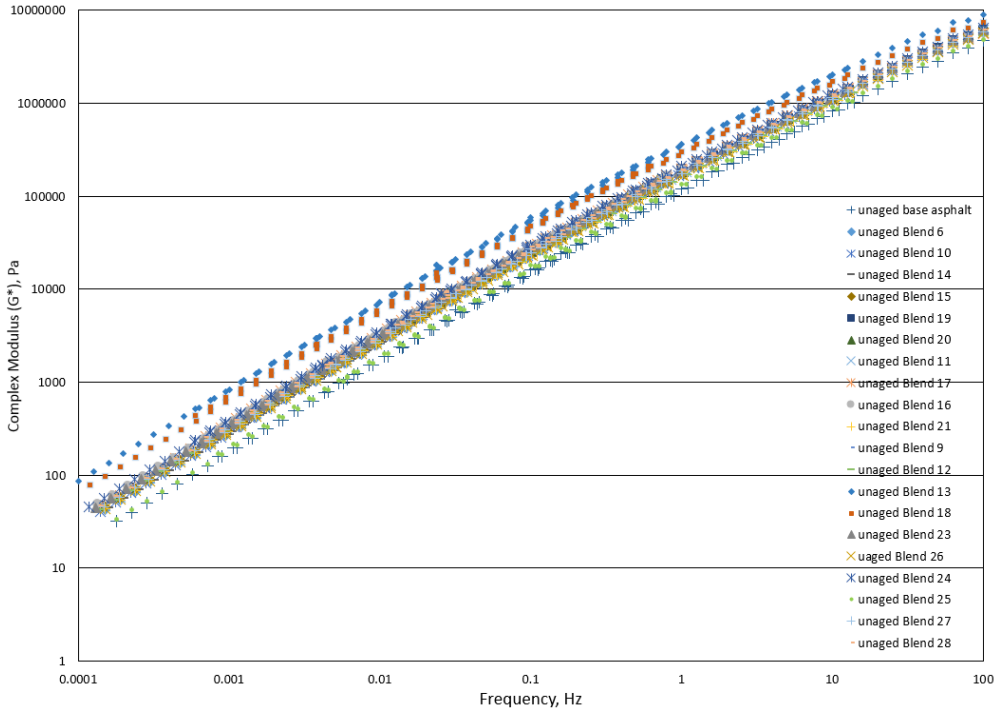

Figure 52. Master curves for unaged bio-based polymer modified asphalt binders

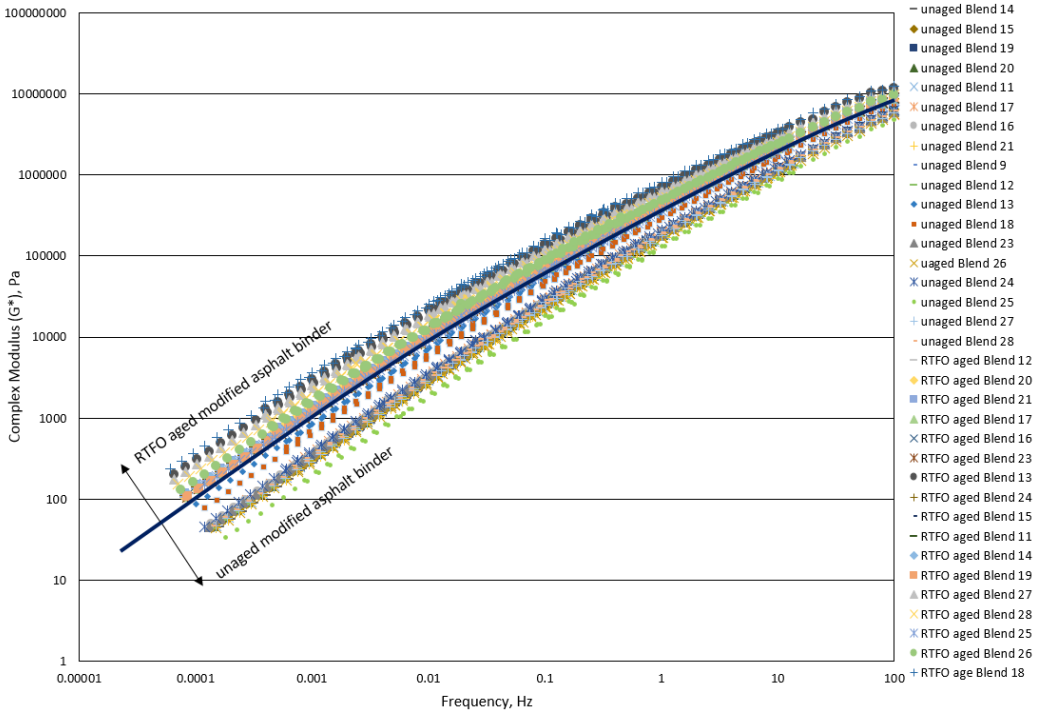

Figure 53. Master curves for the RTFO short-term aged bio-based polymer modified asphalt binders and unaged bio-based modified asphalt binders

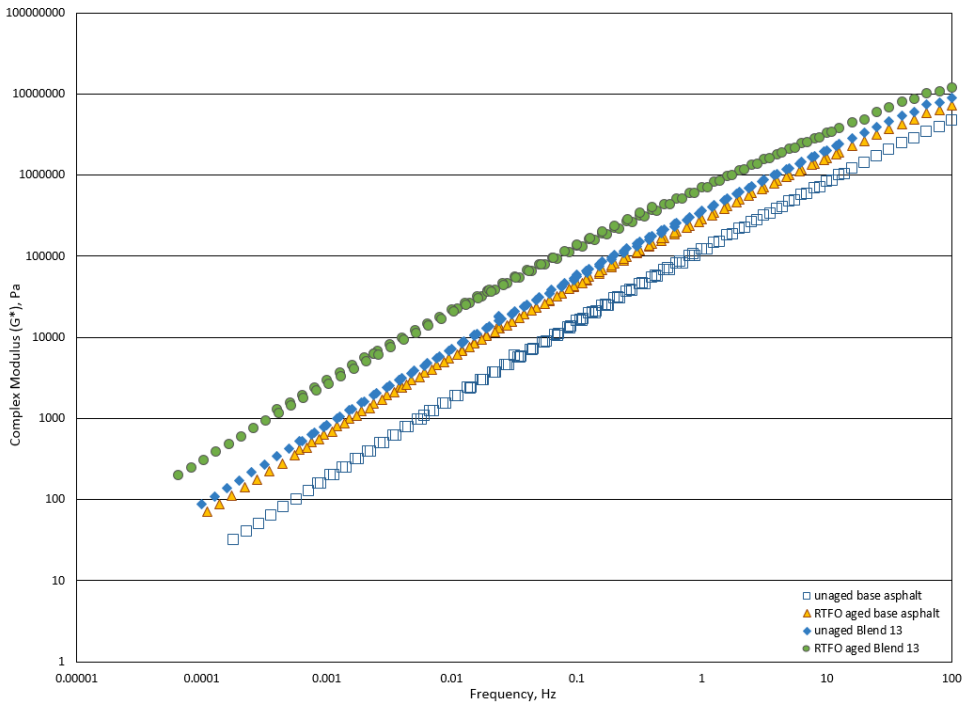

Figure 54.Master curves for unaged and the RTFO short-term aged blend 13 and base asphalt binders

BLACK DIAGRAM FOR BIO-BASED POLYMER MODIFIED ASPHALT BINDER

In order to evaluate the changes in complex modulus (G*) and phase angle (δ) corresponding to testing temperatures and frequencies, black diagrams were developed for better describing of the rheological behavior for modified asphalt binders. The black diagrams for unaged modified asphalt binders were developed as described in Chapter 3.

According to the black diagrams in Figure 55, it can be observed that for both unaged and the RTFO short-term aged modified blends at high stiffness values (high G*) corresponding to lower temperatures and higher frequency, the black diagrams showed a shift towards lower phase angles (δ) which indicated the hardening and aging of the polymer modified binders. Furthermore, in the black diagrams the RTFO short-term aged blends tends to have lower phase angles, which indicated these blends have improved elastic properties. For a better understanding, blend 13 was selected to compare against the base asphalt binder (control group) in Figure 56. At lower temperatures, a phase angle shift of five to ten degrees was observed for the unaged binder between blend 13 and the base asphalt (control group), while a phase angle shift of 10 to 15 degrees was observed between blend 13 and the base asphalt (control group) after the RTFO short-term aging process. This shift/trend in phase angles was also observed with a smaller change of one to three degrees at higher temperatures (low complex modulus), which means the polymer used made the base asphalt more elastic.

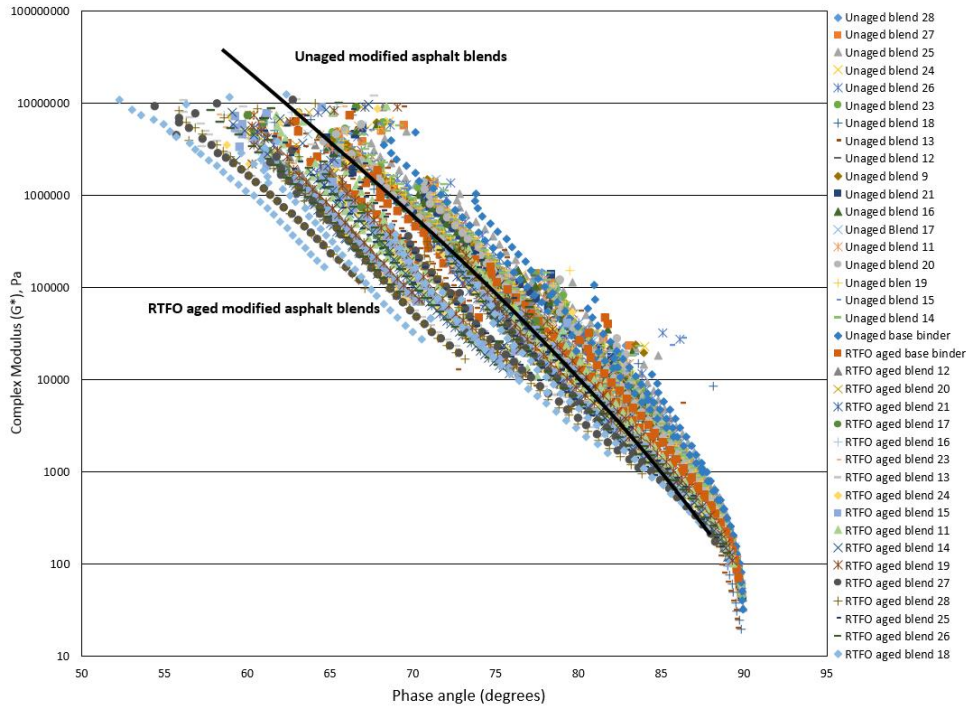

Figure 55. Black diagrams for unaged and the RTFO short-term aged modified asphalt binders

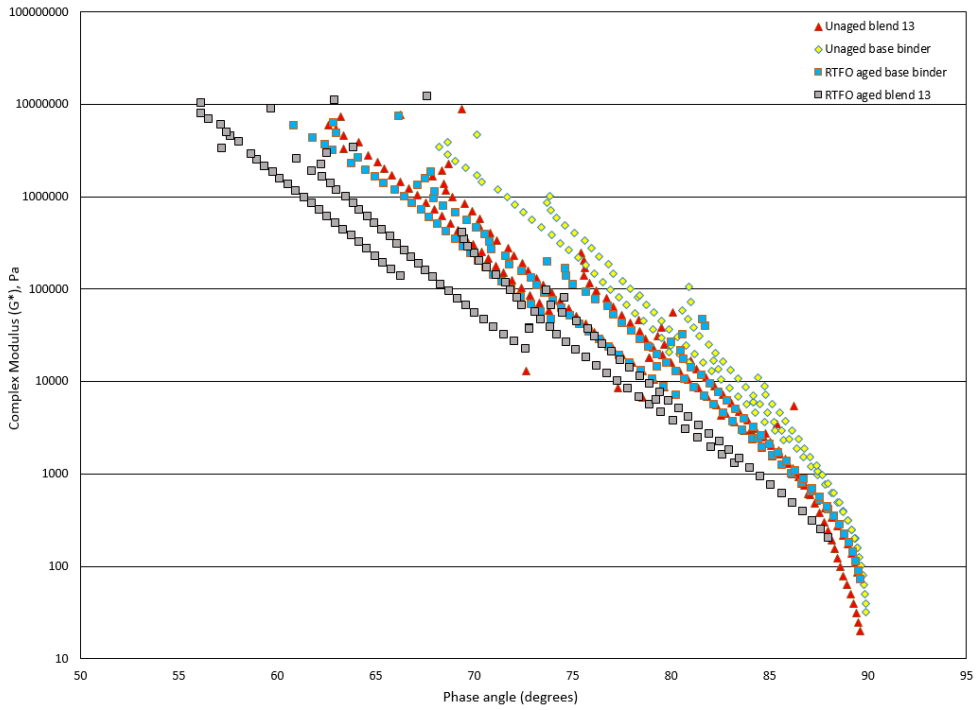

Figure 56. Black diagrams for unaged and the RTFO short-term aged blend 13 and base asphalt binders

STATISTICAL ANALYSIS

In order to investigate the factors that would affect the test results (G*/sin(δ) for high temperature, and the m-value and stiffness for low temperature) in this experimental study, several possible experimental factors were selected for statistical analysis. These factors can be classified into three important factors: styrene molecular weight (MW, kDa), styrene content (%), and test temperature (°C) for prediction modeling and two less important factors: polymer reaction duration (in hours) and shear blending method (A: shear blended at 180°C for 3hr, B: shear blended at 190°C for 3hr, and C: shear blended at 120°C for 30min and 195°C for 60min) for statistical analysis. Other outside variables have been controlled to reduce random error variation during testing, for example, the same operator did all of the shear blending by using the same shear mixer, high temperature tests (DSR), required aging processes (RTFO and PAV), and low temperature tests (BBR).

Statistical analysis on the effects of polymer reaction duration

As the shear blending experimental plan shows in Table 5 in Chapter 3, the effects of polymer reaction duration can be estimated by using the PS-PAESO bio-based polymer with the same styrene molecular weight (30kDa) and same styrene content (30%) at different reaction durations. The high temperature G*/sin(δ) resulted from six test temperatures (20, 30, 40, 46, 52, and 58°C) were used as responses. The blends used in the statistical software JMP for running the fit model were blends 21, 14, 9, 15, 17, 19, 16, and 20. A summarized statistical analysis for these blends is shown in Table 13. A least square means comparison (the Turkey's HSD test with α=0.05) was made and summarized in Table 14, and a least square plot is shown in Figure 57.

According to the statistical results show in Table 13 obtained from F-test, it was found that there was no statistically significant difference between polymer reaction time (in hours). Furthermore, based on Table 14 all levels of polymer reaction duration were connected by the same letter "A" which means there was no statistically significant difference between any of these polymer reaction durations. The lateral-like line with no amplitudes in Figure 57 also presented the same result. It is thus reasonable to conclude that there is no statistically significant difference in polymer reaction duration.

Table 13. ANOVA table for modified asphalt binders G*/sin(δ) at different reaction durations and test temperatures

Source	DF	Sum of Squares	Mean Square	F Ratio	Prob>F
Reaction duration, hr	6	323.23	53.87	0.4980	0.7914
Test temp, °C	5	488077.75	97615.55	902.755	<.0001*
Reaction duration*Test temp	30	1055.53	35.18	0.3252	0.9818
Error	6	649.06	108.2		
C. Total	47	523785.82			

Note: statistically significant at $\alpha<0.05$.

Table 14. Least square means differences for modified asphalt binders G*/sin(δ) at different reaction durations

α	Q	
0.05	4.16861	
Level		Least Sq Mean
4	A	54.034917
5	A	54.357117
8	A	59.986208
9	A	60.011250
10	A	60.187683
11	A	61.040883
12	A	59.450717

Note: Levels not connected by same letter are significantly different.

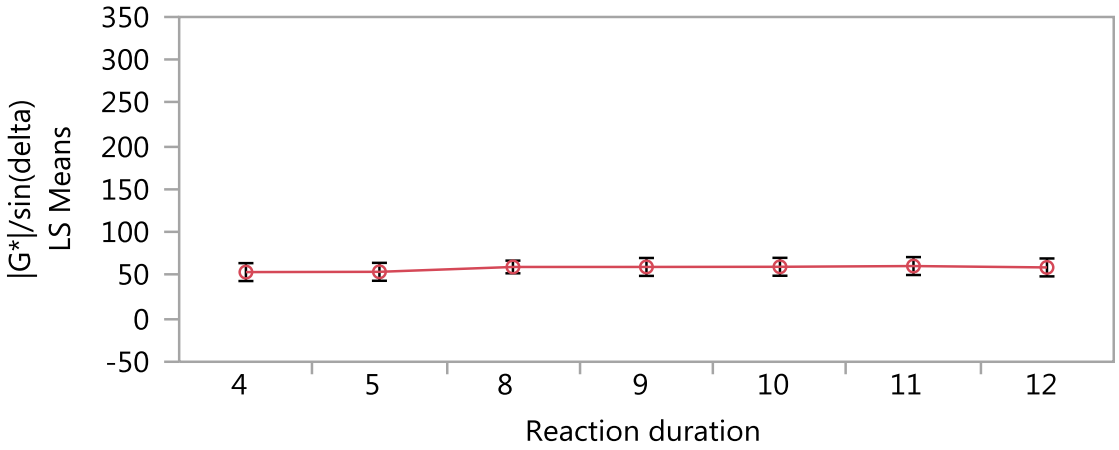

.

Figure 57. Least square means plot for modified asphalt binders G*/sin(δ) at different reaction durations

To reduce the random error variation that caused by the difference between the modified blends for evaluating the effects of polymer reaction duration, blocking design was performed to make the blends uniform within each block based on the least square means from the HSD table. Because the polymer reaction durations of four and five hours have close least square mean while they are off approximately five from the rest of the durations, two blocks were designed by using short and long which stands for the short polymer duration and the long polymer duration. The ANOVA table from F-test for the block design statistical analysis is shown as Table 15. The least squares means is shown in Table 16 with a least mean plot shows in Figure 58. The Student's t-test at α=0.05 was also performed to evaluate the statistical significant difference of the blocks (Table 17).

According to the ANOVA table (Table 15), there is statistically significant difference between the two blocks which means the long and short reaction durations were statistically different since the p-value from the F-test is smaller than 0.05. The same results were obtained from the Student's t-tests (Table 17), which shows different letter level between the long and short blocks that indicates the statistically significant difference between the two blocks.

Table 15. ANOVA table for modified blends with blocks of polymer reaction duration

Source	DF	Sum of Squares	Mean Square	F Ratio	Prob>F
Block	1	314.83	314.8	7.5354	0.0089
Test temp, °C	5	521758.01	104351.6	2497.642	<.0001*
Error	41	1712.98	41.8		
C. Total	47	523785.82			

Note: statistically significant at $\alpha<0.05$.

Table 16. Least square means table of the blocks (long reaction duration and short reaction duration)

Level	Least Sq Mean	Std Error	Mean
long	60.110492	1.0772914	60.1105
short	54.196017	1.8659234	54.1960

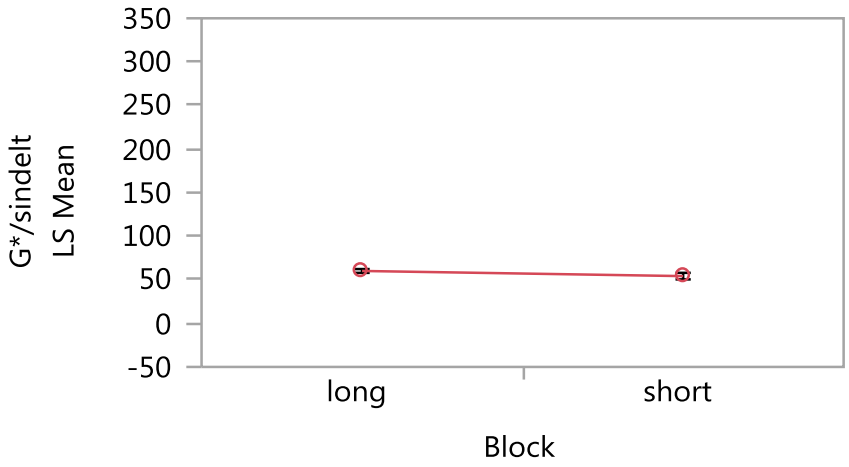

Figure 58. Least square means plot of blocks (long and short reaction duration)

Table 17. Least square means differences student's t table of long and short reaction durations

α	t	
0.05	2.01954	
Level		Least Sq Mean
long	A	60.110492
short	B	54.196017

Note: Levels not connected by same letter are significantly different.

Statistical analysis on the effects of shear blending methods

Three different shear blending methods (method A, method B, and method C) were applied in this study. The statistical analysis on effects of different shear blending methods were investigated by running the fit model on the blends using the same PS-PAESO bio-based polymer with the same styrene molecular weight (30kDa) and styrene content (25%) at 8 hours reaction duration. The high temperature G*/sin(δ) resulted from three test temperatures (46, 52, and 58°C) were used as responses. The blends used in the statistical software JMP for running the fit model were blends 2, 3, 8, and 12.

The statistical analysis for these blends is summarized in Table 18, which shows there was no statistically significant difference between shear blending methods. The same results can also be observed in Table 19 due to these three methods were all in the same connecting level "A" when using the Turkey's HSD test with α=0.05, although the least square plot in Figure 59 shows method A has a slightly higher least square mean value as compared to the other two methods results.

Table 18. ANOVA table for modified asphalt binders G*/sin(δ) by using different shear blending methods at different test temperatures

Source	DF	Sum of Squares	Mean Square	F Ratio	Prob>F
Shear blending method	2	1.119396	0.559698	1.2477	0.4033
Test temp, °C	2	16.712854	8.356427	18.6290	0.0203*
Shear blending method*Test temp	4	0.492201	0.123050	0.2743	0.8782
Error	3	1.345715	0.44857		
C. Total	11	23.584379			

Note: statistically significant at α<0.05.

Table 19. Least square means differences for modified asphalt binders G*/sin(δ) by different shear blending methods

α	Q	
0.05	4.17871	
Level		Least Sq Mean
A	A	2.4199862
B	A	1.8362667
C	A	1.784233

Note: Levels not connected by same letter are significantly different.

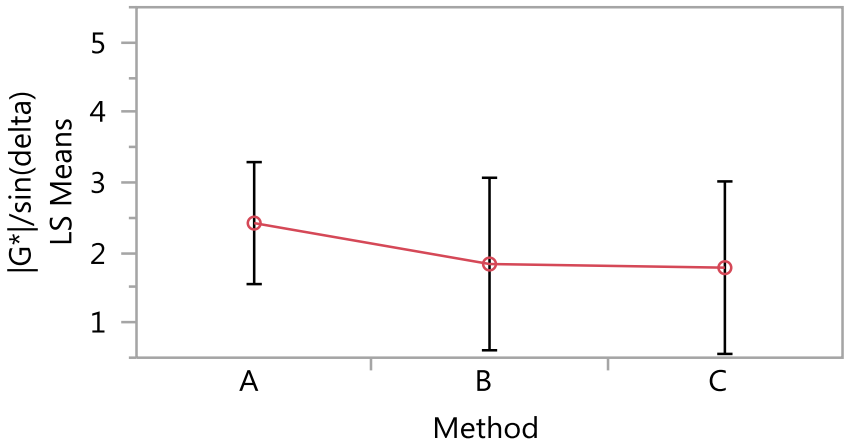

Figure 59. Least square means plot for modified asphalt binders G*/sin(δ) by different shear blending methods

In order to reduce the random error variation and make the different shear blending methods effects easier to observe, the block design was performed based on the difference among the least square means. Because the shear blending method A has higher least square mean, while the method B and method C have close least square mean with a difference less than 0.1, the two blocks were formed by using the higher least square mean and the lower least square mean. The ANOVA table from F-test with the block design is shown as Table 20. The least squares means is shown in Table 21 with a least mean plot showing in Figure 60. The Student's t-test at $\alpha=0.05$ was also performed to evaluate the statistical significant difference of the blocks (Table 22).

The ANOVA table (Table 20) shows no statistically significant difference between the blocks which means the shear blending methods were not statistically different due to the p-value is 0.0589 that is larger than 0.05. However, the p-value is with only 17.8% off to 0.05. Based on the multi-lab variability in the practical experiments, there was a possibility that the shear blending methods could have statistically significant difference towards the test results. The Student's t-test result (Table 22) shows the same results that obtained from the F-test. The two blocks of higher and lower are in the same letter level which means there is no statistically significant difference between the shear blending methods.

Table 20. ANOVA table for modified blends with blocks of shear blending method

Source	DF	Sum of Squares	Mean Square	F Ratio	Prob>F
Block	1	1.115335	1.11533	4.8441	0.0589
Test temp, °C	2	20.627068	10.31353	44.7933	<.0001*
Error	8	1.841977	41.8		
C. Total	11	23.584379			

Note: statistically significant at α<0.05.

Table 21. Least square means table of the blocks (method A with higher least square mean and method B & method C with lower least square means)

Level	Least Sq Mean	Std Error	Mean
higher	2.4199862	0.19589417	2.41999
lower	1.8102500	0.19589417	1.81025

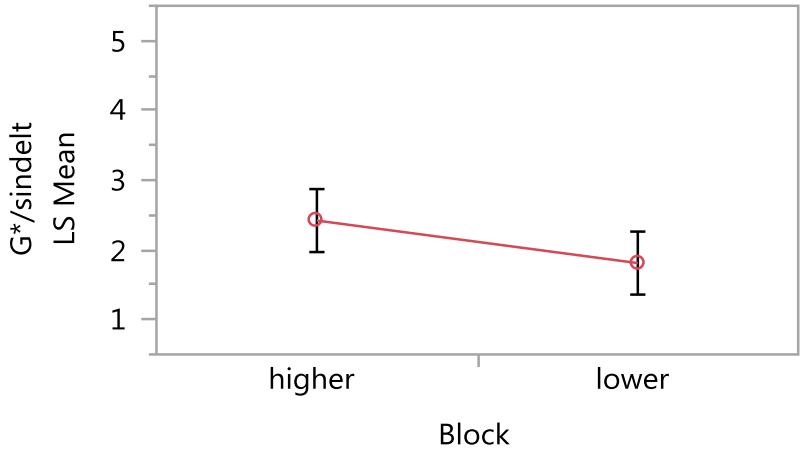

Figure 60. Least square means plot of blocks (method A with higher least square mean and method B & method C with lower least square means)

Table 22. Least square means differences student's t table of higher and lower shear blending methods' least square means

α	t	
0.05	2.306	
Level		Least Sq Mean
higher	A	2.4199862
lower	A	1.8102500

According to the statistical analysis results, the two factors, the polymer reaction duration and the shear blending method, were proved to have no statistically significant difference from the treatment factors test results for F-tests. However, after conducting the block designs within the treatments for each statistical analysis, the ANOVA tables form the F-test and the student's test results showed statistically significant difference between the long and short polymer reaction durations but no statistically significant difference between the shear blending methods.

Response surface modeling for shear blending results

The response surface modeling was used for predicting the optimum styrene molecular weight and styrene content in producing bio-based polymers for asphalt modification at both high temperature and low temperature.

The DSR results (high temperature) G*/sin (δ) for unaged modified asphalt blends, the DSR results (high temperature) G*/sin (δ) for RTFO short-term aged modified asphalt blends, and the BBR results (low temperature) m-value and stiffness for PAV long-term aged modified asphalt blends were used as responses respectively with factors of styrene molecular weight, styrene content, and test temperature in the response surface modeling. The final set of prediction models can be performed through the step-down regression process by eliminating high p-value process for unmodified state, a logarithm base 10 transformed state, and root square transformed state as described in Chapter 3. The final prediction models using the statistical software JMP provides output for each state with corresponding residual distributions and standard deviations and are summarized in Appendix B. By comparing the residuals of all these prediction models, one followed the normal distribution conditions and same standard deviation were selected as the model for predicting the recommended bio-based polymer styrene parameters (styrene molecular weight and styrene content).

The final model chosen for the unaged modified asphalt blend DSR results (high temperature) G*/sin (δ) was the logarithm base 10 transformed state model with a 99.2% R^2 value whose residuals follow a normal distribution condition. The ANOVA table and the corresponding coefficient values table of the final logarithm base 10 transformed state model are shown in Table 23 and Table 24. The finalized prediction model is presented in Equation 4.

Table 23. ANOVA of Log10 transformed model for unaged modified asphalt blends DSR results G*/sin (δ)

Source	DF	Sum of Squares	Mean Square	F Ratio	Prob>F
Styrene MW,kDa_X1	1	0.0394668	0.039467	6.1420	0.0146*
Styrene content,%_X2	1	0.0514770	0.051477	8.0111	0.0055*
Test Temp,°C_X3	1	3.9912734	3.991273	621.1445	<.0001*
X1^2	1	0.0344727	0.034473	5.3648	0.0223*
X2^2	1	0.0420303	0.042030	6.5410	0.0118*
X3^2	1	0.3465335	0.346534	53.9295	<.0001*

Note: statistically significant at $\alpha<0.05$.

Table 24. Coefficient value based on the Log10 transformed model for unaged modified asphalt blends DSR results G*/sin (δ)

Coefficient	Value
β_0	5.2072488
β_1	-0.034097
β_2	-0.038773
β_3	-0.097251
β_{11}	0.0007949
β_{22}	0.0005626
β_{33}	0.0003648

$$\left(\frac{G^*}{\sin\delta}\right) = 10^{(\beta_0+\beta_1\times x_1+\beta_2\times x_2+\beta_3\times x_3+\beta_{11}\times x_1^2+\beta_{22}\times x_2^2+\beta_{33}\times x_3^2)} \quad (4)$$

The final model selected for the RTFO short-term aged modified asphalt blend DSR results (high temperature) G*/sin (δ) was the logarithm base 10 transformed state model with a 98.9% R^2 value whose residuals follow a normal distribution condition. The ANOVA table and the corresponding coefficient values table of the final logarithm base 10 transformed state model are shown in Table 25 and Table 26. The finalized prediction model is summarized in Equation 5.

Table 25. ANOVA of Log10 transformed model for RTFO short-term aged modified asphalt blends DSR results G*/sin (δ)

Source	DF	Sum of Squares	Mean Square	F Ratio	Prob>F
Styrene MW,kDa_X1	1	0.1867863	0.186786	21.1752	<.0001*
Styrene content,%_X2	1	0.4408357	0.440836	49.9757	<.0001*
Test Temp,°C_X3	1	3.4373152	3.437315	389.6739	<.0001*
X2^2	1	0.5410697	0.541070	61.3388	<.0001*
X3^2	1	0.1987523	0.198752	22.5317	<.0001*

Note: statistically significant at α<0.05.

Table 26. Coefficient value based on the Log10 transformed model for RTFO short-term aged modified asphalt blends DSR results G*/sin (δ)

Coefficient	Value
β_0	6.214795
β_1	-0.004307
β_2	-0.113069
β_3	-0.09025
β_{22}	0.0020146
β_{33}	0.0002762

$$\left(\frac{G^*}{\sin\delta}\right) = 10^{(\beta_0+\beta_1\times x_1+\beta_2\times x_2+\beta_3\times x_3+\beta_{22}\times x_2^2+\beta_{33}\times x_3^2)} \quad (5)$$

For the low temperature BBR results for the m-value, the final model selected for the PAV long-term aged modified asphalt blends was the root square transformed state model with a 75.5% R^2 value whose residuals follow a normal distribution condition. The ANOVA table and the corresponding coefficient values table of the final root square transformed state model are shown in Table 27 and Table 28. The finalized prediction model is presented in Equation 6.

Table 27. ANOVA of root square transformed model for PAV long-term aged modified asphalt blends BBR results m-value

Source	DF	Sum of Squares	Mean Square	F Ratio	Prob>F
Test Temp,°C_X3	1	0.09854171	0.0985417	361.1216	<.0001*
X1^2	1	0.00483513	0.0048351	17.7191	<.0001*

Note: statistically significant at α<0.05.

Table 28. Coefficient value based on the root square transformed model for PAV long-term aged modified asphalt blends BBR results m-value

Coefficient	Value
β_0	0.7646011
β_3	0.0093219
B_{11}	0.0000165

$$(\text{m} - \text{value}) = (\boldsymbol{\beta_0} + \boldsymbol{\beta_3} \times \mathbf{x_3} + \boldsymbol{\beta_{11}} \times \mathbf{x_1^2})^2 \quad (6)$$

For the low temperature BBR results for the stiffness, the final model selected for the PAV long-term aged modified asphalt blends was the root square transformed state model with a 90.4%R^2 value whose residuals follow a normal distribution condition. The ANOVA table and the corresponding coefficient values table of the final logarithm base 10 transformed state model are shown in Table 29 and Table 30. The finalized prediction model is shown in Equation 7.

Table 29. ANOVA of root square transformed model for PAV long-term aged modified asphalt blends BBR results stiffness

Source	DF	Sum of Squares	Mean Square	F Ratio	Prob>F
Styrene content,%_X2	1	0.0226964	0.022696	7.3846	0.0075*
Test Temp,°C_X3	1	3.3961662	3.396166	1104.991	<.0001*
X1*X2	1	0.0449096	0.044910	14.6120	0.0002*
X2^2	1	0.0341395	0.034140	11.1078	0.0011*

Note: statistically significant at $\alpha<0.05$.

Table 30. Coefficient value based on the root square transformed model for PAV long-term aged modified asphalt blends BBR results stiffness

Coefficient	Value
β_0	1.3949165
β_2	-0.025458
β_3	-0.054725
β_{12}	-0.000072
β_{22}	0.0005025

$$(\text{stiffness}) = \mathbf{10}^{(\boldsymbol{\beta_0}+\boldsymbol{\beta_2}\times\mathbf{x_2}+\boldsymbol{\beta_3}\times\mathbf{x_3}+\boldsymbol{\beta_{12}}\times\mathbf{x_1}\times\mathbf{x_2}+\boldsymbol{\beta_{22}}\times\mathbf{x_2^2})} \quad (7)$$

Each prediction model needs to be combined with corresponding coefficient values in each coefficient values table to determine a formulation of the block co-polymer for use in an asphalt binder. In order to determine the appropriate styrene molecular weight and styrene content corresponding to a performance grade of an asphalt binder, each prediction model should meet its criteria according to the Superpave standard specifications as summarized here:

- Equation 4 should be equal to 1.0 (kPa), which is the G*/sin (δ) critical limit for high temperature rutting deformation of unaged asphalt binder;
- Equation 5 should be equal to 2.2 (kPa), which is the G*/sin (δ) critical limit for high temperature rutting deformation of the RTFO short-term aged asphalt binder;
- Equation 6 should be equal to or greater than 0.300 (MPa), which is the m-value critical limit for low temperature thermal cracking of the PAV long-term aged asphalt binder; and
- Equation 7 should be equal to or less than 300 (MPa), which is the stiffness critical limit for low temperature thermal cracking of the PAV long-term aged asphalt binder.

As calculated, the predicted polymers with the recommended styrene molecular weight and styrene content that could modify the base asphalt to be as PG 64-28 are shown in Table 31.

Table 31. The recommended polymer

Predicted Polymer					
Styrene MW, kDa	5	10	35	40	40
Styrene Content,%	5	5	5	5	10
Critical high temp(unaged)	66	64	65	68	65
Critical high temp (RTFO aged)	77.5	77	74.5	74	66
Critical low temp@-18°C(m-value)	0.357	0.358	0.381	0.3884	0.388
Critical low temp@-18°C(stiffness)	183.42	148.61	178.91	178.17	140.23

CHAPTER 5. CONCLUSIONS AND RECOMMENDATIONS

This chapter presents an overview of the technical merit and scientific value gained from the study and an overview of the lessons learned. The conclusions are presented based on the laboratory results, statistical analysis, and statistical prediction modeling, followed by recommendations for future research and practice.

The specific objectives of this study were to evaluate the rheological properties and performance grades of the based asphalt binder (PG XX-34) modified by bio-based polymers with various styrene molecular weights (MW, kDa) and styrene contents (PS-PAESO and PS-PAESO-Cl) at 3% by total weight of the asphalt-polymer blend via different blending approaches. By means of statistical analysis and statistical prediction modeling, the prediction model was expected to be investigated based on laboratory test results to predict the optimum bio-based polymer styrene parameters (styrene molecular weight and styrene content) that improve the elasticity of the base asphalt binders at high temperature.

GENERAL CONCLUSIONS

The overall conclusions about the application of bio-based polymers (PS-PAESO, PS-PAESO-Cl) used as modifiers in base asphalt binder can be summarized as follows:

- The bio-based polymer (PS-PAESO, PS-PAESO-Cl) modified blends by solvent blending approach presented an average critical high temperature at 65.2°C for unaged modified blends, which is approximately 9°C higher than the modified blends by traditional shear blending approach. A possible reason is that solvent blending provides better compatibility between polymers and the base asphalt binder. However, solvent blending should not be recommended for industry bitumen modification due to the high price of available solvent (e.g. THF) and the time-consuming processes (air drying and oven drying) to pull out of the solvent from asphalt blends;
- By evaluating the shear blending results of both unaged and the RTFO short-term aged modified asphalt blends, the bio-based polymers helped increase the critical high temperature from 53.4°C to 53.7–62.0°C;
- Based on the critical low temperature results, 12 out of the 18 bio-based polymer modified blends were graded as -34°C which was the same as the base asphalt binder, whereas the other six of the bio-based polymer modified blends increased 1 or 2°C than

the base asphalt binder. Therefore, the bio-based polymers used in this study had no effect on improving the low temperature performance grades, which means these polymer did not substantially improve the resistance to thermal cracking.;

- According to the continuous performance grade range results, 11 out of the 18 modified blends presented higher ranges than the base asphalt binder, which resulted in reducing the temperature susceptibility of the base asphalt. This conclusion matches to the finding reported by Williams et al. (2014);
- The master curves showed a trend of the complex modulus (G*) improvement of all bio-based polymer modified asphalt blends, which indicated the establishment of a rubber-elastic network within the modified blends. All modified blends became stiffer especially at lower frequency higher temperatures, which means the bio-based polymers improved the rutting resistance of asphalt binder. This conclusion also matches the finding reported by Williams et al. (2014);
- According to the black diagrams, higher G* (stiffness) corresponding to lower temperatures higher frequency with a shift/trend towards lower phase angles were observed, which means the hardening and aging of the base asphalt binder due to polymer modification;
- By assessing the rheological properties of modified blends, it can be concluded that bio-based polymers improve the rheological properties of base asphalt binder especially at higher temperatures. Accordingly, an assumption is that a type of PS-PAESO with lower molecular weight and lower styrene content can act as a better bio-based polymer;
- The three different shear blending methods used in this study were proved no statistically significant difference corresponding to the laboratory results of the G*/sin(δ) for high temperature performance;
- The different polymer reaction durations were proved no statistically significant difference corresponding to the laboratory results of the G*/sin(δ) for high temperature performance; However, the further block design performed on the reaction duration shows there is statistically significant difference between the short (four and five hours) and long (eight hours and longer than eight hours) reaction durations;
- Based on the prediction model obtained from statistical response surface modeling, bio-based polymers with lower molecular weight and lower styrene content were

recommended to improve the elasticity of the modified blends at high temperature. The same recommendation on bio-based polymer styrene parameters can also be proposed based on laboratory results.

RECOMMENDATIONS FOR FUTURE RESEARCH

Performing this study raised several areas for future research:

- The bio-based polymers (PS-PAESO) as predicted styrene parameters (styrene molecular weight and styrene content) should be produced for rheology tests to verify the prediction models;
- A dosage study should be conducted, for example 2%, 3%, 4%, and 5% by weight, to achieve the optimum dosage of the bio-based polymer in asphalt modification with desirable rheology properties; and
- A shear blending duration study should also be conducted, for example shear blending for 1.5, 2.0, 2.5, and 3.0 hours, to achieve the optimum blending duration of the bio-based polymer.

WORKS CITED

Abraham, H. (1918). Asphalts and allied substances: their occurrence, modes of production, uses in the arts and methods of testing. D. van Nostrand.

Adekunle, K. F. (2014). Bio-Based Polymers for Technical Applications: A Review—Part 2. *Open Journal of Polymer Chemistry*, *4*(04), 95.

Agilent Technologies (2015). Foundation GPC Polymers and Molecular Weight Slides.

Airey, G. D. (2003). Rheological properties of styrene butadiene styrene polymer modified road bitumens. *Fuel*, *82*(14), 1709-1719.

Airey, G. D. (2004). Styrene butadiene styrene polymer modification of road bitumens. *Journal of Materials Science*, *39*(3), 951-959.

Alonso, S., Medina-Torres, L., Zitzumbo, R., and Avalos, F. (2010). Rheology of asphalt and styrene–butadiene blends. *Journal of materials science*, *45*(10), 2591-2597.

Andjelkovic, D. D., Li, F., and Larock, R. C. (2006). Novel polymeric materials from soybean oils: synthesis, properties, and potential applications. In *ACS symposium series* (Vol. 921, pp. 67-81). Oxford University Press.

Andjelkovic, D. D., Valverde, M., Henna, P., Li, F., and Larock, R. C. (2005). Novel thermosets prepared by cationic copolymerization of various vegetable oils—synthesis and their structure–property relationships. *Polymer*, *46*(23), 9674-9685.

ASTM. (2008). "Standard Test Method for Determining the Flexural Creep Stiffness of Asphalt Binder Using the Bending Beam Rheometer (BBR)." Annual book of ASTM standards, ASTM D6648, West Conshohocken, PA.

ASTM. (2008). "Standard Test Method for Determining the Rheological Properties of Asphalt Binder Using a Dynamic Shear Rheometer." Annual book of ASTM standards, ASTM D7175, West Conshohocken, PA.

ASTM. (2013). "Standard Practice for Accelerated Aging of Asphalt Binder Using a Pressurized Aging Vessel (PAV)." Annual book of ASTM standards, ASTM D6521, West Conshohocken, PA.

ASTM. (2015). "Standard Specification for Performance Graded Asphalt Binder." Annual book of ASTM standards, ASTM D6373, West Conshohocken, PA.

Babu, R., O'Connor, K., and Seeram, R. (2013). Current progress on bio-based polymers and their future trends. *Progress in Biomaterials*, *2*(8).

Bahia, H. U. and Anderson, D. A. (1995). The Pressure Aging Vessel (PAV): a test to simulate rheological changes due to field aging. ASTM special technical publication, 1241, 67-88.

Bahia, H. U., and Anderson, D. A. (1995). The new proposed rheological properties of asphalt binders: why are they required and how do they compare to conventional properties (No. STP 1241,).

Baumann, H., Bühler, M., Fochem, H., Hirsinger, F., Zoebelein, H., and Falbe, J. (1988). Natural fats and oils—renewable raw materials for the chemical industry. *Angewandte Chemie International Edition in English*, *27*(1), 41-62.

BMT, 2013. Rutting problem on the asphalt surface. http://bmt-institute.vn/cong-trinh/van-de-dun-troi-be-tong-nhua/?lang=en.

Bonnaillie, L. M., and Wool, R. P. (2007). Thermosetting foam with a high bio-based content from acrylated epoxidized soybean oil and carbon dioxide.*Journal of applied polymer science*, *105*(3), 1042-1052.

Browarzik, D., Laux, H., and Rahimian, I. (1999). Asphaltene flocculation in crude oil systems. *Fluid phase equilibria*, *154*(2), 285-300.

Brûlé, B., Brion, Y. V. O. N. N. I. C. K., and Tanguy, A. (1988). Paving Asphalt Polymer Blends: Relationships between Composition, Structure and Properties (With Discussion). In *Association of Asphalt Paving Technologists Proc* (Vol. 57).

Bunger, J. W., Thomas, K. P., and Dorrence, S. M. (1979). Compound types and properties of Utah and Athabasca tar sand bitumens. *Fuel*, *58*(3), 183-195.

Bunker, S. P., and Wool, R. P. (2002). Synthesis and characterization of monomers and polymers for adhesives from methyl oleate. *Journal of Polymer Science Part A: Polymer Chemistry*, *40*(4), 451-458.

Bunker, S., Staller, C., Willenbacher, N., and Wool, R. (2003). Miniemulsion polymerization of acrylated methyl oleate for pressure sensitive adhesives.*International journal of adhesion and adhesives*, *23*(1), 29-38.

Cakmakli, B., Hazer, B., Tekin, I. O., Kizgut, S., Koksal, M., and Menceloglu, Y. (2004). Synthesis and characterization of polymeric linseed oil grafted methyl methacrylate or styrene. *Macromolecular bioscience*, *4*(7), 649-655.

Chailleux, E., Audo, M., Queffélec, C., Bujoli, B., Legrand, J., and Lepine, O. (2012). Alternative Binder from microalgae: Algoroute project. In *Alternative Binders for Sustainable Asphalt Pavements*.

Chaiya, C. (2011). Production of bio-oil from coffee residue using pyrolysis process. In *Proceedings of the World Congress on Engineering and Computer Science* (Vol. 2, pp. 19-21).

Chen, G., Chen, J., Srinivasakannan, C., and Peng, J. (2012). Application of response surface methodology for optimization of the synthesis of synthetic rutile from titania slag. Applied Surface Science, 258(7), 3068-3073.

Chen, G. Q., and Patel, M. K. (2011). Plastics derived from biological sources: present and future: a technical and environmental review. *Chemical reviews*, *112*(4), 2082-2099.

Chen, J., Liao, M., and Shiah, M. (2002). Asphalt Modified by Styrene-Butadiene Styrene Triblock Copolymer: Morphology and Modal. *Journal of Materials in Civil Engineering*, 224-229.

Corbett, L. W. (1969). Composition of asphalt based on generic fractionation, using solvent deasphaltening, elution-adsorption chromatography, and densimetric characterization. *Analytical Chemistry*, *41*(4), 576-579.

Corun, R. (2015). Section 1- Introduction to Asphalt Modification. Presentation Slides Prepared for the Association of Modified Asphalt Producers Training Program.

Crivello, J. V., and Narayan, R. (1992). Epoxidized triglycerides as renewable monomers in photoinitiated cationic polymerization. *Chemistry of materials*, *4*(3), 692-699.

Cuperus, F. P., and Derksen, J. T. P. (1996). High value-added applications from vernolic acid.

Cutright, T. J., & Meza, L. (2007). Evaluation of the aerobic biodegradation of trichloroethylene via response surface methodology. Environment international, 33(3), 338-345.

Fernandes, M. R. S., Forte, M. M. C., and Leite, L. F. M. (2008). Rheological evaluation of polymer-modified asphalt binders. *Materials research*, *11*(3), 381-386.

Fini, E. H., Kalberer, E. W., and Shahbazi, A. (2011). Biobinder from swine manure: Sustainable alternative for asphalt binder. In *Transportation Research Board 90th Annual Meeting* (No. 11-3453).

Galià, M., de Espinosa, L. M., Ronda, J. C., Lligadas, G., and Cádiz, V. (2010). Vegetable oil-based thermosetting polymers. *European journal of lipid science and technology*, *112*(1), 87-96.

Gultekin, M., Beker, U., Guner, F. S., Erciyes, A. T., and Yagci, Y. (2000). Styrenation of castor oil and linseed oil by macromer method. *Macromolecular Materials and Engineering*, *283*(1), 15-20.

Guo, A., Demydov, D., Zhang, W., and Petrovic, Z. S. (2002). Polyols and polyurethanes from hydroformylation of soybean oil. *Journal of Polymers and the Environment*, *10*(1-2), 49-52.

Guo, A., Javni, I., and Petrovic, Z. (2000). Rigid polyurethane foams based on soybean oil. *Journal of Applied Polymer Science*, *77*(2), 467-473.

Harmelink, D. S. (1997). Special Polymer Modified Asphalt Cements: Final Report (No. CDOT-DTD-R-97-3).

Harold, V. Q. (2004). Polymer-Modified Asphalts- Enhancin g HMA P erformance. AMAP Annual Meeting. February 10.

Hasan, Z., Kamran, R., Mohammad, F., Ahmad, G., and Hosein, F. (2012). Evaluation of different conditions on the mixing bitumen and carbon nano-tubes. International Journal of Civil & Environmental Engineering IJCEE-IJENS, 12(06).

Hernández, N., Yan, M., Williams, R. C., and Cochran, E. W. (2015). Thermoplastic elastomers from vegetable oils via reversible addition-fragmentation chain transfer polymerization. In *ABSTRACTS OF PAPERS OF THE AMERICAN CHEMICAL SOCIETY* (Vol. 248). 1155 16TH ST, NW, WASHINGTON, DC 20036 USA: AMER CHEMICAL SOC.

Hill, D. R., and Jennings, A. A. (2011). *Bioasphalt from urban yard waste carbonization: A student study* (No. FHWA/OH-2011/13). Ohio Department of Transportation, Research & Development.

Hines, M. L. (1993). Asphalt Cement Performance Improved by Styrelf- Laboratory and Field Data. Koch Materials Company.

Isacsson, U. L. F., and Lu, X. (1999). Characterization of bitumens modified with SEBS, EVA and EBA polymers. *Journal of Materials Science*, *34*(15), 3737-3745.

Kluttz, B. (2012). An Introduction to Modified Asphalt Binders. Presentation Slides. Nebraska Asphalt Paving Conference. February 15.

La Scala, J., and Wool, R. P. (2005). Property analysis of triglyceride-based thermosets. *Polymer*, *46*(1), 61-69.

Lewandowski, L. H. (1994). Polymer modification of paving asphalt binders. *Rubber Chemistry and Technology*, *67*(3), 447-480.

Lewandowski, L.H. (2004). Historical Performance of Polymer Modified Asphalt Pavements: Part I. Presentation Slides. Goodyear Chemical. June 23.

Lewis, M. (2006). Australian building: a cultural investigation. http://www.mileslewis.net/australian-building/. Accessed in Oct. 23, 2015.

Li, F., and Larock, R. C. (2003). Synthesis, structure and properties of new tung oil-styrene-divinylbenzene copolymers prepared by thermal polymerization.*Biomacromolecules*, *4*(4), 1018-1025.

Lu, J., Khot, S., and Wool, R. P. (2005). New sheet molding compound resins from soybean oil. I. Synthesis and characterization. *Polymer*, *46*(1), 71-80.

Lu, X., and Isacsson, U. (1997). Compatibility and storage stability of styrene-butadiene-styrene copolymer modified bitumens. *Materials and Structures*, *30*(10), 618-626.

Lu, X., and Isacsson, U. (2000). Modification of road bitumens with thermoplastic polymers. *Polymer Testing*, *20*(1), 77-86.

Lukkassen, D. and Meidell, A. (2011). Advanced materials and structures and their fabrication processes. Book manuscript, Narvik University College, HiN.

Masson, J. F., Collins, P., Robertson, G., Woods, J. R., and Margeson, J. (2003). Thermodynamics, phase diagrams, and stability of bitumen-polymer blends. *Energy & Fuels*, *17*(3), 714-724.

Matyjaszewski, K., Patten, T. E., and Xia, J. (1997). Controlled/"living" radical polymerization. Kinetics of the homogeneous atom transfer radical polymerization of styrene. *Journal of the American Chemical Society*, *119*(4), 674-680.

McIntosh, J. (2008). The ancient Indus Valley: new perspectives. Abc-Clio.

Mills-Beale, J., You, Z., Fini, E., Zada, B., Lee, C. H., and Yap, Y. K. (2012). Aging Influence on Rheology Properties of Petroleum-Based Asphalt Modified with Biobinder. *Journal of Materials in Civil Engineering*, *26*(2), 358-366.

Moad, G., Rizzardo, E., and Thang, S. H. (2005). Living radical polymerization by the RAFT process. *Australian journal of chemistry*, *58*(6), 379-410.

Moad, G., Rizzardo, E., and Thang, S. H. (2006). Living radical polymerization by the RAFT process—a first update. *Australian Journal of Chemistry*, *59*(10), 669-692.

Murgich, J., Rodríguez, J., and Aray, Y. (1996). Molecular recognition and molecular mechanics of micelles of some model asphaltenes and resins.*Energy & Fuels*, *10*(1), 68-76.

National Asphalt Pavement Association. (2011). The Asphalt Paving Industry, A Global Perspective.

Nevin, C. S. (1966). Vicinal acryloxy hydroxy long chain fatty compounds and polymers thereof. *U.S. Patent 3,256,225,* issued June 14.

Onay, O., and Koçkar, O. M. (2006). Pyrolysis of rapeseed in a free fall reactor for production of bio-oil. *Fuel*, *85*(12), 1921-1928.

Park, S. J., Jin, F. L., and Lee, J. R. (2004). Synthesis and thermal properties of epoxidized vegetable oil. *Macromolecular Rapid Communications*, *25*(6), 724-727.

Peterson, C. and Anderson, H. (1998). Interstate 70 Polymerized Asphalt Pavement Evaluation. Unpublished report. Utah Department of Transportation, Material Division. February.

Podolsky, J. H., Hernández, N., Chen, C., Williams, R. C., and Cochran, E. W. (2015). Use of Bioadvantaged Materials for Use in Bituminous Modification. To be submitted to TRA.

Pryde, E. H. (1979). Natural fatty acids and their sources. *Fatty Acids*, 1-28.

Raouf, M. A., and Williams, R. C. (2010). Rheology of fractionated cornstover bio-oil as a pavement material. *International Journal of Pavements*, *9*(1-2-3).

Road Science, (2015). Distress Guide. http://www.roadscience.net/services/distress-guide.

Roberts, F. L., Kandhal, P. S., Brown, E. R., Lee, D. Y., and Kennedy, T. W. (1996). Hot mix asphalt materials, mixture design and construction.2nd Ed. Lanham, Maryland.

Romagosa, H. (2008). SBS Polymer Supply Outlook. The Association of Modified Asphalt Producers.

Rowlett, R. D., Martinez, D. F., Mofor, D. A., Ramine, R. A., and Tahmoressi, M. (1990). Performance of Asphalt Modifiers: Classification of Modifiers and Literature Review. *Centre for Construction Materials Technology, SWL, Houston*.

Rus, A. Z. M. (2010). Polymers from renewable materials. *Science progress*, *93*(3), 285-300.

Şensöz, S., and Kaynar, İ. (2006). Bio-oil production from soybean (Glycine max L.); fuel properties of Bio-oil. *Industrial Crops and Products*, *23*(1), 99-105.

Shanks, R. and Kong, I. (2012). Thermoplastic Elastomer. In *Thermoplastic Elastomers*, E1-Sonbati, A., Ed. InTech.

Shuler, S. and Epps, J. A. (1982). Paper no.41 presented at a meeting of the Rubber Division. American Chemical Society. Philadelphis, PA, May 4-7.

SMD. (1996). Superpave Series No. 2 (SP-2). Superpave Mix Design. *Asphalt Institute, Lexington, KY.*

Softic, A., Hohmann, A., Hernández, N., Bergman, J., and Cochran, E. (2014). RAFT Polymerization using MMA Poster. NSF Engineering Research Center for Biorenewable Chemicals.

Terrel, R. L. and Epps, J. A. (1988). Asphalt modifiers-a user's manual for additives and modifiers in asphalt pavement. National Asphalt Pavement Association. *Draft report NAPA*.

Thompson, D. C., and Hoiberg, A. J. (1979). Bituminous materials: Asphalt tars and pitches.

Tripathy, A. (2004). Fluorescence Microscopy. Class Slides. Texas A&M University.

Uzun, B. B., Apaydin-Varol, E., Ateş, F., Özbay, N., and Pütün, A. E. (2010). Synthetic fuel production from tea waste: characterisation of bio-oil and bio-char. *Fuel*, *89*(1), 176-184.

Wade, L.G. (2003). Chapter 13 Nuclear Magnetic Resonance Spectroscopy Slides. Organic Chemistry 5th Edition.

Wikipedia, (2015). Asphalt. Access 6-18-2015. https://en.wikipedia.org/wiki/Asphalt.

Williams, R. C., Cascione, A. A., Cochran, E. W., and Hernández, N. B. (2014). Development of Bio-Based Polymers for Use in Asphalt. InTrans Project Reports. Paper 29. Iowa State University.

Wool, R., Kusefoglu, S., Palmese, G., Khot, S., and Zhao, R. (2000). High modulus polymers and composites from plant oils. *U.S. Patent No. 6,121,398*, issued September 19.

Wool, R., Kusefoglu, S., Palmese, G., Khot, S., and Zhao, R. (2000). *U.S. Patent No. 6,121,398*. Washington, DC: U.S. Patent and Trademark Office.

Yang, J, et al. (2007). Polymer modified bitumen. Chemical Industry Press. Beijing.

Yang, L., Dai, C., Ma, L., and Lin, S. (2011). Conjugation of soybean oil and it's free-radical copolymerization with acrylonitrile. *Journal of Polymers and the Environment*, *19*(1), 189-195.

Yildirim, Y. (2007). Polymer modified asphalt binders. *Construction and Building Materials*, *21*(1), 66-72.

Zhang, C., Xia, Y., Chen, R., Huh, S., Johnston, P. A., and Kessler, M. R. (2013). Soy-castor oil based polyols prepared using a solvent-free and catalyst-free method and polyurethanes therefrom. *Green Chemistry*, *15*(6), 1477-1484.

APPENDIX A. DATA FOR CHAPTER 4

Table 32. DSR results for unaged unmodified asphalt binder and unaged modified asphalt binders shear blending at 120°C for 30 minutes and 195°C for 90minutes (total blending length:120 minutes)

		Blend Code				
Temp	Measurement	0	7	6	8	10
46°C	|G*| (Pa)	2375	3179	3218	3234	3129
	δ (degrees)	85.99	84.95	84.9	85.12	85.04
	|G*|/sin(δ) (kPa)	2.381	3.191	3.231	3.246	3.141
52°C	|G*| (Pa)	1072	1406	1435	1446	1389.5
	δ (degrees)	87.45	86.6	86.55	86.79	86.7
	|G*|/sin(δ) (kPa)	1.073	1.409	1.437	1.449	1.392
58°C	|G*| (Pa)	494.1	643	657.6	657.8	657.8
	δ (degrees)	88.53	87.9	87.88	88.08	88.08
	|G*|/sin(δ) (kPa)	0.494	0.644	0.658	0.658	0.658
PG Failing Temp (°C)		53.35	55.82	56.12	56.30	55.80

Note: The blending codes refer to Chapter 3.

Table 33. DSR results for unaged unmodified asphalt binders and unaged modified asphalt binders shear blending at 190°C for 3hours (180minutes) (Part 1)

		Blend Code						
Temp	Measurement	0	7	14	15	19	20	11
46°C	|G*| (Pa)	2375	3179	3358	3480	3614	3542	3505
	δ (degrees)	85.99	84.95	84.52	84.48	84.61	84.2	84.56
	|G*|/sin(δ) (kPa)	2.381	3.191	3.373	3.496	3.630	3.560	3.521
52°C	|G*| (Pa)	1072	1406	1505.5	1551	1597	1563	1529
	δ (degrees)	87.45	86.6	86.255	86.29	86.355	86.05	86.385
	|G*|/sin(δ) (kPa)	1.073	1.409	1.509	1.554	1.600	1.566	1.532
58°C	|G*| (Pa)	494.1	643	690.7	706.2	714.6	712.2	681.8
	δ (degrees)	88.53	87.9	87.68	87.73	87.72	87.55	87.82
	|G*|/sin(δ) (kPa)	0.494	0.644	0.691	0.707	0.715	0.713	0.6823
PG Failing Temp (°C)		53.35	53.35	55.82	56.80	57.26	56.92	56.72

Note: The blending codes refer to in Chapter 3.

Table 34. DSR results for unaged unmodified asphalt binders and unaged modified asphalt binders shear blending at 190°C for 3hours (180minutes) (Part 2)

		Blend Code						
Temp	Measurement	0	7	17	16	21	9	12
46°C	|G*| (Pa)	2375	3179	3724	3767	3338	3694	3357
	δ (degrees)	85.99	84.95	84.39	84.05	84.29	84.33	84.08
	|G*|/sin(δ) (kPa)	2.381	3.191	3.742	3.787	3.354	3.715	3.375
52°C	|G*| (Pa)	1072	1406	1628	1655.5	1472	1625.5	1467
	δ (degrees)	87.45	86.6	86.24	85.96	86.17	86.21	85.97
	|G*|/sin(δ) (kPa)	1.073	1.409	1.632	1.660	1.476	1.629	1.4705
58°C	|G*| (Pa)	494.1	643	742.5	752.6	668.4	729.6	662.6
	δ (degrees)	88.53	87.9	87.70	87.44	87.61	87.66	87.46
	|G*|/sin(δ) (kPa)	0.494	0.644	0.743	0.753	0.669	0.730	0.663
PG Failing Temp (°C)		53.35	55.82	55.82	57.80	56.45	56.36	56.27

Note: The blending codes refer to Chapter 3.

Table 35. DSR results for unaged unmodified asphalt binders and unaged modified asphalt binders shear blending at 190°C for 3hours (180minutes) (Part 3)

		Blend Code						
Temp	Measurement	0	7	13	18	23	26	24
46°C	|G*| (Pa)	2375	3179	-	-	3409	3291	3430
	δ (degrees)	85.99	84.95	-	-	84.56	84.73	84.34
	|G*|/sin(δ) (kPa)	2.381	3.191	-	-	3.425	3.305	3.447
52°C	|G*| (Pa)	1072	1406	2954	2565.5	1526.5	1459.5	1514
	δ (degrees)	87.45	86.6	84.06	83.86	86.29	86.44	86.045
	|G*|/sin(δ) (kPa)	1.073	1.409	2.970	2.581	1.530	1.463	1.518
58°C	|G*| (Pa)	494.1	643	1302	1185	697	668.5	693.1
	δ (degrees)	88.53	87.9	85.94	85.78	87.69	87.8	87.39
	|G*|/sin(δ) (kPa)	0.494	0.644	1.305	1.188	0.698	0.669	0.694
64°C	|G*| (Pa)	-	-	608.75	584.65	-	-	-
	δ (degrees)	-	-	68.99	87.22	-	-	-
	|G*|/sin(δ) (kPa)	-	-	0.610	0.585	-	-	-
PG Failing Temp (°C)		53.35	55.82	60.74	60.01	56.80	56.49	56.47

Note: The blending codes refer to Chapter 3.

Table 36. DSR results for unaged unmodified asphalt binders and unaged modified asphalt binders shear blending at 190°C for 3hours (180minutes) (Part 4)

		Blend Code				
Temp	Measurement	0	7	25	27	28
46°C	|G*| (Pa)	2375	3179	2553	3472	3597
	δ (degrees)	85.99	84.95	85.74	84.4	84.27
	|G*|/sin(δ) (kPa)	2.381	3.191	2.560	3.489	3.615
52°C	|G*| (Pa)	1072	1406	1140.5	1550	1587
	δ (degrees)	87.45	86.6	87.30	86.19	86.15
	|G*|/sin(δ) (kPa)	1.073	1.409	1.142	1.554	1.591
58°C	|G*| (Pa)	494.1	643	523	708.1	717.2
	δ (degrees)	88.53	87.9	88.45	87.62	87.63
	|G*|/sin(δ) (kPa)	0.494	0.644	0.523	0.709	0.718
PG Failing Temp (°C)		53.35	55.82	55.82	57.50	56.90

Note: The blending codes refer to Chapter 3.

Table 37. Mass loss results for RTFO aged modified asphalt binders

Blend Code	Bottle	Binder	After RTFO	Mass Loss, %	Average, %
3	177.8	35.8	213.5	0.28	0.36
	179.1	34.8	213.7	0.57	
	178.8	35.4	214.1	0.28	
	178.9	35.1	213.9	0.28	
12	177.0	35.6	212.6	0.00	0.50
	181.3	35.0	216.1	0.57	
	179.1	35.0	213.9	0.57	
	175.9	35.0	210.6	0.86	
13	175.1	35.3	210.3	0.28	0.43
	169.8	35.5	205.1	0.56	
	170.9	35	205.8	0.29	
	174.3	35	209.1	0.57	
18	173	35.3	208.1	0.57	0.35
	164.9	35	199.8	0.29	
	174.2	35.5	209.6	0.28	
	177	35.3	212.2	0.28	
23	166.5	35.4	201.6	0.85	0.78
	169.6	35.1	204.4	0.85	
	174	35.2	209	0.57	
	173.6	35.3	208.6	0.85	
24	173.2	35.4	208.4	0.56	0.71
	177.9	35.3	212.9	0.85	
	179.1	35.3	214.2	0.57	
	181.3	35.5	216.5	0.85	
25	172.9	35.4	208	0.85	0.71
	174.2	35	209	0.57	
	169.4	35.5	204.6	0.85	

Blend Code	Bottle	Binder	After RTFO	Mass Loss, %	Average, %
	175	35.1	209.9	0.57	
26	177	35.2	211.9	0.85	0.93
	173.2	35	207.7	1.43	
	173.9	35	208.6	0.86	
	181.2	35.4	216.4	0.56	
27	165	35.3	199.7	1.70	0.92
	174.3	35.3	209.5	0.28	
	169.8	35.1	204.6	0.85	
	171	35.5	206.2	0.85	
28	177.9	35.1	213.1	-0.28	0.50
	166.5	35.2	201.3	1.14	
	173.5	35.2	208.4	0.85	
	179.1	35.2	214.2	0.28	

Note: The blending codes refer to Chapter 3.

Table 38. DSR results for RTFO aged unmodified asphalt binders and RTFO aged modified asphalt binders shear blending at 120°C for 30 minutes and 195°C for 90minutes (total blending length:120 minutes)

		Blend Code				
Temp	Measurement	0	7	6	8	10
46°C	|G*| (Pa)	5562	7051	10540	7746	-
	δ (degrees)	82.19	80.73	78.19	80.07	-
	|G*|/sin(δ) (kPa)	5.614	7.145	10.77	7.864	-
52°C	|G*| (Pa)	2407	2968.5	4483.5	3350	-
	δ (degrees)	84.46	83.33	81.09	82.70	-
	|G*|/sin(δ) (kPa)	2.419	2.989	4.539	3.377	-
58°C	|G*| (Pa)	1076	1311	1959	1468	4914
	δ (degrees)	86.35	85.46	83.60	84.96	77.5
	|G*|/sin(δ) (kPa)	1.078	1.315	1.972	1.474	5.034
62°C	|G*| (Pa)	-	-	-	-	2337
	δ (degrees)	-	-	-	-	80.27
	|G*|/sin(δ) (kPa)	-	-	-	-	2.371
70°C	|G*| (Pa)	-	-	-	-	1118
	δ (degrees)	-	-	-	-	82.75
	|G*|/sin(δ) (kPa)	-	-	-	-	1.127
PG Failing Temp (°C)		53.67	55.49	57.52	54.50	66.81

Note: The blending codes refer to Chapter 3.

Table 39. DSR results for RTFO aged unmodified asphalt binders and RTFO aged modified asphalt binders shear blending at 190°C for 3hours (180minutes) (Part 1)

		Blend Code						
Temp	Measurement	0	7	14	15	19	20	11
46°C	|G*| (Pa)	5562	7051	8983	7868	8204	8091	7638
	δ (degrees)	82.19	80.73	78.89	79.50	79.84	79.46	80.34
	|G*|/sin(δ) (kPa)	5.614	7.145	9.155	8.002	8.334	8.23	7.748
52°C	|G*| (Pa)	2407	2968.5	3857	3402.5	3535.5	3542	3323
	δ (degrees)	84.46	83.33	81.64	82.16	82.495	82.01	82.87
	|G*|/sin(δ) (kPa)	2.419	2.989	3.899	3.435	3.566	3.577	3.348
58°C	|G*| (Pa)	1076	1311	1701	1507	1564	1548	1476
	δ (degrees)	86.35	85.46	83.99	84.48	84.75	84.27	85.04
	|G*|/sin(δ) (kPa)	1.078	1.315	1.711	1.514	1.571	1.556	1.482
PG Failing Temp (°C)		53.67	55.49	55.87	54.79	55.25	55.21	54.60

Note: The blending codes refer to Chapter 3.

Table 40. DSR results for RTFO aged unmodified asphalt binder and RTFO aged modified asphalt binders shear blending at 190°C for 3hours (180minutes) (Part 2)

		Blend Code						
Temp	Measurement	0	7	17	16	21	9	12
46°C	|G*| (Pa)	5562	7051	8281	8630	9161	8425	8662
	δ (degrees)	82.19	80.73	79.4	79.29	78.90	79.56	78.96
	|G*|/sin(δ) (kPa)	5.614	7.145	8.425	8.783	9.335	8.567	8.825
52°C	|G*| (Pa)	2407	2968.5	3573.5	3692	3951.5	3645.5	3767
	δ (degrees)	84.46	83.33	82.08	82.01	81.63	82.185	81.58
	|G*|/sin(δ) (kPa)	2.419	2.989	3.608	3.729	3.995	3.680	3.808
58°C	|G*| (Pa)	1076	1311	1576	1625	1708	1597	1674
	δ (degrees)	86.35	85.46	84.38	84.34	83.92	84.48	83.90
	|G*|/sin(δ) (kPa)	1.078	1.315	1.584	1.633	1.717	1.605	1.683
PG Failing Temp (°C)		53.67	55.49	55.21	55.64	56.04	55.49	55.71

Note: The blending codes refer to Chapter 3.

Table 41. DSR results for RTFO aged modified asphalt binders and RTFO aged modified asphalt binders shear blending at 190°C for 3hours (180minutes) (Part 3)

		Blend Code						
Temp	Measurement	0	7	13	18	23	26	24
46°C	|G*| (Pa)	5562	7051	-	-	8179	9812	8488
	δ (degrees)	82.19	80.73	-	-	79.34	78.64	78.96
	|G*|/sin(δ) (kPa)	5.614	7.145	-	-	8.323	10.01	8.648
52°C	|G*| (Pa)	2407	2968.5	6267.5	7273.5	3506.5	4196	3656
	δ (degrees)	84.46	83.33	79.29	78.11	82.00	81.43	81.72
	|G*|/sin(δ) (kPa)	2.419	2.989	6.379	7.433	3.541	4.243	3.695
58°C	|G*| (Pa)	1076	1311	2706	3125	1553	1842	1614
	δ (degrees)	86.35	85.46	81.95	81.07	84.34	83.86	84.14
	|G*|/sin(δ) (kPa)	1.078	1.315	2.733	3.163	1.56	1.853	1.622
64°C	|G*| (Pa)	-	-	1283.5	1471.5	-	-	-
	δ (degrees)	-	-	84.02	83.435	-	-	-
	|G*|/sin(δ) (kPa)	-	-	1.291	1.481	-	-	-
PG Failing Temp (°C)		53.67	55.49	60.42	62.04	55.21	56.89	55.54

Note: The blending codes refer to Chapter 3.

Table 42. DSR results for RTFO aged unmodified asphalt binder and RTFO aged modified asphalt binders shear blending at 190°C for 3hours (180minutes) (Part 4)

		Blend Code				
Temp	Measurement	0	7	25	27	28
46°C	|G*| (Pa)	5562	7051	7016	-	-
	δ (degrees)	82.19	80.73	80.45	-	-
	|G*|/sin(δ) (kPa)	5.614	7.145	7.115	-	-
52°C	|G*| (Pa)	2407	2968.5	3005	5429.5	4736
	δ (degrees)	84.46	83.33	83.04	79.52	79.56
	|G*|/sin(δ) (kPa)	2.419	2.989	3.028	5.522	4.816
58°C	|G*| (Pa)	1076	1311	2099	2375	2099
	δ (degrees)	86.35	85.46	82.28	82.18	82.28
	|G*|/sin(δ) (kPa)	1.078	1.315	2.118	2.397	2.118
64°C	|G*| (Pa)	-	-	-	1139	1010
	δ (degrees)	-	-	-	84.32	84.49
	|G*|/sin(δ) (kPa)	-	-	-	1.145	1.015
PG Failing Temp (°C)		53.67	55.49	56.25	59.11	58.19

Note: The blending codes refer to Chapter 3.

Table 43. BBR results for PAV long-term aged bio-polymers modified asphalt binders

Blend code	Sample #	Testing Temperature [C]	Stiffness [MPa] (<300 MPa)	m-value (>0.3)	Continuous Grade
16	1	-18	82.90	0.380	-35.478
	2		98.20	0.371	
	3		90.50	0.407	
	1	-24	238.00	0.328	
	2		222.00	0.314	
	3		203.00	0.309	
20	1	-18	101.00	0.364	-34.583
	2		91.20	0.378	
	3		113.00	0.384	
	1	-24	243.00	0.327	
	2		221.00	0.289	
	3		207.00	0.304	
21	1	-18	116.00	0.386	-32.788
	2		116.00	0.363	
	3		109.00	0.384	
	1	-24	221.00	0.298	
	2		172.00	0.230	
	3		252.00	0.313	
17	1	-18	119.00	0.387	-34.324
	2		114.00	0.372	
	3		110.00	0.336	
	1	-24	195.00	0.285	
	2		254.00	0.310	
	3		229.00	0.315	
9	1	-18	106.00	0.373	-34.576
	2		118.00	0.359	

Blend code	Sample #	Testing Temperature [C]	Stiffness [MPa] (<300 MPa)	m-value (>0.3)	Continuous Grade
	3		102.00	0.362	
	1	-24	223.00	0.308	
	2		223.00	0.297	
	3		269.00	0.312	
15	1	-18	92.70	0.397	-34.653
	2		87.20	0.383	
	3		81.40	0.395	
	1	-24	119.00	0.313	
	2		183.00	0.297	
	3		218.00	0.317	
19	1	-18	97.10	0.374	-37.024
	2		90.10	0.363	
	3		95.50	0.348	
	1	-24	211.00	0.322	
	2		211.00	0.317	
	3		235.00	0.323	
11	1	-18	99.30	0.359	-37.415
	2		110.00	0.377	
	3		96.20	0.357	
	1	-24	191.00	0.326	
	2		166.00	0.319	
	3		224.00	0.325	
14	1	-18	99.60	0.374	-35.157
	2		93.50	0.360	
	3		107.00	0.364	
	1	-24	218.00	0.318	
	2		233.00	0.310	

Blend code	Sample #	Testing Temperature [C]	Stiffness [MPa] (<300 MPa)	m-value (>0.3)	Continuous Grade
	3		226.00	0.304	
13	1	-18	128.00	0.349	-32.570
	2		131.00	0.367	
	3		128.00	0.347	
	1	-24	209.00	0.294	
	2		283.00	0.284	
	3		265.00	0.271	
18	1	-18	133.00	0.343	-31.535
	2		145.00	0.334	
	3		137.00	0.332	
	1	-24	255.00	0.268	
	2		270.00	0.270	
	3		311.00	0.286	
12	1	-18	108.00	0.381	-41.212
	2		105.00	0.365	
	3		114.00	0.372	
	1	-24	197.00	0.332	
	2		256.00	0.366	
	3		235.00	0.321	
23	1	-18	110.00	0.366	-33.500
	2		112.00	0.375	
	3		99.40	0.368	
	1	-24	214.00	0.287	
	2		251.00	0.309	
	3		207.00	0.285	
24	1	-18	105.00	0.373	-34.090
	2		117.00	0.369	

Blend code	Sample #	Testing Temperature [C]	Stiffness [MPa] (<300 MPa)	m-value (>0.3)	Continuous Grade
	3		113.00	0.360	
	1	-24	254.00	0.305	
	2		223.00	0.295	
	3		232.00	0.303	
25	1	-18	85.50	0.384	-35.406
	2		80.10	0.370	
	3		92.40	0.383	
	1	-24	207.00	0.317	
	2		190.00	0.311	
	3		222.00	0.317	
26	1	-18	98.30	0.380	-33.305
	2		103.00	0.369	
	3		105.00	0.380	
	1	-24	221.00	0.312	
	2		185.00	0.296	
	3		243.00	0.262	
27	1	-18	104.00	0.338	-33.472
	2		98.30	0.351	
	3		120.00	0.356	
	1	-24	227.00	0.278	
	2		187.00	0.323	
	3		253.00	0.285	
28	1	-18	118.00	0.349	-34.394
	2		125.00	0.350	
	3		128.00	0.347	
	1	-24	274.00	0.296	
	2		233.00	0.327	

Blend code	Sample #	Testing Temperature [C]	Stiffness [MPa] (<300 MPa)	m-value (>0.3)	Continuous Grade
	3		261.00	0.286	
6	1	-18	134.00	0.396	-35.562
	2		104.00	0.366	
	3		119.00	0.322	
	1	-24	260.00	0.307	
	2		275.00	0.322	
	3		278.00	0.309	
10	1	-18	110.00	0.388	-34.000
	2		103.00	0.363	
	3		114.00	0.378	
	1	-24	272.00	0.296	
	2		225.00	0.305	
	3		267.00	0.299	
8	1	-18	97.50	0.455	-33.801
	2		101.00	0.363	
	3		106.00	0.373	
	1	-24	238.00	0.299	
	2		237.00	0.291	
	3		224.00	0.300	

Note: The blending codes refer to Chapter 3.

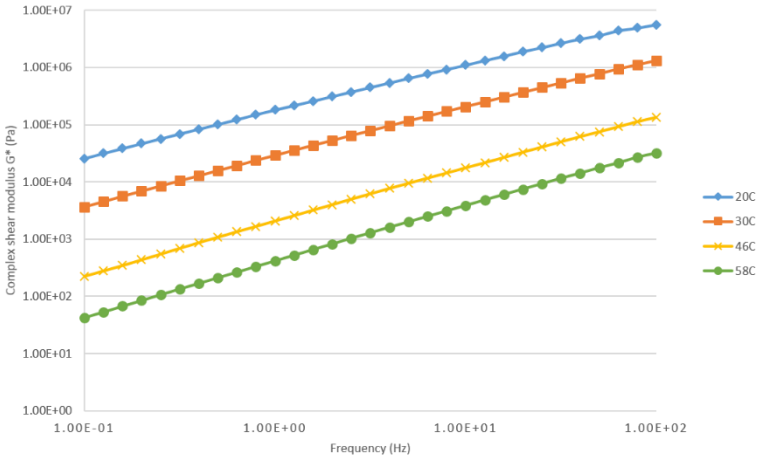

Figure 61. Complex modulus (G*) of unaged blend 6

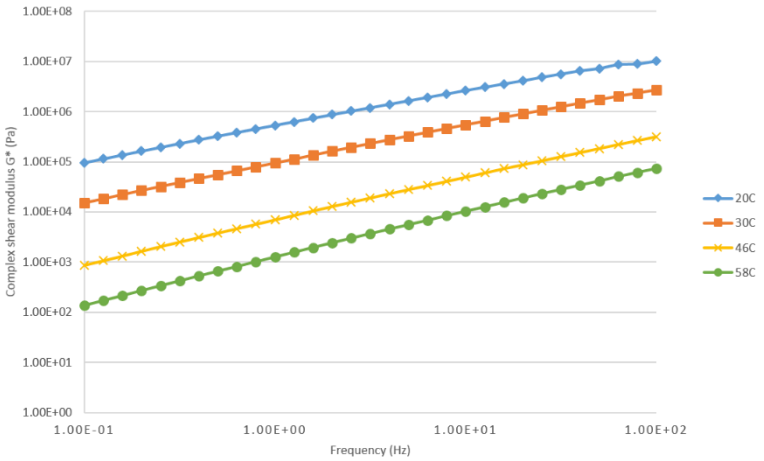

Figure 62. Complex modulus (G*) of RTFO aged blend 6

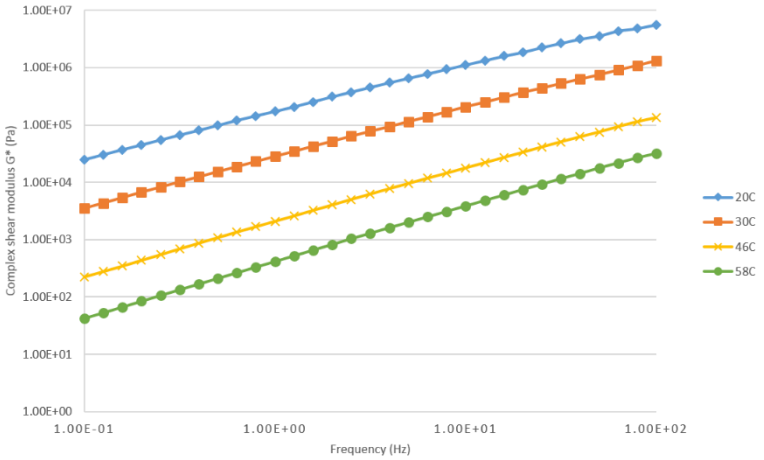

Figure 63. Complex modulus (G*) of unaged blend 8

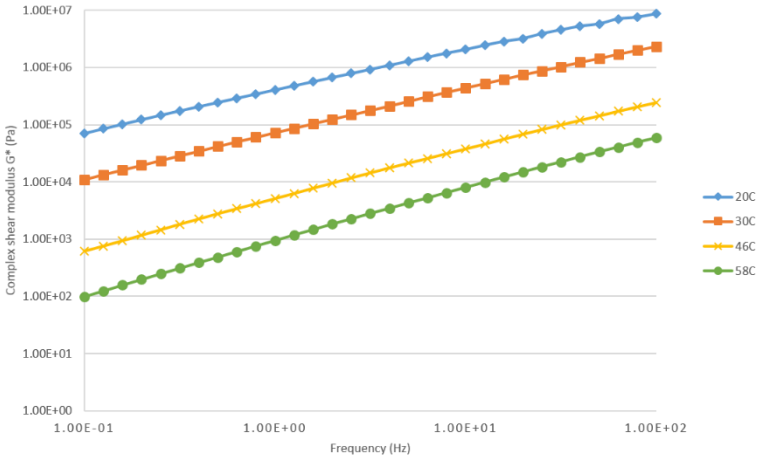

Figure 64. Complex modulus (G*) of RTFO aged blend 8

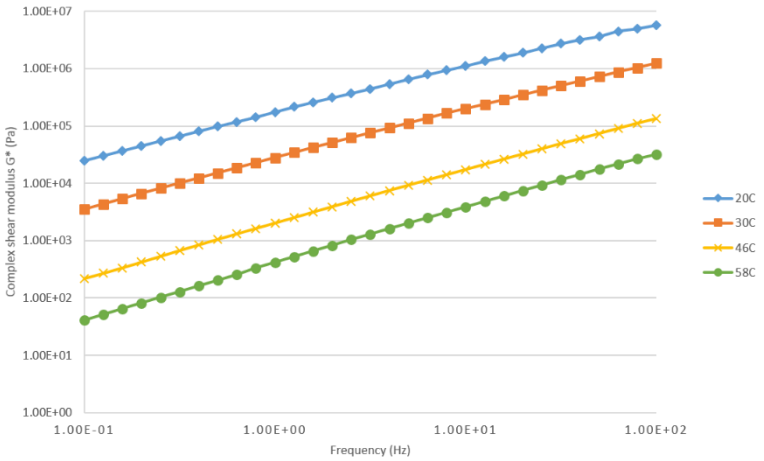

Figure 65. Complex modulus (G*) of unaged blend 10

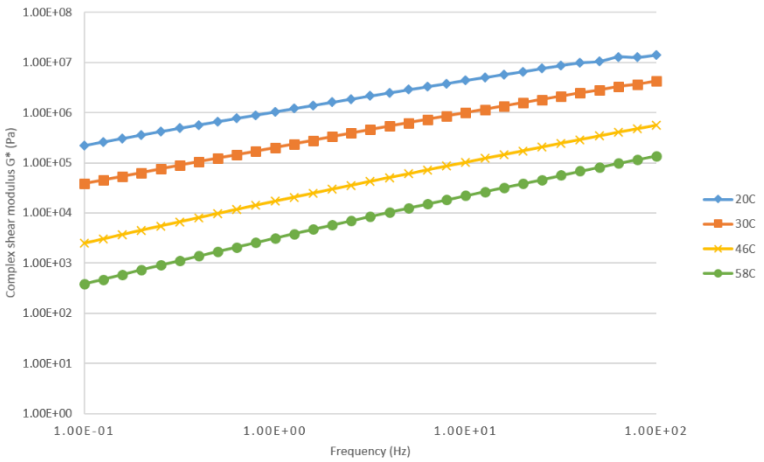

Figure 66. Complex modulus (G*) of RTFO aged blend 10

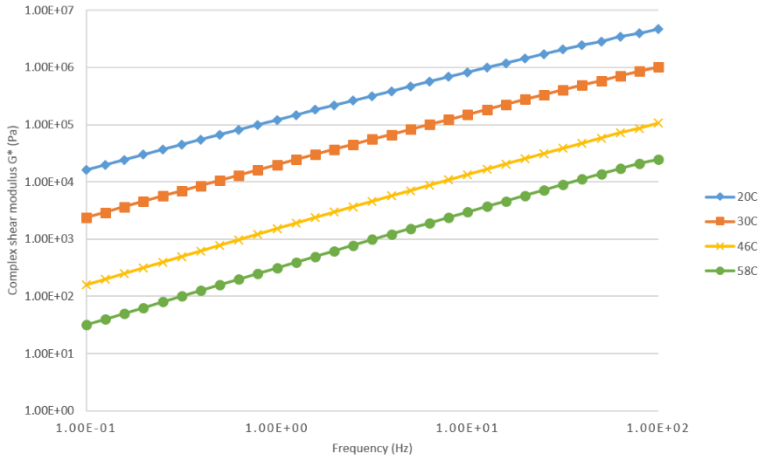

Figure 67. Complex modulus (G*) of unaged base asphalt binder

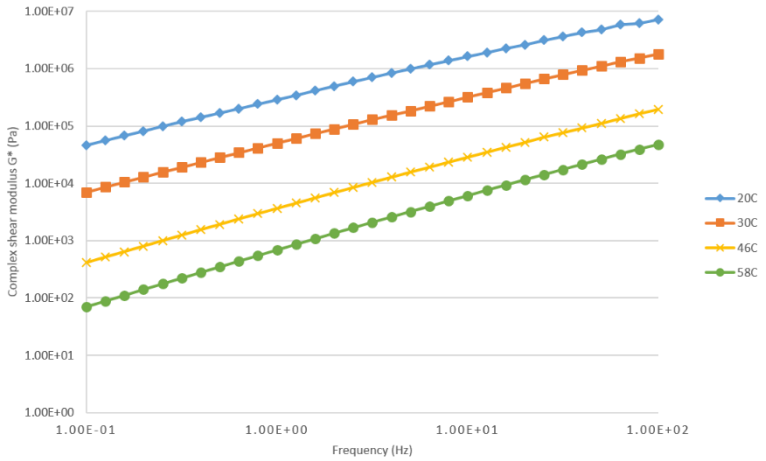

Figure 68. Complex modulus (G*) of RTFO aged base asphalt binder

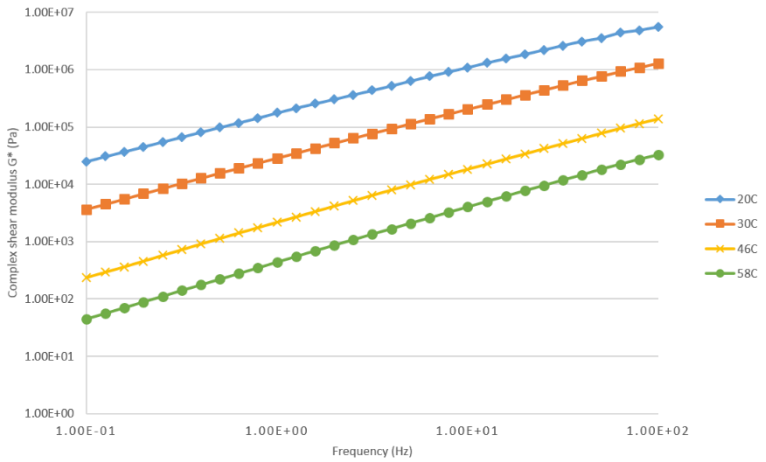

Figure 69. Complex modulus (G*) of unaged blend 14

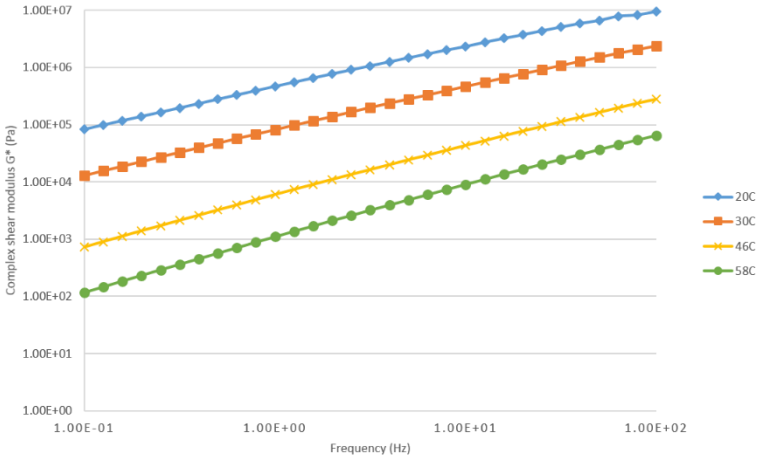

Figure 70. Complex modulus (G*) of RTFO aged blend 14

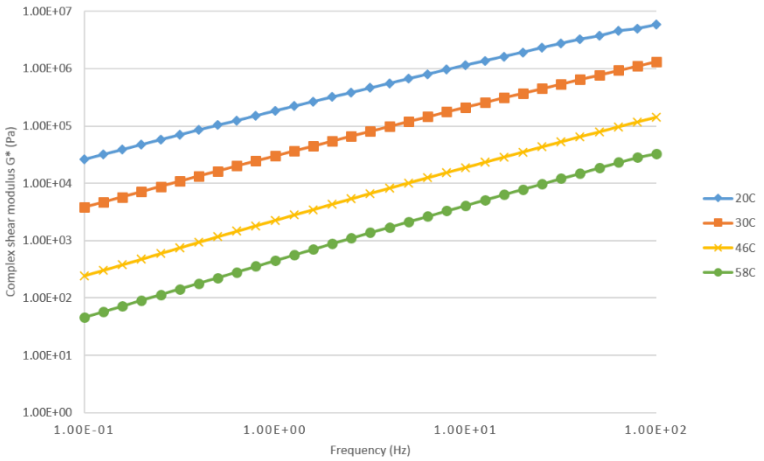

Figure 71. Complex modulus (G*) of unaged blend 15

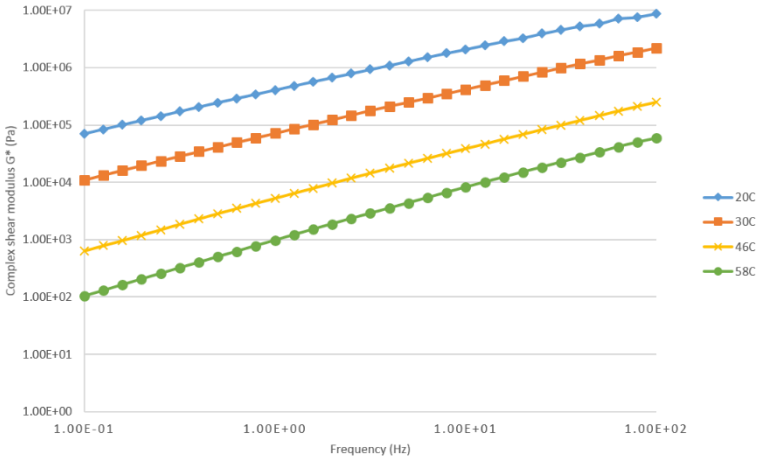

Figure 72. Complex modulus (G*) of RTFO aged blend 15

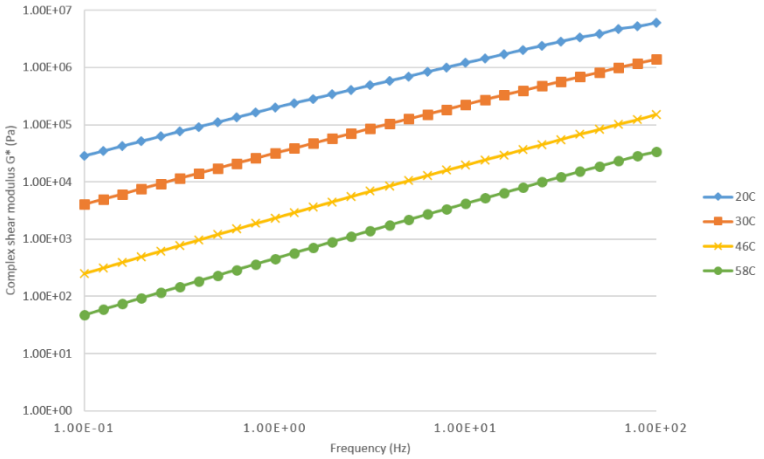

Figure 73. Complex modulus (G*) of unaged blend 19

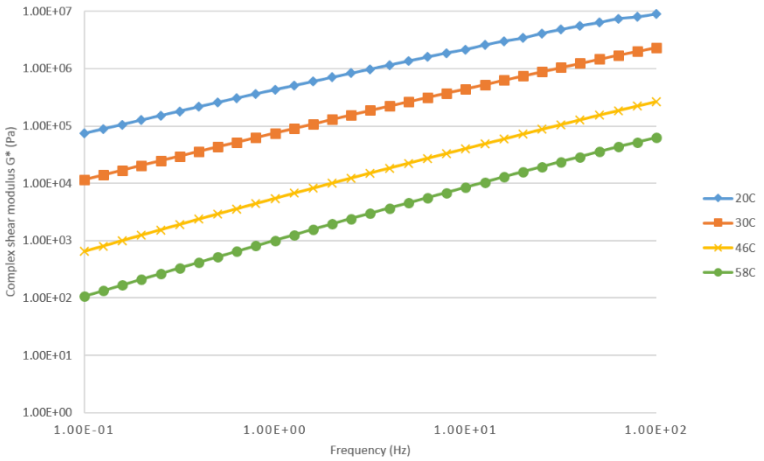

Figure 74. Complex modulus (G*) of RTFO aged blend 19

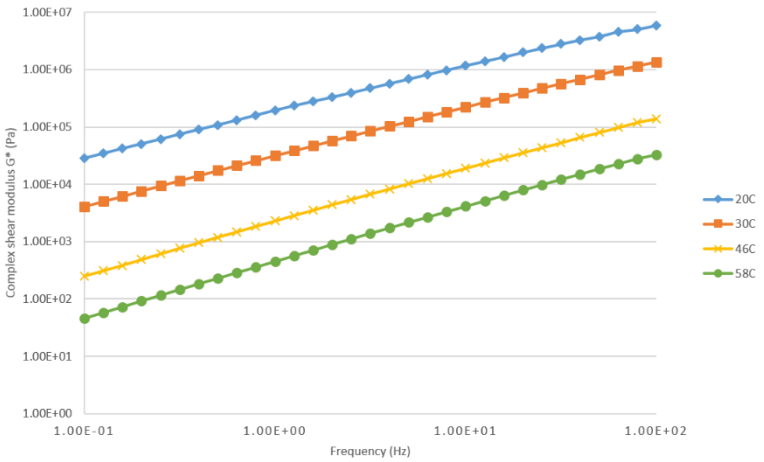

Figure 75. Complex modulus (G*) of unaged blend 20

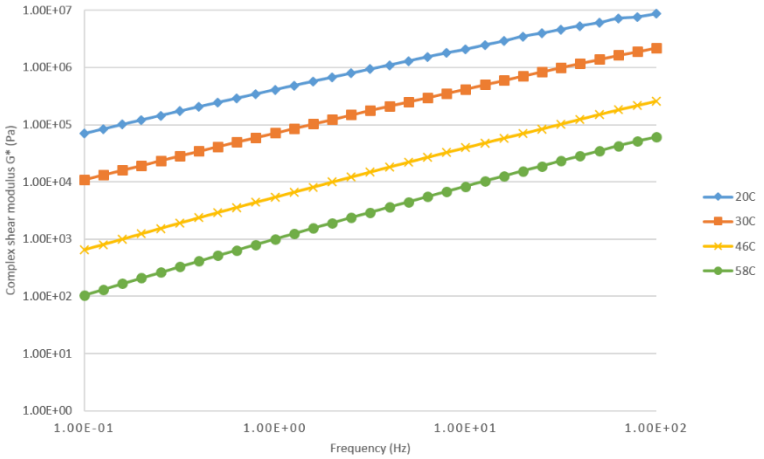

Figure 76. Complex modulus (G*) of RTFO aged blend 20

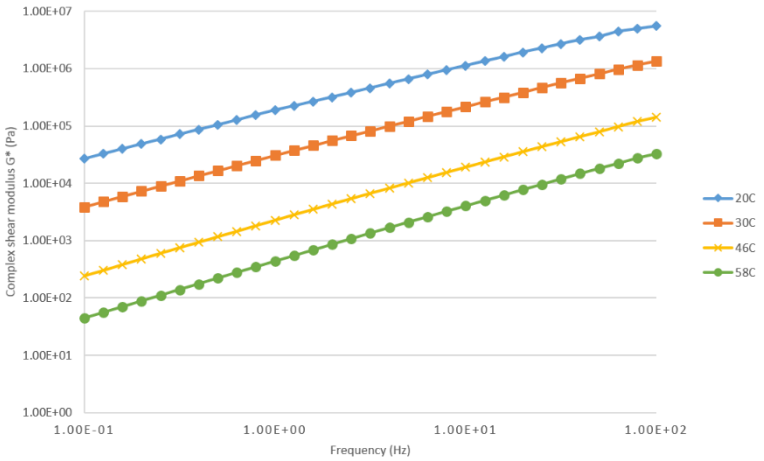

Figure 77. Complex modulus (G*) of unaged blend 11

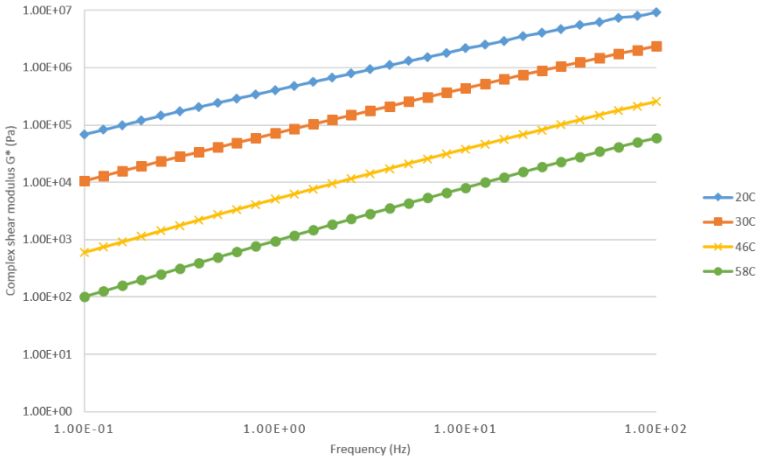

Figure 78. Complex modulus (G*) of RTFO aged blend 11

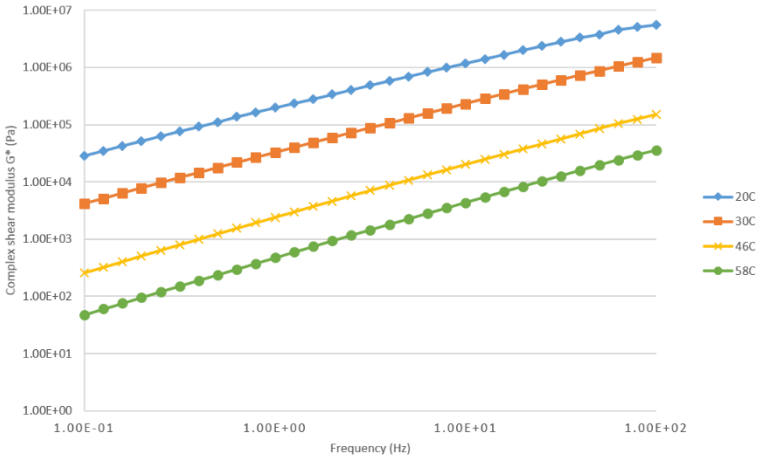

Figure 79. Complex modulus (G*) of unaged blend 17

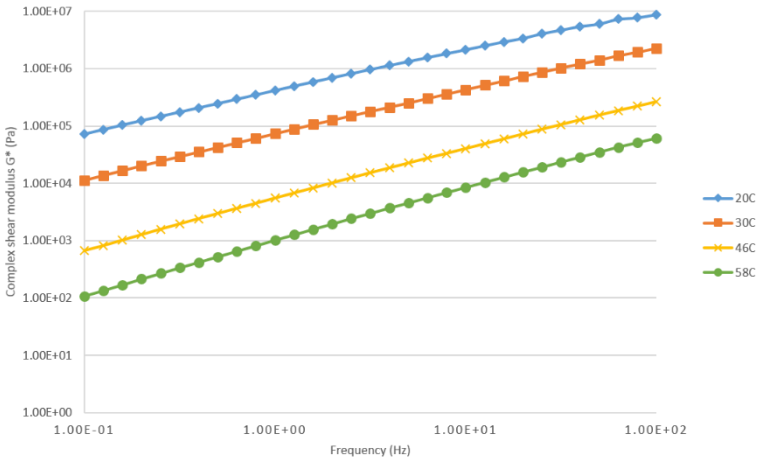

Figure 80. Complex modulus (G*) of RTFO aged blend 11

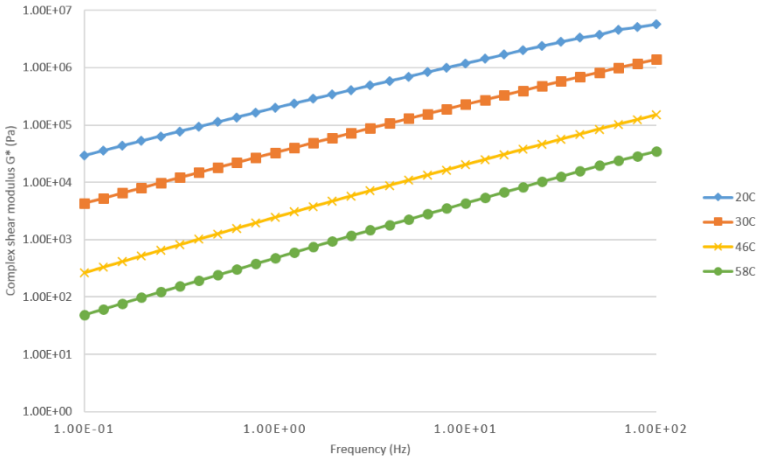

Figure 81. Complex modulus (G*) of unaged blend 16

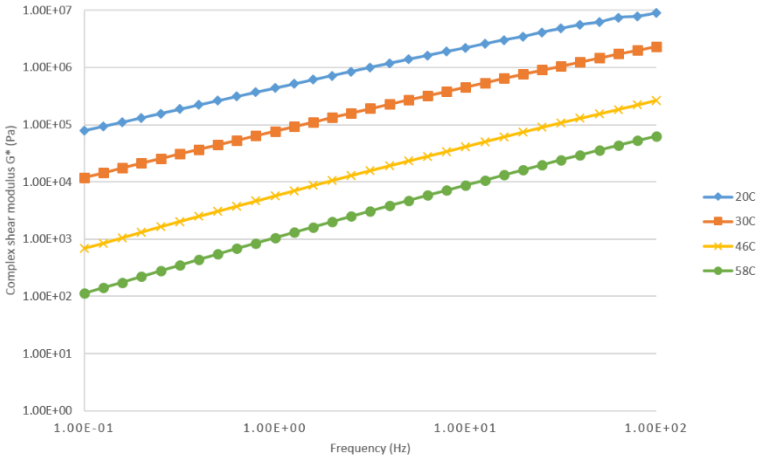

Figure 82. Complex modulus (G*) of RTFO aged blend 16

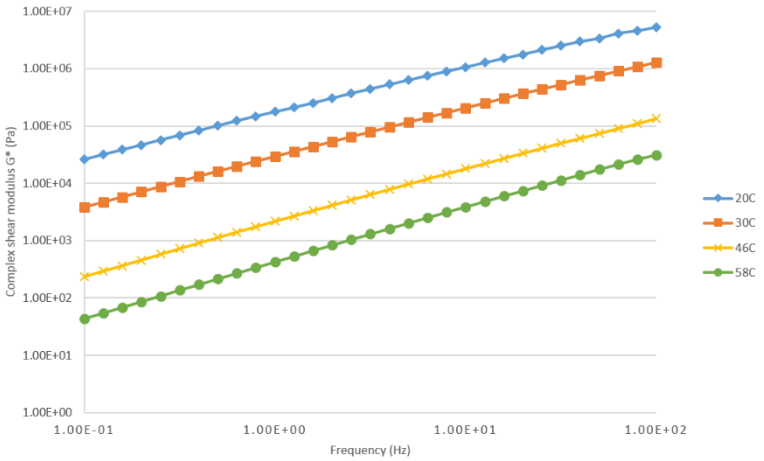

Figure 83. Complex modulus (G*) of unaged blend 21

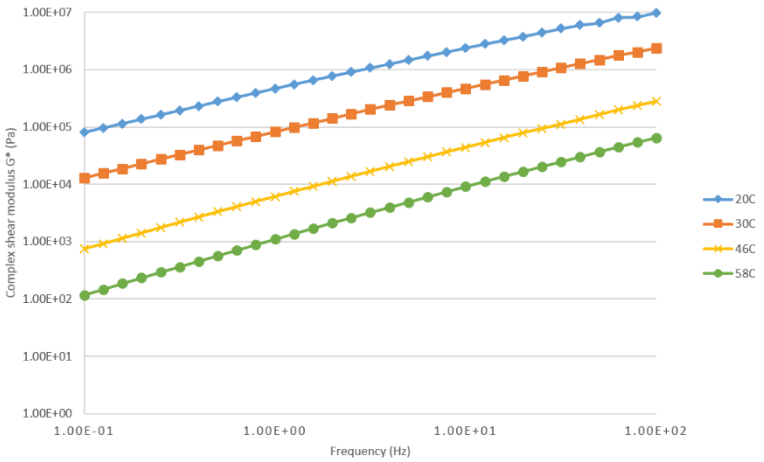

Figure 84. Complex modulus (G*) of RTFO aged blend 21

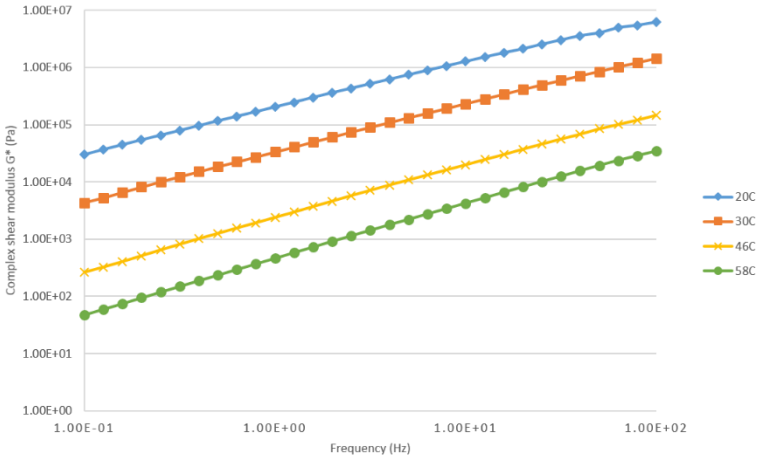

Figure 85. Complex modulus (G*) of unaged blend 9

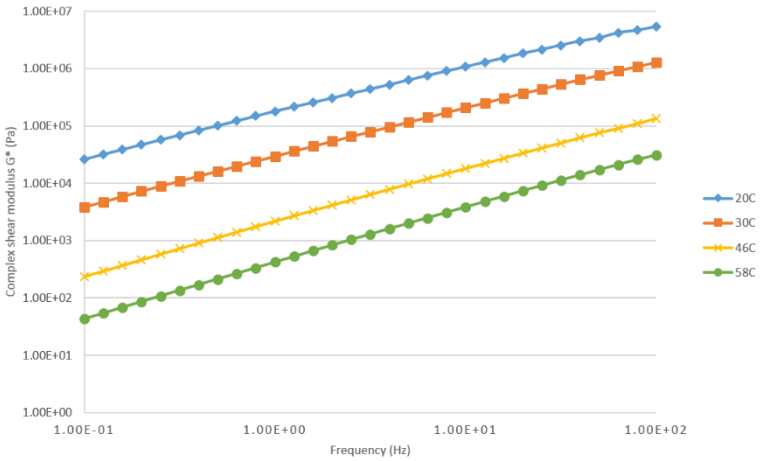

Figure 86. Complex modulus (G*) of unaged blend 12

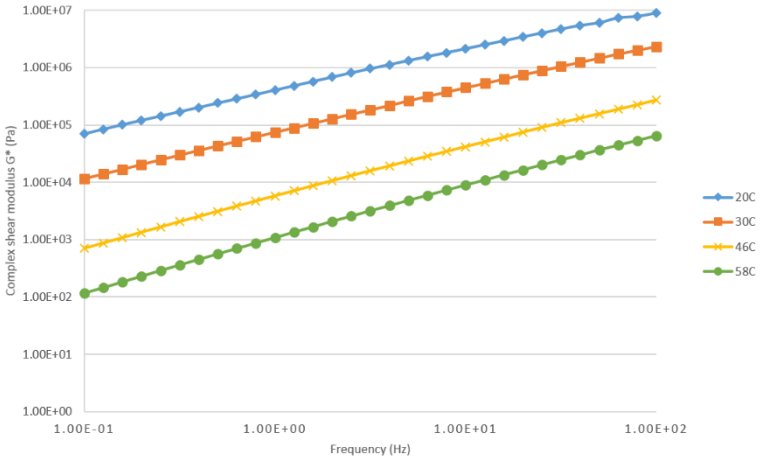

Figure 87. Complex modulus (G*) of RTFO aged blend 12

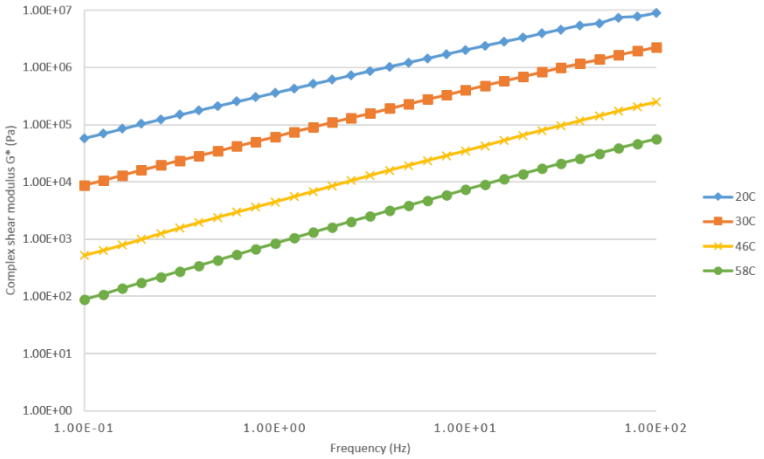

Figure 88. Complex modulus (G*) of unaged blend 13

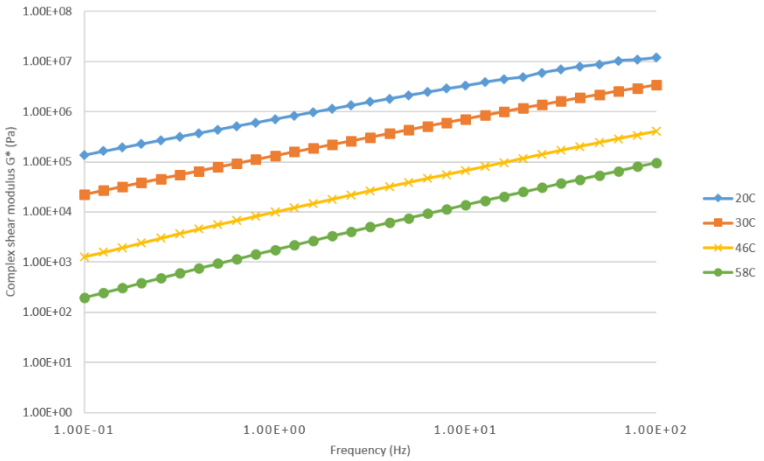

Figure 89. Complex modulus (G*) of RTFO aged blend 13

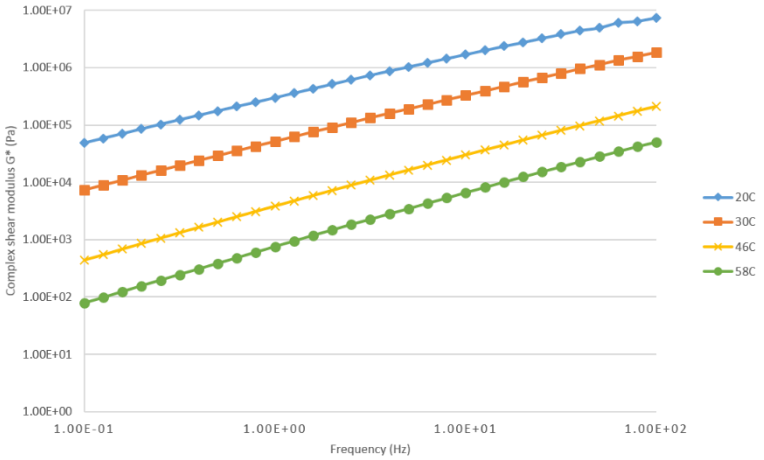

Figure 90. Complex modulus (G*) of unaged blend 18

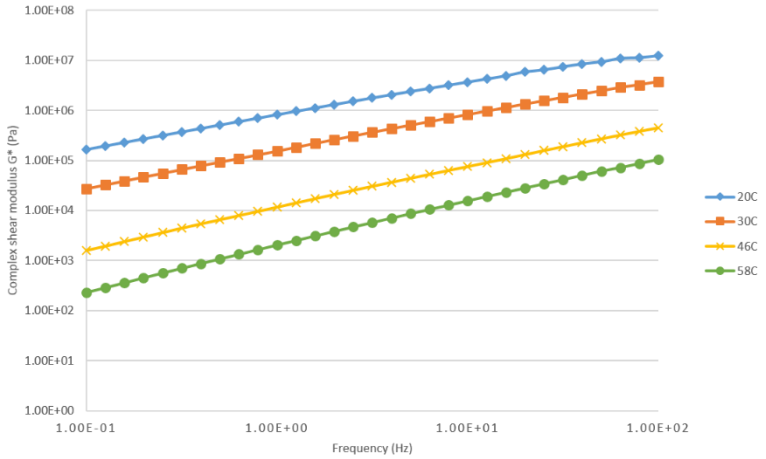

Figure 91. Complex modulus (G*) of RTFO aged blend 13

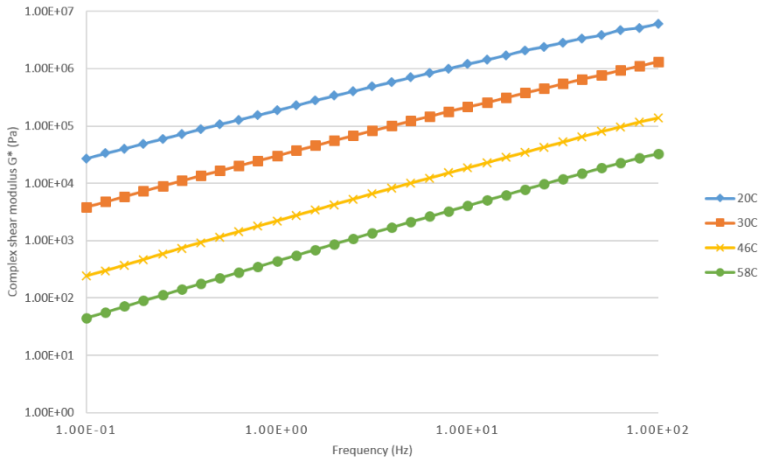

Figure 92. Complex modulus (G*) of unaged blend 23

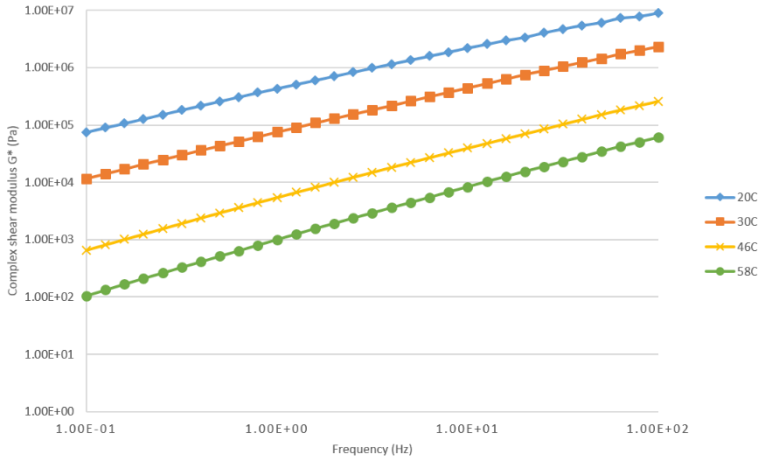

Figure 93. Complex modulus (G*) of RTFO aged blend 23

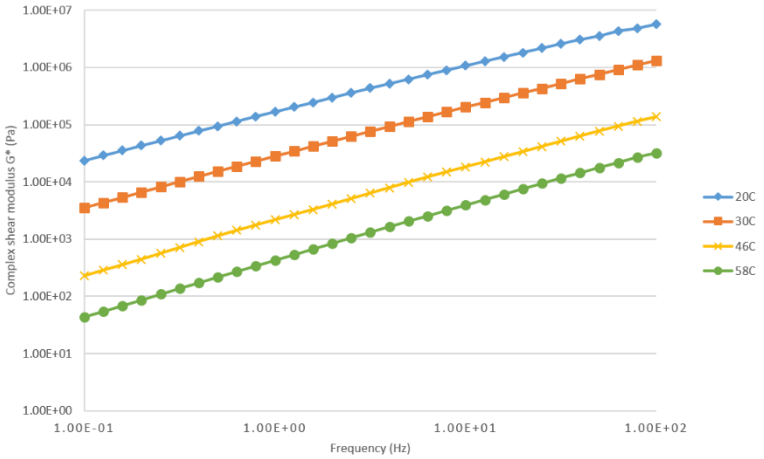

Figure 94. Complex modulus (G*) of unaged blend 26

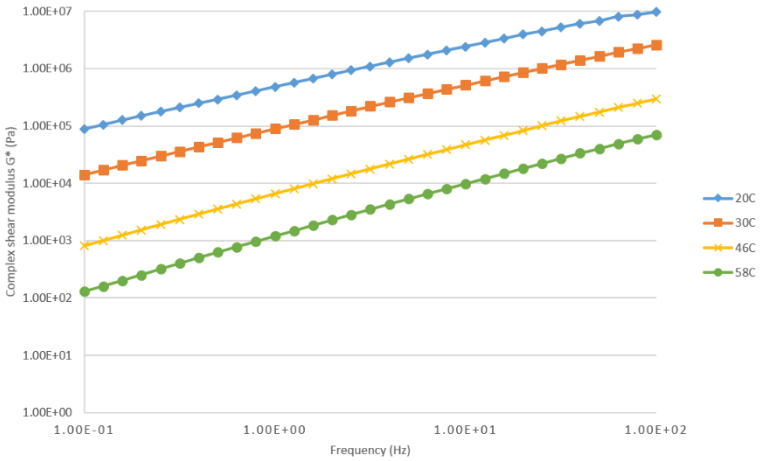

Figure 95. Complex modulus (G*) of RTFO aged blend 26

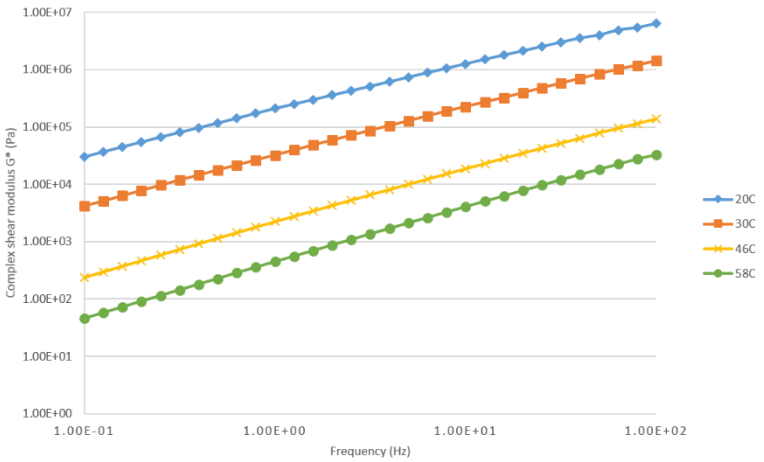

Figure 96. Complex modulus (G*) of unaged blend 24

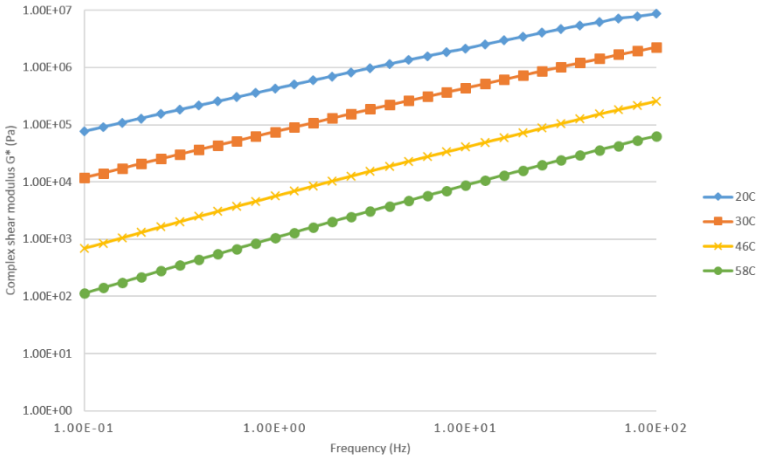

Figure 97. Complex modulus (G*) of RTFO aged blend 24

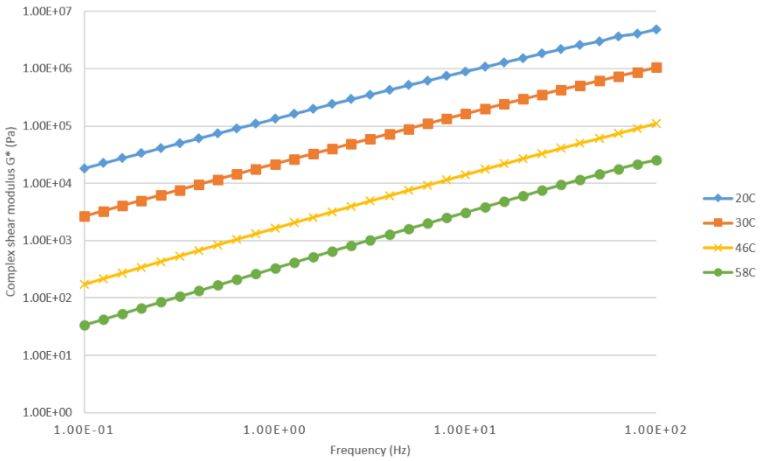

Figure 98. Complex modulus (G*) of unaged blend 25

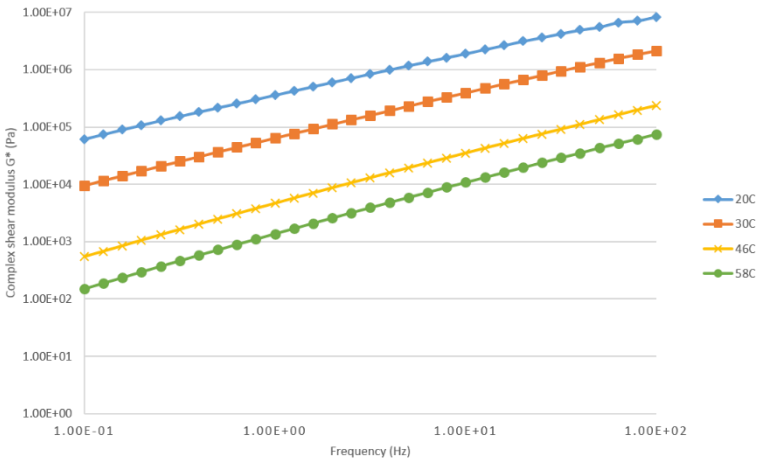

Figure 99. Complex modulus (G*) of RTFO aged blend 25

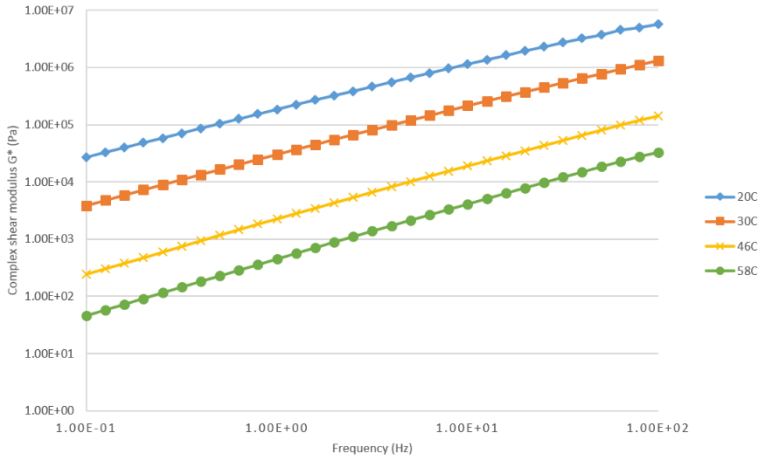

Figure 100. Complex modulus (G*) of unaged blend 27

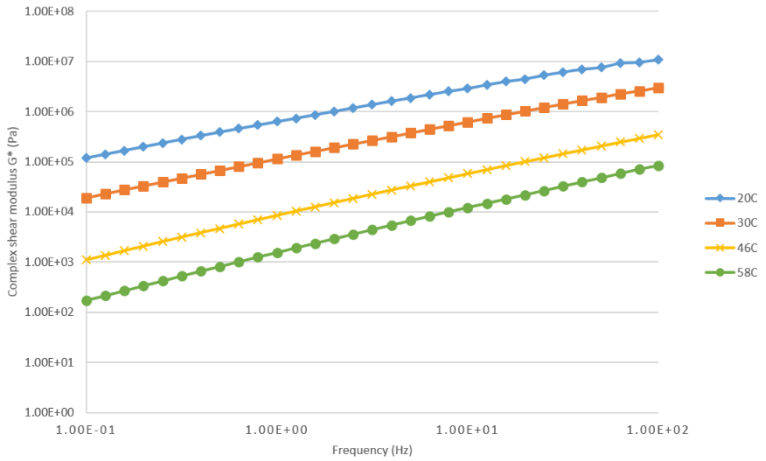

Figure 101. Complex modulus (G*) of RTFO aged blend 27

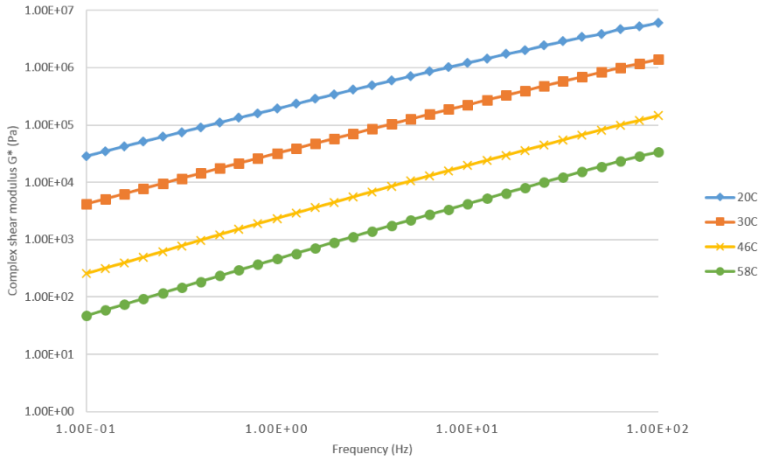

Figure 102. Complex modulus (G*) of unaged blend 28

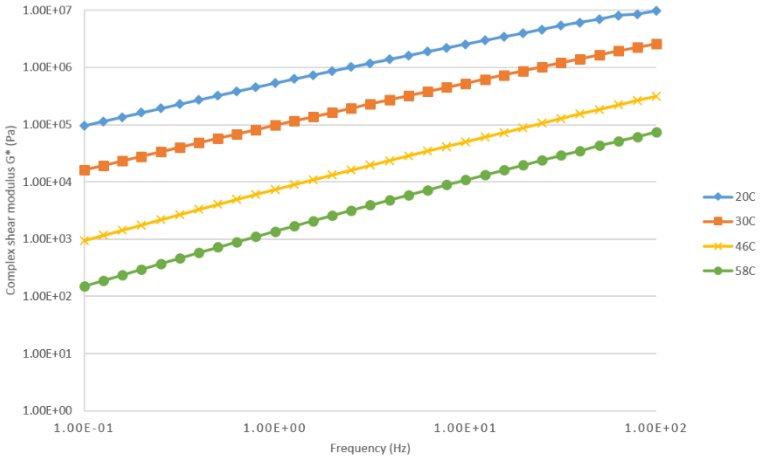

Figure 103. Complex modulus (G*) of RTFO aged blend 27

APPENDIX B. JMP OUTPUT FOR CHAPTER 4

Fit model for reaction duration

Response |G*|/sin(delta)

Effect Summary

Source	LogWorth	PValue
Testing Temp,°C_X3	7.814	0.00000
Reaction duration	0.102	0.79144
Reaction duration*Testing Temp,°C_X3	0.008	0.98180

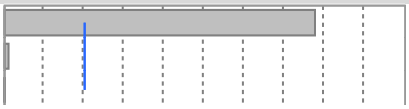

Summary of Fit

RSquare	0.998761
RSquare Adj	0.990293
Root Mean Square Error	10.40078
Mean of Response	58.63187
Observations (or Sum Wgts)	48

Analysis of Variance

Source	DF	Sum of Squares	Mean Square	F Ratio
Model	41	523136.76	12759.4	117.9505
Error	6	649.06	108.2	Prob > F
C. Total	47	523785.82		<.0001*

Effect Tests

Source	DF	Sum of Squares	Mean Square	F Ratio	Prob > F
Reaction duration	6	323.23	53.87	0.4980	0.7914
Testing Temp,°C_X3	5	488077.75	97615.55	902.3755	<.0001*
Reaction duration*Testing Temp,°C_X3	30	1055.53	35.18	0.3252	0.9818

Effect Details

Reaction duration

Least Squares Means Table

Level	Least Sq Mean	Std Error	Mean
4	54.034917	4.2461000	54.0349
5	54.357117	4.2461000	54.3571
8	59.986208	3.0024461	59.9862
9	60.011250	4.2461000	60.0113
10	60.187683	4.2461000	60.1877
11	61.040883	4.2461000	61.0409
12	59.450717	4.2461000	59.4507

LS Means Plot

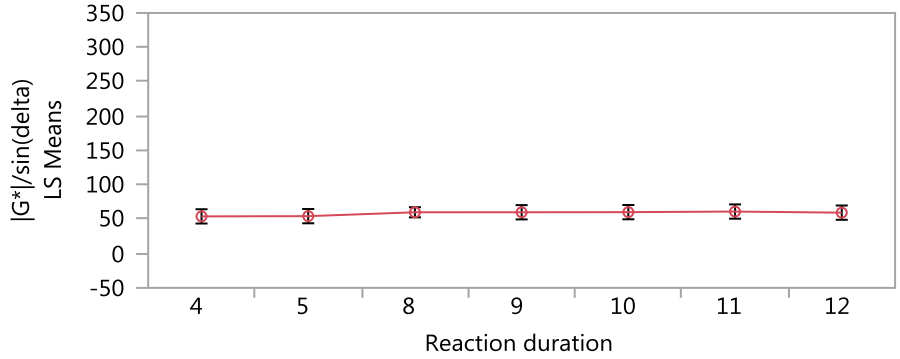

LSMeans Differences Tukey HSD

α= 0.050 Q= 4.16861

Level		Least Sq Mean
11	A	61.040883
10	A	60.187683
9	A	60.011250
8	A	59.986208
12	A	59.450717
5	A	54.357117
4	A	54.034917

Levels not connected by same letter are significantly different.

Fit model for reaction duration with block design

Response G*/sindelta

Summary of Fit

RSquare	0.99673
RSquare Adj	0.996251
Root Mean Square Error	6.463748
Mean of Response	58.63187
Observations (or Sum Wgts)	48

Analysis of Variance

Source	DF	Sum of Squares	Mean Square	F Ratio
Model	6	522072.84	87012.1	2082.625
Error	41	1712.98	41.8	**Prob > F**
C. Total	47	523785.82		<.0001*

Effect Tests

Source	DF	Sum of Squares	Mean Square	F Ratio	Prob > F
Block	1	314.83	314.8	7.5354	0.0089*
Testing temp	5	521758.01	104351.6	2497.642	<.0001*

Effect Details

Block

Least Squares Means Table

Level	Least Sq Mean	Std Error	Mean
long	60.110492	1.0772914	60.1105
short	54.196017	1.8659234	54.1960

t

LS Means Plot

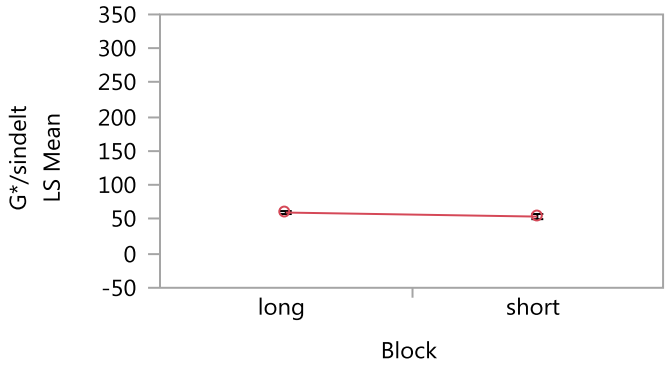

LSMeans Differences Student's t

α=0.050 t=2.01954

LSMean[i] By LSMean[j]

Mean[i]-Mean[j] Std Err Dif Lower CL Dif Upper CL Dif	long	short
long	0 0 0 0	5.91448 2.15458 1.56321 10.2657
short	-5.9145 2.15458 -10.266 -1.5632	0 0 0 0

Level	Least Sq Mean
long	60.110492
short	54.196017

Levels not connected by same letter are significantly different.

Fit model for shear blending methods (A, B, and C) with block design

Response G*/sindelta

Summary of Fit

RSquare	0.921898
RSquare Adj	0.89261
Root Mean Square Error	0.479841
Mean of Response	2.115118
Observations (or Sum Wgts)	12

Analysis of Variance

Source	DF	Sum of Squares	Mean Square	F Ratio
Model	3	21.742402	7.24747	31.4769
Error	8	1.841977	0.23025	**Prob > F**
C. Total	11	23.584379		<.0001*

Effect Tests

Source	DF	Sum of Squares	Mean Square	F Ratio	Prob > F
Block	1	1.115335	1.11533	4.8441	0.0589
Testing temp	2	20.627068	10.31353	44.7933	<.0001*

Effect Details

Block

Least Squares Means Table

Level	Least Sq Mean	Std Error	Mean
higher	2.4199862	0.19589417	2.41999
lower	1.8102500	0.19589417	1.81025

LS Means Plot

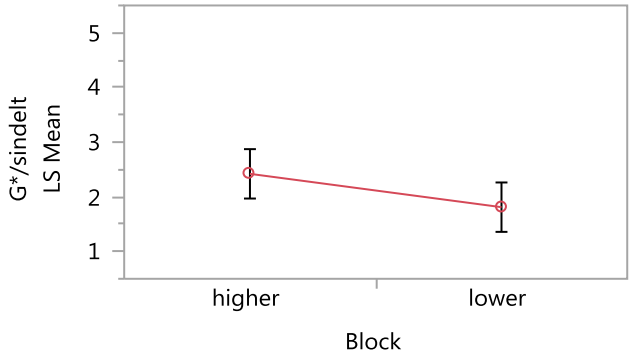

LSMeans Differences Student's t

α=0.050 t=2.306

LSMean[i] By LSMean[j]

Mean[i]-Mean[j] Std Err Dif Lower CL Dif Upper CL Dif	higher	lower
higher	0 0 0 0	0.6097 4 0.2770 4 - 0.0291 1.2485 8
lower	-0.6097 0.27704 -1.2486 0.02911	0 0 0 0

Level		Least Sq Mean
higher	A	2.4199862
lower	A	1.8102500

Levels not connected by same letter are significantly different.

Fit model for shear blending methods (A, B, and C)

Response |G*|/sin(delta)

Effect Summary

Source	LogWorth	PValue
Testing Temp,°C_X3	1.692	0.02034
Method	0.394	0.40334
Method*Testing Temp,°C_X3	0.056	0.87821

Summary of Fit

RSquare	0.94294
RSquare Adj	0.790782
Root Mean Square Error	0.669755
Mean of Response	2.115118
Observations (or Sum Wgts)	12

Analysis of Variance

Source	DF	Sum of Squares	Mean Square	F Ratio
Model	8	22.238665	2.77983	6.1971
Error	3	1.345715	0.44857	Prob > F
C. Total	11	23.584379		0.0806

Effect Tests

Source	DF	Sum of Squares	Mean Square	F Ratio	Prob > F
Method	2	1.119396	0.559698	1.2477	0.4033
Testing Temp,°C_X3	2	16.712854	8.356427	18.6290	0.0203*
Method*Testing Temp,°C_X3	4	0.492201	0.123050	0.2743	0.8782

Effect Details

Method

Least Squares Means Table

Level	Least Sq Mean	Std Error	Mean
A	2.4199862	0.27342628	2.41999
B	1.8362667	0.38668315	1.83627
C	1.7842333	0.38668315	1.78423

LS Means Plot

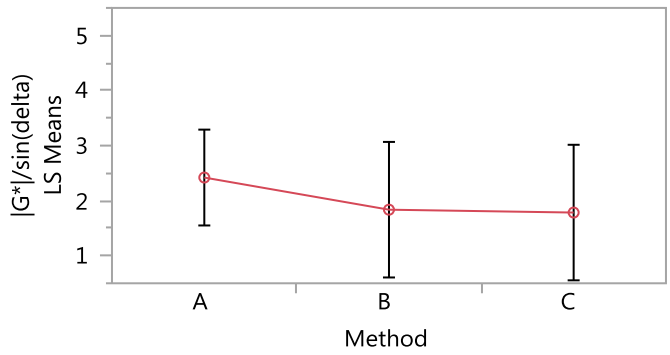

LSMeans Differences Tukey HSD

α= 0.050 Q= 4.17871

Level		Least Sq Mean
A	A	2.4199862
B	A	1.8362667
C	A	1.7842333

Levels not connected by same letter are significantly different.

Response surface model for shear blending results at G*/sin(δ) of unaged modified blends

Unmodified State: Fit Model, Residual Distribution, and Standard Deviation

Response Unmodified |G*|/sin(delta)

Effect Summary

Source	LogWorth	PValue
Testing Temp,°C_X3	37.940	0.00000
X3^2	31.376	0.00000
Styrene MW,kDa_X1	2.114	0.00769
X1*X3	1.673	0.02123

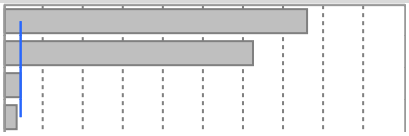

Summary of Fit

RSquare	0.880729
RSquare Adj	0.876786
Root Mean Square Error	39.792
Mean of Response	61.21526
Observations (or Sum Wgts)	126

Analysis of Variance

Source	DF	Sum of Squares	Mean Square	F Ratio
Model	4	1414766.5	353692	223.3743
Error	121	191591.8	1583	**Prob > F**
C. Total	125	1606358.3		<.0001*

Lack Of Fit

Source	DF	Sum of Squares	Mean Square	F Ratio
Lack Of Fit	13	100297.49	7715.19	9.1270
Pure Error	108	91294.29	845.32	**Prob > F**
Total Error	121	191591.78		<.0001*
				Max RSq
				0.9432

Parameter Estimates

Term	Estimate	Std Error	t Ratio	Prob>|t|
Intercept	956.75508	45.5016	21.03	<.0001*
Styrene MW,kDa_X1	-3.431655	1.266039	-2.71	0.0077*
Testing Temp,°C_X3	-39.50344	2.050703	-19.26	<.0001*
X1*X3	0.0687589	0.029456	2.33	0.0212*
X3^2	0.39955	0.024656	16.21	<.0001*

Effect Tests

Source	DF	Sum of Squares	Mean Square	F Ratio	Prob > F
Styrene MW,kDa_X1	1	11633.34	11633.3	7.3471	0.0077*
Testing Temp,°C_X3	1	587564.95	587565.0	371.0773	<.0001*
X1*X3	1	8627.80	8627.8	5.4489	0.0212*
X3^2	1	415808.34	415808.3	262.6042	<.0001*

Distributions

Residual Unmodified |G*|/sin(delta)

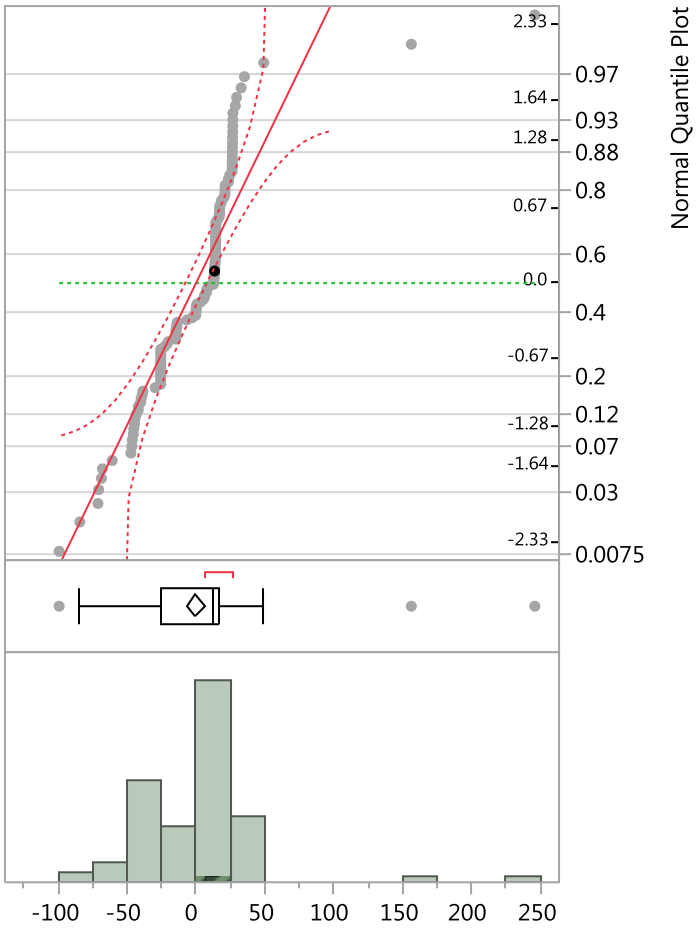

Quantiles

100.0%	maximum	246.15842932
99.5%		246.15842932
97.5%		46.737983806
90.0%		26.550321034
75.0%	quartile	17.165500943
50.0%	median	12.78389581
25.0%	quartile	-25.61820127
10.0%		-44.83931123
2.5%		-71.15408965
0.5%		-99.44157068
0.0%	minimum	-99.44157068

Summary Statistics

Mean	-2.2e-14
Std Dev	39.15015
Std Err Mean	3.4877726
Upper 95% Mean	6.9027348
Lower 95% Mean	-6.902735

N 126

Fit Group

Oneway Analysis of Residual Unmodified |G*|/sin(delta) By Styrene MW,kDa_X1

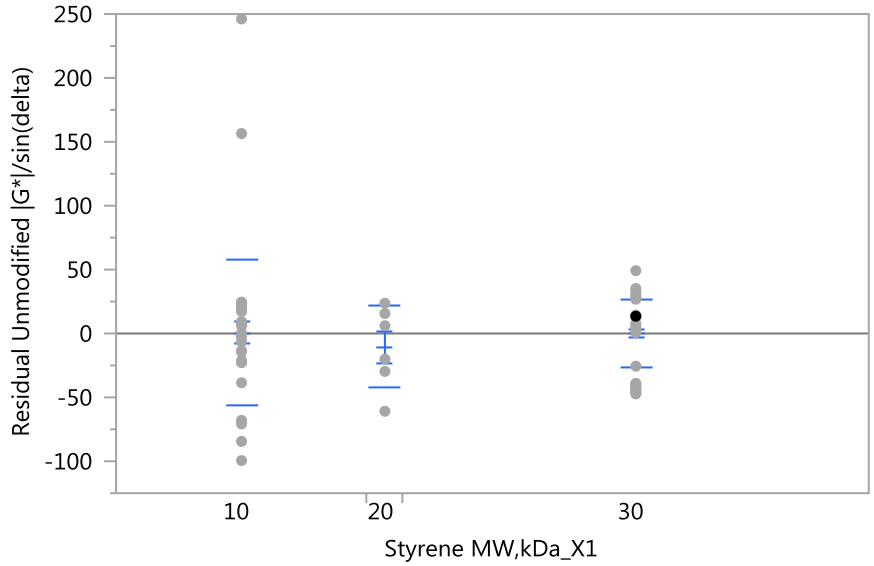

Means and Std Deviations

Level	Number	Mean	Std Dev	Std Err Mean	Lower 95%	Upper 95%
10	42	0.778	56.5909	8.732	-16.86	18.413
20	6	-10.886	31.9991	13.064	-44.47	22.695
30	78	0.419	26.5844	3.010	-5.58	6.413

Oneway Analysis of Residual Unmodified |G*|/sin(delta) By Testing Temp,°C_X3

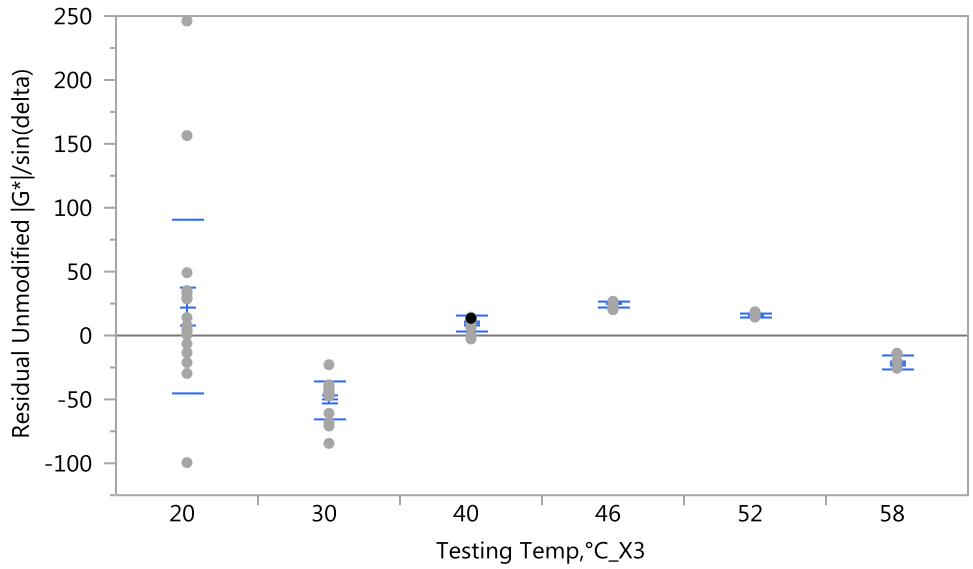

Means and Std Deviations

Level	Number	Mean	Std Dev	Std Err Mean	Lower 95%	Upper 95%
20	21	22.266	68.2344	14.890	-8.79	53.33

Level	Number	Mean	Std Dev	Std Err Mean	Lower 95%	Upper 95%
30	21	-50.101	14.7527	3.219	-56.82	-43.39
40	21	9.266	6.1029	1.332	6.49	12.04
46	21	24.804	2.4037	0.525	23.71	25.90
52	21	15.384	1.5649	0.341	14.67	16.10
58	21	-21.619	5.3868	1.176	-24.07	-19.17

Oneway Analysis of Residual Unmodified |G*|/sin(delta) By X1*X3

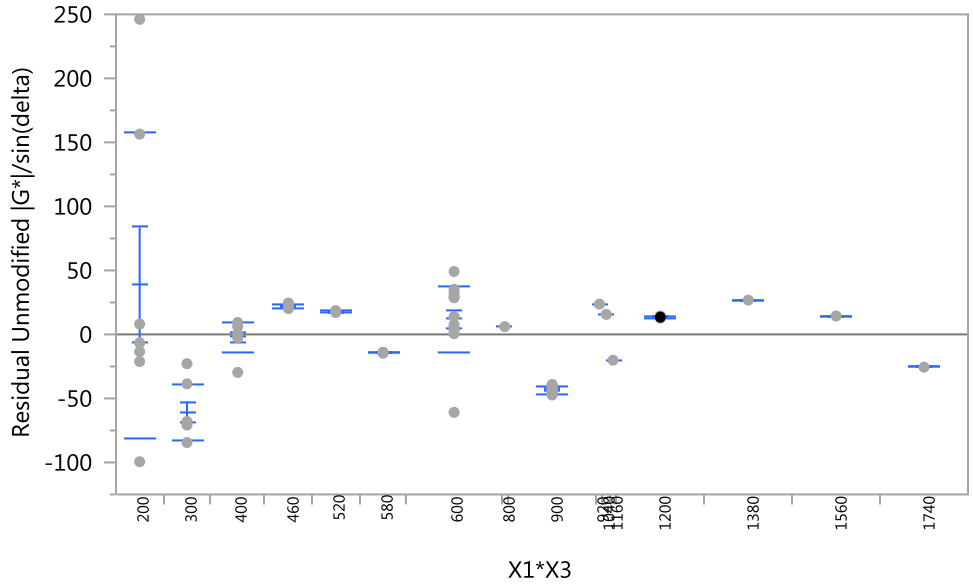

Means and Std Deviations

Level	Number	Mean	Std Dev	Std Err Mean	Lower 95%	Upper 95%
200	7	38.587	119.216	45.059	-71.67	148.8
300	7	-60.655	21.661	8.187	-80.69	-40.6
400	8	-2.110	11.816	4.178	-11.99	7.8
460	7	21.835	1.576	0.596	20.38	23.3
520	7	17.443	0.665	0.252	16.83	18.1
580	7	-14.372	0.292	0.110	-14.64	-14.1
600	14	11.876	25.845	6.907	-3.05	26.8
800	1	6.078	.	.	.	.
900	13	-43.589	2.745	0.761	-45.25	-41.9
920	1	23.635	.	.	.	.
1040	1	15.627	.	.	.	.
1160	1	-20.100	.	.	.	.
1200	13	13.516	0.560	0.155	13.18	13.9
1380	13	26.492	0.208	0.058	26.37	26.6
1560	13	14.257	0.084	0.023	14.21	14.3
1740	13	-25.637	0.034	0.00938	-25.66	-25.6

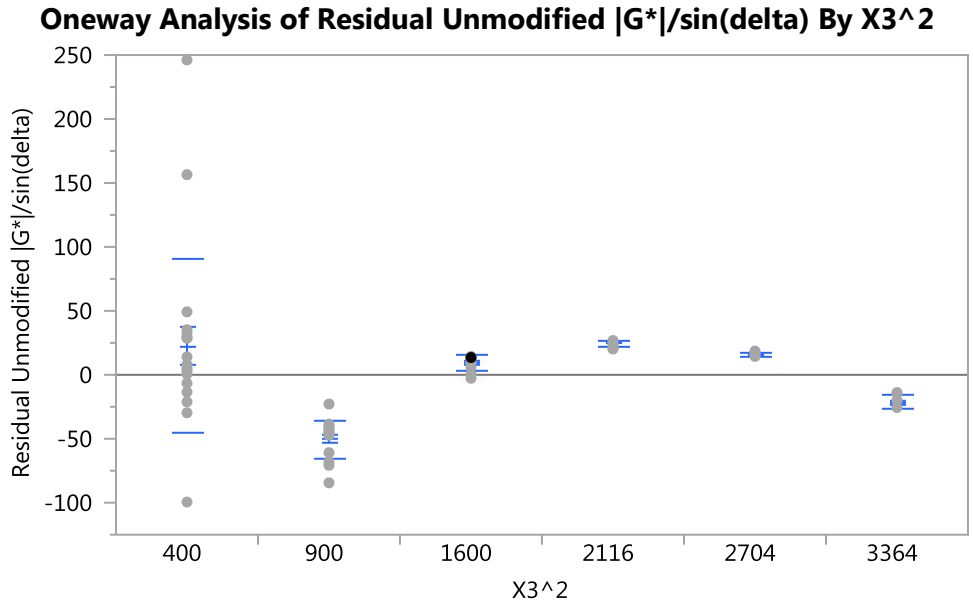

Means and Std Deviations

Level	Number	Mean	Std Dev	Std Err Mean	Lower 95%	Upper 95%
400	21	22.266	68.2344	14.890	-8.79	53.33
900	21	-50.101	14.7527	3.219	-56.82	-43.39
1600	21	9.266	6.1029	1.332	6.49	12.04
2116	21	24.804	2.4037	0.525	23.71	25.90
2704	21	15.384	1.5649	0.341	14.67	16.10
3364	21	-21.619	5.3868	1.176	-24.07	-19.17

Log10 State: Fit Model, Residual Distribution, and Standard Deviation

Response Log10_|G*|/sin(delta)

Effect Summary

Source	LogWorth	PValue
Testing Temp,°C_X3	48.329	0.00000
X3^2	10.549	0.00000
Styrene content,%_X2	2.263	0.00546
X2^2	1.928	0.01180
Styrene MW,kDa_X1	1.836	0.01460
X1^2	1.653	0.02226

Summary of Fit

RSquare	0.992411
RSquare Adj	0.992028
Root Mean Square Error	0.08016
Mean of Response	0.958364
Observations (or Sum Wgts)	126

Analysis of Variance

Source	DF	Sum of Squares	Mean Square	F Ratio
Model	6	99.99285	16.6655	2593.575
Error	119	0.76466	0.0064	**Prob > F**
C. Total	125	100.75751		<.0001*

Lack Of Fit

Source	DF	Sum of Squares	Mean Square	F Ratio
Lack Of Fit	41	0.48681338	0.011873	3.3333
Pure Error	78	0.27784203	0.003562	**Prob > F**
Total Error	119	0.76465542		<.0001*
				Max RSq
				0.9972

Parameter Estimates

Term	Estimate	Std Error	t Ratio	Prob>|t|
Intercept	5.2072488	0.252398	20.63	<.0001*
Styrene MW,kDa_X1	-0.034097	0.013758	-2.48	0.0146*
Styrene content,%_X2	-0.038773	0.013699	-2.83	0.0055*
Testing Temp,°C_X3	-0.097251	0.003902	-24.92	<.0001*
X1^2	0.0007949	0.000343	2.32	0.0223*
X2^2	0.0005626	0.00022	2.56	0.0118*
X3^2	0.0003648	4.967e-5	7.34	<.0001*

Effect Tests

Source	DF	Sum of Squares	Mean Square	F Ratio	Prob > F
Styrene MW,kDa_X1	1	0.0394668	0.039467	6.1420	0.0146*
Styrene content,%_X2	1	0.0514770	0.051477	8.0111	0.0055*
Testing Temp,°C_X3	1	3.9912734	3.991273	621.1445	<.0001*
X1^2	1	0.0344727	0.034473	5.3648	0.0223*
X2^2	1	0.0420303	0.042030	6.5410	0.0118*
X3^2	1	0.3465335	0.346534	53.9295	<.0001*

Prediction Expression

5.2072488052848

+ -0.0340971317281 * Styrene MW,kDa_X1

+ -0.0387726978106 * Styrene content,%_X2

+ -0.0972513573485 * Testing Temp,°C_X3

+ 0.00079494344695 * X1^2

+ 0.00056255546958 * X2^2

+ 0.00036475156716 * X3^2

Distributions

Residual Log10_|G*|/sin(delta)

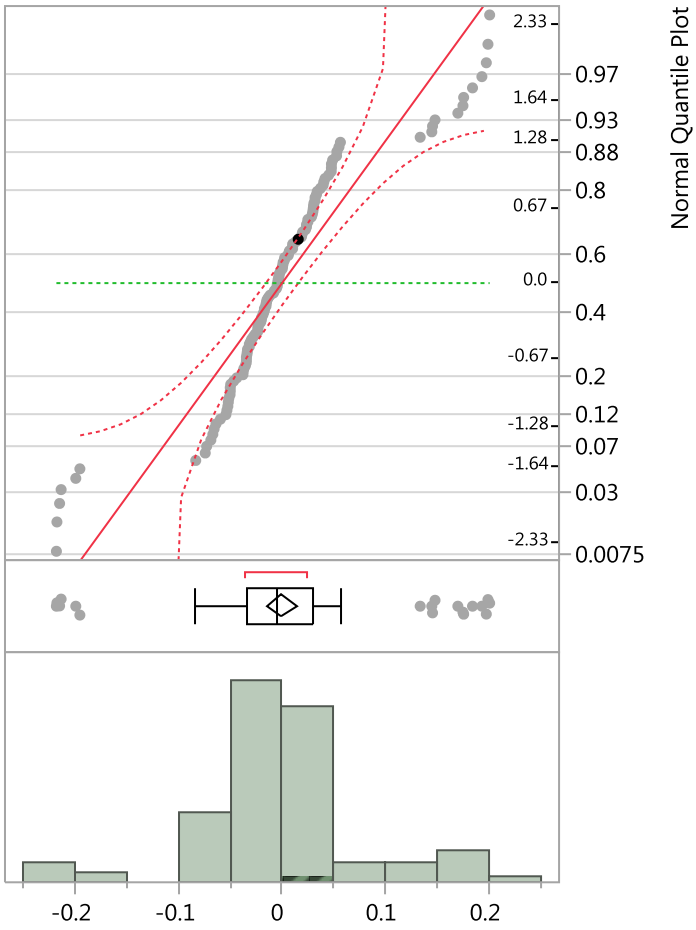

Quantiles

100.0%	maximum	0.2011154995
99.5%		0.2011154995
97.5%		0.1971389525
90.0%		0.0797282289
75.0%	quartile	0.0302771179
50.0%	median	-0.004283029
25.0%	quartile	-0.034509753
10.0%		-0.064526834
2.5%		-0.215228191
0.5%		-0.21856581
0.0%	minimum	-0.21856581

Summary Statistics

Mean	-5.06e-16
Std Dev	0.0782128
Std Err Mean	0.0069678
Upper 95% Mean	0.01379

Lower 95% Mean	-0.01379
N	126

Fit Group

Oneway Analysis of Residual Log10_|G*|/sin(delta) By Styrene MW,kDa_X1

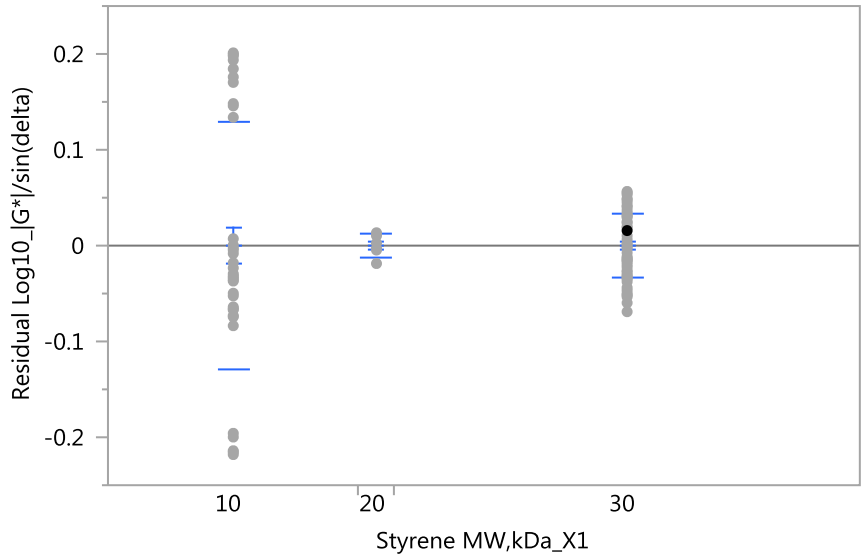

Means and Std Deviations

Level	Number	Mean	Std Dev	Std Err Mean	Lower 95%	Upper 95%
10	42	-4.29e-16	0.128213	0.01978	-0.0400	0.03995
20	6	-4.77e-17	0.011602	0.00474	-0.0122	0.01218
30	78	-5.82e-16	0.034189	0.00387	-0.0077	0.00771

Oneway Analysis of Residual Log10_|G*|/sin(delta) By Styrene content,%_X2

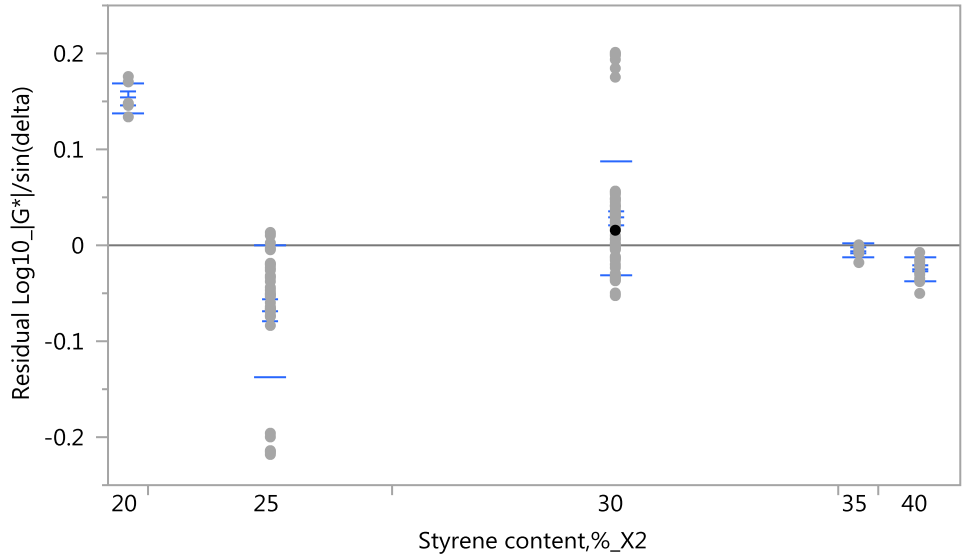

Means and Std Deviations

Level	Number	Mean	Std Dev	Std Err Mean	Lower 95%	Upper 95%
20	6	0.15319	0.016315	0.00666	0.1361	0.1703
25	36	-0.06840	0.068677	0.01145	-0.0916	-0.0452
30	66	0.02836	0.059050	0.00727	0.0138	0.0429
35	6	-0.00561	0.006945	0.00284	-0.0129	0.0017
40	12	-0.02460	0.012044	0.00348	-0.0322	-0.0169

Oneway Analysis of Residual Log10_|G*|/sin(delta) By Testing Temp,°C_X3

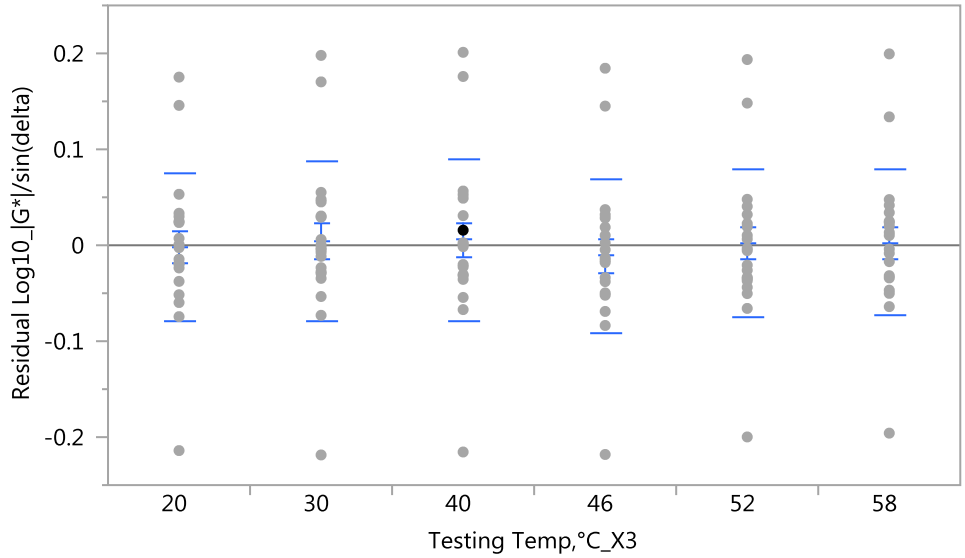

Means and Std Deviations

Level	Number	Mean	Std Dev	Std Err Mean	Lower 95%	Upper 95%
20	21	-0.00251	0.077091	0.01682	-0.0376	0.03258
30	21	0.00438	0.082618	0.01803	-0.0332	0.04199
40	21	0.00545	0.083613	0.01825	-0.0326	0.04351
46	21	-0.01140	0.080347	0.01753	-0.0480	0.02518
52	21	0.00192	0.077614	0.01694	-0.0334	0.03725
58	21	0.00216	0.076095	0.01661	-0.0325	0.03680

Oneway Analysis of Residual Log10_|G*|/sin(delta) By X1^2

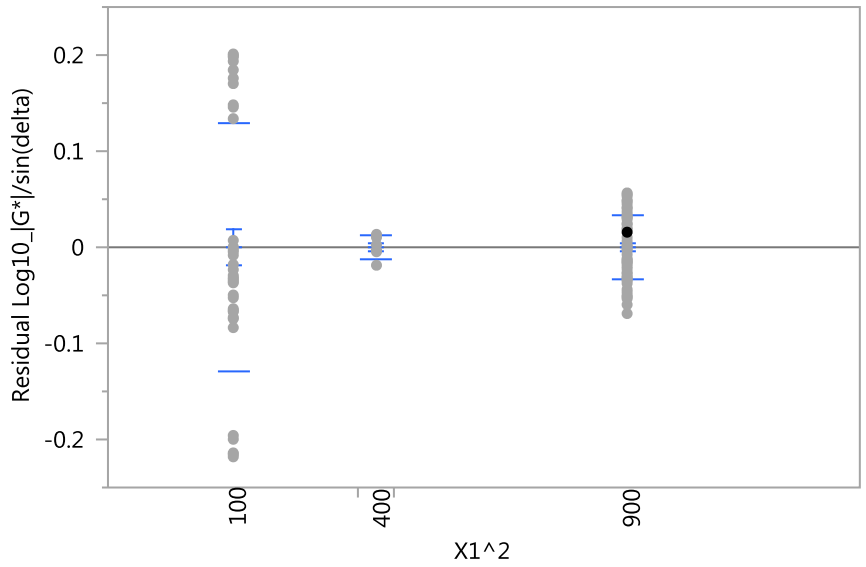

Means and Std Deviations

Level	Number	Mean	Std Dev	Std Err Mean	Lower 95%	Upper 95%
100	42	-4.29e-16	0.128213	0.01978	-0.0400	0.03995
400	6	-4.77e-17	0.011602	0.00474	-0.0122	0.01218
900	78	-5.82e-16	0.034189	0.00387	-0.0077	0.00771

Oneway Analysis of Residual Log10_|G*|/sin(delta) By X2^2

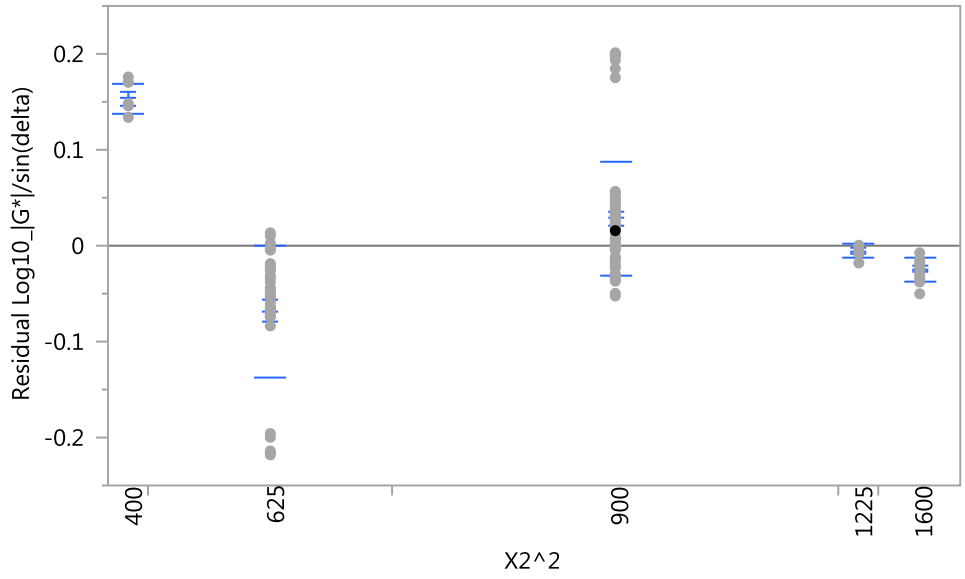

Means and Std Deviations

Level	Number	Mean	Std Dev	Std Err Mean	Lower 95%	Upper 95%
400	6	0.15319	0.016315	0.00666	0.1361	0.1703
625	36	-0.06840	0.068677	0.01145	-0.0916	-0.0452
900	66	0.02836	0.059050	0.00727	0.0138	0.0429

Level	Number	Mean	Std Dev	Std Err Mean	Lower 95%	Upper 95%
1225	6	-0.00561	0.006945	0.00284	-0.0129	0.0017
1600	12	-0.02460	0.012044	0.00348	-0.0322	-0.0169

Oneway Analysis of Residual Log10_|G*|/sin(delta) By X3^2

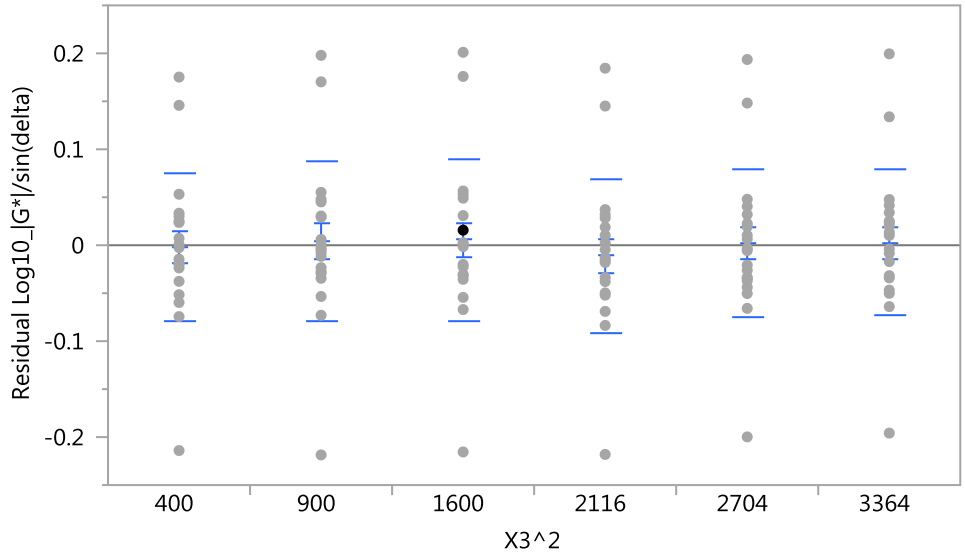

Means and Std Deviations

Level	Number	Mean	Std Dev	Std Err Mean	Lower 95%	Upper 95%
400	21	-0.00251	0.077091	0.01682	-0.0376	0.03258
900	21	0.00438	0.082618	0.01803	-0.0332	0.04199
1600	21	0.00545	0.083613	0.01825	-0.0326	0.04351
2116	21	-0.01140	0.080347	0.01753	-0.0480	0.02518
2704	21	0.00192	0.077614	0.01694	-0.0334	0.03725
3364	21	0.00216	0.076095	0.01661	-0.0325	0.03680

SQRT State: Fit Model, Residual Distribution, and Standard Deviation

Response SQRT_|G*|/sin(delta)

Effect Summary

Source	LogWorth	PValue
styrene MW, kDa-X1	10.885	0.00000
X1^2	10.677	0.00000
Testing Temp,°C_X3	9.940	0.00000

Summary of Fit

RSquare	0.858425
RSquare Adj	0.845152
Root Mean Square Error	0.541167
Mean of Response	2.46946
Observations (or Sum Wgts)	36

Analysis of Variance

Source	DF	Sum of Squares	Mean Square	F Ratio
Model	3	56.823502	18.9412	64.6761
Error	32	9.371580	0.2929	**Prob > F**
C. Total	35	66.195082		<.0001*

Lack Of Fit

Source	DF	Sum of Squares	Mean Square	F Ratio
Lack Of Fit	5	4.0477398	0.809548	4.1056
Pure Error	27	5.3238400	0.197179	**Prob > F**
Total Error	32	9.3715798		0.0067*
				Max RSq
				0.9196

Parameter Estimates

Term	Estimate	Std Error	t Ratio	Prob>|t|
Intercept	3.2468464	1.245425	2.61	0.0138*
styrene MW, kDa-X1	0.6635144	0.064873	10.23	<.0001*
Testing Temp,°C_X3	-0.172111	0.018411	-9.35	<.0001*
X1^2	-0.010789	0.001076	-10.03	<.0001*

Effect Tests

Source	DF	Sum of Squares	Mean Square	F Ratio	Prob > F
styrene MW, kDa-X1	1	30.636049	30.63605	104.6092	<.0001*
Testing Temp,°C_X3	1	25.593453	25.59345	87.3909	<.0001*
X1^2	1	29.464544	29.46454	100.6090	<.0001*

Distributions

Residual SQRT_|G*|/sin(delta)

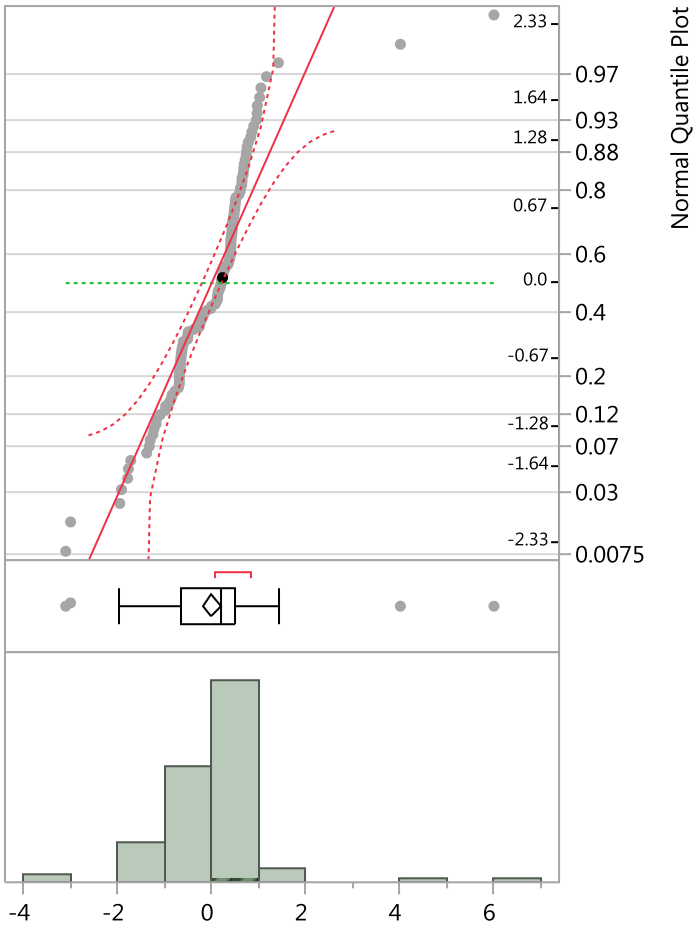

Quantiles

100.0%	maximum	6.0163427086
99.5%		6.0163427086
97.5%		1.3786300711
90.0%		0.7956897226
75.0%	quartile	0.4939713725
50.0%	median	0.2030331613
25.0%	quartile	-0.655564094
10.0%		-1.197948075
2.5%		-1.950522373
0.5%		-3.110357721
0.0%	minimum	-3.110357721

Summary Statistics

Mean	3.204e-15
Std Dev	1.0495796
Std Err Mean	0.093504
Upper 95% Mean	0.185056

Lower 95% Mean	-0.185056
N	126

Fit Group

Oneway Analysis of Residual SQRT_|G*|/sin(delta) By Styrene MW,kDa_X1

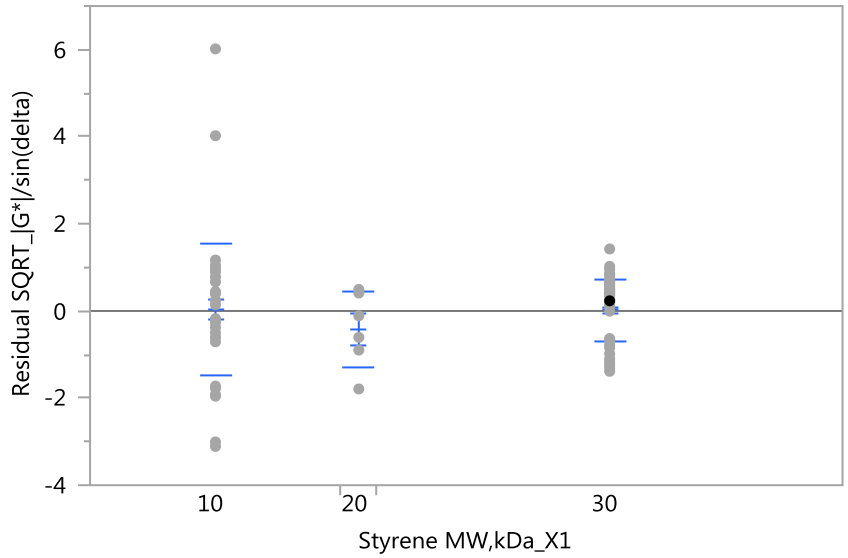

Means and Std Deviations

Level	Number	Mean	Std Dev	Std Err Mean	Lower 95%	Upper 95%
10	42	0.02974	1.52387	0.23514	-0.445	0.50461
20	6	-0.41642	0.86743	0.35413	-1.327	0.49389
30	78	0.01602	0.69910	0.07916	-0.142	0.17364

Oneway Analysis of Residual SQRT_|G*|/sin(delta) By Testing Temp,°C_X3

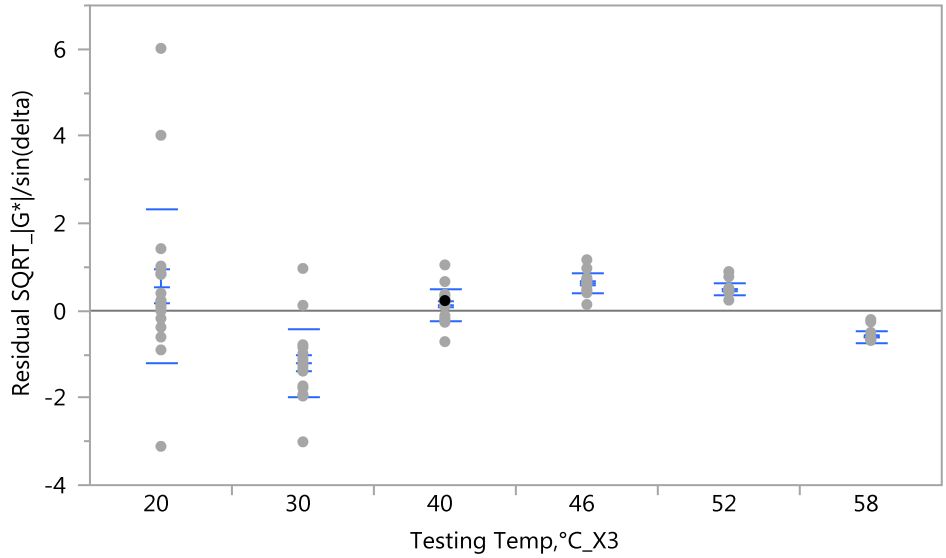

Means and Std Deviations

Level	Number	Mean	Std Dev	Std Err Mean	Lower 95%	Upper 95%
20	21	0.5520	1.77333	0.38697	-0.255	1.359
30	21	-1.2137	0.78603	0.17152	-1.572	-0.856
40	21	0.1450	0.36390	0.07941	-0.021	0.311
46	21	0.6271	0.21421	0.04674	0.530	0.725
52	21	0.4791	0.13374	0.02918	0.418	0.540
58	21	-0.5895	0.13685	0.02986	-0.652	-0.527

Oneway Analysis of Residual SQRT_|G*|/sin(delta) By X1*X3

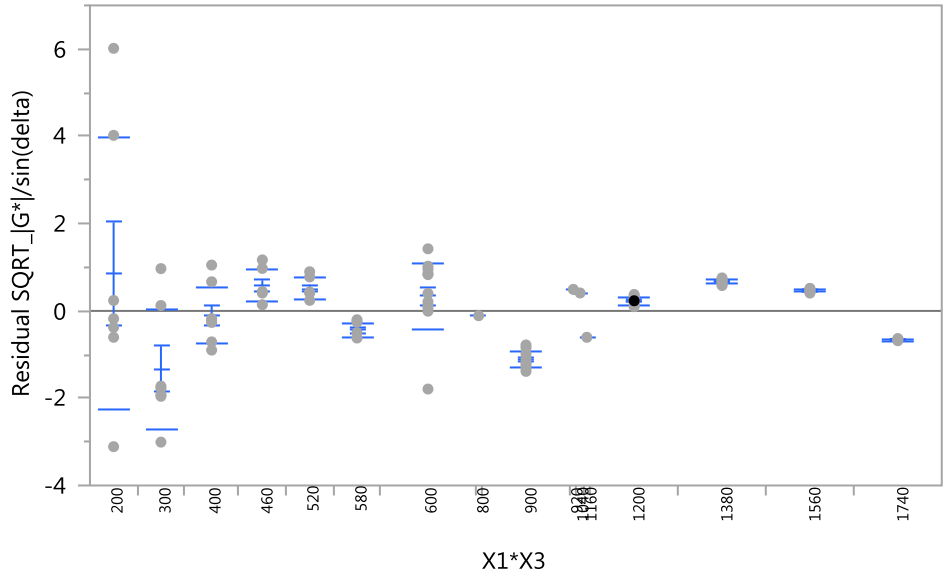

Means and Std Deviations

Level	Number	Mean	Std Dev	Std Err Mean	Lower 95%	Upper 95%
200	7	0.8584	3.09554	1.1700	-2.004	3.721
300	7	-1.3270	1.37289	0.5189	-2.597	-0.057
400	8	-0.0987	0.65336	0.2310	-0.645	0.448
460	7	0.5616	0.36643	0.1385	0.223	0.900
520	7	0.5130	0.23415	0.0885	0.296	0.730
580	7	-0.4430	0.15322	0.0579	-0.585	-0.301
600	14	0.3350	0.75791	0.2026	-0.103	0.773
800	1	-0.1099	.	.	.	.
900	13	-1.1084	0.20027	0.0555	-1.229	-0.987
920	1	0.4939	.	.	.	.
1040	1	0.4108	.	.	.	.
1160	1	-0.6049	.	.	.	.
1200	13	0.2343	0.09338	0.0259	0.178	0.291
1380	13	0.6727	0.05573	0.0155	0.639	0.706
1560	13	0.4662	0.03405	0.0094	0.446	0.487
1740	13	-0.6671	0.02022	0.0056	-0.679	-0.655

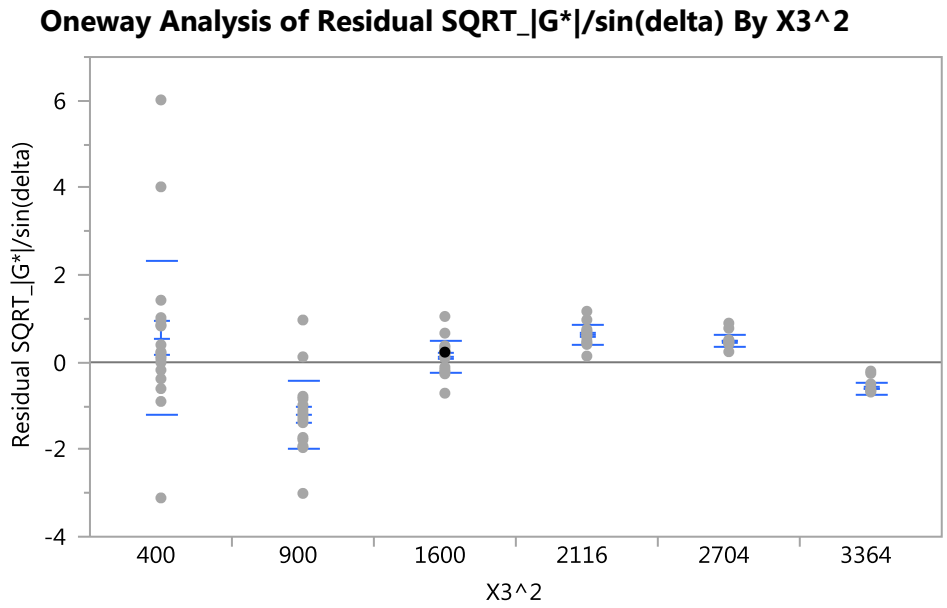

Means and Std Deviations

Level	Number	Mean	Std Dev	Std Err Mean	Lower 95%	Upper 95%
400	21	0.5520	1.77333	0.38697	-0.255	1.359
900	21	-1.2137	0.78603	0.17152	-1.572	-0.856
1600	21	0.1450	0.36390	0.07941	-0.021	0.311
2116	21	0.6271	0.21421	0.04674	0.530	0.725
2704	21	0.4791	0.13374	0.02918	0.418	0.540
3364	21	-0.5895	0.13685	0.02986	-0.652	-0.527

Comparing Residuals in Graph Builder

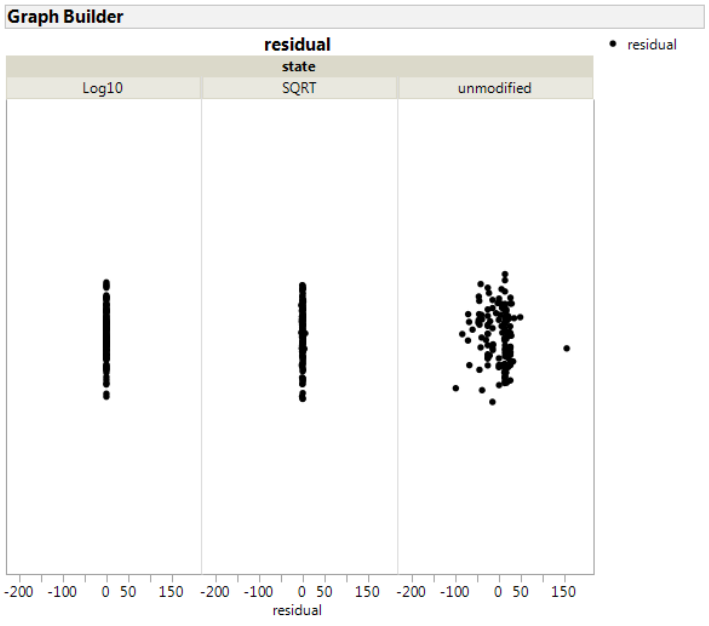

Response surface model for shear blending results at G*/sin(δ) of RTFO short-term aged modified blends

Unmodified State: Fit Model, Residual Distribution, and Standard Deviation

Response Unmodified |G*|/sin(delta)

Effect Summary

Source	LogWorth	PValue
X3^2	25.452	0.00000
Testing Temp,°C_X3	19.033	0.00000
X2^2	4.249	0.00006
X2*X3	3.330	0.00047
Styrene MW,kDa_X1	2.183	0.00656
X1*X3	1.773	0.01688

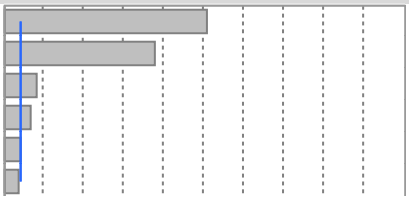

Summary of Fit

RSquare	0.849059
RSquare Adj	0.841449
Root Mean Square Error	121.686
Mean of Response	162.201
Observations (or Sum Wgts)	126

Analysis of Variance

Source	DF	Sum of Squares	Mean Square	F Ratio
Model	6	9911985	1651998	111.5650
Error	119	1762092	14807	**Prob > F**
C. Total	125	11674077		<.0001*

Lack Of Fit

Source	DF	Sum of Squares	Mean Square	F Ratio
Lack Of Fit	41	1018443.7	24840.1	2.6054
Pure Error	78	743648.0	9533.9	**Prob > F**
Total Error	119	1762091.7		0.0001*
				Max RSq
				0.9363

Parameter Estimates

Term	Estimate	Std Error	t Ratio	Prob>|t|
Intercept	2094.4506	162.7635	12.87	<.0001*
Styrene MW,kDa_X1	-11.02212	3.9829	-2.77	0.0066*
Testing Temp,°C_X3	-85.05923	7.758058	-10.96	<.0001*
X1*X3	0.2253772	0.092995	2.42	0.0169*
X2*X3	-0.626114	0.173992	-3.60	0.0005*
X2^2	0.5025038	0.120272	4.18	<.0001*
X3^2	1.0315426	0.075399	13.68	<.0001*

Effect Tests

Source	DF	Sum of Squares	Mean Square	F Ratio	Prob > F
Styrene MW,kDa_X1	1	113400.1	113400	7.6583	0.0066*

Source	DF	Sum of Squares	Mean Square	F Ratio	Prob > F
Testing Temp,°C_X3	1	1779993.5	1779994	120.2090	<.0001*
X1*X3	1	86972.6	86973	5.8736	0.0169*
X2*X3	1	191748.4	191748	12.9494	0.0005*
X2^2	1	258483.3	258483	17.4562	<.0001*
X3^2	1	2771566.4	2771566	187.1732	<.0001*

Distributions

Residual Unmodified |G*|/sin(delta)

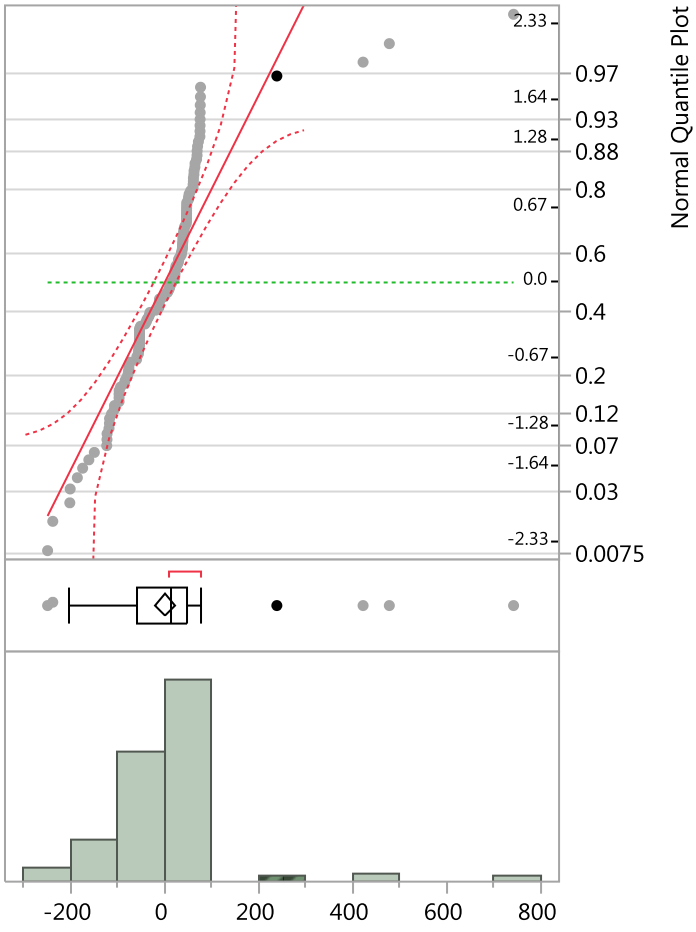

Quantiles

100.0%	maximum	743.43961748
99.5%		743.43961748
97.5%		390.55039183
90.0%		72.735041564
75.0%	quartile	46.669249737
50.0%	median	15.123905696
25.0%	quartile	-59.58052394
10.0%		-118.0884083
2.5%		-202.1645543
0.5%		-249.6068555
0.0%	minimum	-249.6068555

Summary Statistics

Mean	-6.19e-14
Std Dev	118.72966
Std Err Mean	10.577279
Upper 95% Mean	20.933748
Lower 95% Mean	-20.93375
N	126

Fit Group

Oneway Analysis of Residual Unmodified |G*|/sin(delta) By Styrene MW,kDa_X1

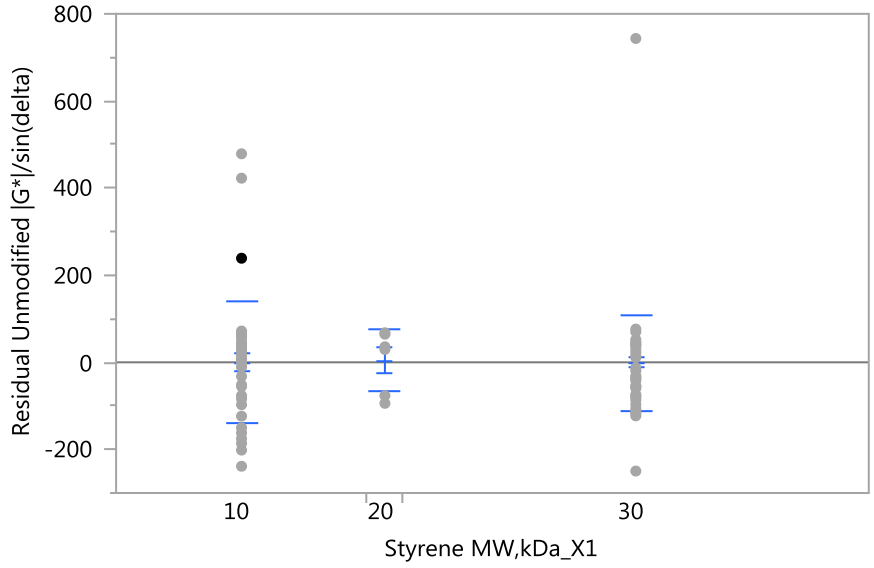

Means and Std Deviations

Level	Number	Mean	Std Dev	Std Err Mean	Lower 95%	Upper 95%
10	42	-0.3215	140.351	21.657	-44.06	43.415
20	6	4.5012	71.414	29.155	-70.44	79.445
30	78	-0.1731	109.831	12.436	-24.94	24.590

Oneway Analysis of Residual Unmodified |G*|/sin(delta) By Testing Temp,°C_X3

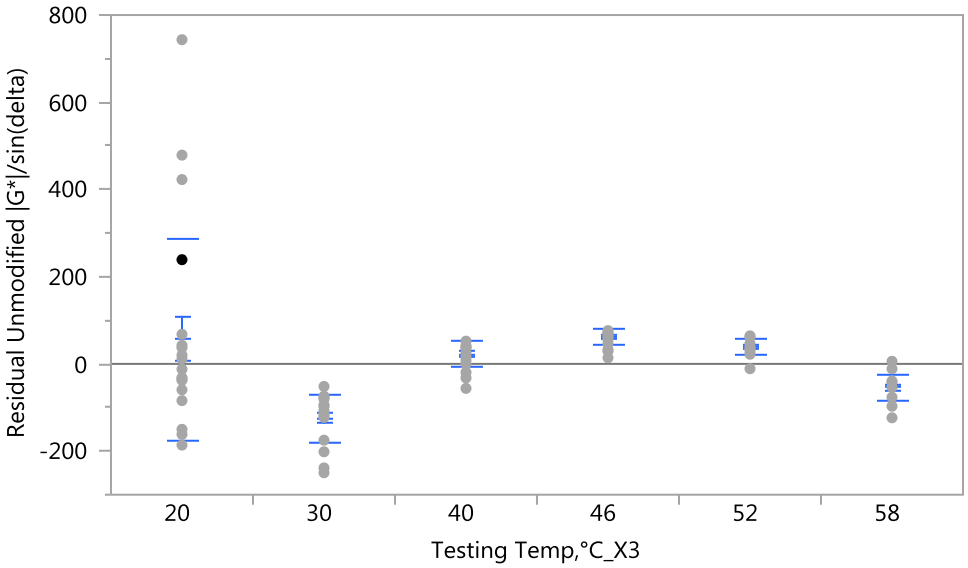

Means and Std Deviations

Level	Number	Mean	Std Dev	Std Err Mean	Lower 95%	Upper 95%
20	21	55.68	231.263	50.466	-49.6	161.0
30	21	-124.98	55.763	12.168	-150.4	-99.6
40	21	22.15	29.294	6.392	8.8	35.5
46	21	62.43	17.748	3.873	54.3	70.5
52	21	39.29	17.958	3.919	31.1	47.5
58	21	-54.57	31.726	6.923	-69.0	-40.1

Oneway Analysis of Residual Unmodified |G*|/sin(delta) By X1*X3

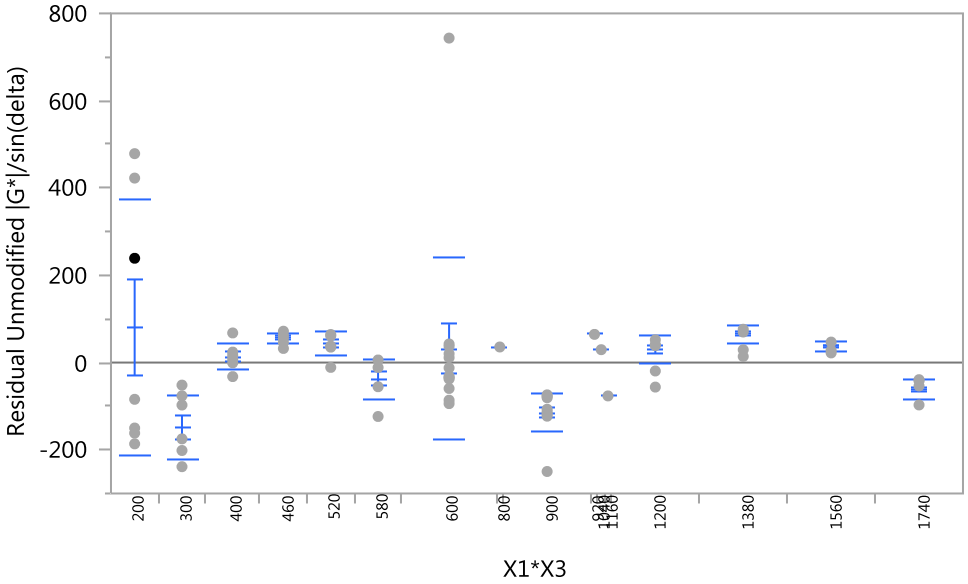

Means and Std Deviations

Level	Number	Mean	Std Dev	Std Err Mean	Lower 95%	Upper 95%
200	7	79.73	291.792	110.29	-190.1	349.6
300	7	-148.95	72.712	27.48	-216.2	-81.7
400	8	13.19	28.546	10.09	-10.7	37.1
460	7	55.82	13.051	4.93	43.8	67.9
520	7	44.04	27.075	10.23	19.0	69.1
580	7	-37.96	44.450	16.80	-79.1	3.1
600	14	32.09	209.258	55.93	-88.7	152.9
800	1	35.68	.	.	.	.
900	13	-114.44	44.767	12.42	-141.5	-87.4
920	1	64.60	.	.	.	.
1040	1	29.52	.	.	.	.
1160	1	-76.47	.	.	.	.
1200	13	30.13	31.476	8.73	11.1	49.2
1380	13	65.82	20.039	5.56	53.7	77.9
1560	13	37.48	12.095	3.35	30.2	44.8
1740	13	-61.82	20.782	5.76	-74.4	-49.3

Oneway Analysis of Residual Unmodified |G*|/sin(delta) By X2*X3

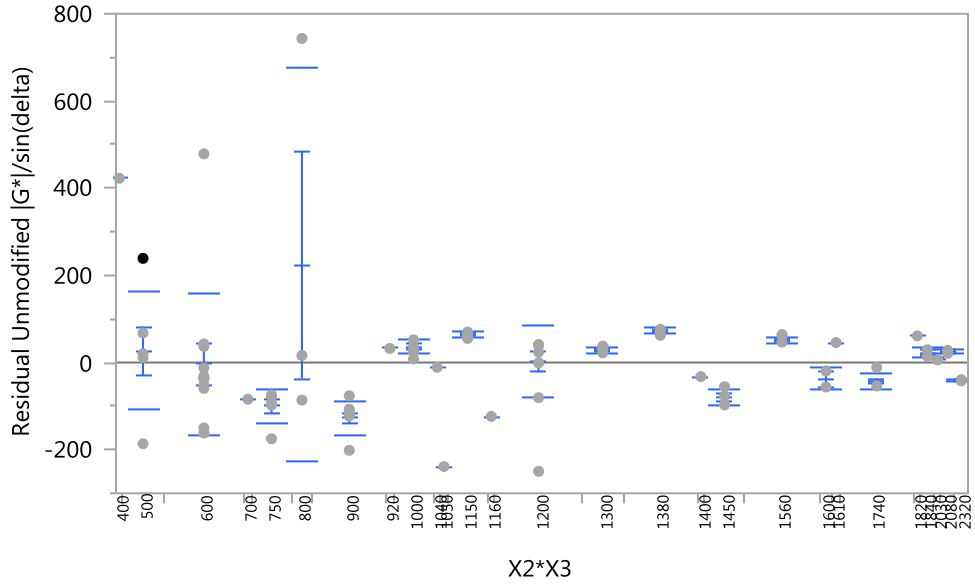

Means and Std Deviations

Level	Number	Mean	Std Dev	Std Err Mean	Lower 95%	Upper 95%
400	1	422.71	.	.	.	.
500	6	27.03	136.117	55.57	-115.8	170
600	12	-3.36	163.589	47.22	-107.3	101
700	1	-84.22	.	.	.	.
750	6	-99.27	38.287	15.63	-139.5	-59
800	3	224.51	452.312	261.14	-899.1	1348
900	11	-128.04	38.741	11.68	-154.1	-102
920	1	32.30	.	.	.	.
1000	6	36.78	17.907	7.31	18.0	56
1040	1	-11.10	.	.	.	.

Level	Number	Mean	Std Dev	Std Err Mean	Lower 95%	Upper 95%
1050	1	-238.60	.	.	.	.
1150	6	64.78	5.798	2.37	58.7	71
1160	1	-123.60	.	.	.	.
1200	13	0.43	82.518	22.89	-49.4	50
1300	6	28.00	7.291	2.98	20.3	36
1380	11	72.82	5.311	1.60	69.2	76
1400	1	-32.20	.	.	.	.
1450	6	-79.90	20.501	8.37	-101.4	-58
1560	11	50.72	7.148	2.16	45.9	56
1600	2	-37.75	26.071	18.44	-272.0	196
1610	1	45.77	.	.	.	.
1740	11	-42.50	19.388	5.85	-55.5	-29
1820	1	61.14	.	.	.	.
1840	2	21.64	10.819	7.65	-75.6	119
2030	1	5.94	.	.	.	.
2080	2	24.57	4.675	3.31	-17.4	67
2320	2	-40.65	2.005	1.42	-58.7	-23

Oneway Analysis of Residual Unmodified |G*|/sin(delta) By X2^2

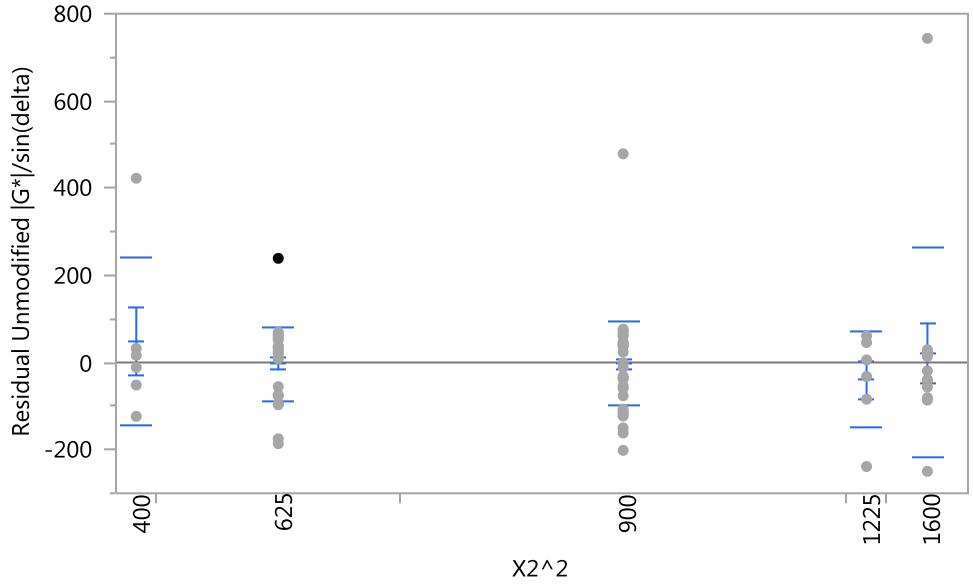

Means and Std Deviations

Level	Number	Mean	Std Dev	Std Err Mean	Lower 95%	Upper 95%
400	6	47.481	192.111	78.429	-154.1	249.09
625	36	-3.765	83.394	13.899	-32.0	24.45
900	66	-2.574	96.929	11.931	-26.4	21.25
1225	6	-40.361	110.594	45.150	-156.4	75.70
1600	12	21.890	239.753	69.211	-130.4	174.22

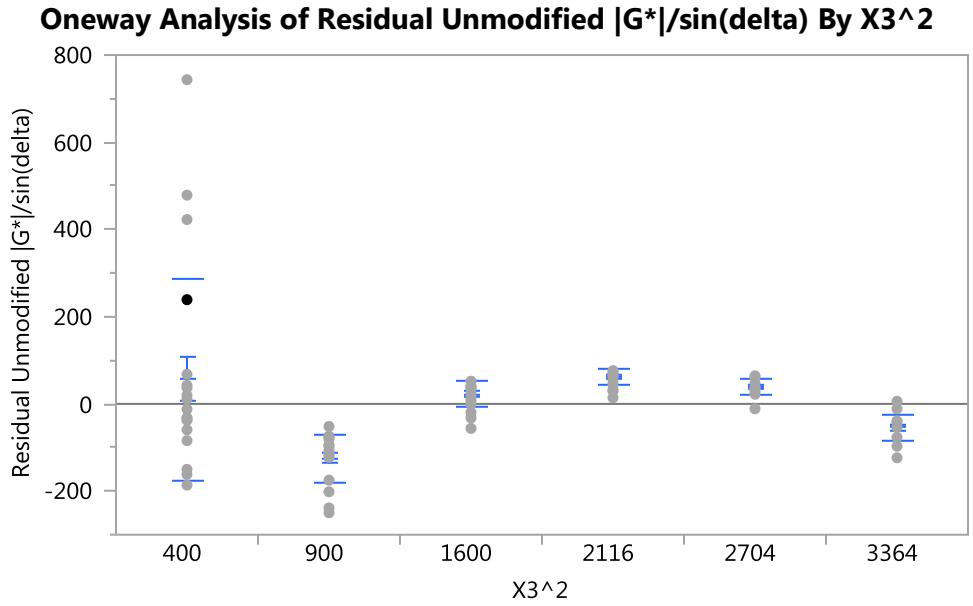

Means and Std Deviations

Level	Number	Mean	Std Dev	Std Err Mean	Lower 95%	Upper 95%
400	21	55.68	231.263	50.466	-49.6	161.0
900	21	-124.98	55.763	12.168	-150.4	-99.6
1600	21	22.15	29.294	6.392	8.8	35.5
2116	21	62.43	17.748	3.873	54.3	70.5
2704	21	39.29	17.958	3.919	31.1	47.5
3364	21	-54.57	31.726	6.923	-69.0	-40.1

Log10 State: Fit Model, Residual Distribution, and Standard Deviation

Response Log10_|G*|/sin(delta)

Effect Summary

Source	LogWorth	PValue
Testing Temp,°C_X3	38.768	0.00000
X2^2	11.668	0.00000
Styrene content,%_X2	9.953	0.00000
X3^2	5.239	0.00001
Styrene MW,kDa_X1	4.979	0.00001

Summary of Fit

RSquare	0.98956
RSquare Adj	0.989125
Root Mean Square Error	0.09392
Mean of Response	1.387448
Observations (or Sum Wgts)	126

Analysis of Variance

Source	DF	Sum of Squares	Mean Square	F Ratio
Model	5	100.33367	20.0667	2274.881
Error	120	1.05852	0.0088	**Prob > F**
C. Total	125	101.39219		<.0001*

Lack Of Fit

Source	DF	Sum of Squares	Mean Square	F Ratio
Lack Of Fit	42	0.0819022	0.001950	0.1557
Pure Error	78	0.9766184	0.012521	**Prob > F**
Total Error	120	1.0585206		1.0000
				Max RSq
				0.9904

Parameter Estimates

Term	Estimate	Std Error	t Ratio	Prob>|t|
Intercept	6.214795	0.256012	24.28	<.0001*
Styrene MW,kDa_X1	-0.004307	0.000936	-4.60	<.0001*
Styrene content,%_X2	-0.113069	0.015994	-7.07	<.0001*
Testing Temp,°C_X3	-0.09025	0.004572	-19.74	<.0001*
X2^2	0.0020146	0.000257	7.83	<.0001*
X3^2	0.0002762	5.819e-5	4.75	<.0001*

Effect Tests

Source	DF	Sum of Squares	Mean Square	F Ratio	Prob > F
Styrene MW,kDa_X1	1	0.1867863	0.186786	21.1752	<.0001*
Styrene content,%_X2	1	0.4408357	0.440836	49.9757	<.0001*
Testing Temp,°C_X3	1	3.4373152	3.437315	389.6739	<.0001*
X2^2	1	0.5410697	0.541070	61.3388	<.0001*
X3^2	1	0.1987523	0.198752	22.5317	<.0001*

Prediction Expression

6.21479500272401

+ -0.0043074663798 * Styrene MW,kDa_X1

+ -0.1130694592589 * Styrene content,%_X2

+ -0.0902504979509 * Testing Temp,°C_X3

+ 0.00201463564881 * X2^2

+ 0.0002762362214 * X3^2

Distributions

Residual Log10_|G*|/sin(delta)

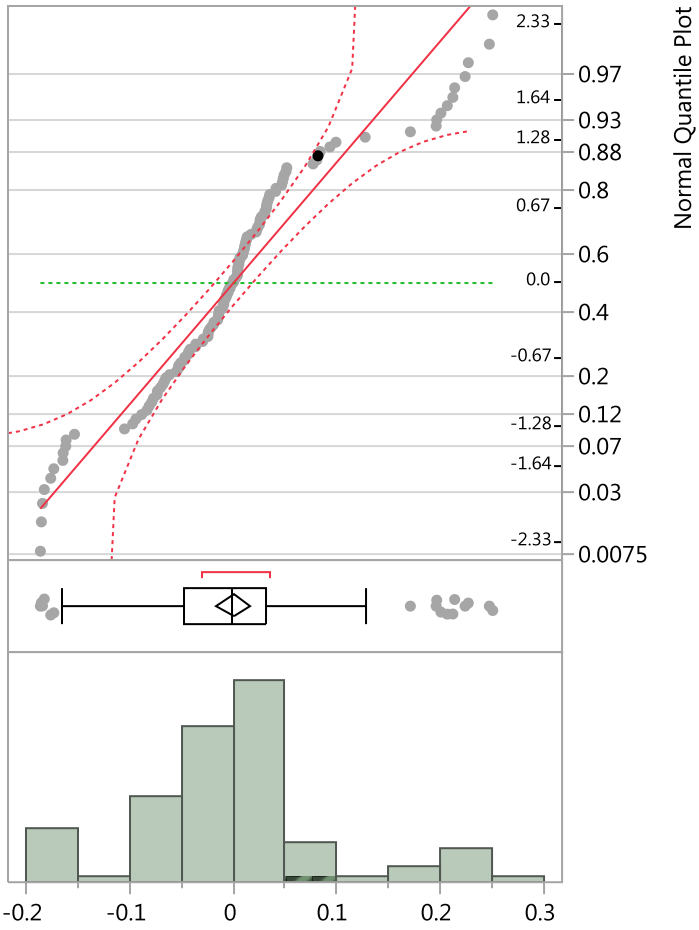

Quantiles

100.0%	maximum	0.2511948687
99.5%		0.2511948687
97.5%		0.2269943092
90.0%		0.1077954891
75.0%	quartile	0.0319014369
50.0%	median	-0.000711344
25.0%	quartile	-0.047199058
10.0%		-0.099976204
2.5%		-0.18464555
0.5%		-0.186986915
0.0%	minimum	-0.186986915

Summary Statistics

Mean	1.384e-16
Std Dev	0.0920226
Std Err Mean	0.008198
Upper 95% Mean	0.0162249
Lower 95% Mean	-0.016225

N 126

Fit Group

Oneway Analysis of Residual Log10_|G*|/sin(delta) By Styrene MW,kDa_X1

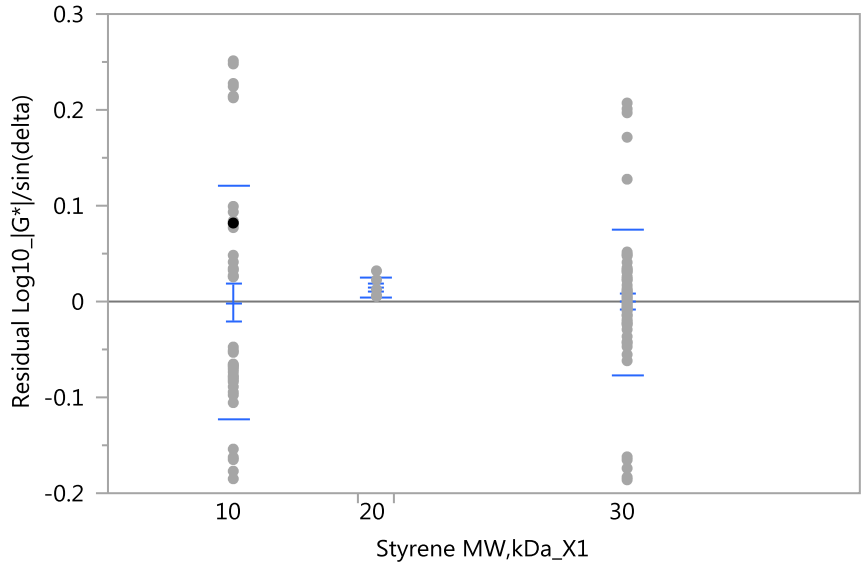

Means and Std Deviations

Level	Number	Mean	Std Dev	Std Err Mean	Lower 95%	Upper 95%
10	42	-0.00108	0.122668	0.01893	-0.0393	0.03714
20	6	0.01518	0.010300	0.00421	0.0044	0.02599
30	78	-0.00058	0.075558	0.00856	-0.0176	0.01645

Oneway Analysis of Residual Log10_|G*|/sin(delta) By Styrene content,%_X2

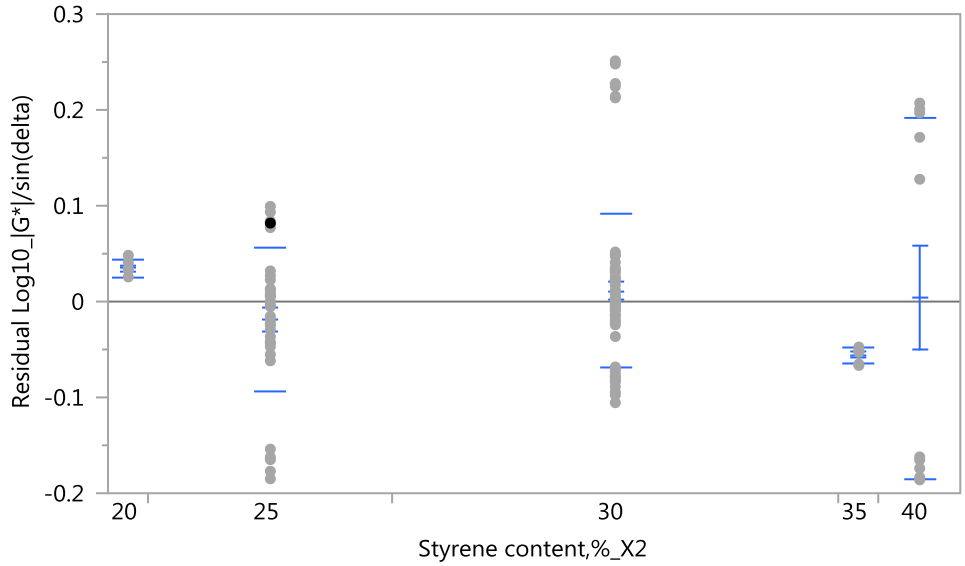

Means and Std Deviations

Level	Number	Mean	Std Dev	Std Err Mean	Lower 95%	Upper 95%
20	6	0.03463	0.008967	0.00366	0.0252	0.0440

Level	Number	Mean	Std Dev	Std Err Mean	Lower 95%	Upper 95%
25	36	-0.01851	0.075172	0.01253	-0.0439	0.0069
30	66	0.01140	0.080355	0.00989	-0.0084	0.0312
35	6	-0.05614	0.007887	0.00322	-0.0644	-0.0479
40	12	0.00359	0.189056	0.05458	-0.1165	0.1237

Oneway Analysis of Residual Log10_|G*|/sin(delta) By Testing Temp,°C_X3

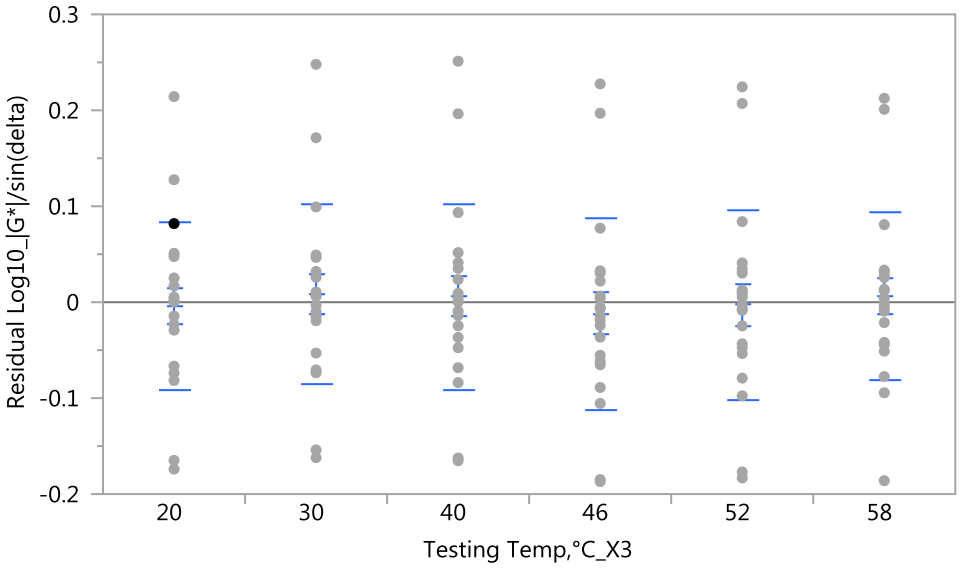

Means and Std Deviations

Level	Number	Mean	Std Dev	Std Err Mean	Lower 95%	Upper 95%
20	21	-0.00454	0.086918	0.01897	-0.0441	0.03503
30	21	0.00836	0.092771	0.02024	-0.0339	0.05059
40	21	0.00577	0.096526	0.02106	-0.0382	0.04971
46	21	-0.01225	0.099443	0.02170	-0.0575	0.03302
52	21	-0.00311	0.098155	0.02142	-0.0478	0.04157
58	21	0.00576	0.087130	0.01901	-0.0339	0.04543

Oneway Analysis of Residual Log10_|G*|/sin(delta) By X2^2

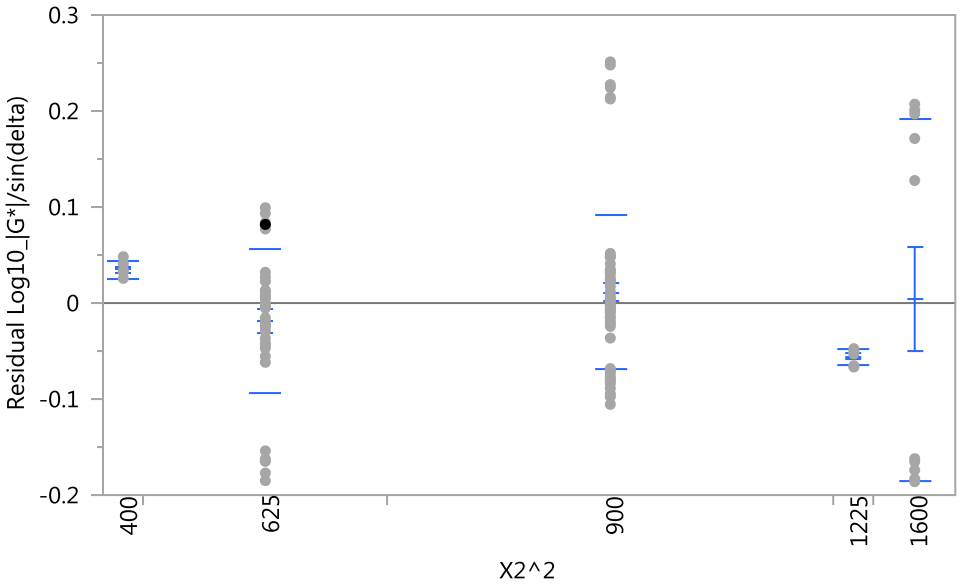

Means and Std Deviations

Level	Number	Mean	Std Dev	Std Err Mean	Lower 95%	Upper 95%
400	6	0.03463	0.008967	0.00366	0.0252	0.0440
625	36	-0.01851	0.075172	0.01253	-0.0439	0.0069
900	66	0.01140	0.080355	0.00989	-0.0084	0.0312
1225	6	-0.05614	0.007887	0.00322	-0.0644	-0.0479
1600	12	0.00359	0.189056	0.05458	-0.1165	0.1237

Oneway Analysis of Residual Log10_|G*|/sin(delta) By X3^2

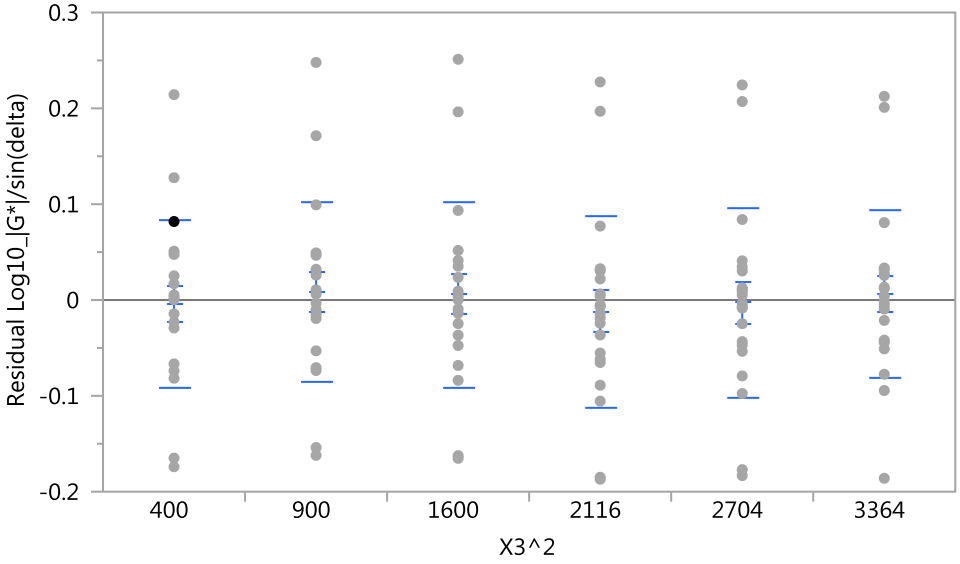

Means and Std Deviations

Level	Number	Mean	Std Dev	Std Err Mean	Lower 95%	Upper 95%
400	21	-0.00454	0.086918	0.01897	-0.0441	0.03503
900	21	0.00836	0.092771	0.02024	-0.0339	0.05059
1600	21	0.00577	0.096526	0.02106	-0.0382	0.04971
2116	21	-0.01225	0.099443	0.02170	-0.0575	0.03302
2704	21	-0.00311	0.098155	0.02142	-0.0478	0.04157
3364	21	0.00576	0.087130	0.01901	-0.0339	0.04543

SQRT State: Fit Model, Residual Distribution, and Standard Deviation

Response SQRT_|G*|/sin(delta)

Effect Summary

Source	LogWorth	PValue
X3^2	40.841	0.00000
Testing Temp,°C_X3	37.635	0.00000
X2^2	3.949	0.00011
Styrene MW,kDa_X1	2.623	0.00238
X2*X3	2.513	0.00307
X1*X3	1.934	0.01164
Styrene content,%_X2	1.673	0.02121

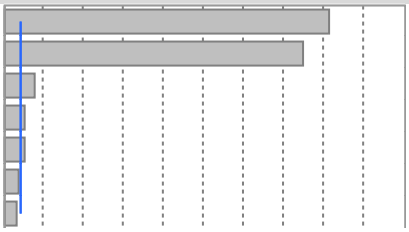

Summary of Fit

RSquare	0.961128
RSquare Adj	0.958822
Root Mean Square Error	1.922818
Mean of Response	8.551419
Observations (or Sum Wgts)	126

Analysis of Variance

Source	DF	Sum of Squares	Mean Square	F Ratio
Model	7	10787.073	1541.01	416.8016
Error	118	436.273	3.70	**Prob > F**
C. Total	125	11223.346		<.0001*

Lack Of Fit

Source	DF	Sum of Squares	Mean Square	F Ratio
Lack Of Fit	40	209.53419	5.23835	1.8020
Pure Error	78	226.73867	2.90691	**Prob > F**
Total Error	118	436.27286		0.0134*
				Max RSq
				0.9798

Parameter Estimates

Term	Estimate	Std Error	t Ratio	Prob>|t|
Intercept	78.744585	6.25963	12.58	<.0001*
Styrene MW,kDa_X1	-0.19704	0.06346	-3.10	0.0024*
Styrene content,%_X2	-0.814492	0.348766	-2.34	0.0212*
Testing Temp,°C_X3	-2.423701	0.125412	-19.33	<.0001*

Term	Estimate	Std Error	t Ratio	Prob>|t|
X1*X3	0.0037817	0.001476	2.56	0.0116*
X2*X3	-0.008853	0.002928	-3.02	0.0031*
X2^2	0.0210451	0.005266	4.00	0.0001*
X3^2	0.0249584	0.001191	20.95	<.0001*

Effect Tests

Source	DF	Sum of Squares	Mean Square	F Ratio	Prob > F
Styrene MW,kDa_X1	1	35.6437	35.644	9.6407	0.0024*
Styrene content,%_X2	1	20.1642	20.164	5.4539	0.0212*
Testing Temp,°C_X3	1	1380.8793	1380.879	373.4905	<.0001*
X1*X3	1	24.2857	24.286	6.5686	0.0116*
X2*X3	1	33.7924	33.792	9.1399	0.0031*
X2^2	1	59.0423	59.042	15.9693	0.0001*
X3^2	1	1622.4956	1622.496	438.8411	<.0001*

Distributions

Residual SQRT_|G*|/sin(delta)

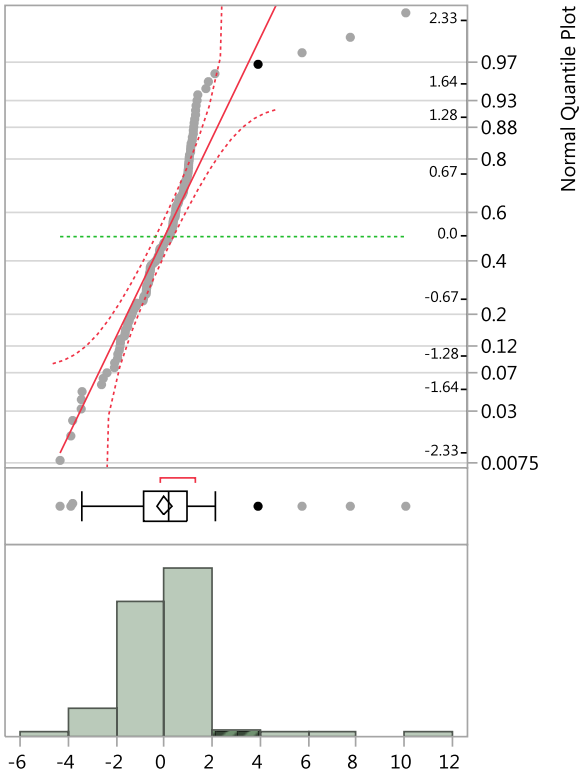

Quantiles

100.0%	maximum	10.084339701
99.5%		10.084339701
97.5%		5.4281031449
90.0%		1.2747654601
75.0%	quartile	0.9742529137
50.0%	median	0.196479053
25.0%	quartile	-0.881276916
10.0%		-1.951206296
2.5%		-3.772959046
0.5%		-4.362000007
0.0%	minimum	-4.362000007

Summary Statistics

Mean	1.319e-14
Std Dev	1.8682031
Std Err Mean	0.1664328
Upper 95% Mean	0.3293911
Lower 95% Mean	-0.329391
N	126

Fit Group

Oneway Analysis of Residual SQRT_|G*|/sin(delta) By Styrene MW,kDa_X1

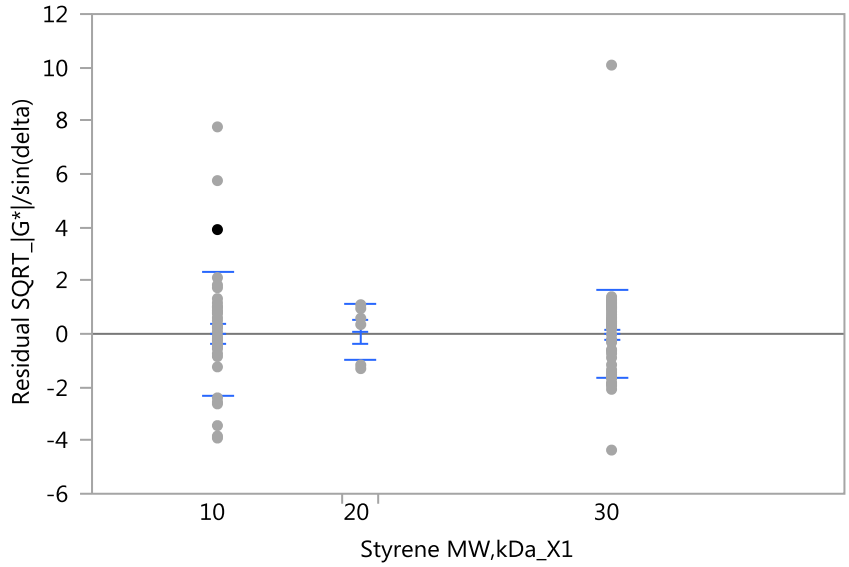

Means and Std Deviations

Level	Number	Mean	Std Dev	Std Err Mean	Lower 95%	Upper 95%
10	42	-0.00601	2.31014	0.35646	-0.726	0.7139
20	6	0.08419	1.05731	0.43165	-1.025	1.1938
30	78	-0.00324	1.65863	0.18780	-0.377	0.3707

Oneway Analysis of Residual SQRT_|G*|/sin(delta) By Styrene content,%_X2

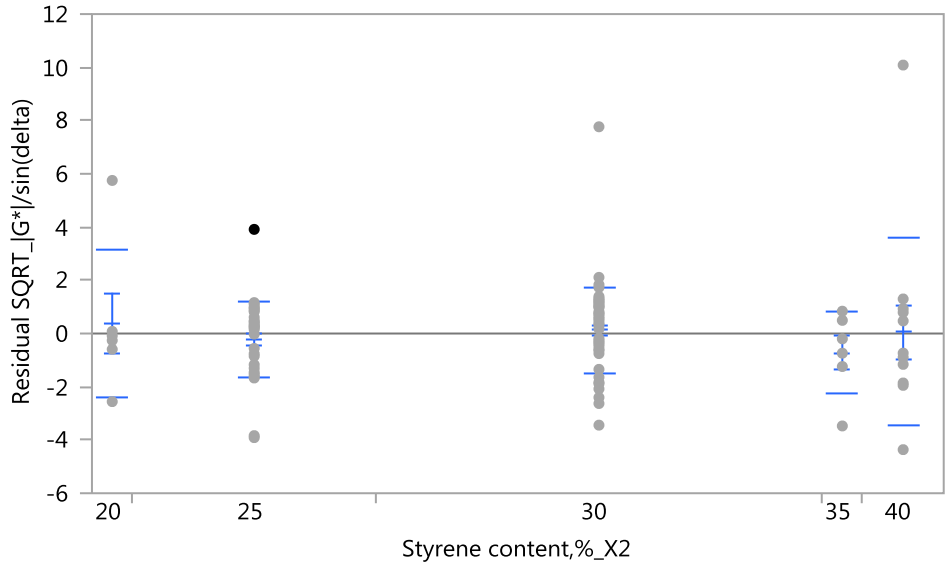

Means and Std Deviations

Level	Number	Mean	Std Dev	Std Err Mean	Lower 95%	Upper 95%
20	6	0.38900	2.79746	1.1421	-2.547	3.3248
25	36	-0.21287	1.43322	0.2389	-0.698	0.2721

Level	Number	Mean	Std Dev	Std Err Mean	Lower 95%	Upper 95%
30	66	0.13616	1.60991	0.1982	-0.260	0.5319
35	6	-0.71973	1.55042	0.6330	-2.347	0.9073
40	12	0.05512	3.54009	1.0219	-2.194	2.3044

Oneway Analysis of Residual SQRT_|G*|/sin(delta) By Testing Temp,°C_X3

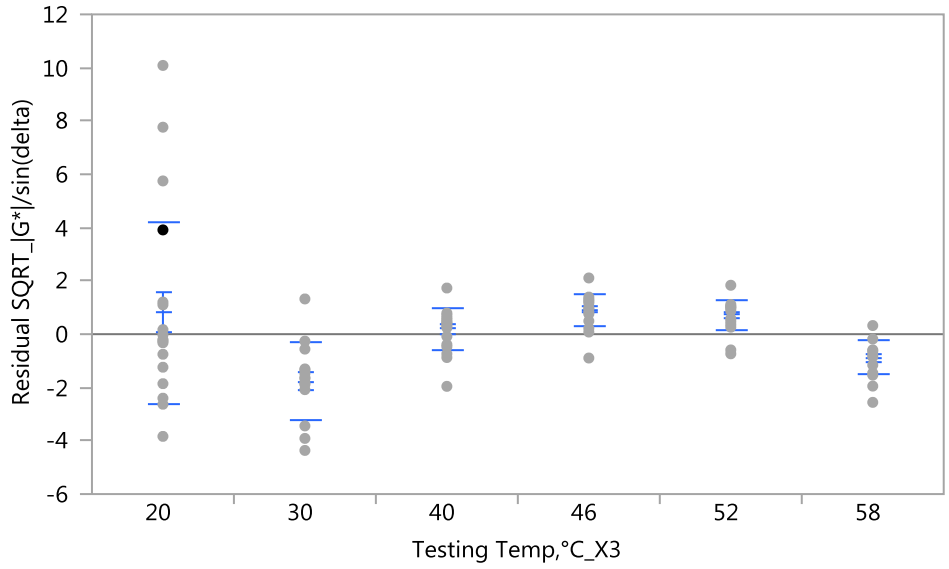

Means and Std Deviations

Level	Number	Mean	Std Dev	Std Err Mean	Lower 95%	Upper 95%
20	21	0.8052	3.42355	0.74708	-0.753	2.364
30	21	-1.7637	1.47565	0.32201	-2.435	-1.092
40	21	0.1890	0.75392	0.16452	-0.154	0.532
46	21	0.9234	0.60116	0.13118	0.650	1.197
52	21	0.7171	0.57902	0.12635	0.454	0.981
58	21	-0.8710	0.65900	0.14380	-1.171	-0.571

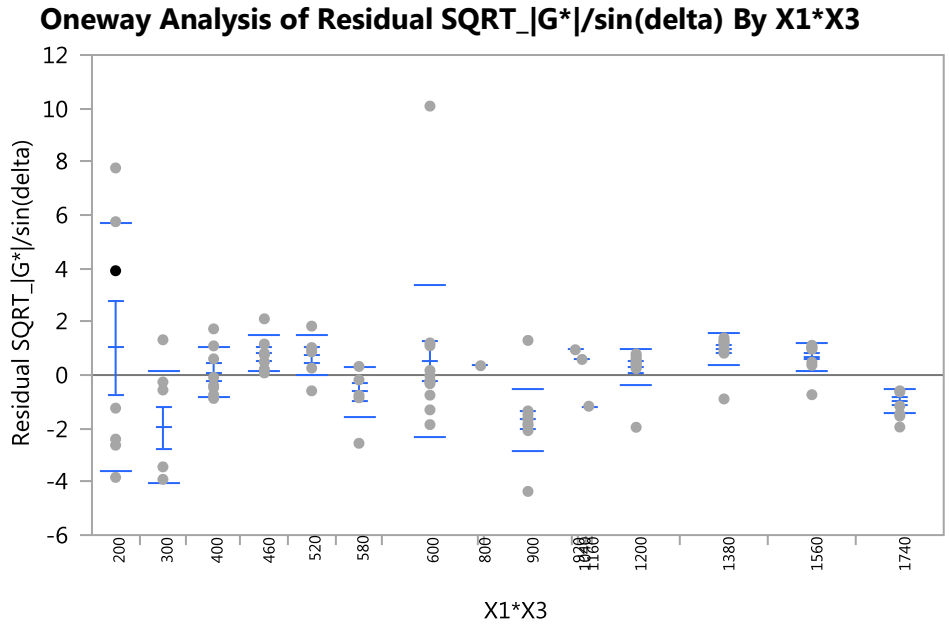

Means and Std Deviations

Level	Number	Mean	Std Dev	Std Err Mean	Lower 95%	Upper 95%
200	7	1.0459	4.65378	1.7590	-3.258	5.350
300	7	-1.9718	2.09052	0.7901	-3.905	-0.038
400	8	0.1090	0.93837	0.3318	-0.675	0.894
460	7	0.8062	0.68214	0.2578	0.175	1.437
520	7	0.7483	0.74997	0.2835	0.055	1.442
580	7	-0.6330	0.93648	0.3540	-1.499	0.233
600	14	0.5135	2.87218	0.7676	-1.145	2.172
800	1	0.3504	.	.	.	.
900	13	-1.6868	1.18106	0.3276	-2.401	-0.973
920	1	0.9492	.	.	.	.
1040	1	0.5860	.	.	.	.
1160	1	-1.1688	.	.	.	.
1200	13	0.2954	0.69509	0.1928	-0.125	0.715
1380	13	0.9844	0.59796	0.1658	0.623	1.346
1560	13	0.7104	0.52487	0.1456	0.393	1.028
1740	13	-0.9762	0.48257	0.1338	-1.268	-0.685

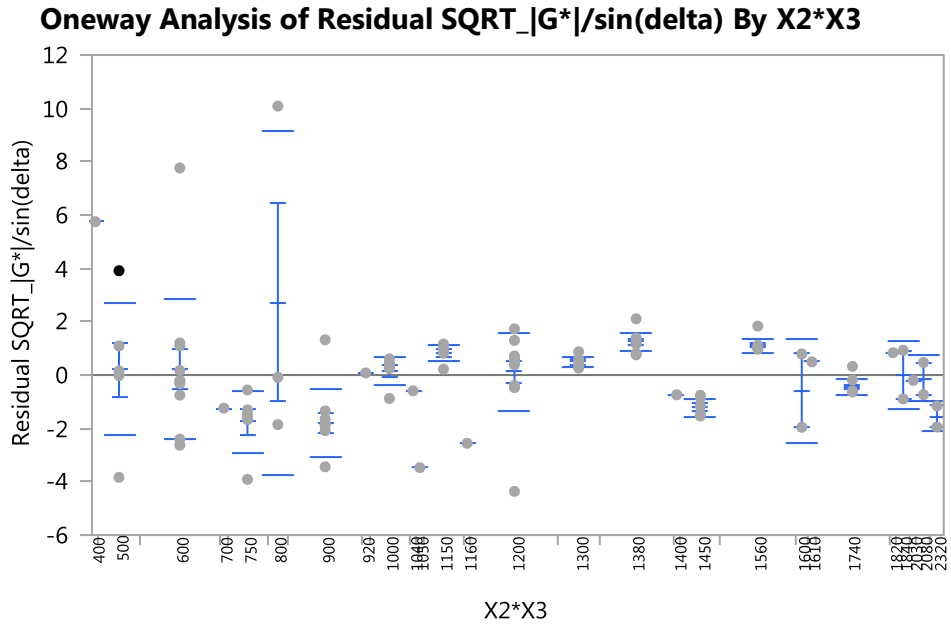

Means and Std Deviations

Level	Number	Mean	Std Dev	Std Err Mean	Lower 95%	Upper 95%
400	1	5.7497	.	.	.	.
500	6	0.2102	2.48872	1.0160	-2.40	2.82
600	12	0.2209	2.63777	0.7615	-1.46	1.90
700	1	-1.2403	.	.	.	.
750	6	-1.7578	1.12983	0.4613	-2.94	-0.57
800	3	2.7139	6.44416	3.7205	-13.29	18.72
900	11	-1.7904	1.25893	0.3796	-2.64	-0.94
920	1	0.0797	.	.	.	.
1000	6	0.1773	0.53178	0.2171	-0.38	0.74
1040	1	-0.5913	.	.	.	.
1050	1	-3.4722	.	.	.	.
1150	6	0.8232	0.32223	0.1316	0.49	1.16
1160	1	-2.5586	.	.	.	.
1200	13	0.1410	1.47075	0.4079	-0.75	1.03
1300	6	0.4882	0.21864	0.0893	0.26	0.72
1380	11	1.2585	0.34785	0.1049	1.02	1.49
1400	1	-0.7392	.	.	.	.
1450	6	-1.2183	0.34868	0.1423	-1.58	-0.85
1560	11	1.1042	0.24615	0.0742	0.94	1.27
1600	2	-0.5825	1.94498	1.3753	-18.06	16.89
1610	1	0.4943	.	.	.	.
1740	11	-0.4650	0.31585	0.0952	-0.68	-0.25
1820	1	0.8381	.	.	.	.
1840	2	0.0168	1.28984	0.9121	-11.57	11.61
2030	1	-0.1992	.	.	.	.
2080	2	-0.1315	0.85474	0.6044	-7.81	7.55
2320	2	-1.5541	0.55751	0.3942	-6.56	3.45

Oneway Analysis of Residual SQRT_|G*|/sin(delta) By X2^2

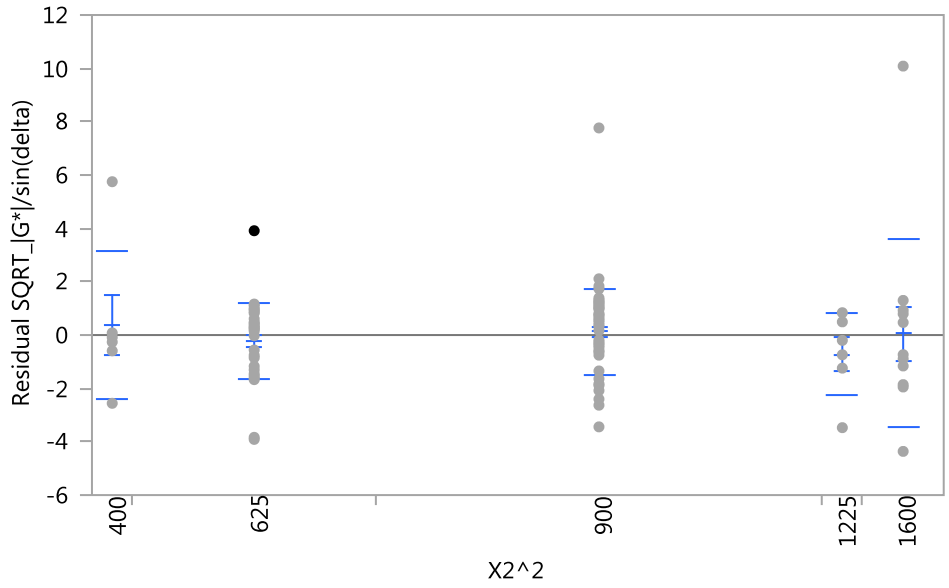

Means and Std Deviations

Level	Number	Mean	Std Dev	Std Err Mean	Lower 95%	Upper 95%
400	6	0.38900	2.79746	1.1421	-2.547	3.3248
625	36	-0.21287	1.43322	0.2389	-0.698	0.2721
900	66	0.13616	1.60991	0.1982	-0.260	0.5319
1225	6	-0.71973	1.55042	0.6330	-2.347	0.9073
1600	12	0.05512	3.54009	1.0219	-2.194	2.3044

Oneway Analysis of Residual SQRT_|G*|/sin(delta) By X3^2

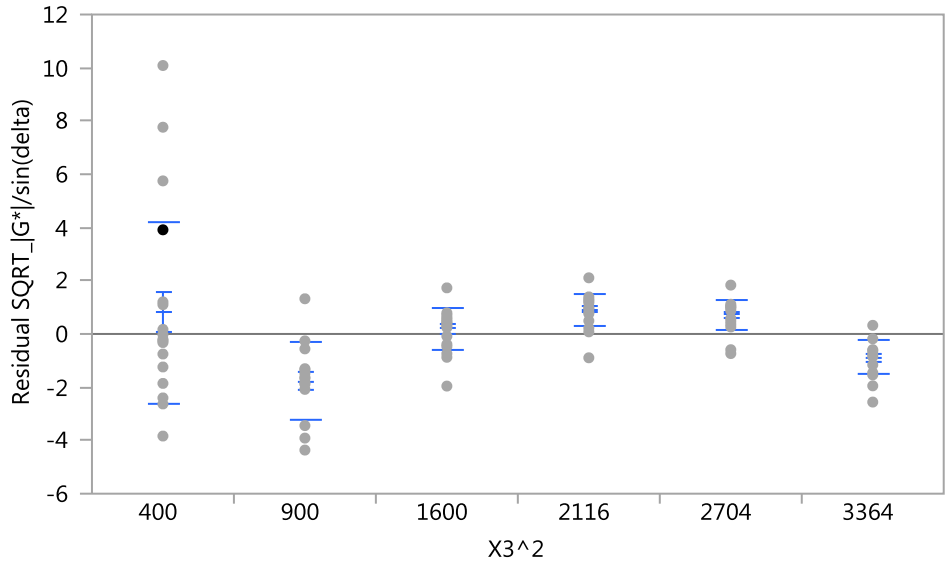

Means and Std Deviations

Level	Number	Mean	Std Dev	Std Err Mean	Lower 95%	Upper 95%
400	21	0.8052	3.42355	0.74708	-0.753	2.364
900	21	-1.7637	1.47565	0.32201	-2.435	-1.092
1600	21	0.1890	0.75392	0.16452	-0.154	0.532
2116	21	0.9234	0.60116	0.13118	0.650	1.197
2704	21	0.7171	0.57902	0.12635	0.454	0.981
3364	21	-0.8710	0.65900	0.14380	-1.171	-0.571

Comparing Residuals in Graph Builder

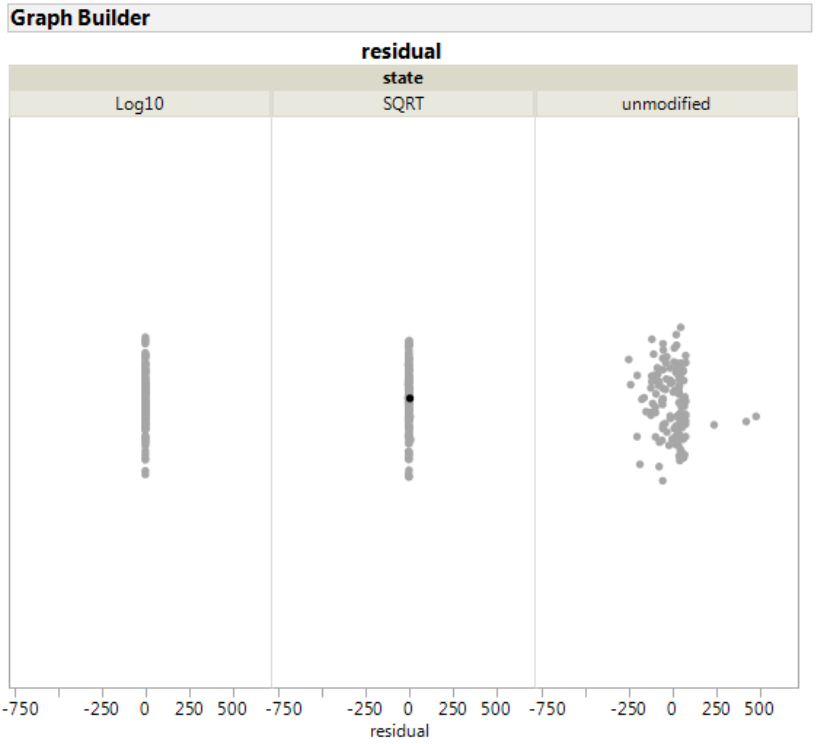

Response surface model for shear blending results at m-value of PAV long-term aged modified blends

Unmodified State: Fit Model, Residual Distribution, and Standard Deviation

Response Unmodified m-value

Effect Summary

Source	LogWorth	PValue
X2*X3	35.382	0.00000
Styrene content,%_X2	22.399	0.00000
X1^2	4.345	0.00005

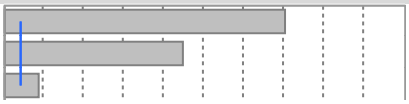

Summary of Fit

RSquare	0.736703
RSquare Adj	0.730228
Root Mean Square Error	0.019854
Mean of Response	0.336214
Observations (or Sum Wgts)	126

Analysis of Variance

Source	DF	Sum of Squares	Mean Square	F Ratio
Model	3	0.13455080	0.044850	113.7848
Error	122	0.04808842	0.000394	**Prob > F**
C. Total	125	0.18263921		<.0001*

Lack Of Fit

Source	DF	Sum of Squares	Mean Square	F Ratio
Lack Of Fit	12	0.00801075	0.000668	1.8322
Pure Error	110	0.04007767	0.000364	**Prob > F**
Total Error	122	0.04808842		0.0514
				Max RSq
				0.7806

Parameter Estimates

Term	Estimate	Std Error	t Ratio	Prob>|t|
Intercept	0.3372696	0.011158	30.23	<.0001*
Styrene content,%_X2	0.0070395	0.000572	12.31	<.0001*
X2*X3	0.0003575	1.988e-5	17.98	<.0001*
X1^2	2.0734e-5	4.9e-6	4.23	<.0001*

Effect Tests

Source	DF	Sum of Squares	Mean Square	F Ratio	Prob > F
Styrene content,%_X2	1	0.05969868	0.0596987	151.4551	<.0001*
X2*X3	1	0.12749170	0.1274917	323.4456	<.0001*
X1^2	1	0.00705851	0.0070585	17.9074	<.0001*

Distributions

Residual Unmodified m-value

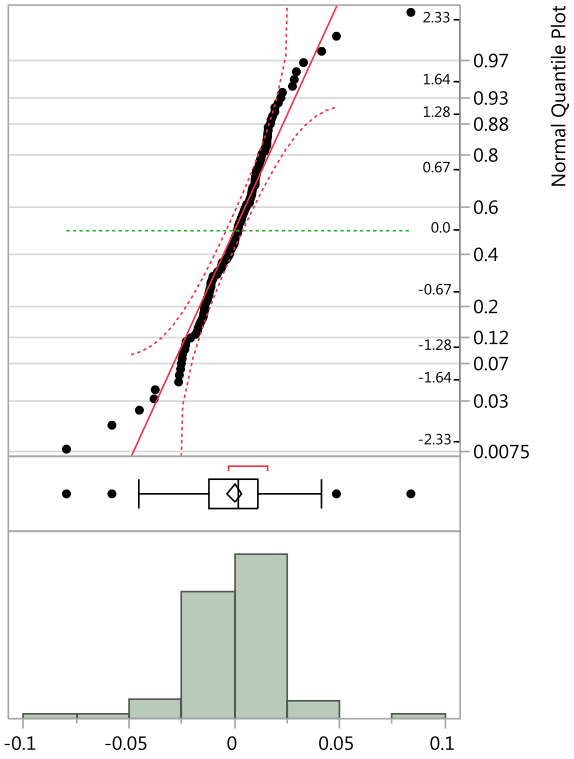

Quantiles

100.0%	maximum	0.083948108
99.5%		0.083948108
97.5%		0.0400465193
90.0%		0.0185836529
75.0%	quartile	0.0108804644
50.0%	median	0.0016202147
25.0%	quartile	-0.011810336
10.0%		-0.023246582
2.5%		-0.043840238
0.5%		-0.079729817
0.0%	minimum	-0.079729817

Summary Statistics

Mean	1.561e-17
Std Dev	0.019614
Std Err Mean	0.0017474
Upper 95% Mean	0.0034582
Lower 95% Mean	-0.003458
N	126

Fit Group

Oneway Analysis of Residual Unmodified m-value By Styrene content,%_X2

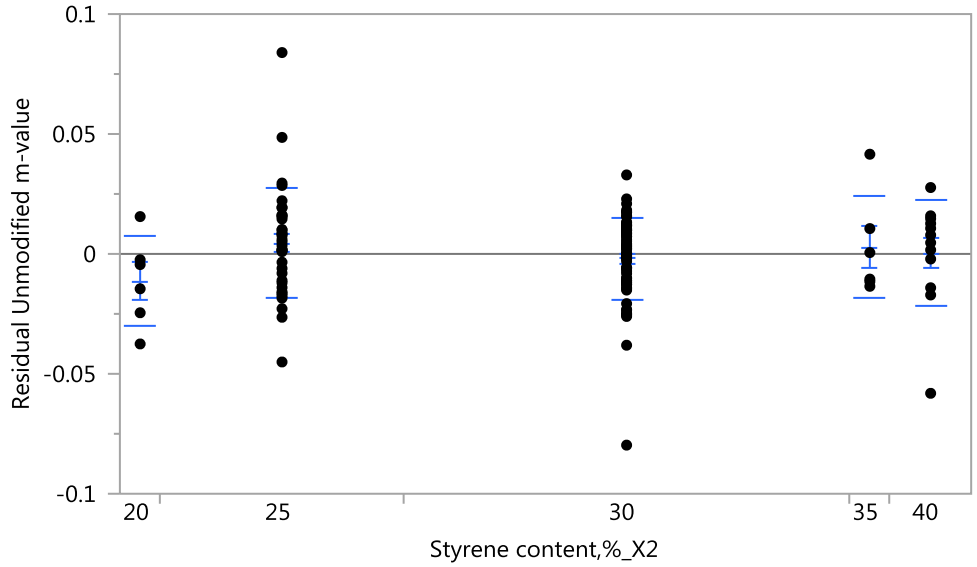

Means and Std Deviations

Level	Number	Mean	Std Dev	Std Err Mean	Lower 95%	Upper 95%
20	6	-0.01132	0.018556	0.00758	-0.0308	0.00815
25	36	0.00449	0.022715	0.00379	-0.0032	0.01217
30	66	-0.00174	0.017042	0.00210	-0.0059	0.00245
35	6	0.00286	0.021050	0.00859	-0.0192	0.02495
40	12	0.00036	0.022296	0.00644	-0.0138	0.01452

Oneway Analysis of Residual Unmodified m-value By X2*X3

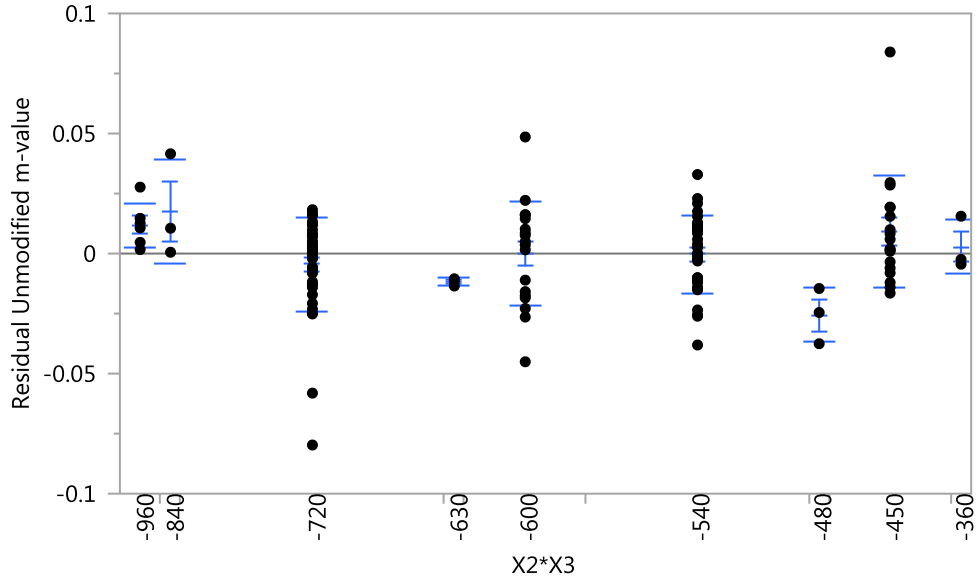

Means and Std Deviations

Level	Number	Mean	Std Dev	Std Err Mean	Lower 95%	Upper 95%
-960	6	0.01200	0.009114	0.00372	0.0024	0.0216
-840	3	0.01756	0.021378	0.01234	-0.0355	0.0707
-720	39	-0.00440	0.019457	0.00312	-0.0107	0.0019
-630	3	-0.01185	0.001528	0.00088	-0.0156	-0.0081
-600	18	-0.00017	0.021862	0.00515	-0.0110	0.0107
-540	33	-0.00034	0.015934	0.00277	-0.0060	0.0053
-480	3	-0.02554	0.011533	0.00666	-0.0542	0.0031
-450	18	0.00915	0.023203	0.00547	-0.0024	0.0207
-360	3	0.00289	0.011015	0.00636	-0.0245	0.0303

Oneway Analysis of Residual Unmodified m-value By X1^2

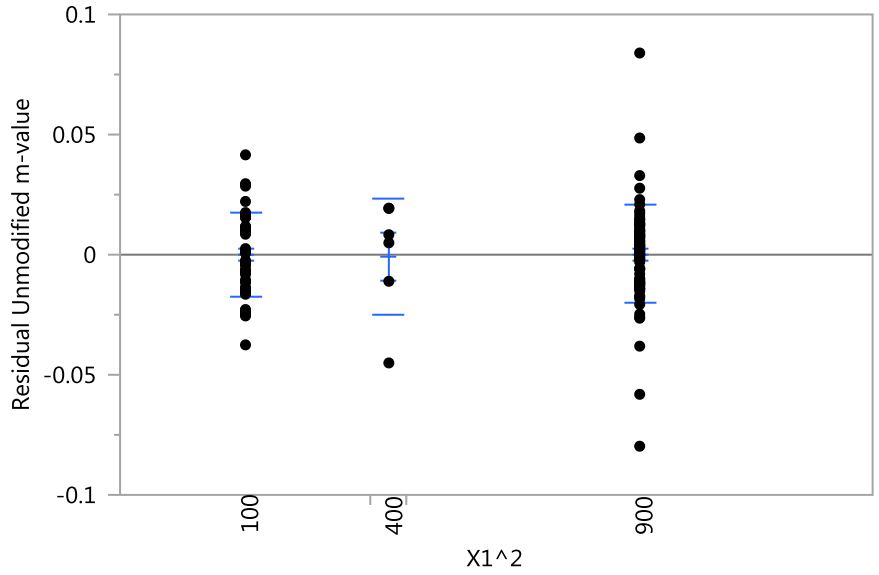

Means and Std Deviations

Level	Number	Mean	Std Dev	Std Err Mean	Lower 95%	Upper 95%
100	42	6.315e-5	0.017775	0.00274	-0.0055	0.00560
400	6	-0.00071	0.024453	0.00998	-0.0264	0.02495
900	78	2.04e-5	0.020431	0.00231	-0.0046	0.00463

Log10 State: Fit Model, Residual Distribution, and Standard Deviation

Response Log10_m-value

Effect Summary

Source	LogWorth	PValue
Testing Temp,°C_X3	37.078	0.00000
X1^2	4.197	0.00006

Summary of Fit

RSquare	0.749272
RSquare Adj	0.745195
Root Mean Square Error	0.025237

Mean of Response	-0.47621
Observations (or Sum Wgts)	126

Analysis of Variance

Source	DF	Sum of Squares	Mean Square	F Ratio
Model	2	0.23410825	0.117054	183.7857
Error	123	0.07833937	0.000637	**Prob > F**
C. Total	125	0.31244762		<.0001*

Lack Of Fit

Source	DF	Sum of Squares	Mean Square	F Ratio
Lack Of Fit	3	0.00145107	0.000484	0.7549
Pure Error	120	0.07688829	0.000641	**Prob > F**
Total Error	123	0.07833937		0.5216
				Max RSq
				0.7539

Parameter Estimates

Term	Estimate	Std Error	t Ratio	Prob>|t|
Intercept	-0.196727	0.016312	-12.06	<.0001*
Testing Temp,°C_X3	0.0140289	0.000749	18.72	<.0001*
X1^2	2.4811e-5	0.000006	4.14	<.0001*

Effect Tests

Source	DF	Sum of Squares	Mean Square	F Ratio	Prob > F
Testing Temp,°C_X3	1	0.22318228	0.2231823	350.4167	<.0001*
X1^2	1	0.01092597	0.0109260	17.1548	<.0001*

Distributions

Residual Log10_m-value

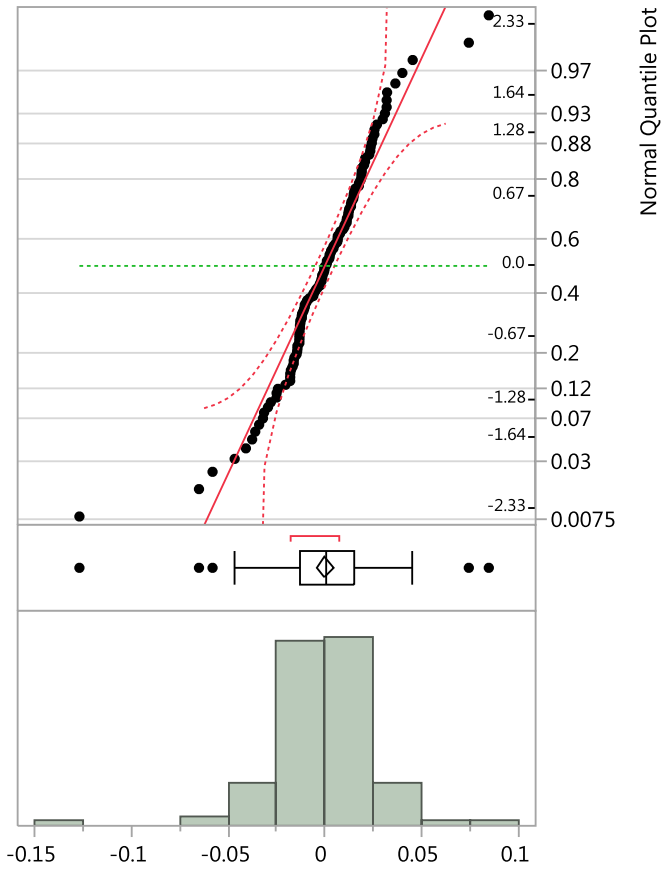

Quantiles

100.0%	maximum	0.0849281442
99.5%		0.0849281442
97.5%		0.0445514147
90.0%		0.0256586662
75.0%	quartile	0.0149024442
50.0%	median	0.0002747212
25.0%	quartile	-0.013176628
10.0%		-0.025915465
2.5%		-0.056197673
0.5%		-0.127182074
0.0%	minimum	-0.127182074

Summary Statistics

Mean	1.983e-17
Std Dev	0.0250343
Std Err Mean	0.0022302
Upper 95% Mean	0.0044139
Lower 95% Mean	-0.004414
N	126

Fit Group

Oneway Analysis of Residual Log10_m-value By Testing Temp,°C_X3

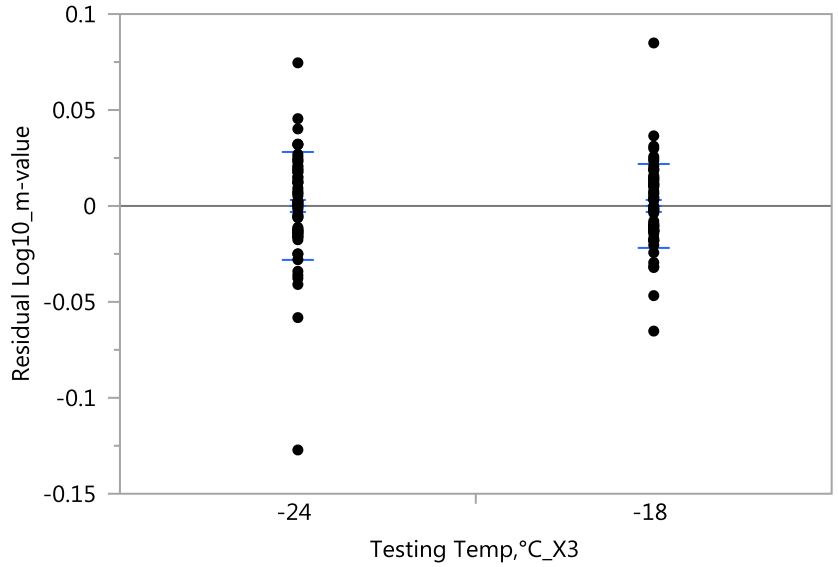

Means and Std Deviations

Level	Number	Mean	Std Dev	Std Err Mean	Lower 95%	Upper 95%
-24	63	1.764e-17	0.028076	0.00354	-0.0071	0.00707
-18	63	2.175e-17	0.021801	0.00275	-0.0055	0.00549

Oneway Analysis of Residual Log10_m-value By X1^2

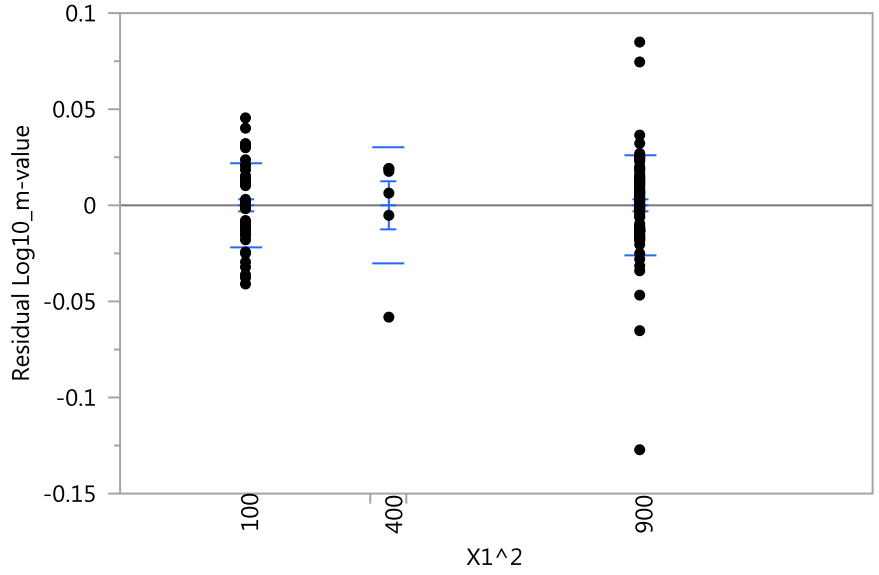

Means and Std Deviations

Level	Number	Mean	Std Dev	Std Err Mean	Lower 95%	Upper 95%
100	42	0.000018	0.022203	0.00343	-0.0069	0.00694
400	6	-0.00020	0.029988	0.01224	-0.0317	0.03127
900	78	5.791e-6	0.026391	0.00299	-0.0059	0.00596

SQRT State: Fit Model, Residual Distribution, and Standard Deviation

Response SQRT_m-value

Effect Summary

Source	LogWorth	PValue
Testing Temp,°C_X3	37.677	0.00000
X1^2	4.310	0.00005

Summary of Fit

RSquare	0.754902
RSquare Adj	0.750917
Root Mean Square Error	0.016519
Mean of Response	0.578902
Observations (or Sum Wgts)	126

Analysis of Variance

Source	DF	Sum of Squares	Mean Square	F Ratio
Model	2	0.10337684	0.051688	189.4204
Error	123	0.03356384	0.000273	**Prob > F**
C. Total	125	0.13694068		<.0001*

Lack Of Fit

Source	DF	Sum of Squares	Mean Square	F Ratio
Lack Of Fit	3	0.00059067	0.000197	0.7166
Pure Error	120	0.03297317	0.000275	**Prob > F**
Total Error	123	0.03356384		0.5440
				Max RSq
				0.7592

Parameter Estimates

Term	Estimate	Std Error	t Ratio	Prob>|t|
Intercept	0.7646011	0.010677	71.61	<.0001*
Testing Temp,°C_X3	0.0093219	0.000491	19.00	<.0001*
X1^2	0.0000165	3.921e-6	4.21	<.0001*

Effect Tests

Source	DF	Sum of Squares	Mean Square	F Ratio	Prob > F
Testing Temp,°C_X3	1	0.09854171	0.0985417	361.1216	<.0001*
X1^2	1	0.00483513	0.0048351	17.7191	<.0001*

Distributions

Residual SQRT_m-value

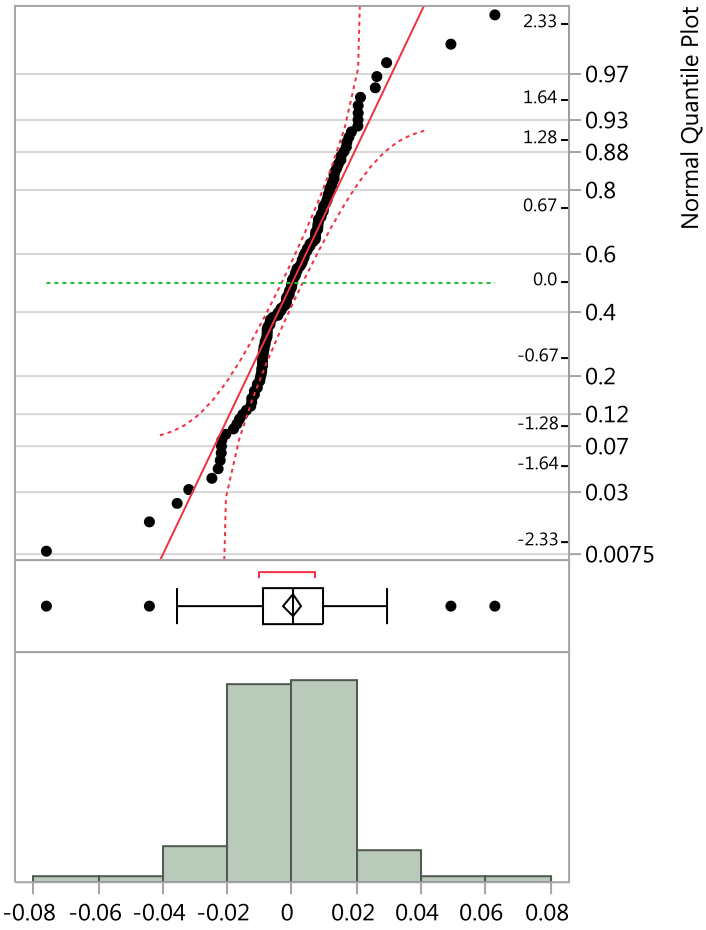

Quantiles

100.0%	maximum	0.0628749118
99.5%		0.0628749118
97.5%		0.0287860706
90.0%		0.0171745131
75.0%	quartile	0.0097608092
50.0%	median	0.0000202131
25.0%	quartile	-0.009167153
10.0%		-0.0173991
2.5%		-0.034986631
0.5%		-0.076147534
0.0%	minimum	-0.076147534

Summary Statistics

Mean	8.04e-18
Std Dev	0.0163863
Std Err Mean	0.0014598
Upper 95% Mean	0.0028891
Lower 95% Mean	-0.002889
N	126

Fit Group

Oneway Analysis of Residual SQRT_m-value By Testing Temp,°C_X3

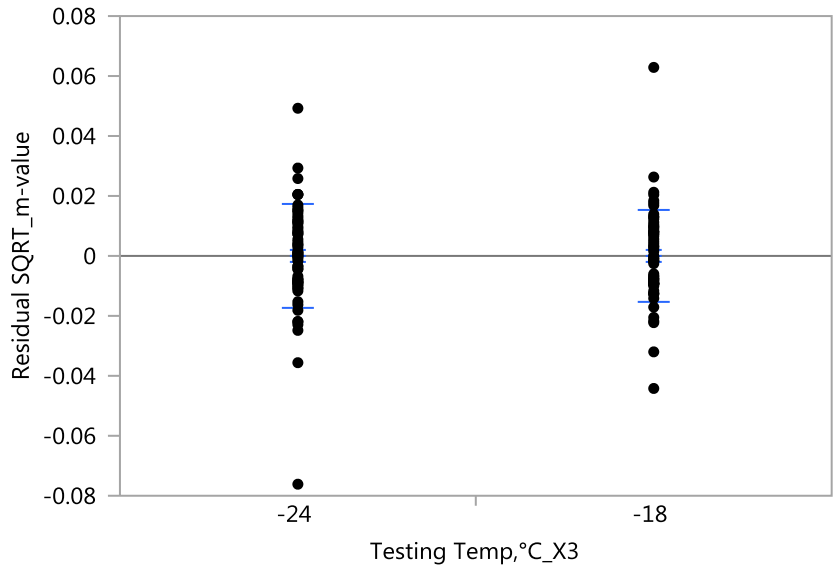

Means and Std Deviations

Level	Number	Mean	Std Dev	Std Err Mean	Lower 95%	Upper 95%
-24	63	-6.55e-18	0.017479	0.00220	-0.0044	0.00440
-18	63	2.266e-17	0.015357	0.00193	-0.0039	0.00387

Oneway Analysis of Residual SQRT_m-value By X1^2

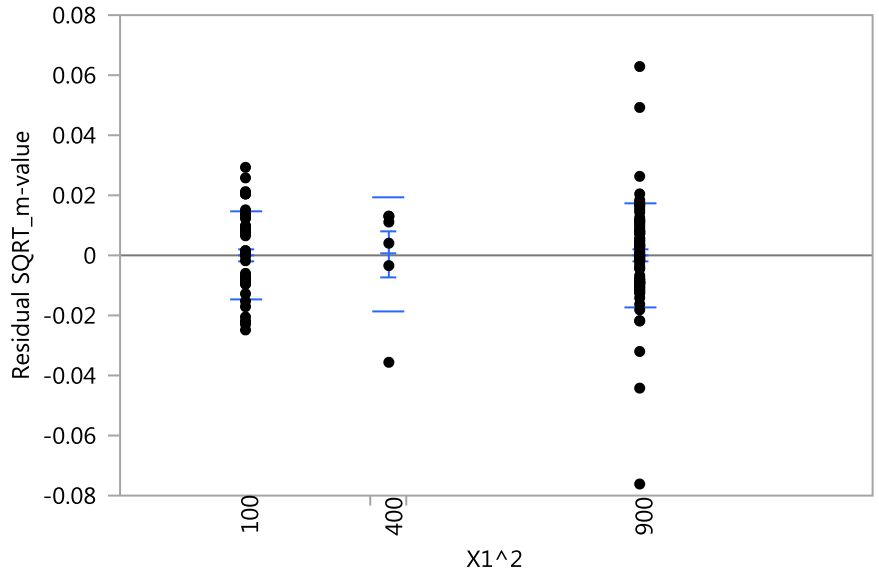

Means and Std Deviations

Level	Number	Mean	Std Dev	Std Err Mean	Lower 95%	Upper 95%
100	42	-3.22e-5	0.014405	0.00222	-0.0045	0.00446
400	6	0.00036	0.018754	0.00766	-0.0193	0.02004
900	78	-0.00001	0.017394	0.00197	-0.0039	0.00391

Comparing Residuals in Graph Builder

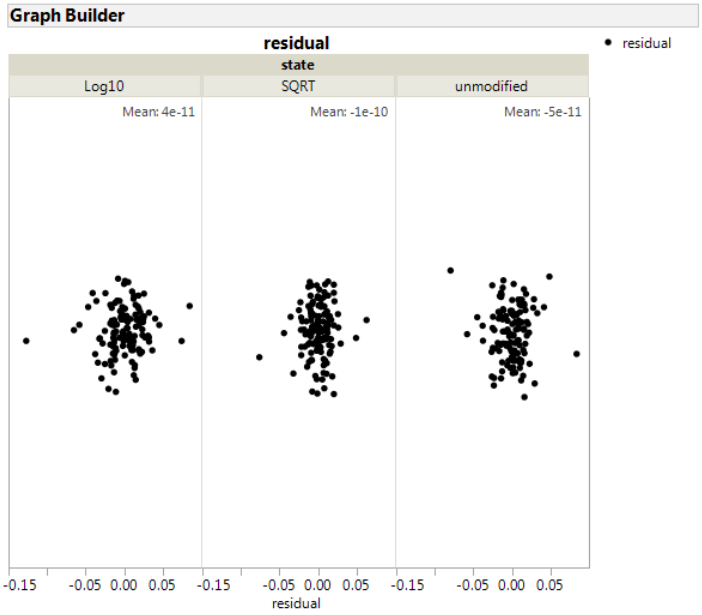

Response surface model for shear blending results at stiffness of PAV long-term aged modified blends

Unmodified State: Fit Model, Residual Distribution, and Standard Deviation

Response Unmodified stiffness

Effect Summary

Source	LogWorth	PValue
Testing Temp,°C_X3	57.510	0.00000
X1*X2	3.209	0.00062
X2^2	2.807	0.00156
Styrene content,%_X2	2.001	0.00998

Summary of Fit

RSquare	0.88649
RSquare Adj	0.882737
Root Mean Square Error	22.63104
Mean of Response	168.3802
Observations (or Sum Wgts)	126

Analysis of Variance

Source	DF	Sum of Squares	Mean Square	F Ratio
Model	4	483985.41	120996	236.2454
Error	121	61971.84	512	**Prob > F**
C. Total	125	545957.24		<.0001*

Lack Of Fit

Source	DF	Sum of Squares	Mean Square	F Ratio
Lack Of Fit	11	8735.343	794.122	1.6409
Pure Error	110	53236.492	483.968	**Prob > F**
Total Error	121	61971.835		0.0971
				Max RSq
				0.9025

Parameter Estimates

Term	Estimate	Std Error	t Ratio	Prob>|t|
Intercept	-121.9343	59.97712	-2.03	0.0442*
Styrene content,%_X2	-10.01158	3.824346	-2.62	0.0100*
Testing Temp,°C_X3	-20.31772	0.672044	-30.23	<.0001*
X1*X2	-0.027057	0.007695	-3.52	0.0006*
X2^2	0.1992163	0.061551	3.24	0.0016*

Effect Tests

Source	DF	Sum of Squares	Mean Square	F Ratio	Prob > F
Styrene content,%_X2	1	3509.94	3509.9	6.8532	0.0100*
Testing Temp,°C_X3	1	468126.48	468126.5	914.0169	<.0001*
X1*X2	1	6331.67	6331.7	12.3626	0.0006*
X2^2	1	5365.31	5365.3	10.4758	0.0016*

Distributions

Residual Unmodified stiffness

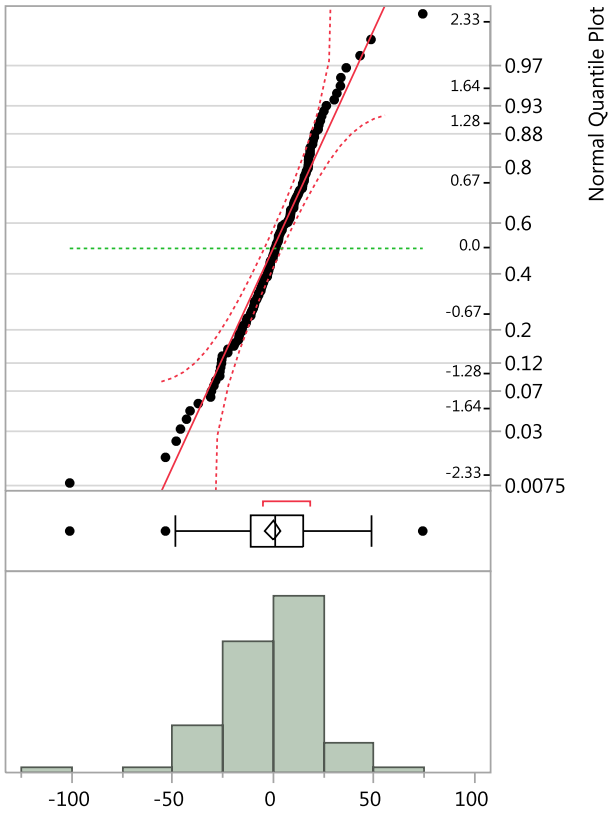

Quantiles

100.0%	maximum	74.478659604
99.5%		74.478659604
97.5%		42.060559536
90.0%		22.94720195
75.0%	quartile	14.879793299
50.0%	median	0.9659513293
25.0%	quartile	-11.15590946
10.0%		-26.5339011
2.5%		-47.91278709
0.5%		-101.2872233
0.0%	minimum	-101.2872233

Summary Statistics

Mean	1.203e-14
Std Dev	22.265998
Std Err Mean	1.9836128
Upper 95% Mean	3.9258159
Lower 95% Mean	-3.925816
N	126

Fit Group

Oneway Analysis of Residual Unmodified stiffness By Styrene content,%_X2

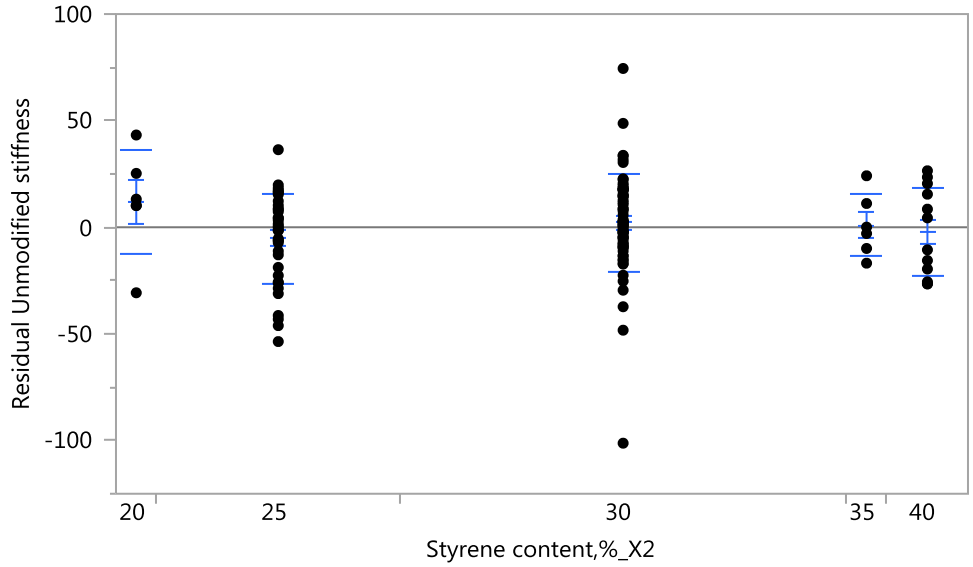

Means and Std Deviations

Level	Number	Mean	Std Dev	Std Err Mean	Lower 95%	Upper 95%
20	6	11.885	24.4447	9.9795	-13.77	37.538
25	36	-5.231	21.1743	3.5290	-12.39	1.934
30	66	2.076	23.2925	2.8671	-3.65	7.802
35	6	0.931	14.7902	6.0381	-14.59	16.452
40	12	-2.136	20.7934	6.0025	-15.35	11.076

Oneway Analysis of Residual Unmodified stiffness By Testing Temp,°C_X3

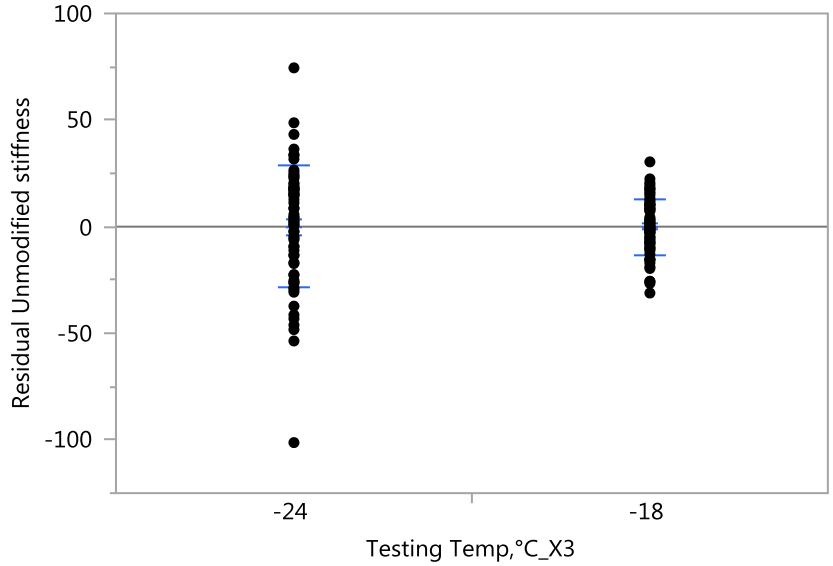

Means and Std Deviations

Level	Number	Mean	Std Dev	Std Err Mean	Lower 95%	Upper 95%
-24	63	4.021e-14	28.6985	3.6157	-7.228	7.2276
-18	63	-1.56e-14	13.2644	1.6712	-3.341	3.3406

Oneway Analysis of Residual Unmodified stiffness By X1*X2

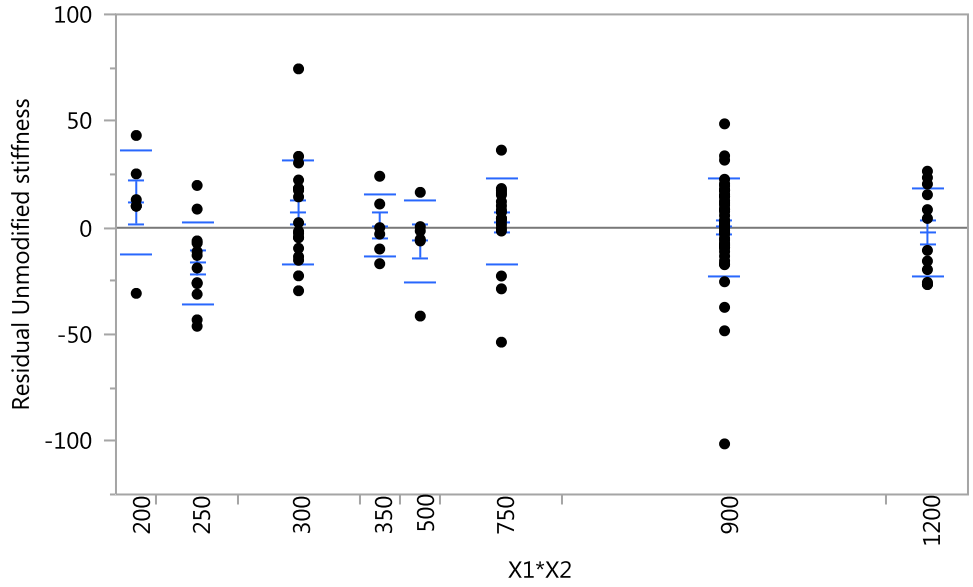

Means and Std Deviations

Level	Number	Mean	Std Dev	Std Err Mean	Lower 95%	Upper 95%
200	6	11.885	24.4447	9.9795	-13.77	37.54
250	12	-16.669	19.4954	5.6278	-29.06	-4.28
300	18	7.121	24.6344	5.8064	-5.13	19.37
350	6	0.931	14.7902	6.0381	-14.59	16.45
500	6	-6.214	19.1136	7.8031	-26.27	13.84
750	18	2.723	20.2488	4.7727	-7.35	12.79
900	48	0.185	22.7469	3.2832	-6.42	6.79
1200	12	-2.136	20.7934	6.0025	-15.35	11.08

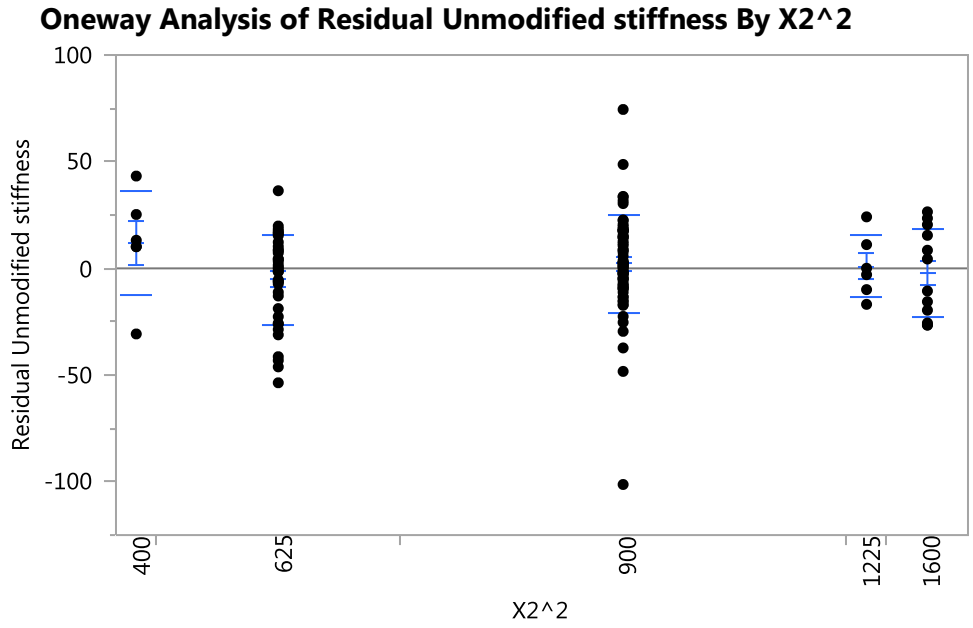

Means and Std Deviations

Level	Number	Mean	Std Dev	Std Err Mean	Lower 95%	Upper 95%
400	6	11.885	24.4447	9.9795	-13.77	37.538
625	36	-5.231	21.1743	3.5290	-12.39	1.934
900	66	2.076	23.2925	2.8671	-3.65	7.802
1225	6	0.931	14.7902	6.0381	-14.59	16.452
1600	12	-2.136	20.7934	6.0025	-15.35	11.076

Log10 State: Fit Model, Residual Distribution, and Standard Deviation

Response Log10_stiffness

Effect Summary

Source	LogWorth	PValue
Testing Temp,°C_X3	61.963	0.00000
X1*X2	3.678	0.00021
X2^2	2.943	0.00114
Styrene content,%_X2	2.122	0.00754

Summary of Fit

RSquare	0.903854
RSquare Adj	0.900675
Root Mean Square Error	0.055439
Mean of Response	2.191612
Observations (or Sum Wgts)	126

Analysis of Variance

Source	DF	Sum of Squares	Mean Square	F Ratio
Model	4	3.4960842	0.874021	284.3751
Error	121	0.3718910	0.003073	**Prob > F**

Source	DF	Sum of Squares	Mean Square	F Ratio
C. Total	125	3.8679752		<.0001*

Lack Of Fit

Source	DF	Sum of Squares	Mean Square	F Ratio
Lack Of Fit	11	0.05368570	0.004881	1.6871
Pure Error	110	0.31820529	0.002893	**Prob > F**
Total Error	121	0.37189099		0.0855
				Max RSq
				0.9177

Parameter Estimates

Term	Estimate	Std Error	t Ratio	Prob>|t|
Intercept	1.3949165	0.146925	9.49	<.0001*
Styrene content,%_X2	-0.025458	0.009368	-2.72	0.0075*
Testing Temp,°C_X3	-0.054725	0.001646	-33.24	<.0001*
X1*X2	-0.000072	1.885e-5	-3.82	0.0002*
X2^2	0.0005025	0.000151	3.33	0.0011*

Effect Tests

Source	DF	Sum of Squares	Mean Square	F Ratio	Prob > F
Styrene content,%_X2	1	0.0226964	0.022696	7.3846	0.0075*
Testing Temp,°C_X3	1	3.3961662	3.396166	1104.991	<.0001*
X1*X2	1	0.0449096	0.044910	14.6120	0.0002*
X2^2	1	0.0341395	0.034140	11.1078	0.0011*

Prediction Expression

1.39491650195118

+ -0.0254583829823 * Styrene content,%_X2

+ -0.0547252737222 * Testing Temp,°C_X3

+ -0.0000720589763 * X1*X2

+ 0.00050252310653 * X2^2

Distributions

Residual Log10_stiffness

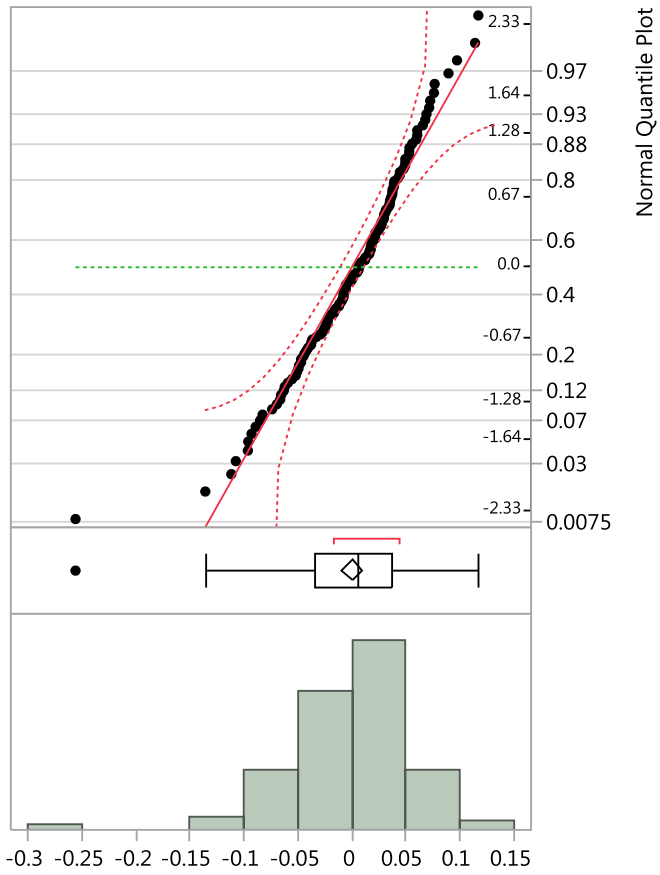

Quantiles

100.0%	maximum	0.1175357042
99.5%		0.1175357042
97.5%		0.0963777761
90.0%		0.0608203323
75.0%	quartile	0.0367413876
50.0%	median	0.006467195
25.0%	quartile	-0.033759015
10.0%		-0.067317021
2.5%		-0.111056586
0.5%		-0.256442338
0.0%	minimum	-0.256442338

Summary Statistics

Mean	1.961e-16
Std Dev	0.0545447
Std Err Mean	0.0048592
Upper 95% Mean	0.009617
Lower 95% Mean	-0.009617
N	126

Fit Group

Oneway Analysis of Residual Log10_stiffness By Styrene content,%_X2

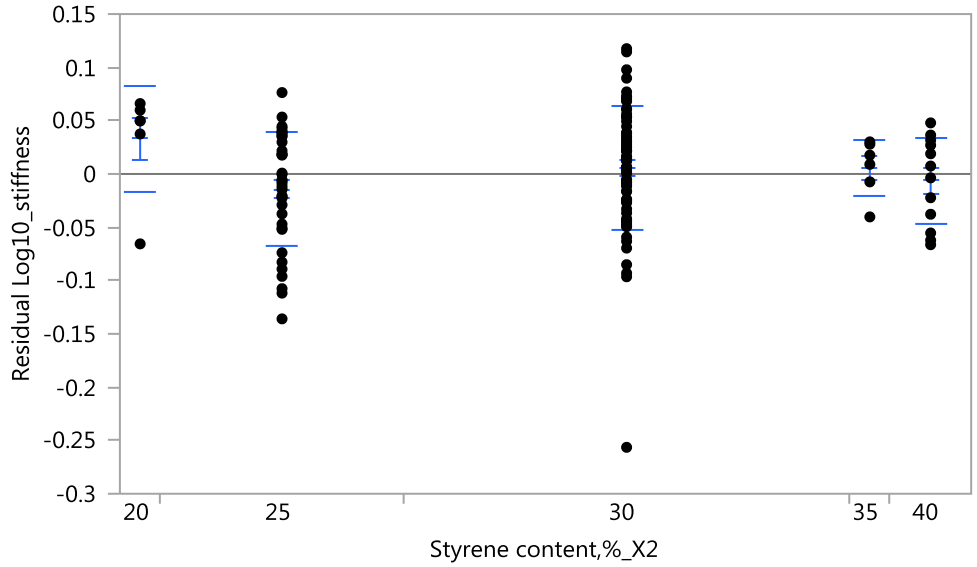

Means and Std Deviations

Level	Number	Mean	Std Dev	Std Err Mean	Lower 95%	Upper 95%
20	6	0.03290	0.049238	0.02010	-0.0188	0.08457
25	36	-0.01428	0.052981	0.00883	-0.0322	0.00365
30	66	0.00542	0.058564	0.00721	-0.0090	0.01982
35	6	0.00615	0.026562	0.01084	-0.0217	0.03403
40	12	-0.00651	0.041062	0.01185	-0.0326	0.01958

Oneway Analysis of Residual Log10_stiffness By Testing Temp,°C_X3

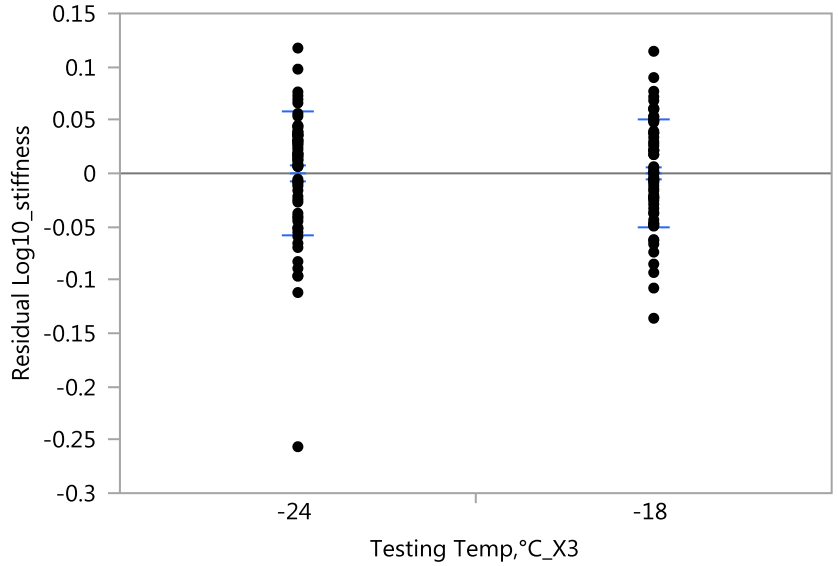

Means and Std Deviations

Level	Number	Mean	Std Dev	Std Err Mean	Lower 95%	Upper 95%
-24	63	2.485e-16	0.058967	0.00743	-0.0149	0.01485
-18	63	1.424e-16	0.050211	0.00633	-0.0126	0.01265

Oneway Analysis of Residual Log10_stiffness By X1*X2

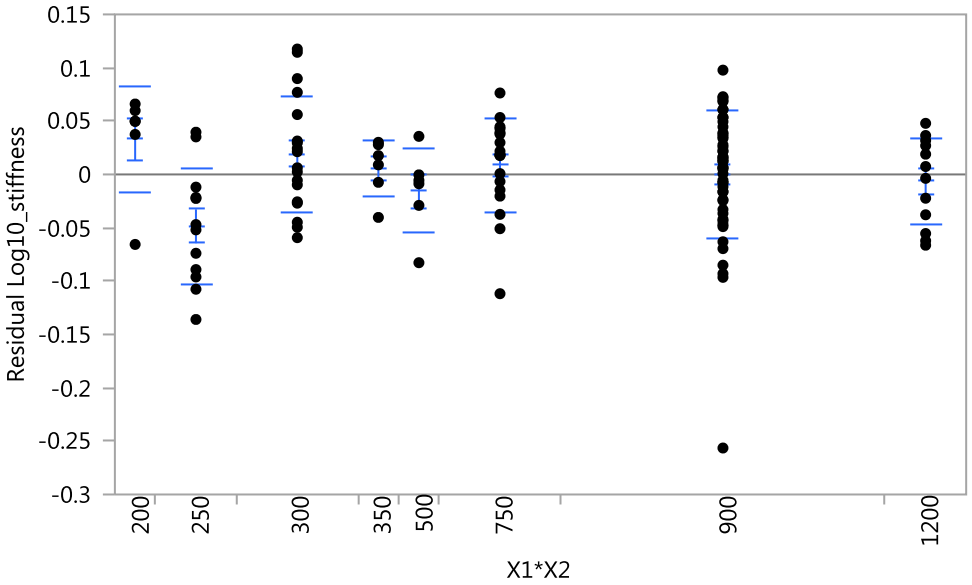

Means and Std Deviations

Level	Number	Mean	Std Dev	Std Err Mean	Lower 95%	Upper 95%
200	6	0.03290	0.049238	0.02010	-0.0188	0.0846
250	12	-0.04857	0.054958	0.01586	-0.0835	-0.0137
300	18	0.01938	0.054093	0.01275	-0.0075	0.0463
350	6	0.00615	0.026562	0.01084	-0.0217	0.0340
500	6	-0.01511	0.039238	0.01602	-0.0563	0.0261
750	18	0.00886	0.044437	0.01047	-0.0132	0.0310
900	48	0.00019	0.059853	0.00864	-0.0172	0.0176
1200	12	-0.00651	0.041062	0.01185	-0.0326	0.0196

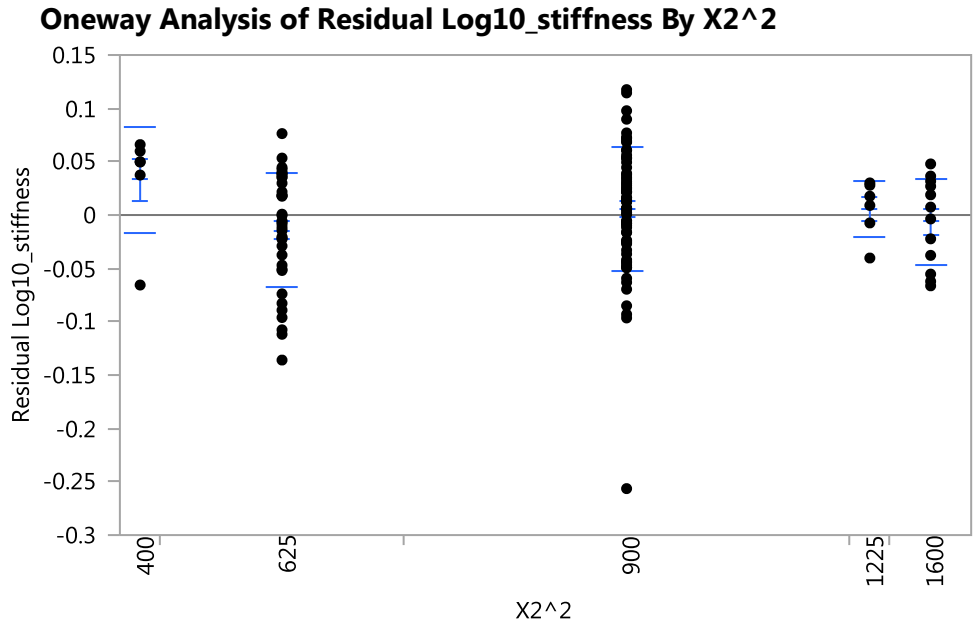

Means and Std Deviations

Level	Number	Mean	Std Dev	Std Err Mean	Lower 95%	Upper 95%
400	6	0.03290	0.049238	0.02010	-0.0188	0.08457
625	36	-0.01428	0.052981	0.00883	-0.0322	0.00365
900	66	0.00542	0.058564	0.00721	-0.0090	0.01982
1225	6	0.00615	0.026562	0.01084	-0.0217	0.03403
1600	12	-0.00651	0.041062	0.01185	-0.0326	0.01958

SQRT State: Fit Model, Residual Distribution, and Standard Deviation

Response SQRT_stiffness

Effect Summary

Source	LogWorth	PValue
Testing Temp,°C_X3	60.832	0.00000
X1*X2	3.518	0.00030
X2^2	2.932	0.00117
Styrene content,%_X2	2.100	0.00795

Summary of Fit

RSquare	0.899746
RSquare Adj	0.896432
Root Mean Square Error	0.823373
Mean of Response	12.72345
Observations (or Sum Wgts)	126

Analysis of Variance

Source	DF	Sum of Squares	Mean Square	F Ratio
Model	4	736.20403	184.051	271.4841
Error	121	82.03121	0.678	Prob > F

Source	DF	Sum of Squares	Mean Square	F Ratio
C. Total	125	818.23523		<.0001*

Lack Of Fit

Source	DF	Sum of Squares	Mean Square	F Ratio
Lack Of Fit	11	10.976701	0.997882	1.5448
Pure Error	110	71.054506	0.645950	**Prob > F**
Total Error	121	82.031207		0.1258
				Max RSq
				0.9132

Parameter Estimates

Term	Estimate	Std Error	t Ratio	Prob>|t|
Intercept	1.215121	2.182117	0.56	0.5787
Styrene content,%_X2	-0.375544	0.139139	-2.70	0.0079*
Testing Temp,°C_X3	-0.79356	0.024451	-32.46	<.0001*
X1*X2	-0.001042	0.00028	-3.72	0.0003*
X2^2	0.0074462	0.002239	3.33	0.0012*

Effect Tests

Source	DF	Sum of Squares	Mean Square	F Ratio	Prob > F
Styrene content,%_X2	1	4.93873	4.9387	7.2849	0.0079*
Testing Temp,°C_X3	1	714.12223	714.1222	1053.365	<.0001*
X1*X2	1	9.38263	9.3826	13.8398	0.0003*
X2^2	1	7.49573	7.4957	11.0566	0.0012*

Distributions

Residual SQRT_stiffness

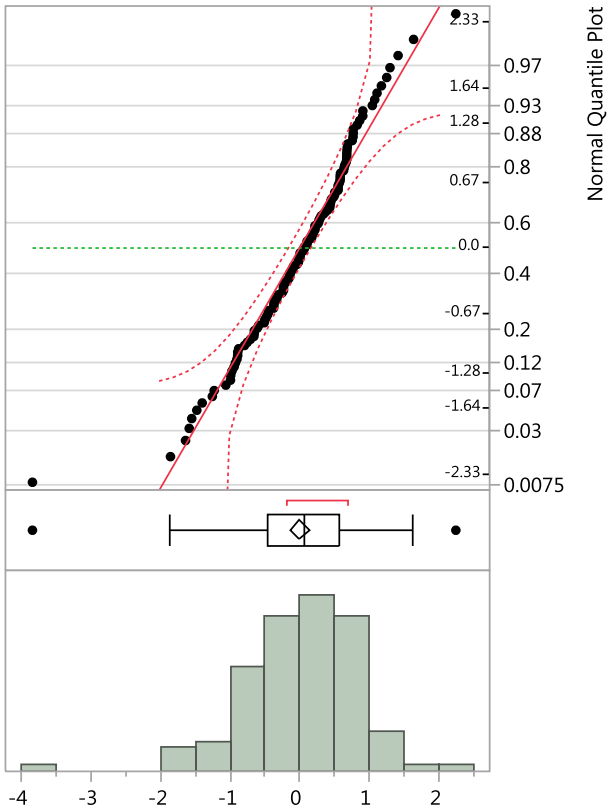

Quantiles

100.0%	maximum	2.251827271
99.5%		2.251827271
97.5%		1.3991419908
90.0%		0.8407283504
75.0%	quartile	0.5743041577
50.0%	median	0.0673357458
25.0%	quartile	-0.453743208
10.0%		-0.980201011
2.5%		-1.634300172
0.5%		-3.849721711
0.0%	minimum	-3.849721711

Summary Statistics

Mean	2.262e-15
Std Dev	0.8100924
Std Err Mean	0.0721688
Upper 95% Mean	0.1428309
Lower 95% Mean	-0.142831
N	126

Fit Group

Oneway Analysis of Residual SQRT_stiffness By Styrene content,%_X2

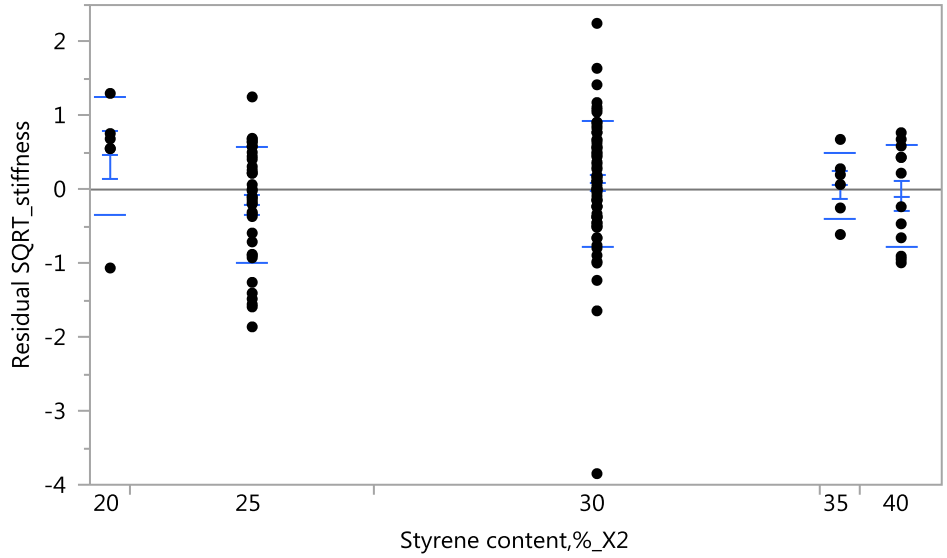

Means and Std Deviations

Level	Number	Mean	Std Dev	Std Err Mean	Lower 95%	Upper 95%
20	6	0.46602	0.798581	0.32602	-0.3720	1.3041
25	36	-0.20367	0.780304	0.13005	-0.4677	0.0603
30	66	0.07909	0.860077	0.10587	-0.1323	0.2905
35	6	0.06203	0.446443	0.18226	-0.4065	0.5305
40	12	-0.08801	0.682735	0.19709	-0.5218	0.3458

Oneway Analysis of Residual SQRT_stiffness By Testing Temp,°C_X3

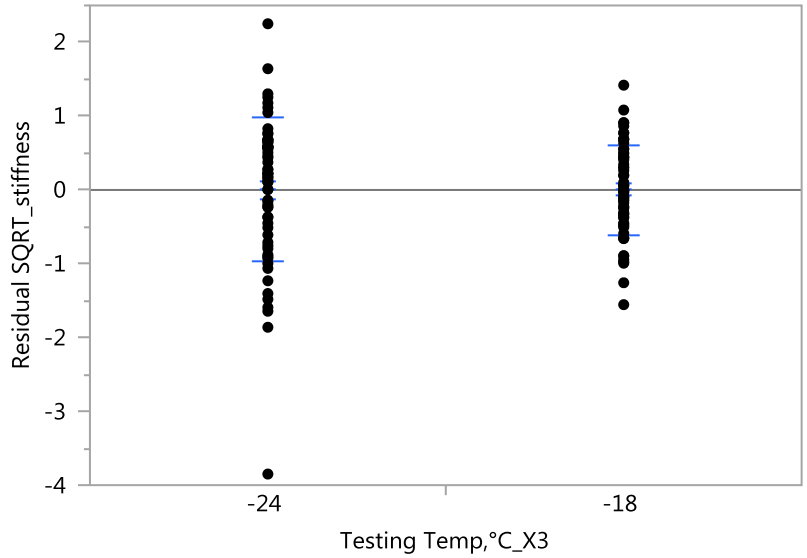

Means and Std Deviations

Level	Number	Mean	Std Dev	Std Err Mean	Lower 95%	Upper 95%
-24	63	3.23e-15	0.977750	0.12318	-0.2462	0.24624
-18	63	1.262e-15	0.605879	0.07633	-0.1526	0.15259

Oneway Analysis of Residual SQRT_stiffness By X1*X2

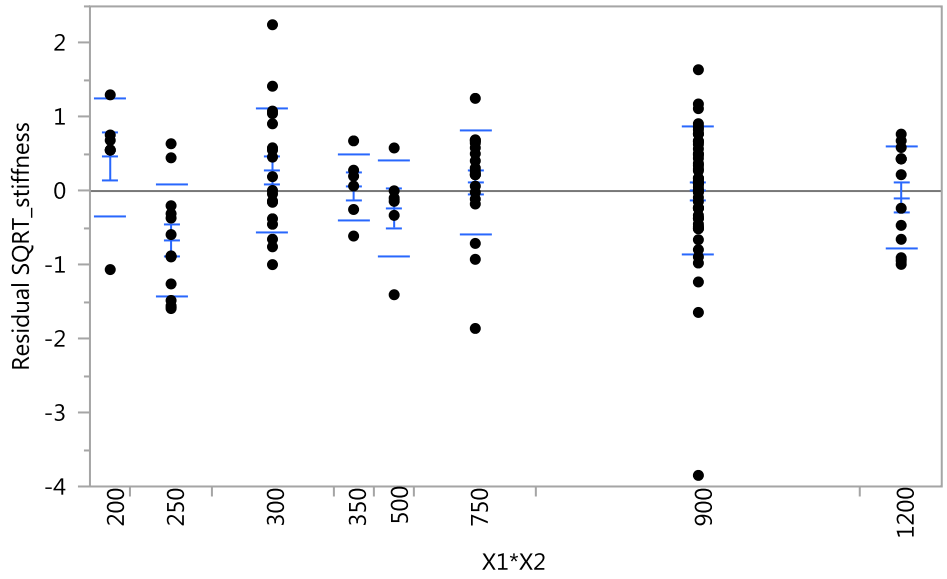

Means and Std Deviations

Level	Number	Mean	Std Dev	Std Err Mean	Lower 95%	Upper 95%
200	6	0.46602	0.798581	0.32602	-0.372	1.304
250	12	-0.66856	0.747807	0.21587	-1.144	-0.193
300	18	0.27568	0.843287	0.19876	-0.144	0.695
350	6	0.06203	0.446443	0.18226	-0.406	0.531
500	6	-0.22998	0.652642	0.26644	-0.915	0.455
750	18	0.11502	0.711411	0.16768	-0.239	0.469
900	48	0.00537	0.863403	0.12462	-0.245	0.256
1200	12	-0.08801	0.682735	0.19709	-0.522	0.346

Oneway Analysis of Residual SQRT_stiffness By X2^2

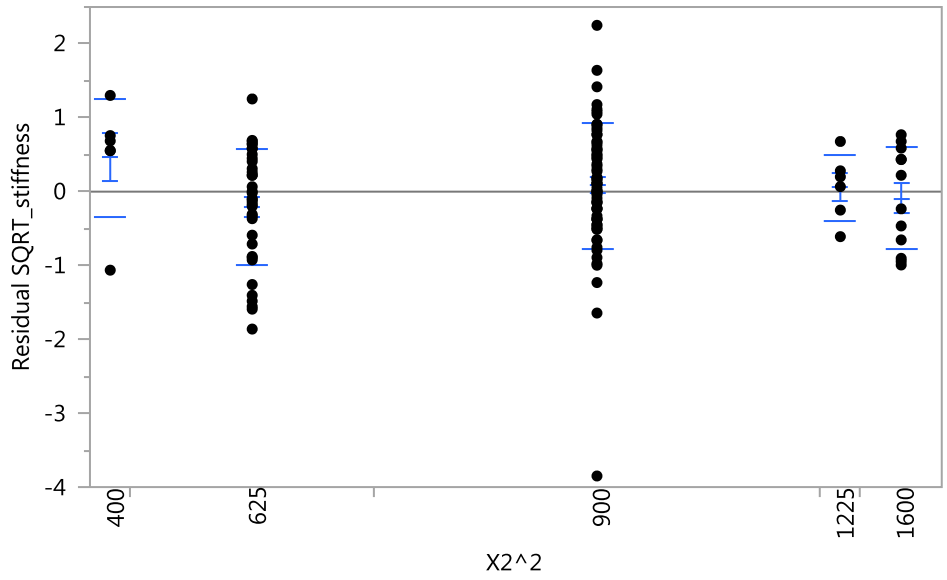

Means and Std Deviations

Level	Number	Mean	Std Dev	Std Err Mean	Lower 95%	Upper 95%
400	6	0.46602	0.798581	0.32602	-0.3720	1.3041
625	36	-0.20367	0.780304	0.13005	-0.4677	0.0603
900	66	0.07909	0.860077	0.10587	-0.1323	0.2905
1225	6	0.06203	0.446443	0.18226	-0.4065	0.5305
1600	12	-0.08801	0.682735	0.19709	-0.5218	0.3458

Comparing Residuals in Graph Builder